EXPERIMENTAL CELL RESEARCH

Published under the auspices of

THE INTERNATIONAL SOCIETY FOR CELL BIOLOGY

EDITORS:

H. BAUER · T. CASPERSSON · A. ENGSTRÖM · E. FAURÉ-FREMIET

H. B. FELL · D. MAZIA · G. MONTALENTI · J. T. RANDALL · J. RUNNSTRÖM

F. O. SCHMITT · E. C. SLATER · P. WEISS · R. W. G. WYCKOFF

VOLUME 12 · JUNE 1957 · NUMBER 3

ACADEMIC PRESS INC., PUBLISHERS, NEW YORK, N. Y.

EXPERIMENTAL CELL RESEARCH

EDITORS:

H. Bauer, Max Planck Institut f. Meeresbiologie, Wilhelmshaven 23, Germany
T. Caspersson, Department of Cell Research, Karolinska Inst., Stockholm 60, Sweden
A. Engström, Department of Medical Physics, Karolinska Inst., Stockholm 60, Sweden
E. Fauré-Fremiet, Collège de France, Paris V:e, France
Honor B. Fell, Strangeways Laboratory, Cambridge, England
D. Mazia, University of California, Berkeley, Calif., U.S.A.
G. Montalenti, Istituto di Genetica dell'Università di Napoli, Naples, Italy
J. T. Randall, Wheatstone Physics Laboratory, King's College, London W. C. 2, England
J. Runnström, Wenner-Gren Institute for Experimental Biology, Stockholm Va., Sweden
F. O. Schmitt, Massachusetts Institute of Technology, Cambridge 39, Mass., U.S.A.
E. C. Slater, University of Amsterdam, The Netherlands.
P. Weiss, Rockefeller Institute for Medical Research, New York 21, N.Y., U.S.A.
R. W. G. Wyckoff, Laboratory of Physical Biology, National Institute of Health, Bethesda, Md., U.S.A.

Editorial Secretaries: L. Ernster and Vera Reio, Norrtullsgatan 16, Stockholm Va., Sweden.
Papers should be submitted to one of the editors or to the Editorial Office, Norrtullsgatan 16, Stockholm Va., Sweden.

ADVISORY BOARD:

W. Bloom (Chicago), J. Brachet (Bruxelles), F. Buchthal (Copenhagen), W. S. Bullough (London), A. Buzzati-Traverso (La Jolla, Calif.), R. Chambers (New York), E. Chargaff (New York), M. Chèvremont (Liège), J. F. Danielli (London), C. D. Darlington (London), J. N. Davidson (Glasgow), M. Demerec (Cold Spring Harbor, N.Y.), J. Engelbreth-Holm (Copenhagen), A. Fischer (Copenhagen), A. Forssberg (Stockholm), A. Frey-Wyssling (Zürich), N. Fries (Uppsala), S. Gard (Stockholm), R. J. Gautheret (Paris), L. Geitler (Wien), G. Gomori (Chicago), T. Gustafson (Stockholm), A. Haddow (London), E. Hammarsten (Stockholm), B. Hanström (Lund), E. Newton Harvey (Princeton, N. J.), L. V. Heilbrunn (Philadelphia, Pa.), G. C. Heringa (Amsterdam), A. Hollaender (Oak Ridge, Tenn.), H. Holter (Copenhagen), J. Holtfreter (Rochester, N.Y.), T. Hultin (Stockholm), G. Klein (Stockholm), P. Koller (London), F. Lehmann (Bern), P. L'Héritier (Paris), G. Levi (Torino), P. E. Lindahl (Uppsala), O. Lindberg (Stockholm), G. Lindeberg (Ås, Norway), C. C. Lindegren (Carbondale, Ill.), R. J. Ludford (London), S. E. Luria (Urbana, Ill.), A. Lwoff (Paris), A. Mirsky (New York), H. Okkels (Copenhagen), O. Olivo (Bologna), A. W. Pollister (New York), S. Ranzi (Milano), W. J. Schmidt (Giessen), F. Schrader (New York), F. Sjöstrand (Stockholm), T. M. Sonneborn (Bloomington, Ind.), J. M. Sosa (Montevideo), J. Spek (Rostock), W. M. Stanley (Berkeley, Calif.), E. Suomalainen (Helsingfors), E. L. Tatum (New York), T. Teorell (Uppsala), A Tyler (Pasadena, Calif.), W. Wilbrandt (Bern), E. Zeuthen (Copenhagen).

Subscriptions

EXPERIMENTAL CELL RESEARCH

is published in two volumes annually, at $ 13.00 per volume. Please send your subscription orders to Academic Press Inc., 111 Fifth Avenue, New York 3, New York.

Experimental Cell Research **12**, *427–506 (1957)*

CHLOROPHYLL-LETALE UND DER SUBMIKROSKOPISCHE FORMWECHSEL DER PLASTIDEN[1]

D. von WETTSTEIN

Forstliche Forschungsanstalt, Stockholm
und Biochemisches Institut der Universität, Uppsala, Schweden

Eingegangen am 15. Oktober 1956

Die Physiologie der Genwirkung versucht die Zusammenhänge zwischen dem Erbfaktor und der ihm zugeordneten Eigenschaft aufzudecken. Sie fragt etwa: Auf welche Weise, zu welchem Zeitpunkt und an welchem Ort beeinflusst und kontrolliert ein Gen die Entwicklung eines Organismus, eines Organes oder einer Zelle? Da zahlreiche Genwirkungen miteinander verknüpft sind, kennen wir Polygenie — mehrere Gene beeinflussen dieselbe Eigenschaft — und Polyphänie oder Pleiotropie — ein Gen beeinflusst mehrere Eigenschaften. Die eben gestellten Fragen werden auf verschiedene Weise analysiert. Einerseits kann man von den Chromosomen, dem Sitz der Gene, ausgehen und z. B. die Wirkung gewebe- und funktionsspezifischer Strukturmodifikationen der Chromomeren in den Riesenchromosomen der Dipteren verfolgen. Andererseits lässt sich die Wirkkette von der Eigenschaft her aufrollen, indem einzelne spontane oder induzierte Mutanten in den verschiedensten Eigenschaften und Entwicklungsstadien mit dem Normaltypus verglichen werden. Eine solche Analyse kann in der makroskopischen oder mikroskopischen Morphologie erfolgen und letale Mutanten von *Drosophila* [59, 147] sind dafür ebenso geeignet wie vitale Mutanten der Gerste [159, 160, 30].

In den letzten Jahren haben biochemische Analysen bei Mikroorganismen, vor allem dem Pilz *Neurospora*, uns gelehrt, wie man Letalfaktoren zur Feststellung der natürlichen Synthese von Stoffen ausnutzen kann [11, 12, 73]. Bei der dabei entwickelten Technik fasst man vor allem solche Mutanten, deren Stoffwechseldefekt durch spezifische, von aussen zugeführte Stoffe behoben werden kann. Das führte zur Erkenntnis, dass viele Gene mit einzelnen und vielfach nur diesen einzelnen Synthesestufen verknüpft sind, indem sie die dazu notwendigen Enzyme bereitstellen. Auch bei Insekten ist eine solche einfache Genwirkkette, die zur Augenausfärbung notwendig ist, klargelegt [19, 18, 80]. Bei der Ausbildung der Augenpigmente konnte in

[1] Gedruckt mit Unterstützung des „Längmanska Kulturfonden".

Verbindung mit histologischer und Transplantationstechnik ein Knotenpunkt zweier Genwirkketten aufgeklärt werden, indem für die Pigmentbildung einmal eine Wirkkette der Umwandlung von Tryptophan in 3-Oxykynurenin in zwei Stufen notwendig ist und zum anderen eine Genwirkkette, die Eiweissträger für das 3-Oxykynurenin bereitstellt, an denen sich dann die weitere Pigmentsynthese vollzieht [81].

Gibt es eine morphologische Pleiotropie, so ist auch eine biochemische Pleiotropie zu erwarten, die mit Hilfe der Papierchromatographie für Aminosäuren, Peptide und verschiedene fluoreszierende Stoffe bei *Drosophila* und *Ephestia* eindrucksvoll aufgezeigt worden ist [59, 60, 61]. Eine Mutation kann weitreichende Veränderungen im Muster fluoreszierender Stoffe bewirken, ohne dass dies morphologisch oder bezüglich der Vitalität in Erscheinung tritt wie bei der Mutante „biochemica" von *Ephestia*, die in einem scheinbar „reinen" Wildstamm aufgefunden wurde [82].

Wir haben von der Wirkung der Gene im morphologischen, mikroskopischen und biochemischen Bereich gesprochen; was aber für Manifestationsmuster zeigen uns die Gene im submikroskopischen Bereich, in dem die engste Verknüpfung zwischen biochemischer und struktureller Analyse gegeben ist? Hierher gehören die Befunde an Virusmutanten, bei denen nach elektrophoretischen Untersuchungen eine Änderung in der Faltung bzw. Spiralisierung und dem räumlichen Feinbau der Proteide als Folge der Mutation erfolgt ist, ohne dass die Zusammensetzung an Nuklein- und Aminosäuren verändert ist [18, 133, 134]. Auch beim Menschen kennen wir einen ganz ähnlichen Fall, die Sichelzellanämie. Pauling [111] hat diese durch ein Gen bedingte Abweichung der roten Blutkörperchen als „molekuläre Krankheit" bezeichnet. Das Sichelzellhämoglobin unterscheidet sich von dem normalen durch seine veränderte Löslichkeit im reduzierten Zustand und seine elektrophoretischen Eigenschaften, nach denen es mehr freie positive Ladungen besitzt. Es besteht kein Unterschied im Röntgen-Beugungsdiagramm, und die Aminosäurezusammensetzung der beiden Hämoglobine ist zumindest sehr ähnlich. Beide müssen also in ihrem Aufbau weitgehend ähnlich sein und das pleiotrope Muster der Sichelzellanämie scheint auf eine kleine genbedingte Änderung der Oberfläche des Globulines zurückführbar zu sein [111, 135, 115].

Es ist Aufgabe der vorliegenden Arbeit, an Chlorophyllmutanten der Gerste zu untersuchen, welche Wirkung mutierte Gene auf die Entwicklung der submikroskopischen Chloroplastenstrukturen haben. Chlorophyllmutationen sind bei der Gerste die häufigsten Mutanten, die nach Bestrahlung auftreten, und finden in der experimentellen Mutationsforschung auf mannigfaltige

Art als Testmutationen Verwendung, zuletzt insbesondere für die Frage der gerichteten Mutabilität ([50, 51, 55, 29, 30, 107] und dort zit. Lit.). Chlorophylldefekte werden vorwiegend durch Faktormutationen bedingt. In jedem einzelnen Fall ist dies aber zu prüfen, da man etwa beim Mais Chlorophyllmutanten kennt, die mit Deficiencies verbunden sind [95] und eine grosse Zahl von ausserkaryotisch vererbten Chlorophylldefekten bekannt ist [24, 121]. Gustafsson [55] schätzt die Zahl der Loci, die die Chlorophyllsynthese und Chloroplastenentwicklung bei der Gerste beeinflussen, auf 250–300. Phänotypisch lassen sich die Chlorophyllmutanten in vier Gruppen einteilen: *albina* (ganz weisse Keiminge), *viridis* (gelb- oder hellgrüne Keimlinge), *xantha* (gelbe bis gelbrote Keimlinge) und in verschiedener Weise gemusterte Keimlinge (*alboviridis, tigrina, striata, maculata* etc.). Einzelne *viridis*-Typen sind vital, während die meisten dieses Typus und alle anderen Chlorophyll-Letale darstellen, die im Keimlingsstadium absterben. Nach eigenen Untersuchungen waren von 615 spontan, nach Röntgen- und Neutronenbestrahlung erhaltenen Chlorophyllmutanten 46% *albina*, 33% *viridis*, 8% *xantha* und 13% seltene gemusterte Typen. Diese Verteilung entspricht der von Gustafsson, Ehrenberg und Nybom festgestellten und gibt eine gewisse Vorstellung über die Verteilung der 250–300 Loci. Dabei ist zu berücksichtigen, dass Allelismus in der *xantha*-Gruppe offenbar häufiger ist als bei *albina* [51]. Beim Mais finden wir ähnliche Befunde über Chlorophyllmutanten. Genauer beschrieben sind 80 Loci — verteilt über alle 9 Chromosomen —, die die Ausbildung der Blattpigmente beeinflussen und von 13 näher untersuchten *albina*-Mutanten wurden keine allel befunden [26, 31].

Die Entwicklung der Präparationsmethoden für die Elektronenmikroskopie macht nunmehr eine direkte Analyse der submikroskopischen Strukturen möglich, und die Chloroplasten erwiesen sich dabei als besonders geeignete Objekte ([75, 35, 36, 47, 90, 91, 146, 161] u.a.). Auf der anderen Seite ist eine Analyse der Blattpigmente in den Chlorophyllmutanten leicht durchführbar [69, 71, 106]. Es wurde daher versucht, an den hier untersuchten Chlorophyll-Letalen *albina* und *xantha*-3 und normal grünen Keimlingen den Verlauf der Bildung von Chlorophyll *a*, *b* und der Carotinoide in der Keimlingsentwicklung festzulegen und mit der submikroskopischen Entwicklung ihrer Chloroplasten zu korrelieren.

Das Studium der genbedingten Syntheseblocke bei *Neurospora* hat gezeigt, dass Zwischenprodukte des Stoffwechsels angehäuft werden. Oft sind es jene Vorstufen, deren weitere Verwendung in der Synthese durch die Genveränderung unmöglich ist, etwa die Anhäufung von Anthranilsäure in Mutanten, die Tryptophan nicht synthetisieren können [152]. Besonders ein-

drucksvoll ist die Synthese von Methionin aus Cystein über Homocystein [72, 73]. Von zwei Mutanten, die Cystein nicht in Homocystein umwandeln können, akkumuliert die eine einen Stoff, der von der anderen Mutante zur Synthese von Homocystein verwendet werden kann. Dieser Stoff wurde dann isoliert und als Cystathionin identifiziert.

Die „Mutantenanalyse" hat sich auch für die Chlorophyll- und Carotinoidsynthese bewährt, wobei vor allem *Chlorella* untersucht wird. Wenn auch eine exakte genetische Analyse bei *Chlorella* nicht möglich ist, so macht doch die beschriebene Konstanz der Abweicher ein mutatives Ereignis wahrscheinlich. Granick [45, 46] hat die Synthesekette des Chlorophylls vom Protoporphyrin IX mit Hilfe solcher Mutanten in groben Zügen klarlegen können. Auch eine mutative Trennung der Licht- und Dunkelsynthese des Chlorophylls ist möglich [45]. Entsprechende Befunde liegen für die Carotinoidsynthese vor [22]. Ein anderer Typus von Mutanten [25] kann die Chromatophorenpigmente weitgehend normal bilden, aber der Photosynthese-Mechanismus selbst ist unterbrochen. Zweifellos sind unter den zahlreichen bekannten Chlorophyll-Letalen und Schecken der höheren Pflanzen beide Typen vertreten, d.h. solche, deren Plastidendefekt durch eine Blockierung in der Pigmentsynthese bedingt ist und solche, deren Defekt in einer Störung der Photosynthese zu suchen ist (vergl. hierzu [132, 151]).

Mag oft die Lokalisation bestimmter Substanzen lichtmikroskopisch in der Zelle mit erheblichen Schwierigkeiten verbunden sein, so sind unsere Kenntnisse über die Cytochemie der elektronenmikroskopisch darstellbaren Strukturen noch sehr gering. Osmiumtetroxyd wird vorwiegend als Fixiermittel in der Elektronenmikroskopie verwendet und seine Reduktion zu niederen Oxyden und metallischem Osmium durch das biologische Material steigert den Kontrast im elektronenmikroskopischen Bild. Dies beruht auf dem hohen Elektronenstreuungsvermögen des Osmiumatomes [4]. Es ist von grossem Interesse, mit welchen Stoffen Osmiumtetroxyd reagiert. Einige vorbildliche Studien über die Mannigfaltigkeit und Unspezifität der Osmiumreaktion sind veröffentlicht [4, 5]. Man hat weiter versucht, die Farbstoffe der Lichtmikroskopie durch geeignete Metallverbindungen mit hoher Elektronenstreuung und spezifischem Reaktionsvermögen gegenüber bestimmten Stoffen oder Radikalen zu ersetzen [3, 6, 63].

Es soll uns hier die Frage beschäftigen, ob Mutanten, die einen genbedingten Syntheseblock aufweisen, zur Lokalisation von Substanzen im elektronenmikroskopischen Bild verwendet werden können. Zufolge einer Mutation angehäufte Stoffwechselzwischenprodukte sind chemisch zu fassen und zu analysieren. Sind sie bestimmten Strukturen im makromolekularen

Bereich zugeordnet, so sollte auch eine Anhäufung der Strukturen — in unserem Fall im Chloroplasten — elektronenmikroskopisch nachweisbar sein. Eine indirekte Methode zur Lokalisation von Stoffen im submikroskopischen Bereich ist damit gegeben.

Über den Aufbau und die Entwicklung der Chloroplasten der Gerste liegen bisher keine elektronenmikroskopischen Analysen vor. Eine Zusammenfassung dieser Arbeit ist im „Symposium on Fine Structure of Cells" Leiden 1954 erschienen [162].

MATERIAL UND METHODIK

Zur Untersuchung gelangten die Gerstenmutanten *albina* 49/1117,29 und *xantha*-3. Die *albina* Mutante wurde 1949 aus einer X_2-Generation nach Bestrahlung mit 10000 r isoliert und zeigte in den folgenden Jahren eine Spaltung von 68 grün : 24 weiss, was einem Verhältnis von 3:1 gut entspricht (Heterogenitätstest: $0.5 > P > 0.3$). Sie ist von der Muttersorte, Bonusgerste, durch ein rezessives Gen, das im homozygoten Zustand weisse Keimlinge bedingt, getrennt. *Xantha*-3 wurde von Nilsson-Ehle Anfang der 20iger Jahre in Goldgerste, einer alten schwedischen Landsorte, als spontane Mutation aufgefunden und ihr monofaktorieller Erbgang wurde mehrfach erwiesen. Die hier untersuchten Individuen entstammen einer Nachkommenschaft von 30 Pflanzen. Von diesen Pflanzen spalteten 20 für *xantha* und 10 waren homozygot normal, ein zufällig ideales Verhältnis. Die 20 heterozygoten Pflanzen spalteten in 296 grün : 98 gelb, was eine gute Übereinstimmung mit dem geforderten 3:1 Verhältnis ergibt (Heterogenitätstest: $0.5 > P > 0.3$). Diese Übereinstimmung verdeckt allerdings mehrere beträchtliche Spaltungsabweichungen in den einzelnen Pflanzen, eine Tatsache die Gustafsson [50, 53] analysiert hat. Er hat nachgewiesen, dass ein beträchtlicher Überschuss oder ein starkes Defizit der homozygot Rezessiven nur physiologische Ursachen hat, wie umweltabhängige Konkurrenzfähigkeit der Gameten und rascher Keimfähigkeitsverlust der homozygot Rezessiven. Nachdem diese Störungen offenbar keinen genetischen Hintergrund haben, können wir *xantha*-3 ebenfalls als einen einfachen rezessiven Letalfaktor betrachten. *Xantha*-3 wurde mehrfach unter verschiedenen Gesichtspunkten bearbeitet, insbesondere in der Frage der monohybriden Heterosis [50, 53, 54, 56, 57]. Biochemische Untersuchungen an dieser Mutante haben v. Euler und Moritz [33] ausgeführt und Pigmentanalysen aus neuerer Zeit liegen von Holm [71] vor. Dabei ist beachtenswert, dass die Heterozygoten auch in Bezug auf Chlorophyll *a*, *b* und Carotinoide monohybride Heterosis zeigen.

Als Vergleichspflanzen zu diesen Chlorophyll-Letalen wurden homozygot normale Keimlinge von Gold- und Bonusgerste (beides reine Linien) und zwar Geschwisterpflanzen der letalen Individuen verwendet. (Die Heterozygoten wurden bei dieser Untersuchung nicht herangezogen.) Da die Chloroplasten dieser beiden normalen Linien in ihrer Struktur und Entwicklung nicht zu unterscheiden waren, seien sie im folgenden ungetrennt behandelt.

Die zur Einbettung und zur Pigmentbestimmung gelangenden Individuen wurden

unter Gewächshausbedingungen bei ca. 18°C herangezogen und waren dem gleichen Wechsel der äusseren Bedingungen unterworfen. Leider konnte die Pigmentanalyse und die Einbettung nicht an denselben Individuen sondern nur gleichzeitig an verschiedenen Keimlingen ausgeführt werden. Auf der anderen Seite erwiesen sich zu verschiedenen Zeitpunkten genommene Keimlinge in der elektronenmikroskopischen Analyse als gleichwertig. Die Keimlinge wurden nach 6–10 Tagen zur Analyse verwendet, d.h. wenn das Primärblatt eine durchschnittliche Länge von 10 cm erreicht hat. Am selben Keimling kann man im 2–6 mm langen Sekundärblatt die Chloroplastenentwicklung studieren. Die Chlorophyll-Letalen sterben bald nach diesem Zeitpunkt, welcher in den normalen Keimlingen den Kompensationspunkt darstellt, bei dem durch die beginnende Assimilation der Trockengewichtsverlust während der Keimung ausgeglichen ist [30 a].

Die von Herrn Dr. Leyon und mir verwendete routinemässige Herstellung von Dünnschnitten und die Untersuchung in einem modifizierten Elektronenmikroskop Modell Siemens 1941 ist an anderer Stelle mehrfach ausführlich beschrieben (85, 86, 87, 91). Hinzuzufügen ist, dass neben gepufferter Osmiumtetroxydlösung auch Osmiumräucherung mit Erfolg verwendet wurde.

Vergleichende lichtmikroskopische Untersuchungen wurden mit Ortholux, apochromatischer Optik und der Phasenkontrasteinrichtung von Leitz ausgeführt.

Die Pigmentanalyse erfolgte nach der von Holm [71] und Nybom [106] ausgearbeiteten Methodik mit Hilfe eines Hilger „Uvispek". Die Blätter wurden in einem Mörser mit reinem Aceton und einer Spur von Magnesiumcarbonat extrahiert, auf 5 oder 10 cm³ verdünnt und direkt in eine 1 cm Küvette filtriert. Die Extinktion dieses Extraktes wurde in den Wellenlängen 662,0 mμ, 644,0 mμ, den Absorptionsmaxima von Chlorophyll *a* resp. *b*, und im blauen Teil des Spektrums bei 440,5 mμ, wo Chlorophyll *a* und *b* die gleiche Absorption besitzen, bestimmt. Bei Kenntnis der spezifischen Absorptionskoeffizienten für Chlorophyll *a*, *b* und die Carotinoide in diesen Wellenlängen, lassen sich die absoluten Konzentrationen der einzelnen Pigmente in einem Gemisch auf Grund des Beerschen Gesetzes nach folgenden Gleichungen errechnen ([23, 167, 143, 43] und dort cit. Lit.):

$$E_{662,0} = C_a \cdot \alpha^{a}_{662,0} + C_b \quad \cdot \alpha^{b}_{662,0};$$

$$E_{644,0} = C_a \cdot \alpha^{a}_{644,0} + C_b \quad \cdot \alpha^{b}_{644,0};$$

$$E_{440,5} = C_c \cdot \alpha^{c}_{440,5} + C_{a+b} \cdot \alpha^{a=b}_{440,5};$$

E = Extinktion; C_i = Konzentration in g/l; α = spezifischer Absorptionskoefficient (Extinktion einer Lösung von 1 g Pigment in 1 l; a = Chlorophyll *a*; b = Chlorophyll *b*; c = Carotinoide.

Folgende spezifische Absorptionskoeffizienten für Aceton fanden Verwendung:

$$\alpha^{a=b}_{440,5} = 57{,}0; \quad \alpha^{a}_{644,0} = 22{,}68; \quad \alpha^{a}_{662,0} = 104{,}50;$$

$$\alpha^{c}_{440,5} = 213{,}0; \quad \alpha^{b}_{644,0} = 47{,}72; \quad \alpha^{b}_{662,0} = 4{,}83.$$

Eine Auflösung der obigen Gleichungen ergibt mit diesen Koeffizienten:

$$C_a = 9{,}784 \cdot E_{662{,}0} - 0{,}990 \cdot E_{644{,}0};$$

$$C_b = 21{,}426 \cdot E_{644{,}0} - 4{,}650 \cdot E_{662{,}0};$$

$$C_c = 4{,}695 \cdot E_{440{,}5} - 0{,}268 \cdot C_{(a+b)}.$$

Man erhält die Konzentration (C) in mg Pigment per l Lösung.

Der Vorteil einer solchen spektrophotometrischen Methode ist minimale Veränderung der Pigmente im Anschluss an die Extraktion. Alle Manipulationen von der Extraktion bis zur Ablesung der Photometerwerte lassen sich in wenigen Minuten und in schwachem künstlichen Licht ausführen. Die biologische Variabilität ist grösser, als die durch die photometrische Methode eingeführten Fehler (siehe [106]). Es wurde sorgfältig darauf geachtet, dass im Verlaufe der Extraktion keine Pigmente an der Wand des Mörsers antrockneten. Die analytischen Werte sind von der spektralen Bandweite abhängig und Comar und Zscheile [23] haben die zulässigen Grenzen für verschiedene Wellenlängen festgelegt. Bei der hier verwendeten Bandweite von 5 Å sind diese in allen Fällen weit unterboten.

Ein Nachteil der Untersuchung von Pigmentgemischen ist, dass nur die Gesamtheit der gelben Pigmente bestimmt werden kann, da die Ähnlichkeit ihrer Absorptionskoeffizienten keine Trennung erlaubt.

Besondere Beachtung verdienen andere Stoffe, die in den untersuchten Wellenlängen absorbieren. Die Werte der Wellenlängen über 630 mμ werden von Carotinoiden und von einer unbekannten Substanz, die bei 626,5 mμ absorbiert [23], nicht beeinflusst. Flavone und Anthocyanine, die im Bereich der Carotinoide absorbieren, sind im Gerstenblatt in zu vernachlässigender Menge vorhanden. Ein anderes Pigment, das in diesem Zusammenhang Beachtung verdient, ist das Protochlorophyll, die Vorstufe des Chlorophyll *a* [77, 140, 141, 79, ältere Lit. bei 28]. Über die Anwesenheit von Protochlorophyll in normalen belichteten Blättern liegt nur eine kurze Angabe vor [140], und die vorkommende Menge dürfte allgemein gering sein. In Chlorophyllmutanten hingegen ist eine Anhäufung dieses Pigmentes denkbar. Die spezifischen Absorptionskoeffizienten des Protochlorophylls sind bei 662 mμ 0,1–0,2, bei 644 mμ 1,1–1,2 und bei 440,5 mμ ca 220 [77, 79, 76]. Während also eine Anwesenheit von Protochlorophyll die hier bestimmten Werte der Chlorophylle nur wenig beeinflusst, ist sein Einfluss auf die Carotinoidmenge beträchtlich. Da die Absorptionskoeffizienten für Carotinoide und das Protochlorophyll bei 440,5 mμ ungefähr gleich gross sind, dürfte die aus der Absorption bei 440,5 mμ bestimmte Pigmentmenge bei Anwesenheit von Protochlorophyll in Annäherung der Summe von Carotinoiden und Protochlorophyll entsprechen.

Der ausdifferenzierte Gerstenchloroplast

In Schnitten durch das Parenchym 10 cm langer Primärblätter erhält man Übersichtsbilder wie Abb. 1.[1] Im wandständigen Plasma liegen längsgeschnittene Chloroplasten dicht nebeneinander. Sie zeigen eine Länge von

[1] Abb. 1–21 und 24–101 siehe S. 488–506.

4–6 μ und besitzen eine durchschnittliche Dicke von 0.8–2,5 μ. Häufig sind 1–2 Stärkekörner — durch ihren geringen Kontrast im Elektronenmikroskop (Abb. 2 und 3) und ihre Schrumpfung auffallend — in den Chloroplasten zu finden. Letztere sind aus den typischen Strukturelementen, den Lamellen des Stromas und der Grana aufgebaut. Die Schichten und Lamellen sind von einer feinkörnigen Grundsubstanz, die sich zuweilen zu fibrillären oder netzartigen Strukturen verdichtet, umgeben (Abb. 1–5). Vielfach liegen kugelige „osmiophile" Körner oder Tropfen mit einem, soweit festgestellt, homogenen Aufbau zwischen den Lamellen (Abb. 1, 3, 15). Für diese stark elektronenstreuenden Körper, deren allgemeine Verbreitung in den Chloroplasten festgestellt ist (z.B. [47, 90]), sei hier im folgenden der Ausdruck *Globuli* verwendet.

Der Chloroplast erscheint in den Elektronmikrographien von einer doppelten Membran begrenzt (Abb. 1 und 2). Jede Teilmembran weist einen Durchmesser von ca 50 Å auf und der Zwischenraum misst 75–100 Å, so dass sich eine totale Dicke von ca 200 Å für die zusammengesetzte Membran ergibt. Auffallend sind oft beobachtete Durchbrechungen dieser Membran, welche zuweilen in regelmässigen Abständen aufscheinen (Abb. 1, 2, 3, und 5). Ob diese Durchbrechungen als Poren aufzufassen sind oder lediglich Fixierungsartefakte darstellen, bleibt zu untersuchen.

Wie bei anderen Objekten (vgl. [88]) lässt sich auch beim Gerstenchloroplasten eine dichte äussere Randschicht mit einem granulären Aufbau aufzeigen. Sie dürfte dem „Peristromium" Senns [136, 83, 64] entsprechen. Besonders deutlich tritt diese Randschicht mit einem maximalen Durchmesser von 0,15 μ im oberen Chloroplasten der Abb. 1 und in Abb. 2 hervor. In anderen Chloroplastenbildern kann sie mehr oder weniger vollständig fehlen. In jüngeren Chloroplasten scheint sie stärker ausgeprägt zu sein. Ein pseudopodienartiger Fortsatz dieser Randschicht ist in Abb. 2 links unten sichtbar.

Zwischen den Chloroplasten lassen sich im Plasma zwei Organellen feststellen: Das eine, kleinere (Abb. 1 *a*, *b*) ist durch seinen sehr dichten Aufbau und starke Elektronenstreuung in den Mikrogrammen gekennzeichnet. Diese Körper mit einem gemessenen Durchmesser von 0,2–0,4 μ sind kugelförmig, da sie in den Schnitten stets eine mehr oder weniger kreisförmige Begrenzung zeigen. Einige dieser Körper wie *a* (Abb. 1) erscheinen homogen, etwa wie die *Globuli*, andere wie *b* (Abb. 1) zeichnen sich durch eine dichte retikuläre Struktur aus. Ob es sich um zwei verschiedene Gebilde oder um verschiedene Zustände ein und desselben handelt, bleibt vorerst ungeklärt.

Das andere, etwas grössere Organell (Abb. 1 *c*) mit einem geschätzten

Durchmesser von 0,4–0,6 μ hat häufig eine ovale bis längliche Form und ist von wesentlich geringerer elektronenoptischer Dichte. Es ist durch eine mehr oder weniger deutliche Membran abgegrenzt, von der radiale Stränge gegen die Mitte ziehen. Der zentrale Teil kann von Substanz ausgefüllt oder elektronenoptisch leer sein. Die mögliche Natur der Organellen sei im Zusammenhang mit den Bestandteilen jüngerer Zellen besprochen (S. 442 ff.).

Bei näherer Betrachtung des Chloroplastenaufbaues fällt auf, dass dieser aus 6–12 mehr oder weniger durchgehenden Schichten besteht (Abb. 1–5). Eine solche Schicht (nach Menke [96]) ist in Stroma- und Granabereiche aufgeteilt. Der Durchmesser der Stromalamellen (Abb. 7) beträgt 75 ± 25 Å. Innerhalb einer Schicht variiert ihr Abstand voneinander zwischen 50 und 100 Å. Die Granabereiche sind im Querschnitt scharf abgegrenzt rechteckig und durch eine strenge Parallelität der Lamellen sowie eine stärkere Elektronenstreuung gekennzeichnet (Abb. 1–7). Die Granalamellen wurden zu 40 ± 20 Å und die Zwischenräume zu 50 ± 20 Å Dicke bestimmt. Im Flächenschnitt sind die Grana kreisrund (Abb. 8 und 9) und der Durchmesser solcher Scheiben wechselt von 0,3 bis 0,4 μ.

Solche idealen Flächenschnitte erhält man nur selten, da das Granum als Zylinder aufzufassen ist und ein solcher in zwei seiner Hauptschnittrichtungen ein Rechteck ergibt. Weiter stellen die Chloroplastenschichten Schalen — parallel zur Chloroplastenmembran — dar und die Grana folgen der Schalenkrümmung. Daher sind in den Plastiden nach verschiedenen Ebenen schief geschnittene Grana, wie im linken Ende des unteren Chloroplasten der Abb. 1, häufig.

Es ist für die Entstehung der Granastruktur von Interesse, ob der Durchmesser des Zylinders innerhalb eines Chloroplasten eine elementare Grösse ist oder einer Variation unterworfen ist. Dass der Durchmesser der Grana in verschiedenen Geweben, unter verschiedenen physiologischen Bedingungen und in verschiedenen Arten in weitem Umfang wechselt, ist bekannt [64, 14, 47]. Aber auch innerhalb einzelner Chloroplasten scheint die Variation bedeutend zu sein. Die beiden Scheiben der Abb. 8 und 9 zeigen bei gleicher Vergrösserung schon einen beträchtlichen Unterschied. Längsschnitte sind in diesem Zusammenhang nur sehr bedingt brauchbar. In ihnen lässt sich eine Variation von 0,1–0,6 μ feststellen. Entscheidend sind aber beträchtliche Abweichungen der rechteckigen Form median geschnittener Grana, z.B. im 2. Granum von unten der Abb. 6 oder 7. Hier sind die beiden untersten Granalamellen auf der einen Seite wesentlich verkürzt. Eine Durchmesservariation von 50% innerhalb eines Chloroplasten dürfte kaum zu hoch gegriffen sein.

Dies leitet zur Frage der Lage der Granabereiche im Chloroplasten über. Die Granastapel der einzelnen Schichten können einigermassen übereinander liegen (Abb. 1–7). Diese Anordnung ist aber nicht streng wie Abb. 6 und 7 zeigen. Es kommt sogar eine Lage „auf Lücke", wie an verschiedenen Stellen in Abb. 2, 3 und 4, vor.

Zusammenfassend gibt das den Eindruck, dass der Abstand der Grana voneinander innerhalb einer Chloroplastenschicht ein relativ gleichmässiger ist, während die Lage von Schicht zu Schicht stark variiert.

Die einzelnen Chloroplastenschichten enthalten eine wechselnde Anzahl von Lamellen. In Tabelle I sind 25 Fälle aufgeführt, an denen die Lamellenzahl im Granum und im angrenzenden Stroma einer Schicht bestimmt werden konnte. Die Tabelle enthält in der linken Hälfte — Mitte — die Anzahl Granalamellen und zu beiden Seiten die der angrenzenden Stromalamellen.

In 13 Fällen ergibt sich auf beiden Seiten ein Verhältnis von Stroma- zu Granalamellen wie 1:2. In 6 Fällen, wo nur eine Seite bestimmbar war, ist ebenfalls ein Verhältnis von 1:2 gefunden. Von den übrigen fallen No. 5–7 auf, wo 5 Granalamellen 2 oder 3 Stromalamellen gegenüberstehen. In No. 20 enthalten die beiden Enden der Grana eine verschiedene Anzahl: 6 bzw. 8 mit 3 und 4 angrenzenden Stromalamellen. Hier ist offenbar eine Verzweigung von Lamellen im Granum vorhanden. In den beiden restlichen Fällen (No. 15 und 21) findet ebenfalls ein Wechsel der Zahl im Granum mit oder ohne veränderter Stromazahl statt. Diese Abweichungen — wenn sie echt und nicht durch begrenzte Auflösung oder Fixierung bedingt sind — bieten Anhaltspunkte für eine stattfindende Vermehrung der Lamellen.

Abb. 6 und 7 stellen den gleichen stark vergrösserten Ausschnitt der Abb. 2 in verschiedener Fokuseinstellung dar. Abb. 7 ist im Bereich der Grana kontrastarm, aber die Übergänge von einer Stroma- in zwei Granalamellen lassen sich an mehreren Stellen verfolgen. Auch in Abb. 4, 10, 11 und 12 ist die Aufspaltung einer dicken Stromalamelle am Rande des Granums erkennbar.

Die Anzahl der Lamellen in den Grana der Chloroplastenschichten wechselt von 2–14 (Tab. I). Am häufigsten sind Grana mit 6 und 8 Lamellen. Abgesehen von den bereits erwähnten 5-lamelligen Grana beträgt die Lamellenzahl ein Vielfaches von zwei.

Aus der Anzahl, der durchschnittlichen Dicke der Lamellen und Zwischenräume (40 bzw. 50 Å) lassen sich die Höhen der Grana berechnen und mit den direkt gemessenen Werten vergleichen (Tab. I, rechte Hälfte). Für die 2, 4, 6 und 8-lamelligen Grana ist die Übereinstimmung der Mittelwerte gut. Die gemessenen Höhen der Grana mit 5 Lamellen überschreiten in allen 3 Fäl-

TABELLE I

Anzahl der Granalamellen und angrenzender Stromalamellen und Höhe der Grana einzelner Chloroplastenschichten.

Fall	Anzahl Lamellen im:			Höhe des Granum in mμ	
	Stroma	Granum	Stroma	gemessen	berechnet*
(1)	1	2	1	9	
(2)	1	2	1	9	
(3)	1	2	1	14	
				$M = 11$	13
(4)	—	4	2	32	31
(5)	3	5	3	45	
(6)	2	5	3	45	
(7)	—	5	3	50	
				$M = 47$	40
(8)	3	6	3	63	
(9)	3	6	3	54	
(10)	3	6	3	41	
(11)	3	6	3	45	
(12)	3	6	3	41	
(13)	3	6	—	45	
(14)	—	6	3	54	
				$M = 49$	49
(15)	3	6 (7)	4	63	
(16)	4	8	4	72	
(17)	4	8	4	68	
(18)	—	8	4	71	
(19)	—	8	4	65	
(20)	3	(6) 8	4	68	
				$M = 69$	67
(21)	5	10 (11)	5	95	
(22)	5	10	—	94	85
(23)	6	12	6	109	
(24)	6	12	6	118	103
(25)	7	14	7	131	121
$M =$	3,45	6,84	3,48		

* Bei der Berechnung wurden Dicken von 40 Å für die Granalamellen und 50 Å für die Zwischenräume verwendet.

len die berechnete. Das mag für eine Verdickung einzelner Lamellen und für eine stattfindende Lamellenvermehrung sprechen, vielleicht in der Weise — durch Verdickung und nachfolgende Aufspaltung — wie es für die Chromatophorenschichten von *Fucus* gezeigt ist [161]. Auch die gemessenen Höhen der Grana mit 10–14 Lamellen überschreiten wesentlich die berechneten. Neben schiefgeschnittenen Lamellen mit grösserer Dicke dürfte die Unstimmigkeit vor allem in der grösseren Breite einzelner Zwischenräume zu suchen sein. In Abb. 2–7 beobachtet man in den grossen Granastapeln (soweit sie zu einer Chloroplastenschicht gehören) eine gewisse Längsteilung, indem ein oder zwei Zwischenlamellen breiter sind als die übrigen. Die beiden untersten Grana der Abb. 6 und 7 geben den Eindruck, als ob sie durch Trennung voneinander entstanden sind. So sind die Differenzen am ehesten als eine beginnende Trennung zu „hoch gewordener" Grana aufzufassen, was gleichzeitig zur Bildung einer neuen Chloroplastenschicht führt.

Abb. 6 und 7 bringen zum Ausdruck, dass die Zwischenlamellen im Granum aus einer körnigen Substanz mit stärkerer Elektronenstreuung, als die umgebende Chloroplastengrundsubstanz, bestehen. Die Granalamellen sind im Mikrogramm 6 aus zwei feinen dunklen Konturen mit einem helleren Zwischenraum zusammengesetzt. Soweit feststellbar, sind die beiden Konturen gleich dick und auch der Zwischenraum von derselben Grössenordnung. Die Konturen gehen weitgehend parallel, schmelzen jedoch häufig zusammen. Die Granalamellen sind demnach in 3 Feinschichten von 10–20 Å zu unterteilen. Die Deutung des zusammengesetzten Baues als Schichten ist am wahrscheinlichsten, wenn auch andere Möglichkeiten nicht ausgeschlossen sind.

Wie sieht eine Granalamelle von der Fläche aus, nachdem ihre zusammengesetzte Natur im Schnitt erkennbar ist? Die Scheiben in den Mikrogrammen 8 und 9 zeigen eine klare Begrenzung in Form von elektronenoptisch dichterem Material. Eine solche „Anhäufung" von Material ist auch in den Längsschnitten erkennbar und bedingt häufig einen schlechten Kontrast an den Übergangsstellen vom Stroma in den Granabereich. Die innere Fläche der Granascheibe sieht retikulär oder körnelig strukturiert aus. Es bleibt ungewiss, ob diese Struktur der Granalamelle selbst angehört oder infolge der grossen Tiefenschärfe des Elektronenmikroskopes durch die darunterliegende Struktur der Zwischenlamelle bedingt ist.

Granalamellen, strikt von der Fläche geschnitten, sind von statistisch homogenem Material umgeben, ein Hinweis dafür, dass die Stromalamellen und Zwischenräume „Schichten" und nicht Bänder sind (vgl. hiezu [68]).

Der Übergang zweier Granalamellen in eine dicke Stromalamelle (Abb. 7)

liess vermuten, dass die ca 75 Å dicken Stromalamellen zwei Feinschichten sind, die durch eine Zwischensubstanz mit relativ hoher Elektronenstreuung zusammengehalten werden. In der Tat lässt sich eine Trennung zweier solcher Schichten als Folge von Quellung wahrnehmen (Abb. 13, 14, 15 und 16 Pfeil). Eine Stromalamelle ist aus zwei ca 20 Å dicken Feinschichten und einer Zwischenschicht von ca 35 Å aufgebaut. Eine Aufspaltung in 3 Schichten legt Abb. 7 und 13 nahe. Aus Abb. 5, 7, 10–18 geht hervor, dass den Stromalamellen beiderseitig eine Matrix angelagert ist, etwa von der Dichte der Granazwischenlamellen. Dies gibt den Stromalamellen in den Mikrogrammen eine diffuse Begrenzung. Schliesslich können die Stromalamellen in verschiedener Weise verzweigt sein (Abb. 3, 4, 5, 16, 17, 18 und 19).

Nach diesem Streifzug durch die Mikrogramme lässt sich das Wesentliche der Feinstruktur des Gerstenchloroplasten im Schema der Abb. 22 zusammenfassen (das Schema ist in der Richtung der Schichten auf $\frac{1}{5}$ verkürzt gezeichnet):

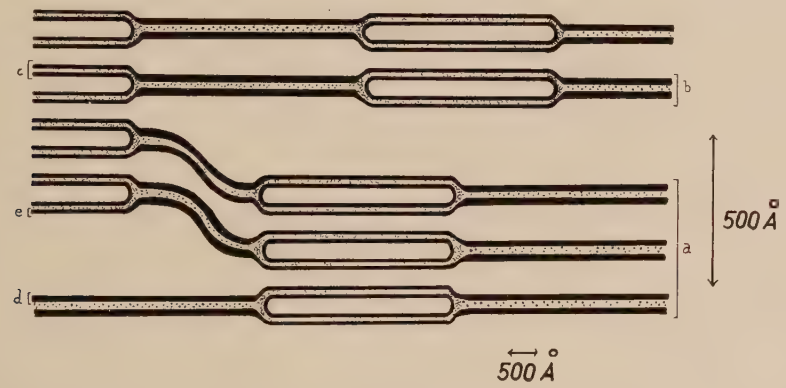

Abb. 22.—Schema der submikroskopischen Organisation des Gerstenchloroplasten. *a* = Schicht, *b* = Stromalamelle, *c* = Granalamelle, *d* = Stromafeinschicht, *e* = Granafeinschicht.

Grundprinzip des Chloroplasten ist die durchgehende Schichten- bezw. Schalenorganisation. Die Chloroplastenschichten (*a*) sind aus den Stroma- (*b*) und Granalamellen (*c*) aufgebaut. Beide lassen sich in je zwei weitere Feinschichten (*d* und *e*) zergliedern. Das Verhältnis von Stroma- zu Granalamellen und das von Stroma- zu Grana-Feinschichten ist 1 : 2.

In einem Punkt muss das Schema hypothetisch bleiben. Die Vereinigung zweier Granafeinschichten — wie gezeichnet — kann nicht mit Sicherheit belegt werden. Eine Aufspaltung einer Stromafeinschicht in die zwei Granafeinschichten ist auch denkbar.

Das Schema wird der Tatsache gerecht, dass die Chloroplastenschichten nicht isoliert, sondern durch Stromalamellen verbunden sind. Das ist in Abb. 1–5 und 18 sichtbar. Um eine Auffassung der Gesamtanordnung der Schichten und ihrer Stromaverbindungen zu gewinnen, sei die schematische Kopie eines Mikrogrammes in Abb. 23 dargestellt. Dabei ist die Feinstruktur der Grana unberücksichtigt. Fast alle Chloroplastenschichten sind durch

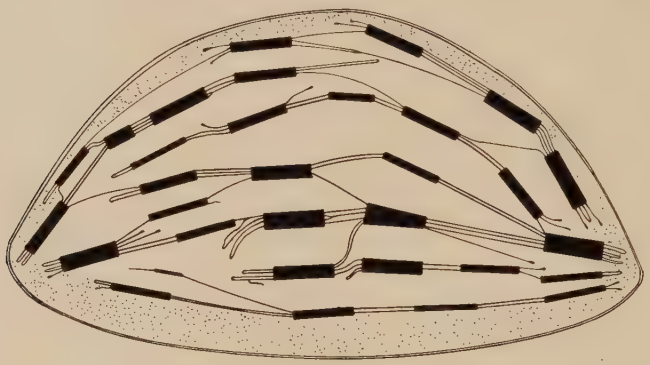

Abb. 23.—Schema der Anordnung der Grana und der Stromalamellen im Gerstenchloroplasten.

einzelne oder auch zwei Stromalamellen miteinander verbunden, so dass sich im Schnitt ein netzartiges Bild ergibt. Die Verbindungen der Chloroplastenschichten sind so angeordnet, dass eine direkte Verbindung von der granulären Randschicht des Chloroplasten weit in das Innere reicht. Wenn trotzdem geschlossene Hohlräume im Schnitt vorzuliegen scheinen, so ist zu berücksichtigen, dass diese sehr wohl in anderen Schnittebenen mit dem äusseren Teil des Chloroplasten in Verbindung stehen können. Der Chloroplastenaufbau kann demnach mit einem System abgeflachter Kanäle verglichen werden, die zu einer vorübergehenden Speicherung der gebildeten Assimilate und ihrer Ableitung geeignet sind [90, 151].

Die Chloroplastenschichten enden mit Stromalamellen. Häufig sind je zwei Stromalamellen an den Enden paarweise vereinigt (Abb. 5, 20, 21 und 23). Ebenso kann das freie Enden von einzelnen Stromalamellen in den Mikrogrammen beobachtet werden (Abb. 1, 3, 5). Dies dürfte so zu verstehen sein, dass die beiden gefundenen Feinschichten eine geschlossene Schleife bilden.

Die granuläre Randschicht kann, wie in Abb. 5 links oben, zahlreiche Lamellen enthalten, die an den Enden verbunden sind und teilweise eine konzentrische Anordnung bilden.

Abb. 4 hält ein lichtmikroskopisch bekanntes Phänomen [102, 119, 64] fest. Oft liegen in den Zellen langgestreckte eingeschnürte Chloroplasten von

biskuitförmigem Aussehen mit einer lichtmikroskopisch helleren Zone. Besonders interessiert die Einschnürungsstelle rechts im Bild. Die Chloroplastenmembran und die Randschicht gehören beiden Plastidenteilen an. Die Einschnürung setzt sich scharf in den Chloroplastenschichten ab. Einzelne Stromalamellen und die im Bild oberste Chloroplastenschicht verbinden die beiden Teile der weitgehend unabhängigen Lamellensysteme. Es ist bekannt, dass diese Plastidenformen zu einer Chloroplastenteilung führen können, aber auch häufig lange Zeit in diesem Zustand weiterbestehen. Abb. 4 spricht dafür, dass eine Teilung ausdifferenzierter Gerstenchloroplasten durch Einschnürung auf ähnliche Weise verläuft, wie es für die *Fucus*-Chromatophoren beschrieben ist [161], d.h. durch Einbuchtung der Schichten und nachfolgende Querteilung.

Abschliessend sei untersucht, wieviel Grana ein Gerstenchloroplast enthält. Dazu sind in Tabelle II einige Werte gesammelt. Diese sind nach steigender Chloroplastenschnittfläche, die mit der Ellipsoidformel erhalten wurde, angeordnet. In der letzten Kolonne sind die per Schnitt gezählten Grana angegeben. Im Grossen und Ganzen steigt gemäss der Erwartung die

Tabelle II

Die Fläche von Chloroplastenschnitten und Anzahl der Grana per Schnitt in stärkefreien und stärkehaltigen Chloroplasten der Gerste.

Länge und Dicke (μ)	Schnittfläche (μ^2)	Anzahl Grana
1. Stärkefreie Chloroplasten		
2,7 × 0,8	1,70	20
3,2 × 0,9	2,26	24
2,8 × 1,2	2,64	27
3,1 × 1,4	3,41	27
3,5 × 1,3	3,57	36
3,3 × 1,4	3,63	19
3,5 × 1,6	4,40	34
4,4 × 1,6	5,53	36
4,9 × 1,9	7,31	47
5,4 × 2,0	8,48	39
2. Stärkehaltige Chloroplasten		
3,5 × 1,1	3,02	33
3,8 × 1,2	3,58	41
4,8 × 1,6	6,03	42
4,9 × 1,6	6,15	42

Granaanzahl mit zunehmender Schnittfläche. Schnitte mit 34–47 Grana dürften als Medianschnitte gelten. Die meisten Schnitte, die Stärke enthalten, fallen in diese Gruppe. Stärke wird mit anderen Worten vor allem in der Mitte des Chloroplasten abgelagert.

Ein Medianschnitt des Gerstenchloroplasten enthält somit ca 40 Grana und bei durchschnittlich 8 Plastidenschichten (S. 435) entfallen 5 Grana auf eine längsgeschnittene Schicht. Der Gerstenchloroplast ist linsenförmig und eine Chloroplastenschicht kann hier schematisch als eine Kreisfläche mit einem Durchmesser von 5 μ angenommen werden. Auf einer solchen Chloroplastenschicht haben 20–25 Grana Platz und wir erhalten für den ganzen Gerstenchloroplasten im 10 cm langen Primärblatt eine Gesamtzahl von 160–200 Grana.

Die Entwicklung der Gerstenchloroplasten

Im mittleren Teil 3–4 mm langer Sekundärblätter erhält man Übersichtsbilder wie Abb. 24. Die Zellen enthalten bereits eine grosse Vakuole und in dem dünnen Plasmabelag entlang der Zellwand liegen eine grosse Zahl im Schnitt rundlicher und ovaler Organellen. Es sei mit diesen Zellen begonnen, da hier eine Unterscheidung der Proplastiden von den übrigen Zellbestandteilen möglich ist. Die in Abb. 24 vorhandenen Partikel können nach morphologischen Gesichtspunkten in 4 Gruppen eingeteilt werden (1–4 der Abb.):

1. Diese Partikel mit 0,3–0,6 μ Durchmesser zeichnen sich durch ihre Homogenität und Kugelform aus. Sie wurden schon im vorigen Abschnitt in älteren Zellen erwähnt. Abb. 28–30 gibt eine Vorstellung über ihre Variabilität im Aussehen. Entweder erscheinen sie homogen geschwärzt (Abb. 28) oder mit einer deutlichen dunklen Randzone und einem Kern von elektronenoptisch geringerer Dichte (Abb. 29 und 30). Die scheinbare Strukturierung in Abb. 30 beruht wohl auf übergelagertem Plasma. Die starke Schwärzung und insbesondere die zuweilen auftretende Randschicht legt nahe, dass der starke Kontrast dieser Partikel eine Folge der Osmiumreaktion ist und deutet auf starken Lipoidgehalt. In der Vakuole finden sich ähnliche Einschlüsse (Abb. 24, 25), sie sind jedoch oft grösser und von unregelmässiger Form (Abb. 27). Sie dürften nicht vollständig homogen sein.

2. Die Proplastiden dieses Stadiums sind durch ihre Grösse, ihre langgestreckte Form mit einzelnen Pseudopodien, durch das Plastidenzentrum und eine beginnende Lamellenbildung gekennzeichnet.

Die beiden restlichen Organellen sind von gleicher Form — im Schnitt rundlich oder oval — und von gleicher Grösse mit 0,4–0,8 μ im Durchmesser. Beide sind von einer zuweilen doppelten Membran umgeben. Sie unter-

scheiden sich durch ihr Vermögen zur Elektronenstreuung und ihre innere Struktur:

3. Dieses Organell fällt durch seine starke Schwärzung und hohe Dichte in den Mikrogrammen auf. Seine Struktur weist zwei Elemente auf, ein granuläres und ein retikuläres System. Die grösseren dieser Körper unterscheiden sich von den Proplastiden nur durch das Fehlen eines Zentrums und gestreckter Lamellen.

4. Im Gegensatz dazu sind die Organellen dieser Gruppe locker strukturiert und besitzen von der Membran nach innen laufende Septen. Sie enthalten bereits die Mitochondrienstruktur, wie sie uns in den älteren Zellen entgegentritt (Abb. 41–45).

Geht man einen Schritt zurück und betrachtet die Zellen 1–2 mm langer farbloser Blättchen, so enthalten diese Zellen 1–3 kleinere Vakuolen und demzufolge an einigen Stellen einen wesentlich breiteren Wandbelag des Plasmas. Die typisch embryonale Plasmastruktur wird sichtbar (Abb. 25–26). Sie fällt gegenüber dem Plasma der eben betrachteten älteren Zellen durch ihre grosse Dichte auf, wie ein Vergleich der Abb. 25 und 26 mit Abb. 24 zeigt. (Dabei unterschreitet die Schnittdicke der Abb. 25, 26 die der Abb. 24.) Das embryonale Plasma ist durch eine doppelte Schicht, den Tonoplasten, mit einem Durchmesser von ca 300 Å gegen die Vakuole abgegrenzt. In den Mikrogrammen ist jede einzelne der beiden Schichten durch eine deutliche und fast regelmässige Punktierung ausgezeichnet (Abb. 26, links). Die Randschicht ist als ein geordnetes Netzwerk von Fibrillen oder von Strängen aus globulären Teilchen in zwei Schichten aufzufassen, wobei die kontrastreichen „Punkte" Querschnitte von Fibrillen mit ca 100 ± 20 Å Durchmesser darstellen. Die Zellwände bestehen bekanntlich aus einer solchen Fibrillentextur und im Schnitt ergibt sich gerade das Bild, wie es auch der Tonoplast zeigt, insbesondere wenn man ihn mit der doppelten Mittellamelle vergleicht (Abb. 25). Die Zellulosefibrillen der Wand sind von geringerem Kontrast als die Fibrillen der Plasma-Randschicht. In die Vakuole vorspringende Plasmastränge sind vom Tonoplasten umgeben (Abb. 25).

Von besonderem Interesse ist, ob die Tonoplastenstruktur auch an der Berührungsstelle von Plasma und Zellwand, das Plasmalemma, vorhanden ist (vgl. hierzu die Diskussion bei Frey-Wyssling [36] und dort cit. Lit.). Liegt das Plasma direkt der Zellwand an, so ist das der Fall (Abb. 25 rechts unten). Ist das Plasma durch die Fixierung von der Wand abgelöst, so bleibt das Plasmalemma an der Zellwand hängen (Abb. 25 und 26). In diesem Fall scheint das Plasma von einer durchgehenden Membran begrenzt. Da diese bei dem Plasma, das der Wand eng anliegt, fehlt, dürfte sie als ein

Artefakt aufzufassen sein. Die beobachtete geordnete Fibrillenstruktur des Plasmalemmas scheint geeignet, der entstehenden und wachsenden Zellwand die Mizellierungsrichtung aufzuprägen [17, 117].

Das dichte Plasma erscheint als ein kompliziertes Maschenwerk fibrillärer Elemente und im Gegensatz zum Tonoplasten nicht geordnet, d.h. mit einer vielgestaltigen Variation der Zwischenräume und zahlreichen verschiedenen „Vakuol"-Systemen. Teilweise haften die fibrillären Elemente direkt dem Tonoplasten in senkrechter Richtung an (vgl. [7]). Die kürzeren oder längeren in verschiedener Weise gefalteten Fibrillen mit einem durchschnittlichen Durchmesser von 60–120 Å erwecken teilweise den Eindruck einer Spiralisierung (z.B. Pfeil in Abb. 26). Oft laufen Fibrillen (oder Lamellen) ein längeres Stück parallel und bilden zumindest einseitig geschlossene Stränge oder Schichten (vgl. auch Abb. 71), die durch eine Masse elektronenoptisch geringer Dichte getrennt sind. Globuläre Einzelteilchen der Grössenordnung um 100 Å sind von quer geschnittenen Fibrillen nicht zu unterscheiden, daher ist über ihre Existenz oder Verteilung nichts auszusagen.

In diesen jungen Blattmeristemzellen sind ebenfalls 4 Partikel vom Plasma abgegrenzt. Die in der obigen Aufzählung unter (1) genannten homogenen Partikel mit 0,3–0,6 μ sind auch in diesen meristematischen Zellen nachweisbar, ebenso wie die unregelmässigen solchen gleicher Dichte in der Vakuole.

Das unter (3) aufgeführte stark elektronenstreuende Organell mit dichter granulärer und retikulärer Struktur ist wieder zu erkennen (Abb. 26, oben links).

Ein weiteres Organell (Abb. 26, 37, 38, 39) zeichnet sich durch seine grossen „Vakuolen" aus. Es ist von einer doppelten Membran umgeben. Die Vakuolen sind durch eine 60–80 Å dicke Schicht begrenzt. Oft ist die Begrenzung nicht vollständig geschlossen, sondern eine durchgehende Membran bildet im Innern des Organells finger- bis blasenförmige Ausstülpungen. Es liegt nahe, diese Membranfalten mit den Septen der Mitochondrien in Verbindung zu setzen (Abb. 41–45). Diese sind allerdings dünner (40–60 Å). Auf der anderen Seite zeigt das rechte Mitochondrion der Abb. 45 im Innern eine durchgehend gefaltete Membran.

Schliesslich tritt ein Organell mit unregelmässiger Form und langen und schmalen Fortsätzen auf (Abb. 26). Seine innere Struktur entspricht auffallend dem des Grundplasmas. Die 120–140 Å dicke Membran bildet einen langen, umgebogenen Fortsatz. Dieser Fortsatz besteht im grössten Teil seiner Länge nur aus den parallelen Membranteilen, die durch einen Zwischenraum von 120–250 Å mit granulärer Substanz getrennt sind.

An zwei Stellen ist dieser Fortsatz erweitert. Die Erweiterung am Ende ist interessant. Ihre innere Struktur entspricht dem seitlich anliegenden Organell mit den grossen „Vakuolen" und gefalteten Membranen.

Es ist möglich, dass diese Gebilde ein frühes Stadium der lichtmikroskopisch festgestellten „Proplastiden" mit amöboidförmiger Gestalt in den Meristemen höherer Pflanzen darstellen.

Zusammenfassend lässt sich über den Inhalt dieser jüngsten untersuchten Blattmeristemzellen folgendes sagen: Die Partikel — abgesehen von den stark elektronenstreuenden — sind vom Grundplasma strukturell in Schnitten nicht einwandfrei zu unterscheiden. Lediglich die Abgrenzung durch eine Membran gibt uns ihre Existenz zu erkennen. Ob alle, ein oder zwei aus dem Plasma kondensiert werden können oder ob sie submikroskopisch kontinuierliche Systeme darstellen, sowie ihre ontogenetischen Beziehungen untereinander und zu den in älteren Meristemzellen charakterisierbaren Mitochondrien und Proplastiden muss in einer gesonderten Arbeit untersucht werden. Ein Zentrum, das die Proplastiden auszeichnen kann, wurde bisher in den jüngsten Blattmeristemzellen der Gerste nicht beobachtet. Ebenso enthält keines der Partikel Stärke. Weiter enthält keines der Partikel die für den ausdifferenzierten Gerstenchloroplasten kennzeichnenden parallelen Schichten, Lamellen oder Grana.

Wir sind daher einstweilen auf eine rein morphologische Beschreibung der Partikel in den Blattmeristemen angewiesen. Zum Abschluss sei in Abb. 27–45 eine Übersicht gegeben.

Abb. 27–30 stellt die homogenen Typen dar (S. 442). Sie sind von den jüngsten Blattmeristemzellen bis zu den ausdifferenzierten Assimilationsgeweben vorhanden.

Abb. 41–45 gibt typische Mitochondrien der Gerste mit den von der Membran mehr oder weniger radiär verlaufenden Cristae mitochondriales [109, 110, 139, 123, 47] wieder. Diese bestehen aus Doppellamellen, die im innern des Mitochondriums geschlossen sind. Eine zentrale Verbindung der Bereiche zwischen den Doppellamellen erscheint aus den Bildern wahrscheinlich. Die Form der Gerstenmitochondrien ist rundlich bis länglich. Auch in länglichen Schnitten sind die Doppellamellen radiär gestellt (Abb. 41, Mitte). Diese Struktur der Mitochondrien wurde von den älteren Blattmeristemzellen bis in die ausdifferenzierten Gewebe gefunden.

Nur in den jüngsten Zellen finden sich die Organellen der Abb. 37–39, deren weitere Entwicklung einstweilen unbekannt ist.

Abb. 31–36 gibt die dichten, stark elektronenstreuenden Organellen wieder, die von den jüngsten untersuchten meristematischen Zellen bis zu

solchen mit ausdifferenzierten Chloroplasten gefunden werden können. Sie wechseln stark an Form und Grösse. Sie erreichen in dem dargestellten Strukturzustand in älteren Meristemzellen Grössen von über 1 μ Durchmesser und übertreffen damit ausdifferenzierte Mitochondrien. Zusätzlich zeigen sie teilweise ausgeprägte amöboide Fortsätze (Abb. 35–36). Die grösseren von ihnen entwickeln sich offenbar zu Chloroplasten. Die zunächst gleichmässig retikulär-granuläre Struktur nimmt die Form gewundener Fibrillen oder Membranen bzw. Kanäle an.

Abb. 40 ist ein Fall, dessen Einordnung nicht leicht ist. Am ehesten stellt dies ein Proplastidstadium mit beginnender Bildung des Plastidenzentrums und einzelnen von ihm ausgehenden Ausbuchtungen (rechts im Bild) dar.

In Plastiden mit einem Durchmesser von 1 μ beginnt das Plastidenzentrum aufzutreten, umgeben von einer Region geringerer Dichte (Abb. 46 und 47). (Der Name Plastidenzentrum sei hier dem Ausdruck „Primärgranum" vorgezogen, da es strukturell nicht den Chloroplastengrana entspricht; vgl. [88, 148, 163].) Das Plastidenzentrum kann entweder sehr dicht und fast homogen erscheinen (Abb. 46, 51 und 52) oder lockerer strukturiert und dann netzgitterartig (Abb. 47, 48, 55 und 58) sein. Besonders klar konnte seine Struktur in der *xantha*-3-Mutante gefasst werden (Abb. 78 und 82). Es scheint aus in allen Richtungen gefalteten Membranen zu bestehen. Offenbar ist das Plastidenzentrum zunächst kugelförmig, da es im Schnitt immer mehr oder weniger rund begrenzt erscheint. Die Lage des Plastidenzentrums ist in vielen Fällen median (Abb. 46–48, 51 und 55), in anderen aber einseitig am Ende der Plastiden wie in Abb. 52, 54 und 56. Diese einseitige Lage mag durch Streckung der zuerst entwickelten Chloroplastenschichten erfolgen, da sie — soweit gesehen — erst hervortritt, wenn bereits einige Schichten gebildet sind. Eine solche Verlagerung des Zentrums ist in den *albina*- und *xantha*-Mutationen, in denen eine Bildung der Chloroplastenschichten unterbleibt, nicht zu bemerken, sondern die Lage bleibt dort median.

Solange nur einzelne Schichten in den Plastiden vorhanden sind, besitzen die Proplastiden amöboide Formen (Abb. 46–48). In diesem Stadium können sie mit ein bis mehreren Stärkekörnern angefüllt sein (Abb. 53). In den stärkehaltigen Proplastiden ist zuweilen das Plastidenzentrum und eine Lamellierung nachweisbar. Mit zunehmender Bildung der Lamellen wird die Stärke abgebaut (Abb. 53, rechts).

Im Plastidenzentrum dürfte das Material angesammelt werden, aus dem die ersten Chloroplastenschichten aufgebaut werden. In Abb. 47 ist das Zentrum durch 100–150 Å dicke gefaltete Schichten oder Membranen ausge-

zeichnet. Je zwei dieser Membranen bilden am äusseren Rand fingerartige geschlossene Ausfaltungen. Zwischen diesen Membranen befindet sich statistisch homogen verteilt eine granuläre Substanz, deren Teilchen den gleichen Durchmesser wie die Membranen besitzen. Dies gibt dem Zentrum seine netzgitterartige Struktur. Eine direkt kristalline Anordnung [65, 89] konnte bisher in diesem Material nicht gefunden werden. Sie scheint aber durch eine vollkommene Streckung der Membranen verständlich.

Abb. 48–51 zeigt die radiäre Ausstrahlung der Chloroplastenschichten aus dem Zentrum. Gleichzeitig treten auch die Globuli hervor. Sehr rasch beginnt eine Differenzierung der Schichten, indem sie in feine Lamellen unterteilt sind.

Einen genaueren Aufschluss über die Vorgänge gibt Abb. 54–58. In Abb. 54 erkennt man auf der rechten Seite die fingerartigen Ausstülpungen, während links die einzelnen Schichten bereits eine Differenzierung in Lamellen zeigen. So eine fingerartige Ausstülpung mit einem Durchmesser von 500–700 Å ist durch eine äussere Membran gekennzeichnet, die homogenes Material umschliesst. Diese Membranen entsprechen vermutlich denen, die zuerst im Plastidenzentrum zu sehen sind. Die ausgestülpten Schichten, im Schnitt an einer Seite 4–6 an der Zahl, lockern sich auf und gleichzeitig nimmt das Proplastid an Grösse zu (Abb. 55, 56 und 57). Die ursprünglichen Membranen des Zentrums und der Ausstülpungen sind dann nicht mehr durchgehend zu verfolgen, vielmehr tritt an den Schichten lokal eine Vermehrung einzelner Lamellen ein. Diese neu entstandenen Lamellen sind jeweils paarweise verbunden (Abb. 48, 51, 55–57). Sie sind von sehr unterschiedlicher Dicke und eine wiederholte Aufspaltung dickerer in feinere Lamellen scheint stattzufinden.

In Abb. 57 kann dieser Prozess untersucht werden. Das Plastidenzentrum ist median. Von ihm gehen radiär die einzelnen Chloroplastenschichten aus. In letzteren liegen einzelne Lamellenpakete aus paaarweise verbundenen Lamellen von ca. 100 Å Durchmesser. In Abb. 58, einem stärker vergrösserten Ausschnitt sieht man, dass die Lamellen geteilt und verzweigt sind, d.h. sie spalten sich in verschiedener Weise dichotom auf. Das Plastidenzentrum ist relativ locker und gleicht strukturell der Grundsubstanz der von ihm ausgehenden Plastidenschichten mit granulären Elementen und gefalteten Lamellenstücken.

Ein etwas fortgeschritteneres Stadium ist in Abb. 62 festgehalten. Die ausgefalteten Chloroplastenschichten sind nunmehr über grössere Bereiche durchgehend lamelliert und bestehen aus 4–10 Lamellen. Zunächst fällt auf, dass zwei Chloroplastenschichten am Ende verbunden sind, während die

übrigen frei münden, wobei aber die einzelnen Lamellen dieser Schichten untereinander paarweise verbunden sind. Das mag darauf hindeuten, dass eine Ausfaltung des Zentrums auch unmittelbar zu zwei Chloroplastenschichten führen kann. Freie Lamellenenden können während der ganzen Entwicklung nicht nachgewiesen werden.

Rechts aussen im Bild ist eine typische Stelle der Lamellenbildung, wie sie schon in den vorigen Bildern auftrat. Die darin zu erkennenden Einzelheiten sind in der eingefällten Zeichnung schematisiert. Solche Stellen lokaler Lamellenvermehrung sind 0,1–0,3 μ lang. Die einzelnen Lamellenstücke sind verschieden dick und auch innerhalb eines Lamellenstückes sind Verdickungen ausgeprägt. Diese Verdickungen spalten offenbar auf und es entstehen zwei getrennte neue Lamellen. Die Verdickung und Spaltung erfolgt gleichzeitig an mehreren Stellen, was dazu führt, dass schliesslich die Lamellen nur noch an wenigen Punkten zusammenhalten. An den Enden sind die Lamellen untereinander verbunden, so dass alle Lamellen einer zusammenhängenden Schicht aus einer einzelnen Lamelle durch diesen Prozess der Verdickung und Spaltung entstanden gedacht werden können. Auch ist zu bemerken, dass die Lamellenvermehrung gleichzeitig in verschiedenen Ordnungen verläuft. Besonders deutlich wird das in der Mitte der Zeichnung, wo zwei Lamellen durch ein breites homogenes Stück verbunden sind und die eine Tochterlamelle bereits wieder eine beginnende Spaltung zeigt.

Die einzelnen Pakete von Lamellenstücken wachsen in die Länge, sei es durch Streckung oder Einlagerung neuer Substanz, bis sie sich berühren. Dann dürfte eine Verschmelzung eintreten, so dass ein durchgehendes Lamellensystem entsteht.

In Abb. 63 ist das weitgehend erfolgt. Das Zentrum mit mehreren Globuli ist geringer ausgeprägt und die strahlenförmige Anordnung der Schichten und Lamellen beginnt einer parallelen Ordnung Platz zu machen. Gleichzeitig setzt die Vermehrung der Lamellen und auch Schichten fort.

Der Chloroplast in Abb. 65 zeigt eine im Ganzen durchgehende und parallele Lamellierung. Wenn auch an einzelnen Stellen noch mehrere Lamellen vereinigt und nicht durchgehend gespalten sind, fällt doch die einheitliche Dicke der Lamellen von 50 ± 20 Å auf. Am Chloroplastenende sind die gleichwertigen Lamellen zu zwei und zwei geschlossen. Das Plastidenzentrum ist verschwunden. Abb. 66 stellt die Verbindung zwischen den Plastidenstadien von Abb. 56, 57, 62 mit denen der Abb. 65 her. Grosse Bereiche sind streng parallel lamelliert, wie am rechten Ende, während in anderen die Vermehrung und das Flächenwachstum der Lamellen noch in

vollem Gange ist. Aus diesem Chloroplasten wurde Abb. 59 mit einem gut orientierten Lamellenbereich herausvergrössert, und Abb. 60 und 61 zeigen im Gegensatz dazu Einzelheiten sich verzweigender und wachsender Lamellen. An verschiedenen Stellen lässt sich auch die Berührung zweier in sich geschlossener Lamellenpaare finden, was die geforderte Verschmelzung bedeuten kann.

Die Plastiden nehmen in diesem Stadium auch ihre typische Linsenform an. Dies verursacht eine gewisse Streckung in Richtung der Lamellenebene und mag zu der streng parallelen Orientierung der Lamellen beitragen.

Auch ein etwas gequollener Chloroplast dieser Stadien in Abb. 67 macht die durchgehenden Chloroplastenschichten und Lamellen mit einzelnen Verzweigungen bzw. Aufspaltungen anschaulich.

Erst in diesen Stadien beginnt an voneinander unabhängigen Stellen der Schichten eine Differenzierung in Granabereiche und Stromalamellen aufzutreten (Abb. 63, 68–70). Sie dürfte durch Einlagerung von Material erfolgen; denn nun beginnen einzelne Bereiche kontrastreicher hervorzutreten und das für den ausdifferenzierten Chloroplasten typische Verhältnis von 2:1 der Grana- und Stromalamellen wird an verschiedenen Stellen sichtbar (Pfeile in Abb. 63, 68–70). Aus der ausdifferenzierten Struktur wissen wir, dass die Lamellen im Granabereich sich einmal mehr „teilen" müssen. Man könnte versucht sein, die lokalen Vermehrungsstellen der Lamellen, die als kontrastreiche Pakete der Schichten in Proplastiden hervortreten (Abb. 54–58 und 62), als Grana zu bezeichnen. Sie haben in diesem Fall nur einen grösseren Kontrast mit den Grana des ausdifferenzierten Chloroplasten gemein. Es scheint mir schwer verständlich, diese Bereiche mit den Grana gleichzusetzen; denn wo blieben die Grana dann im Stadium der durchgehenden Lamellierung wie in Abb. 65 und 67?

Eine andere Beobachtung spricht ebenfalls dafür, dass die Grana erst nach dem Stadium der durchgehenden Lamellierung entstehen. Wir haben beim ausdifferenzierten Chloroplasten von der netzartigen Verbindung der Chloroplastenschichten durch Stromalamellen gesprochen. Die Bereiche der Lamellenbildung liegen in voneinander getrennten Chloroplastenschichten. Gerade der Zustand der durchgehenden parallelen Lamellierung lässt durch Einlagerung von Substanz auch eine „Zusammenfassung" von Lamellen verschiedener Chloroplastenschichten zu. Dadurch kann das typische Bild der Grana in den Chloroplastenschichten mit der netzartigen Verbindung der Stromalamellen entstehen.

Schliesslich bleibt noch das Auftreten der Globuli zu besprechen. Sie werden zuerst im oder um das Plastidenzentrum gebildet und zwar auf einem

relativ frühen Stadium (Abb. 48, 49, 52). Vereinzelt mögen sie vor der Anwesenheit eines Plastidenzentrums vorhanden sein (Abb. 26). Später liegen die Globuli auch zwischen den Plastidenschichten (Abb. 54, 55, 56, 57). Ob sie vom Plastidenzentrum dorthin verfrachtet oder in der Chloroplastengrundsubstanz gebildet werden, ist vorerst nicht zu entscheiden. Besonders zahlreich treten die Globuli im Zusammenhang mit der intensiven Schlussphase der Lamellenbildung (Abb. 64) und einer beginnenden Granadifferenzierung (Abb. 63) auf. Abb. 64 ist im Zusammenhang mit der Mutantenanalyse (S. 453) von Interesse, da es die grösste Menge Globuli zeigt, die in einem normalen Chloroplastenschnitt der Gerste gefunden wurde. Die kugelförmigen Globuli haben einen Durchmesser von 500–800 Å.

Es wurde versucht, ein Bild der Entwicklung des Gerstenchloroplasten auf der Grundlage der submikroskopischen Morphologie verschieden alter Stadien zu zeichnen. Das Bild ist nicht vollständig und zahlreiche Einzelheiten bleiben ungeklärt. Einige Prozesse, die aus den Makromolekülen der ersten Proplastidstadien Schichten, Lamellen und Feinlamellen aufbauen, sind erkennbar. Das Bild mag aber hinreichend sein, um eine Analyse der Chlorophyllmutanten anzugehen.

Zusammenfassend kann die Differenzierung der Gerstenchloroplasten aus den jüngsten Proplastiden folgendermassen dargestellt werden:

1. Im undifferenzierten Proplastid bildet sich das Plastidenzentrum.
2. Zahlreiche Stärkekörner treten in den Proplastiden auf.
3. Aus dem Plastidenzentrum wird das Material für den Aufbau der Chloroplastenschichten radiär ausgefaltet, worauf eine rasche Auflokkerung der Ausfaltungen erfolgt.
4. In den Chloroplastenschichten werden die ersten Lamellenstücke lokal begrenzt und an verschiedenen Stellen gleichzeitig aufgebaut.
5. Es erfolgt eine intensive Vermehrung der Lamellenstücke durch Verdickung und Spaltung.
6. Die stets zumindest paarweise verbundenen Lamellenstücke dehnen sich radial aus, bis sie aneinanderstossen.
7. Die Lamellenstücke verschmelzen und eine durchgehende parallele Lamellierung des Plastids wird hergestellt. Das Plastidenzentrum verschwindet.
8. Die Schichten des Chloroplasten vermehren sich durch Aufteilung.
9. Die Granabereiche werden durch Substanzeinlagerung und eine weitere Aufspaltung der Lamellen differenziert.

10. Während der ganzen Entwicklung sind die Globuli vorhanden. Sie treten zuerst im Plastidenzentrum auf und werden am Ende der Entwicklung häufiger.

Drei Mechanismen scheinen für die Entstehung der Chloroplastenschichten und Lamellen notwendig zu sein: Ausfaltung, Verdickung und Spaltung, sowie Verschmelzung und Querteilung. Es sind dieselben Prozesse, wie sie für die Vermehrung und Teilung der Chromatophorenschichten von *Fucus* gefunden wurden [161]. Beachtenswert scheint mir, dass die durchgehenden Lamellen aus Teilstücken makromolekulärer Grösse aufgebaut werden.

Die angeführte Reihenfolge der verschiedenen Entwicklungsschritte ist nur prinzipiell. Vielfach laufen mehrere dieser Schritte an verschiedenen Stellen im Chloroplasten gleichzeitig ab, wie das bei der Besprechung der Abbildungen hervorgehoben wurde. Eine Teilung der Plastiden während des Aufbaues der lamellaren Organisation konnte bisher nicht beobachtet werden.

Die Plastiden der Mutante albina-49/1117/29

Die Ergebnisse dieser *albina*-Mutante sind in den Abbildungen 71–77 zusammengefasst. Die jüngsten Stadien der Proplastiden (Abb. 72) entsprechen denen normaler Pflanzen. Eine Differenzierung eines Plastidenzentrums ist noch nicht erkennbar. Ein Übersichtsbild einer Zelle aus einem 5 mm langen Sekundärblatt ist in Abb. 71 dargestellt. Die mit *P* bezeichneten Proplastiden sind durch eine doppelte Membran vom Plasma abgegrenzt. Ihre Struktur ist in den jüngsten Stadien kompakt und dicht (oben rechts). Die älteren amöboidartigen Proplastiden sind durch eine Auflockerung ihrer Struktur gekennzeichnet. In einzelnen Plastiden ist das Zentrum erkennbar und einzelne Globuli liegen im bzw. am Plastidenzentrum. Auch Mitochondrien mit ihrer typischen inneren Struktur sind vorhanden.

Abb. 73–76 zeigt einzelne Plastiden verschiedenen Alters. Überall erkennt man die umgebende doppelte Membran und das Plastidenzentrum mit seiner in allen Richtungen gefalteten Membranstruktur. Ein Ausfalten der Chloroplastenschichten und eine Bildung von Lamellen findet nicht statt. Die Globuli sind stets in diesen älteren Stadien vorhanden.

Einlagerung von Stärke, charakteristisch für normale Proplastiden, konnte nicht beobachtet werden.

Offenbar können die Plastiden, trotz fehlender Differenzierung ihrer Innenstruktur, ein beträchtliches Wachstum ausführen. In Primärblättern (Abb. 77) erreichen sie eine Grösse von $3 \times 0{,}8\ \mu$. Das entspricht den klein-

sten voll ausdifferenzierten Chloroplasten (S. 434). Ihre innere Struktur besteht in diesem Stadium aus statistisch homogen verteiltem Material mit teilweise retikulärer Anordnung. Eine geordnete Struktur ist nicht erkennbar. Eine Vakuolisierung der Plastiden, so kennzeichnend für einige Plastidommutanten (vgl. [151]), ist nicht beobachtet worden. Beim Absterben der Zellen scheinen die Plastiden einfach zu zerfallen.

Lichtmikroskopisch sind die Plastiden in den Primärblättern homogen und farblos, lediglich die Chloroplastenwand kann unterschieden werden. Die Proplastiden der sekundären Blätter in den *albina*-Mutanten zeigen eine gelbgrünliche Färbung im Lichtmikroskop, was für die Anwesenheit von geringen Mengen Chlorophyll im Plastidenzentrum und den Globuli spricht.

Offensichtlich verhindert die Genveränderung in dieser Chlorophyll-Letalen das Ausfalten der Plastidenschichten aus dem Plastidenzentrum und die Bildung von Lamellen. Es wird von Interesse sein, zu untersuchen, ob dies auf der Unmöglichkeit der Synthese eines Stoffes beruht oder ob, trotz Anwesenheit aller normal vorkommender Baustoffe, die unterbleibende Differenzierung durch einen Defekt der Orientierung und Bindung von Makromolekülen verursacht ist.

Die Untersuchung anderer *albina*-Mutanten ist vor allem mit einem Ziele begonnen: Gibt es solche, deren Plastidenentwicklung vor der Bildung des Zentrums unterbrochen ist? Dies würde einen Beweis für die Bildung des Plastidenzentrums geben.

Wir können aus der Analyse der *albina*-Mutante schliessen, dass das Grössenwachstum der Chloroplasten weitgehend unabhängig von der inneren Differenzierung ist, wenn auch in diesem Fall eine voll normale Grösse knapp erreicht wird.

Der Plastidenformwechsel der Mutante xantha-3

Der Formwechsel der Plastiden dieser Chlorophyll-Letalen ist in Abb. 78–85 dargestellt. Die Entwicklung der ersten Proplastidstadien entspricht der normalen Entwicklung. Wir beginnen beim Stadium mit dem Plastidenzentrum (Abb. 78). Es ist besonders scharf abgegrenzt und seine innere Struktur — im Schnitt unregelmässig netzartig — ist im Raum, wie schon genannt, wahrscheinlich ein System von in allen Richtungen gefalteten Membranen.

In einzelnen, allerdings nur selten beobachteten Plastidenstadien treten gut orientierte und paarweise geschlossene Schichten auf (Abb. 80 und 81). Sie zeigen einen Durchmesser von ca. 150 Å. Es handelt sich jedenfalls

um die ausgefalteten Schichten des Plastidenzentrums. Letzteres ist in den Mikrogrammen 80 und 81 an der mit Pfeil markierten Stelle in der Mitte der Plastide zu suchen. In diesen Schichten findet man in der normalen Entwicklung, lokal begrenzt, die Lamellenbildung. Sie kann in der *xantha*-Mutante nicht erfolgen. Stattdessen liegen an den Stellen der Lamellenbildung elektronenoptisch homogene und kontrastreiche längliche Pakete (Abb. 78 und 81). In Abb. 81 ist eine „Verklebung" der Schichten durch ein solches Paket homogener Masse erkennbar. Einzelne kleinere Klumpen umschliessen auch die Schichten. Diese Masse gleicht in ihrem elektronenoptischen Verhalten auffallend den Globuli (Abb. 78, 82). Man hat den Eindruck, dass die Masse das Material darstellt, aus dem die Lamellen in den Chloroplastenschichten aufgebaut werden sollten. Die Funktion dieses Materials ist in der Mutante nicht möglich. Wir haben bei der normalen Entwicklung gesehen, dass die Chloroplastenschichten sich auflockern und dann ihre begrenzenden Membranen, die aus dem Plastidenzentrum ausgefaltet wurden, nicht mehr durchgehend erkennbar sind (vergl. auch [90]). Daraus wird verständlich, dass die Schichten der Abb. 80 und 81 verschwinden und dann nicht mehr in der Plastide erkennbar sind. Demnach stellt auch Abb. 78 ein späteres Stadium dar als es auf den ersten Blick vortäuscht. Die ursprünglich ausgefalteten Schichten sind aufgelockert und nicht mehr von der Grundsubstanz der Plastiden unterscheidbar. Nur die dunklen Massen des Materials für den Lamellenaufbau liegen um das Plastidenzentrum.

Das Plastidenzentrum mit seiner ursprünglichen Organisation bleibt in der *xantha*-Mutante im Verhältnis zur Plastidengrösse lange erhalten (Abb. 78 und 82).

Das Auffallendste an den Mutantenplastiden aber ist die enorme Anhäufung der Globuli zunächst um das Plastidenzentrum (Abb. 82). Schliesslich füllen sie fast die ganze Plastide aus (Abb. 83).

Die Globuli sind Kugeln; denn sie sehen immer mehr oder weniger kreisrund aus (vgl. auch Abb. 79). Sie liegen dicht übereinander und wechseln im Durchmesser von 500–1400 Å, wenn die kleinsten Durchmesser als Anschnitte unberücksichtigt bleiben. Die grosse Variation ist in Abb. 83 erkennbar und diese Abbildung demonstriert zugleich an den verschiedentlich übereinander liegenden Globuli die grosse Tiefenschärfe des Elektronenmikroskopes. Eine solch grosse Menge von Globuli konnte in normalen Chloroplasten und Proplastiden nie aufgefunden werden. Die grösste Anzahl in den untersuchten normalen Plastiden ist in Abb. 64 zum Vergleich aufgenommen. Daraus geht auch hervor, dass die Globuli der Mutante einen grösseren Durchmesser zu erreichen scheinen als die der normalen Plastiden.

Die Globuli liegen in einer retikulären Grundsubstanz der Plastide eingebettet. Abb. 79 gibt einen extrem dünnen Schnitt wieder. Man erkennt zwischen und um die Globuli unregelmässig gefaltete und teilweise geschlossene Membranstücke. Die Globuli sind vielleicht homogene einheitliche Riesenmoleküle. Man könnte erwarten, dass sie sich zu grösseren mikroskopischen „Tropfen" zusammenschliessen. Das erfolgt aber offenbar nicht. Sie behalten ihre submikroskopische Grösse, wie dicht sie auch zueinander liegen mögen.

Die Plastiden der Primärblätter erreichen trotz der abgebrochenen inneren Differenzierung eine normale Grösse von 3–5 μ Länge (Abb. 84 und 85). Die Struktur dieser Plastiden ist ungeordnet. Die Globuli liegen weit verstreut in der Plastidensubstanz und sind weniger an Zahl. Sie scheinen teilweise abgebaut; denn sie sind nun bedeutend kleiner. Die grössten zu messenden Durchmesser liegen nun unter 500 Å. Sie sind weiter elektronenoptisch von geringerer Dichte. Das Plastidenzentrum ist verschwunden. Die Plastidensubstanz ist locker retikulär. Eine Vakuolisierung der älteren Plastiden konnte auch in dieser Chlorophyll-Letalen nicht beobachtet werden.

Die Stadien der Abb. 82 und 83 sowie die der Abb. 84 und 85 wurden lichtmikroskopisch im lebenden Zustand untersucht. Die ausgewachsenen Plastiden sind hell gelbgrün gefärbt und zeigen eine schwache Granulierung. Die Plastiden der Stadien in Abb. 82 und 83 mit den zahlreich angehäuften Globuli sind stärker hellgrün gefärbt und in ihnen treten dunkle Körner auf. Die Erkennung der einzelnen Globuli liegt ausserhalb des Bereiches der Auflösung im Lichtmikroskop, aber die einzelnen Gruppen der Globulikugeln sind demnach zu erkennen und geben dem Chloroplasten ein granuliertes Aussehen. Abgesehen von Grössenvariationen lassen sich diese Gruppen von Globuli nicht von den im Lichtmikroskop erkennbaren Grana normaler grüner Chloroplasten unterscheiden. Die im Lichtmikroskop gefundene Färbung deutet darauf hin, dass Chloroplastenpigmente in den Globuli lokalisiert sind. Diese Frage sei im folgenden Abschnitt näher untersucht.

Die grosse Anhäufung der Globuli in den Plastiden der *xantha*-Mutante erinnert unmittelbar an die bekannten biochemischen Ergebnisse der *Neurospora*-Genetik: Die Genmutation bedingt einen Syntheseblock, der die Bildung eines lebensnotwendigen Stoffwechselproduktes verhindert. Die Vorstufe wird als Folge davon angehäuft.

Es wurde hier festgestellt, dass die Lamellenbildung nicht stattfinden kann. Die Anhäufung der Globuli wäre demnach als „die angehäufte Vorstufe" bei der „Synthese" der Lamellen aufzufassen. Viele Beobach-

tungen der normalen Plastidenentwicklung sprachen dafür, dass die Globuli etwas mit der Differenzierung der Lamellen und auch der Granastruktur zu tun haben und — bildlich gesprochen — das Material dazu liefern. Die Befunde der *xantha*-Mutante finden ihre beste Erklärung dadurch. Auch die oben besprochenen „Verklebungen" und „Pakete" gleichen Aussehens wie die Globuli unterstützen diese Ansicht.

Wie dies im einzelnen vor sich geht, werden uns vielleicht andere *xantha*-Mutanten mit einem Block an einer anderen Stelle lehren.

Die *albina*- und *xantha*-Mutanten geben uns Hinweise dafür, dass die Chlorophyll-Letalen geeignet sind, Stadien der normalen submikroskopischen Strukturdifferenzierung näher zu verstehen. Die Plastiden machen gleichsam jeweils in einem bestimmten Stadium Halt. Das prägt sich auch darin aus, dass das Stadium mit der Anhäufung der Globuli alle Plastiden einer Zelle kennzeichnen kann und über relativ weite Blattbereiche gleichmässig zu finden ist. In der normalen Entwicklung finden sich mehrere verschieden weit fortgeschrittene Stadien in der gleichen Zelle und selbst in Zellen mit schon voll ausdifferenzierten Plastiden, kann man noch die jüngsten Proplastidstadien antreffen.

Unabhängig, ob die Deutung der Funktion der Globuli im einzelnen richtig ist, zeigen uns die Befunde, dass Chlorophyll-Letale höherer Pflanzen dieselben Störungen aufweisen können wie die letalen Stoffwechseldefektmutanten der Pilze oder Bakterien. Dieser Typus des Geschehens in den Mutanten umfasst nicht nur die Synthese einzelner Substanzen wie z.B. Aminosäuren oder Pigmente, sondern auch den Aufbau von Proteinen aus Aminosäuren und Peptiden [59, 62]. Dieses Geschehen umfasst weiter, wie hier im Fall der Plastidendifferenzierung, den Aufbau der Strukturen, die im Bereich der submikroskopischen Morphologie sichtbar gemacht werden können.

Pigmentanalysen der normalen und chlorophyll-letalen Keimlinge

Der Pigmentgehalt normaler Keimlinge wurde in drei verschiedenen Entwicklungsstadien untersucht: (1) in ca. 10 cm langen Primärblättern, die also vorwiegend voll ausdifferenzierte Chloroplasten enthalten, (2) in Sekundärblättern des gleichen Pflanzenmateriales mit 5–10 mm Länge und gelbgrüner Farbe, (3) in 1–5 mm langen Sekundärblättern, die weissgelblich gefärbt waren. Diese frühen Entwicklungsstadien wurden makroskopisch nach ihrer Farbe und unabhängig von ihrer exakten Blattlänge für die Pigmentbestimmung zusammengefasst. Sie enthalten die Entwicklungsstadien der Plasti-

den, in denen die Lamellenbildung vor sich geht. Als Mass für die Entwicklung der Blätter und Plastiden wurde das Frischgewicht bestimmt. Die Ergebnisse der Analysen sind in Abb. 102, 103 und Tabelle III wiedergegeben.

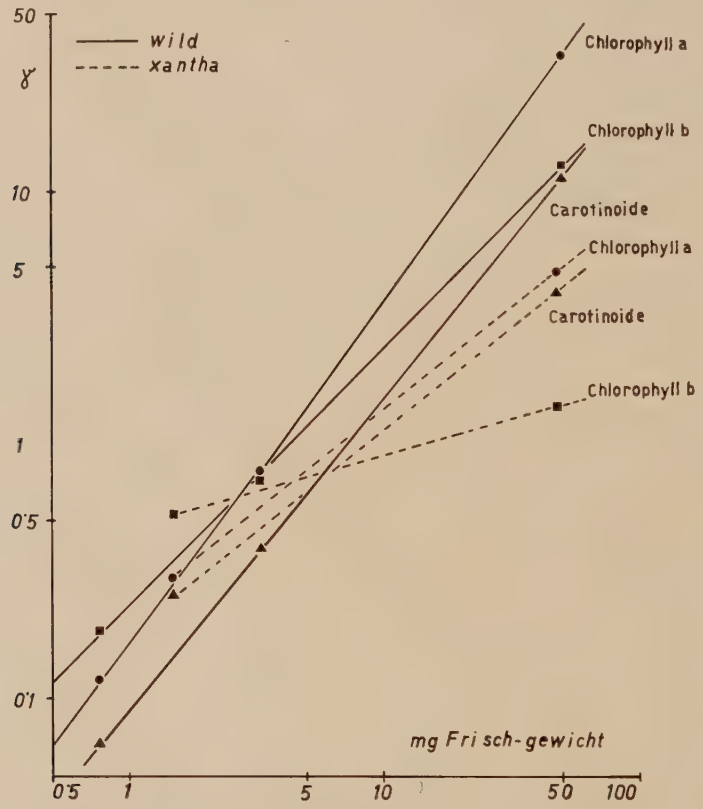

Abb. 102.—Pigmentgehalt normaler Gerstenkeimlinge (wild) und der Mutante *xantha*-3 in verschiedenen Entwicklungsstadien.

In Abb. 102 sind die Absolutmengen der Chlorophylle und Carotinoide in γ gegen das Frischgewicht in mg aufgetragen (logarithmische Skalen). Als eine bessere Bezugsgrösse ist oft das Trockengewicht anzusehen. In diesem Fall ist das von geringerer Bedeutung, da das relative Trockengewicht, d.h. Trockengewicht in % des Frischgewichtes, in verschiedenen Entwicklungsstadien der Gerstenkeimlinge — unter den hier gegebenen Bedingungen — konstant ist und etwa 8% beträgt [30 a].

Chlorophyll *a* und die Carotinoide nehmen mit steigendem Frischgewicht stark zu, wobei die Carotinoidbildung einer etwas flacheren Kurve folgt. Das

Chlorophyll *b* zeigt einen anderen Bildungsverlauf. In Blättern unter 1 mg Frischgewicht ist mehr Chlorophyll *b* als *a* vorhanden. In Blättern mit etwa 1,5 mg Frischgewicht sind sie in gleichen Mengen ausgebildet und in den

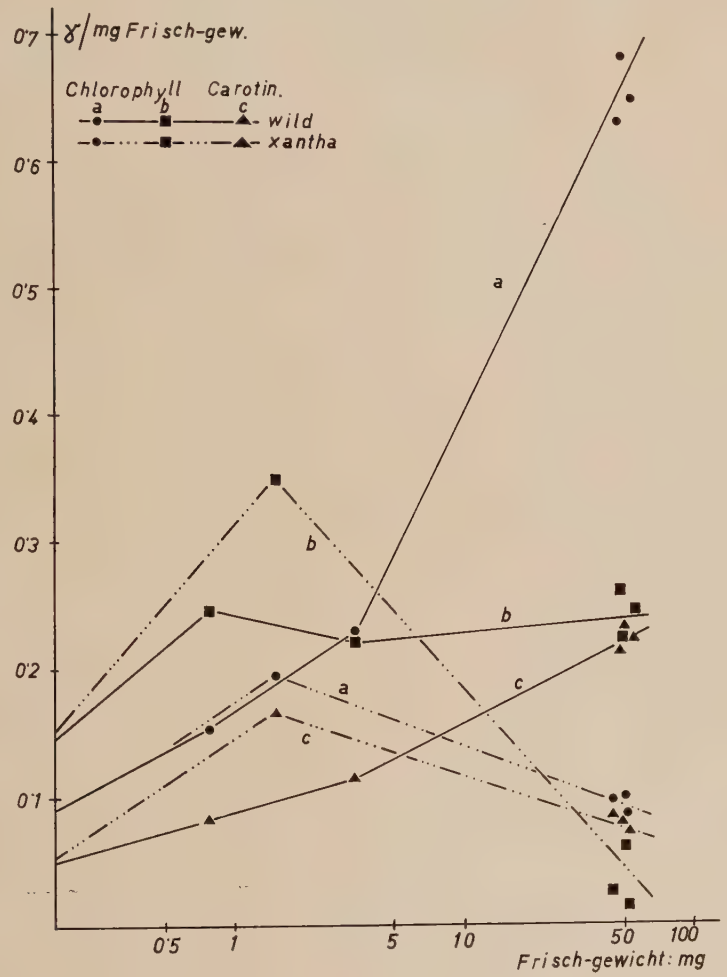

Abb. 103.—Pigmentgehalt per mg Frischgewicht verschiedener Entwicklungsstadien in normalen Gerstenkeimlingen (wild) und der Chlorophyll-Letalen *xantha*-3.

Blättern von 50 mg Frischgewicht hat sich das normale Mengenverhältnis der beiden Chlorophylle eingespielt.

Untersucht man die Menge Pigmente per mg Frischgewicht im Laufe der Entwicklung von Gerstenkeimlingen, so werden Kurven der Abb. 103 er-

halten. Das Chlorophyll *a* nimmt exponentiell zu, d.h. mit zunehmender Entwicklung steigt der Chlorophyllgehalt stärker an als das Frischgewicht. Diese Zunahme erreicht sicher einen Grenzwert, nach dem die Menge Chlorophyll *a* per Frischgewichtseinheit konstant bleibt. Dies dürfte mit den Werten der 50 mg schweren Blätter erreicht sein, da das Verhältnis von *a* zu *b* gerade dem voll entwickelter Blätter entspricht. Der erhaltene Wert stimmt grössenordnungsmässig mit dem Niveau überein, das bei Ergrünung von etiolierten Gerstenkeimlingen erreicht wurde [141].

Die Menge Chlorophyll *b* per mg Frischgewicht bleibt im Laufe dieses Entwicklungsabschnittes konstant, d.h. Chlorophyll *b* wird proportional der Frisch- und Trockengewichtszunahme gebildet. Das trifft für den späteren Entwicklungsverlauf auch beim Chlorophyll *a* zu. Jedoch bei der Keimlingsentwicklung, die mit der hier untersuchten Plastidenentwicklung und -differenzierung zusammenfällt, erreicht das Chlorophyll *b* die Proportionalitätsstufe bedeutend früher als das Chlorophyll *a*. Für den einzelnen Chloroplasten mag das bedeuten, dass schon in den ersten Stadien, zur Zeit der Lamellenbildung, die gesamte Menge Chlorophyll *b*, die der ausdifferenzierte Chloroplast enthält, vorhanden ist und dass diese Menge konstant gehalten wird, während das Chlorophyll *a* den Gleichgewichtszustand erst später, etwa nach der Differenzierung der Granastruktur erreicht. Die Carotinoide folgen in ihrer Bildung dem Chlorophyll *a*, wenn auch ihre Gesamtmenge stets geringer bleibt. Im ausdifferenzierten Gerstenchloroplasten der Primärblätter ist die Menge Chlorophyll *b* und die Menge aller Carotinoide zusammen etwa gleich gross.

In Tabelle III ist zum Vergleich für die Mutanten noch der Chlorophyll *a* und *b* Gehalt in % der Menge (γ/mg Frischgewicht), die in ausdifferenzierten Chloroplasten der Primärblätter vorhanden ist, angegeben. In derselben Weise sind die Carotinoide berücksichtigt. Die Konstanz des Chlorophyll-*b*-Spiegels tritt hervor. Das Verhältnis von Chlorophyll *a*/*b* wechselt im Laufe der Plastidenentwicklung von 0,6 zu 2,7. Letzterer Wert entspricht gut dem allgemein anerkannten von 2,9 für assimilierende Gewebe. Aus der danebenstehenden Spalte $a+b/c$ wird der Anteil der Carotinoide an dem Pigmentgemisch deutlich. In den jüngsten Blättern scheint er etwas grösser, sinkt aber dann sehr bald auf ein konstantes Verhältnis. Schliesslich ist die Gesamtmenge der Pigmente aufgenommen.

Der Pigmentgehalt der *albina*-Mutante ist vorerst ausschliesslich für den Endzustand der Plastidenentwicklung untersucht. Der Pigmentgehalt ist ausserordentlich gering, ganz wie es aus der submikroskopischen Morphologie dieser Mutante zu erwarten ist. Die Carotinoide sind mengenmässig überlegen,

TABELLE III

Pigmentgehalt verschiedener Entwicklungsstadien normaler und chlorophyll-letaler Gerstenkeimlinge.

	Chlorophyll Carotinoide, %					$a+b+c$
	a	b	c	a/b	$a+b/c$	γ/mg Frischgew.
normal,						
Primärblätter 10 cm	100	100	100	2,7	4,0	1,125
Sekundärblätter gelbgrün	35	91	52	1,0	3,9	0,570
Sekundärblätter weissgelb	24	100	39	0,6	4,6	0,487
xantha,						
Primärblätter 10 cm	15	14	37	3,7	1,6	0,212
Sekundärblätter gelblich	30	142	75	0,6	3,3	0,712
albina,						
Primärblätter 10 cm	0,2	0,9	3,2	0,8	0,6	0,011

und offenbar enthalten die Plastiden mehr Chlorophyll *b* als *a*, sofern nicht die Werte überhaupt auf Verunreinigungen beruhen.

Von besonderem Interesse ist die *xantha*-3-Mutante zufolge ihres auffallenden Plastidenformwechsels. Einerseits wurden Primärblätter mit dem Plastidenendzustand (Abb. 84, 85) zur Pigmentanalyse herangezogen und andererseits jenes Stadium mit den grossen Anhäufungen der Globuli (Abb. 82, 83). Das Frischgewicht 10 cm langer Primärblätter der *xantha*-Mutante unterschied sich nicht von dem normaler. Aus Abb. 102 geht hervor, dass Chlorophyll *a*, *b* und die Carotinoide mit steigendem Frischgewicht zunehmen. Die Pigmente werden also bis zum Absterben der Keimlinge gebildet. Der Verlauf der Kurven ist aber ein anderer als in den normalen Keimlingen. Dabei fällt auf, dass im frühen Entwicklungsstadium (1,5 mg Frischgewicht) Chlorophyll *a* in normaler Menge vorhanden ist, während Chlorophyll *b* und die Carotinoide in grösserer Menge auftreten. Chlorophyll *b* nimmt im Laufe der weiteren Frischgewichtserhöhung nur mehr wenig zu, während Chlorophyll *a* und die Carotinoide relativ hohe Werte erreichen.

Betrachten wir die Menge der Pigmente per mg Frischgewicht (Abb. 103), so wird der Unterschied zwischen den normalen Keimlingen und der Mutante deutlich. Während die Pigmentbestimmungen der normalen Keimlinge ansteigende bzw. Sättigungskurven ergeben, zeigt die Mutante Optimumkurven für alle drei Pigmente.

Das Chlorophyll *a* entspricht in seinem Optimum den normalen Keimlingen des gleichen Entwicklungsstadiums. Das Chlorophyll *b* und die Carotinoide erreichen im Optimum Mengen, die über denen vergleichbarer

normaler Entwicklungsstadien liegen. Das bedeutet, dass in den Entwicklungsstadien der Mutante, in denen die Globuli in grosser Menge angehäuft sind, auch eine bedeutende Konzentration von Carotinoiden und vor allem Chlorophyll *b* vorhanden ist. Die Bestimmung der Carotinoide ist nicht einwandfrei (S. 433), da der hohe Wert auch auf eine vermehrte Menge von Protochlorophyll zurückführbar ist. Hingegen die Erhöhung des Chlorophyll-*b*-Gehaltes um ca. 50% (Tabelle III) über das Niveau, welches in den Entwicklungsstadien der Plastiden und in den ausdifferenzierten Chloroplasten zu finden ist, scheint gesichert.

In den Endstadien der Plastidenentwicklung der Mutante ist der Pigmentgehalt per mg Frischgewicht stark gesunken. Chlorophyll *b* ist von diesem Abfall am stärksten betroffen, während die Carotinoide möglicherweise am wenigsten beeinträchtigt werden (vgl. auch Tabelle III: a/b und $a + b/c$). Die Gesamtpigmentmenge ist für das Entwicklungsstadium mit den stark angehäuften Globuli (Abb. 82, 83) ca. 40% grösser als in den vergleichbaren normalen Entwicklungsstadien, während im Endzustand (Abb. 84, 85) die Plastiden nur $\frac{1}{5}$ der Pigmentmenge ausdifferenzierter Chloroplasten zeigen.

Diese Befunde über den Pigmentgehalt in der Mutante haben eine auffallende Parallelität mit dem Verhalten der Globuli in den Chloroplasten. Vor allem der hohe Chlorophyll *b* Gehalt gerade in den Stadien der Anhäufung der Globuli scheint zu zeigen, dass die Globuli zumindest Chlorophyll *b* — möglicherweise alle Pigmente — enthalten. Ein Abbau der Globuli in der weiteren Differenzierung wird durch ihre kleinere Grösse und geringere Zahl in den Endstadien der Chloroplasten (S. 454) nahegelegt. Auch dieser Vorgang findet seine Parallele in der starken Pigmentverminderung.

Die Mutation *xantha*-3 bedingt keine Blockade der Chlorophyllsynthese. Eine bedeutende Verschiebung des Verhältnisses von Chlorophyll *a* zu *b* findet aber statt. Aus Untersuchungen mit C^{14} ist bekannt, dass Chlorophyll *a* und *b* zunächst einen gleichen Syntheseweg haben ([40, 41, 42] u.a.). Erst verhältnissmässig spät findet eine Gabelung der Synthese statt. Eine Umwandlung von Chlorophyll *a* in *b* oder umgekehrt konnte nicht festgestellt werden [125]. Die Befunde der Pigmentbildung während der normalen Entwicklung legen nahe, dass aus der gemeinsamen Vorstufe der beiden Chlorophylle eine entsprechende Menge Chlorophyll *b* zur Erreichung und Erhaltung des konstanten Niveaus im Chloroplasten gebildet wird, während der verfügbare Rest dieser Vorstufe in Chlorophyll *a* umgewandelt wird. In der Mutante *xantha*-3 ist dieser Mechanismus gestört und eine abnormal grosse Menge Chlorophyll *b* entsteht.

Das Vorkommen der Globuli in allen Differenzierungsstadien der normalen

Chloroplasten wurde erwähnt. Ihr Pigmentinhalt würde bedeuten, dass entweder die Pigmentbildung zunächst zu den Globuli führt und die Globuli zum Aufbau des Lipochromoproteides der Chloroplastenschichten und der Grana verwendet werden, oder dass der Überschuss der Pigmente beim Aufbau und der stetigen Erneuerung des Lipochromoproteides in Form der Globuli abgelagert wird. Beide Möglichkeiten vermögen das allgemeine Vorkommen und zugleich die grosse Anhäufung der Globuli bei Unmöglichkeit des Aufbaues der Chloroplastenschichten und Grana in der Mutante zu erklären.

Die *xantha*-Mutante veranschaulicht, dass für das Verstehen der physiologischen und morphologischen Wirkung einzelner Letalfaktoren in den höheren Pflanzen eine Analyse des Entwicklungsvorganges aufschlussreich ist. Gerade in Bezug auf die Pigmente gibt das erreichte Endstadium ein nur sehr beschränktes Bild, indem es ein grosses Defizit der Pigmente zeigt, während man in den früheren Entwicklungsstadien sogar einen Überschuss findet. Die Pigmente zeigen eine biochemische Pleiotropie des *xantha*-3-Faktors. Es wird von besonderem Interesse sein, ob der mutative Block primär das Fehlen einer Protein- oder Lipoidkomponente bedingt oder ob der Block die Bindung der Komponenten zum Lipochromoproteid verhindert. Für die weitere Entwicklung der Plastiden dieser Mutante kann festgestellt werden, dass die primär reichliche Produktion der Pigmente durch die fehlende strukturelle Differenzierung stark zurückgeht und schliesslich nicht den Abbau der Pigmente zu kompensieren vermag.

Zusätzliche Beobachtungen an Proplastiden und anderen Zellbestandteilen

Zur Frage der Kontinuität der Plastidenstrukturen sind einige Befunde an dem Moos *Funaria hygrometrica* von Interesse. Da im Gegensatz zu tierischen Zellen noch wenige elektronenmikroskopische Befunde über die Zellorganellen der Pflanzenzelle — wenn man von den Plastiden absieht — vorliegen, sei auf den Inhalt der Moosspore und den Formwechsel der Mitochondrien in der Braunalge *Fucus vesiculosus* eingegangen.

Strugger und seine Mitarbeiter ([148, 150 a] und dort zit. Lit.) vertreten mit Nachdruck, dass die Grana der ausdifferenzierten Chloroplasten eine kontinuierliche Struktur darstellen. In den Embryonalgeweben der höheren Pflanzen soll nur ein Granum vorhanden sein, aus dem durch Teilung die Grana der ausdifferenzierten Chloroplasten hervorgehen. Dies steht im Widerspruch mit dem bei der Gerste festgestellten Entwicklungsvorgang der Plastiden (zur Diskussion siehe S. 472 ff.).

Kaja [74] hat die Moosplastiden lichtmikroskopisch im Leben untersucht und will die Kontinuität der Granastruktur in allen Stadien bewiesen haben. Nach Kaja erfolgt bei den Moosen keine Reduktion der Plastiden in ein „monogranuläres" Stadium, sondern in allen Teilen des Sporophyten sind „polygranuläre" Plastiden zu finden, die in den Paraphysen nur 3–4 Grana enthalten. In den reifen Sporen von *Mnium horneum* sollen 30–40 Grana vorhanden sein. Auch für *Funaria* gibt er die gleichen Verhältnisse an.

Es ist deshalb von Bedeutung, wie die Grana in reifen, ungekeimten und ungequollenen Sporen von *Funaria* elektronenmikroskopisch aussehen. In Abb. 86 ist ein Übersichtsbild eines Schnittes durch eine Spore wiedergegeben.

Im Blickfeld liegen verhältnissmässig grosse Plastiden. Sie enthalten einen dichteren zentralen Teil und dieser zeigt einzelne mehr oder weniger ungeordnete Lamellen (vgl. auch Abb. 89). Letztere liegen vereinzelt parallel, sind aber häufiger gefaltet und aufgewickelt. Von einer ausgesprochenen Granastruktur, wie sie uns in den ausdifferenzierten Chloroplasten entgegentritt, ist nichts zu bemerken. Auch in diesen Chloroplasten sind die Globuli verstreut vorhanden.

Kaja hat die Plastiden aus den Sporen in 1 molarer Zuckerlösung isoliert, wodurch die Grana gut zu beobachten seien. Es wurden deshalb Sporen in 1 molarer Rohrzuckerlösung eingebracht und anschliessend fixiert. Das Ergebnis mag aus Abb. 70 a entnommen werden. Dieses Medium verursacht offenbar eine bedeutende Quellung der Plastiden. Dabei tritt eine Schichtung und Blasenbildung auf. Streng parallele und begrenzte Lamellenpakete, wie sie für die Granastruktur charakteristisch sind, treten nicht hervor, wenn auch einzelne Lamellenstücke vorhanden sind. Die Globuli sind in gewöhnlicher Menge vorhanden. Man kann erwarten, dass ungequollene Chloroplasten der Abb. 86 und 89 im Lichtmikroskop homogen erscheinen.

Ungekeimte und ungequollene Sporen wurden in 0,1 und 1 molare Rohrzuckerlösungen gelegt und im Blickfeld des Mikroskopes unter Beobachtung gequetscht. Der Sporeninhalt tritt aus und die Plastiden zeichnen sich durch ihre hellgrüne Farbe aus. Beim Austritt aus der Spore sind sie homogen ohne erkennbare Granulierung. In 0,1 molarer Lösung tritt allmählich, nach etwa 30 Min. eine Granulierung auf, während in der 1 molaren Lösung diese Granulierung schon nach wenigen Minuten sichtbar wird. Das Chlorophyll ist offenbar in den Globuli und den Lamellenstücken lokalisiert und bei der auftretenden Quellung und Entmischung gibt dies in Übereinstimmung mit Abb. 91 das Aussehen von „Grana" mikroskopischer Grösse. Auch die Beobachtungen an den Moossporen geben bisher keine

Anhaltspunkte für eine Kontinuität der Granastruktur ausdifferenzierter Chloroplasten.

Die Sporen von *Funaria* sind von einer dreischichtigen Wand umgeben (Abb. 86), wie das aus der Lichtmikroskopie bekannt ist [84, 92]. Die 0,1–0,2 μ breite Intine besitzt die für Zellulosewände charakteristische Fibrillentextur. Daran schliesst sich die etwa gleich breite Exine, die von grosser elektronenoptischer Dichte ist und ebenfalls eine allerdings weniger ausgeprägte Fibrillentextur zeigt. Der Exine sitzt aussen die Perine auf. Sie besteht aus Zapfen und einer dünnen, die Zapfen verbindenden Schicht. Die Perine mit den Zapfen weist eine grössere elektronenoptische Dichte als die Exine auf. Die Zapfen zeigen an der Oberfläche kleine Papillen und sind teilweise in verschiedener Weise aufgespalten. Die Perine und Zapfen sind von einer 150–200 Å dicken homogenen und stark elektronenstreuenden Membran lückenlos umkleidet. Das geht vor allem aus Querschnitten der Zapfen und Papillen hervor.

Das auffallendste lichtmikroskopische Organell der Moosspore ist der grosse lichtbrechende fette Öltropfen, der sich mit dem spezifischen Fettreagenz Sudan IV stark rot anfärbt. Erstaunlicherweise ergibt er im Elektronenmikroskop nach Osmiumfixierung einen nur sehr geringen Kontrast.

Das Plasma einer Spore ist ausserordentlich dicht und mit einer grossen Zahl verschiedener Organellen angefüllt (Abb. 86–95). Trotzdem enthält eine solche Moosspore nach Trockengewichtsbestimmungen etwa 70% Wasser. Die Struktur des Plasmas ist dem embryonalen Cytoplasma der Gerste ähnlich. Durch ihre Septierung lassen sich die Mitochondrien identifizieren (Abb. 86 oben links). Die Septen sind kontrastarm, etwas aufgebläht und gefaltet. Als weiterer Bestandteil sind die tiefschwarzen Kugeln der Abb. 87 mit einem durchschnittlichen Durchmesser von 0,3–0,4 μ zu nennen. Möglicherweise handelt es sich um Fettropfen.

Bisher unbekannt sind die Sporenbestandteile der Abb. 88 und 93. Sie besitzen eine rundliche bis ovale Form und einen mittleren Durchmesser von 0,8–1 μ. Charakteristisch ist die Begrenzung dieser Körper, die im Querschnitt einer Perlenschnur gleicht. In Tangentialschnitten der Oberfläche heben sich „schwarze" Kreise oder Ellipsen von einer weniger dichten Haut ab (Abb. 93). Die Perlenschnur der Querschnitte (Abb. 88, 93) besteht aus einer dünnen Membran und von ihr verbundenen Tropfen. Ob die Membran durch die Mitte der Tropfen läuft oder die Tropfen der Membran innen anhaften ist an Hand des vorliegenden Materials nicht zu klären. Dieselbe Art der Begrenzung zeigt ein grösseres rundliches Organell mit 1,8–2,5 μ Durchmesser. Während die eben besprochenen Partikel elektronenoptisch leer zu

sein scheinen, zeigen diese einen dichten Kern, der von mehreren elektronenoptisch leeren Hohlräumen umgeben ist (Abb. 87, 92 und 94). Die Struktur des Kernes ist wabenartig. An einigen Bildern erkennt man auch eine Struktur von gefalteten Schichten, die durch dichtes Material in Abständen verbunden sind. Die weitere Analyse der eigenartigen Membranstruktur wird sich damit beschäftigen, ob sie einen Typus von Porenfilter darstellt und ob sie von besonderer Bedeutung für die lange Lebensdauer der Sporen ist.

In diesem Zusammenhang sei auch auf die Begrenzung der Plastiden hingewiesen. Sie lässt sich an den Membranen der nahe aneinanderliegenden Plastiden in Abb. 86, 89 und 90 studieren. Jede Plastide ist von einer doppelten Membran begrenzt und zwischen den beiden Doppelmembranen liegt eine granuläre Substanz des Plasmas. Zuweilen ist zwischen den zwei Plastiden eine dritte kontrastarme Mittellamelle sichtbar (Abb. 89 unten, 90). Vielleicht beruht sie auf einer linearen Aggregation der granulären Substanz.

Schliesslich bleiben die zahlreichen Einschlüsse zu besprechen, die am ehesten als Reservesubstanz aufzufassen sind. Einer von diesen Einschlusskörpern ist in Abb. 95 wiedergegeben. Sie sind von ellipsoider Gestalt und können einen Längsdurchmesser von 1 μ erreichen. Oft liegen sie dicht rings um eine Plastide (Abb. 86 und 89). Sie bestehen aus zwei Teilen, einem elektronenoptisch kontrastreichen und weitgehend homogenen Mantel verschiedener Dicke mit einer gewellten Begrenzung und einem elektronenoptisch leeren Raum, der von dem Mantel umschlossen wird. Tangentialschnitte durch den Mantel geben unregelmässig gelappte und gleichmässig dunkle Flächen (Abb. 86). Es ist durchaus möglich, dass dieser Hohlraum von einem Polysaccharid, das ähnlich der Stärke nur geringe Elektronenstreuung bedingt, ausgefüllt ist. Gegen ein Fixierungsartefakt spricht die ebene Begrenzung des „Hohlraumes". Lichtmikroskopisch lassen sich in der Moosspore Einschlüsse dieser Grösse mit Sudan IV rot färben, was eine fetthaltige Mantelsubstanz nahe legt. Während Lorch [92] für zahlreiche Moossporen das Vorkommen von Stärke in den Plastiden beschreibt, konnte an dem vorliegenden Material weder in den Plastiden, noch in anderen Zellbestandteilen mit Jod-Jodkali eine Blaufärbung erzielt werden.

Die eben beschriebenen Einschlüsse ähneln in Aufbau und Struktur solchen aus dem *Fucus*-Ei (Abb. 96 und 97). Die Ähnlichkeit von Abb. 95 aus einer Moosspore mit dem Einschluss der Abb. 97 aus einem *Fucus*-Ei ist bemerkenswert. Ein Querschnitt dieses Einschlusstypus von *Fucus* ist in Abb. 96 zu sehen. Sie sind grösser als die bei *Funaria* und der Mantel zeigt eine feine Strukturierung in Form eines sehr dichten Netzwerkes.

Während wir den Mitochondrienformwechsel der Gerste noch nicht überblicken, kann *Fucus vesiculosus* eine Auffassung darüber geben (Abb. 98–101). In der Eizelle (vgl. [91] und Abb. 98–100) sind die Mitochondrien von einer doppelten Membran umgeben. Sie sind unregelmässig gelappt bzw. amöboid. Die von der Mitochondrienmembran ausgehenden Doppellamellen sind verbunden und bilden somit die charakteristischen Septen. Die Septen oder Cristae eines Mitochondriums sind vorwiegend in einer Richtung orientiert. Diese Richtung kann eine beliebige Lage zu der Form der Mitochondrien einnehmen, sie kann in der Längsachse des Mitochondriums, senkrecht oder diagonal zu ihr liegen. Daraus ergibt sich, dass bei der amöboiden Bewegung der Mitochondrien die Septen nicht senkrecht auf der Mitochondrienmembran stehen bleiben, sondern sie behalten ihre ursprüngliche Richtung bei. Daher erscheinen die Septen auch bei einer Orientierung in der Längsrichtung dünner und dichter gepackt. Das legt nahe, dass die Septen mit der Mitochondrienmembran fest verbunden sind, sei es dass sie Ausfaltungen der inneren Mitochondrienmembran oder in sich geschlossene Lamellen bilden (vgl. [110, 139]). Im einzelnen sind die Septen teilweise gewunden und besitzen unregelmässige Vorsprünge, was in den Schnitten zu geschlossenen Konturen führen kann. Sie bestehen aus drei Schichten, indem zwei kontrastreiche von ca. 40 Å Dicke eine breitere lichte Schicht umschliessen. Diese Mitochondrien entsprechen im Aufbau recht gut dem von Palade [109, 110] dargestellten Schema der Nierenmitochondrien [123, 139]. Aus den männlichen Keimzellen von *Helix* ist ein Mitochondrientypus mit coaxial gestellten Schichten beschrieben [13] und einen ähnlichen Aufbau besitzen Einschlüsse des Seeigeleies [1, 2]. Analog sind im *Fucus*-Ei und auch in anderen *Fucus* — Zellen die Physoden gebaut ([91], Abb. 98 zwischen den zwei linken Mitochondrien).

Die Mitochondrien der jungen Rindenzellen von *Fucus* entsprechen strukturell denen der Eizelle [161]. In älteren Thalluszellen zeigen sie einen anderen Aufbau (Abb. 101). Sie sind etwa doppelt so gross wie die der Eizellen, weitgehend abgerundet und auch von einer doppelten Membran umgeben. Die Septen sind blasenförmig angeschwollen und begrenzen sich auf die Peripherie des Mitochondriums, so dass ein relativ grosser zentraler Hohlraum entsteht. Die Septen sind zahlenmässig weniger geworden. Der Aufbau dieser älteren Mitochondrien entspricht den bei Tabak, *Euglena, Chlamydomonas* und anderen Objekten gefundenen mit den „pocket like bladders" [109, 110, 127, 47, 103].

Der Formwechsel der Mitochondrien in *Fucus* und der Gerste (vgl. S. 443 ff.) zeigt eine Parallele mit dem Formwechsel der Plastiden in diesen

beiden Objekten. In der Eizelle von *Fucus* enthalten die Elementarchromatophoren die für die Photosynthese notwendige und für den ausdifferenzierten Chromatophoren charakteristische Lamellenstruktur. Die Mitochondrien sind mit einer Septenstruktur versehen, wie sie für funktionstüchtige und aktive Mitochondrien typisch sein dürfte. Der Formwechsel der beiden Organellen in *Fucus* besteht in Wachstum, Vermehrung der Lamellen, Teilung bei den Chromatophoren und Wachstum, Umgestaltung der Septen, vielleicht auch Teilung bei den Mitochondrien. Er mündet bei beiden Organellen in einer Degeneration. Bei der Gerste zeigen die embryonalen Plastiden keine Lamellen- und Granastruktur, so dass ihre Identifizierung nicht mit Sicherheit möglich ist. Ihre innere Struktur wird im Laufe der Differenzierung aufgebaut. Auch die Mitochondrien der Gerste besitzen in den embryonalen Zellen nicht die für die älteren Zellen charakteristische Septenstruktur und eine Identifizierung auf Grund dieses Merkmals ist nicht gegeben, d.h. auch diese Struktur wird in der Gerste erst im Laufe der Entwicklung herausdifferenziert.

Somit erfährt die submikroskopische Struktur der Plastiden und Mitochondrien in höheren Pflanzen, wie der Gerste, einen umfassenderen Formwechsel als diese Organelle in Algen, wie *Fucus*.

ALLGEMEINE BETRACHTUNGEN

Aus neuerer Zeit liegen zahlreiche zusammenfassende Darstellungen über die Struktur, den Formwechsel und die genetische Kontinuität der Plastiden vor. Da die Plastidenforschung durch die Verwendung des Elektronenmikroskopes in zunehmendem Masse betrieben wird und zahlreiche neue Ergebnisse zu erwarten sind, soll hier auf eine erneute Zusammenfassung der Plastidenprobleme verzichtet werden. Vielmehr sei auf folgende Arbeiten verwiesen, die eine Einsicht in die ältere Literatur und die verschiedenen gegenwärtig herrschenden Ansichten erlauben: Frey-Wyssling, 1955 [36], Granick, 1955 [47], Gustafsson und v. Wettstein, 1956 [58], Heitz, 1955 [66], Leyon, 1956 [90], Mühlethaler, 1954, 1955, 1956 [104], Pirson, 1955 [116], Strugger, 1954 [148], Strugger und Perner, 1956 [150 a]. Hingegen sei zu solchen Fragen der Plastidenstruktur und Plastidenentwicklung Stellung genommen, die auf Grund der vorliegenden Untersuchung geklärt oder zumindest besser präzisiert werden können.

Terminologie.—Da selbst die gebräuchlichsten Begriffe in verschiedenen Arbeiten recht divergierende Dinge bezeichnen, sei die im Vorstehenden ge-

brauchte Ausdrucksweise definiert und gegenüber der anderer Autoren abgegrenzt. Das Wort *Plastide* bei den höheren Pflanzen umfasst Chloro-, Chromo-, und Leukoplasten einschliesslich ihrer Entwicklungsstadien. Die *Proplastiden* sind die jüngsten Entwicklungsstadien aller Plastiden. Die Grenze zwischen einer Proplastide und einem Chloroplasten ist bei beginnender Schichten- und Lamellenbildung zu legen (vgl. [37]).

Der ausdifferenzierte Chloroplast enthält *Schichten* (engl. layer) [97, 98]. Die Schichten sind in *Lamellen* (engl. lamellae) unterteilt. Dieser Aufbau ist schematisch durch Abb. 22 definiert. Die beiden Begriffe lassen sich auch für die Algenchromatophoren verwenden. Eine weitere Unterteilung der Lamellen wird vorläufig mit dem arbeitstechnischen Ausdruck *Feinschichten* beschrieben.

Der Ausdruck „*Grana*" geht auf die Untersuchungen Schimpers und Meyers [131, 101] zurück, während der Ausdruck *Stroma* von Pringsheim [118] stammt. Diese Forscher sahen, dass die ausdifferenzierten Chloroplasten der höheren Pflanzen nicht homogen sind, sondern aus einer Grundsubstanz, dem Stroma, und besonders chlorophyllreichen Teilchen, den „Grana" zusammengesetzt sind. Heitz [64] hat die allgemeine Verbreitung dieser Grana in den höheren Pflanzen sichergestellt und ihre Scheibenform, wie auch ihre Variabilität erkannt. Aus der Elektronenmikroskopie kennen wir nun den Aufbau der Grana aus *Granalamellen* und wissen, dass auch das Stroma *Stromalamellen* enthält, wobei letztere mit den Granalamellen verbunden sind. Während manche Autoren (z. B. [90]) die Bezeichnung Grana in dem eben dargestellten eingeschränkten Sinne für die ausdifferenzierten Chloroplasten verwenden, sind andere Autoren dazu übergegangen, die verschiedensten lichtmikroskopisch sichtbaren Teilchen in den Plastiden und Chromatophoren als Grana zu bezeichnen. So bezeichnen Strugger und seine Mitarbeiter [148, 150] z. B. alle Teilchen mit Chlorophyllfluoreszens als Grana. Eine Definition der Grana auf Grund einer unterschiedlichen Verteilung der Chlorophyllfluoreszens gibt etwa auch Metzner [100]. Ebenfalls Heitz [66] hat diese weite Fassung übernommen. Dem Elektronenmikroskopiker treten bei einer solchen weiten Fassung des Begriffes Grana Schwierigkeiten entgegen, da er dann offenbar submikroskopisch verschiedene Strukturen mit dem Ausdruck Grana belegen soll. Lichtmikroskopisch würden etwa Abb. 2 eines normalen Chloroplasten und Abb. 83 eines Chloroplasten der Mutante *xantha* in gleicher Weise als Plastiden mit Grana beschrieben werden. Deshalb ist es angezeigt, in der vorliegenden Arbeit den Ausdruck Grana und Granalamellen nur für die im ausgewachsenen Chloroplasten vorhandenen typischen kontrastreichen Differenzierungen zu verwen-

den. In den Entwicklungsstadien der Chloroplasten werden die beiden Ausdrücke nur für die den Grana homologen Differenzierungen verwendet.

Ganz das Entsprechende gilt für die Verwendung des Begriffes Stromalamellen. Nach der hier und von Leyon verwendeten Ausdrucksweise enthalten alle bisher elektronenmikroskopisch untersuchten Algen (Flagellaten [164, 165], Chlorophyceen [90], Diatomeen [94], Phaeophyceen [91], und Characeen [99]) keine Grana, auch wenn lichtmikroskopisch eine ungleiche Verteilung des Chlorophylles in den gleichen Objekten (vgl. [38, 100]) auftreten mag. Konsequenterweise wären die bei Algen beobachteten Lamellen auch nicht Stromalamellen (vgl. [66]) zu nennen, da eine Homologie der Algenlamellen weder zu den Stroma- noch zu den Granalamellen der höheren Pflanzen gegeben oder bewiesen ist. Ein anderes wichtiges Missverständnis betrifft die Bildung der Schichten und Lamellen in den Proplastiden der höheren Pflanzen. Leyon [88] hat die Bildung der Schichten und Lamellen aus dem Plastidenzentrum zuerst beschrieben. Mühlethaler [103] und Heitz [66, 67] bezeichnen die aus dem Plastidenzentrum entstehenden Schichten als Stromalamellen und geben dadurch diesem Befund eine Deutung, die Leyon durch den Gebrauch der Worte „layers" bzw. „lamina" nicht gemeint hat.

Der Nomenklatur Leyons folgend, halte ich die Verwendung des Ausdrukkes *Plastidenzentrum* (engl. plastid-center or -core) in der Elektronenmikroskopie statt Primärgranum in den Proplastiden für geeignet, da der bisher elektronenmikroskopisch aufgedeckte Zusammenhang zwischen dem Plastidenzentrum und den Grana der ausgewachsenen Chloroplasten ein durchaus indirekter ist, d.h. eine Entstehung der Grana durch Teilung des „Primärgranums" nicht nachgewiesen werden konnte. Zudem ist es wahrscheinlich, dass die lichtmikroskopisch als Primärgranum oder als Grana in den Proplastiden und jungen Chloroplasten bezeichneten und dargestellten Gebilde (vgl. [148, 150, 8, 16, 49, 34, 112]) submikroskopisch verschiedene, nicht homologe Strukturen darstellen. Das Plastidenzentrum ist am besten durch Abb. 78 und 82 definiert. Es kann eine kristalline Ordnung [65, 89] annehmen.

Schliesslich wurde der neutrale Begriff *Globulus* (Mehrz. Globuli) eingeführt. Er bezeichnet die „osmiophilic globules" [90], „Fett- oder Lipoidtröpfchen" [103] „opaque spherical granules" [146], „spheres" [127]. Die Globuli wurden allgemein in den ausdifferenzierten Chloroplasten der höheren Pflanzen und ihren Entwicklungsstadien, wie auch in den Chromatophoren der Algen gefunden. Abb. 79 und 83 mag sie charakterisieren.

Der ausdifferenzierte Chloroplast

Der Aufbau des Gerstenchloroplasten entspricht auffallend gut den Chloroplasten im Mesophyll des Maises [70]. Vor allem das Verhältnis von einer Stroma- zu zwei Granalamellen ist beiden Chloroplasten gemeinsam. Die kontrastreichen Granalamellen wurden beim Mais zu 35 Å bestimmt, was mit den hier gemessenen Werten von 40 ± 20 Å eine Identität ergibt. Der Abstand der Granalamellen voneinander weist beim Mais einen etwas grösseren Wert auf. Die Stromalamellen der Gerste mit ca. 75 Å Durchmesser wurden etwas dünner als die 125 Å messenden des Maises befunden. Beide Objekte zeigen, dass im Elektronenmikroskop eine weitere Auflösung der Lamellen in Feinschichten von 10–20 Å Durchmesser nachzuweisen ist. Die Deutung dieser aufgelösten Feinschichten ist jedoch im Moment nicht in Übereinstimmung zu bringen. Dem Chloroplastenschema (vgl. Abb. 22) der Gerste und des Maises stehen die Chloroplasten von *Aspidistra* [88, 90, 146] und *Chlorophytum* [149] gegenüber. Der auffallendste Unterschied betrifft das bei letzteren festgestellte Verhältnis von 1 zu 1 der Stroma- und Granalamellen. Gleichzeitig tritt bei diesem Chloroplastentypus eine ausgesprochene Paarung der Stromalamellen [88, 90, 149] auf, während eine solche Paarung der Stromalamellen bei der Gerste und beim Mais fehlt. Interessanterweise ist die Dicke der Stromalamellen bei ihnen grösser als die der Granalamellen, während bei *Aspidistra* die Stromalamellen nur halb so dick wie die Granalamellen sind. Im Vorstehenden wurde gezeigt, dass die Stromalamellen der Gerste aus zwei eng gepaarten Feinschichten bestehen. Das würde bedeuten, dass eine Stromalamelle von *Aspidistra* einer Stromafeinschicht des Gerstenchloroplasten entspricht. Leyon ([90] S. 78) hat darauf hingewiesen, dass die Granalamellen von *Aspidistra* möglicherweise aus zwei Feinschichten aufgebaut sind. Somit ist auch bei diesem Objekt eine 1 zu 2 Beziehung der Stroma- und Granalamellen möglich.

Offenbar ist die Affinität der gepaarten Stromalamellen bzw. Stromafeinschichten in den Chloroplasten verschiedener Arten underschiedlich stark ausgeprägt. Es wird von Interesse sein, ob diesen Unterschieden (vgl. auch [151]) der submikroskopischen Chloroplastenstruktur auch ein chemischer Unterschied der Stoffe zwischen den gepaarten Stromalamellen bzw. Feinschichten zu Grunde liegt.

Die Chloroplastenschichten sind in den elektronenmikroskopisch untersuchten Präparaten verschieden deutlich. Während sie bei der Gerste und beim Mais ohne weiteres erkennbar sind, treten sie in den ausgewachsenen Chloroplasten von *Aspidistra* gewöhnlich nicht hervor. Durch eine leichte

dürften die „multigranulären Jungchloroplasten" den Stadien mit der lokalen Lamellenbildung entsprechen. Diese Orte der lokalen Lamellenbildungen erscheinen lichtmikroskopisch als „Grana", obgleich sie diesen nicht direkt homolog sind, und wurden lichtmikroskopisch wohl zuerst von Twiss [154] beim Mais gesehen und abgebildet. Die Grana der ausdifferenzierten Chloroplasten werden erst verhältnismässig spät, nachdem eine durchgehende Lamellierung des Chloroplasten erfolgt ist, aufgebaut. In bestimmten Zellen kann sie, wie beim Mais festgestellt, unterbleiben. Wahrscheinlich enthalten die Orte lokaler Lamellenbildung wie das Plastidenzentrum Chlorophyll und so ist es nicht möglich zu entscheiden, ob Heitz und Maly bzw. Düvel Plastiden im Stadium der Lamellenbildung, solche im Stadium der Granadifferenzierung oder beides beobachtet haben.

Chlorophylldefekte Mutanten und Biochemie der Plastiden

Die genetisch bedingten Chlorophylldefekte umfassen einfarbige und gescheckte, letale und vitale Typen. Trotz morphologischer Ähnlichkeit können sie durch ein stabiles Gen, durch Deficiencies, durch ein labiles Gen, plasmonisch oder plastidomisch bedingt sein.

Die Chloroplasten der vitalen hellgrünen bis gelbgrünen Typen dürften eine normale submikroskopische Struktur erreichen, wie das etwa für eine gelbgrüne Mutante vom Mais festgestellt ist, die sich in ihrer Chloroplastenstruktur elektronenmikroskopisch nicht von den normalen Chloroplasten unterscheiden liess [70]. Hier handelt es sich offenbar um eine quantitative mutative Beeinflussung der Synthese und der Lichtempfindlichkeit des Chlorophylls. Für diese Typen ist charakteristisch, dass Variationen der Temperatur, Lichtintensität und Nährstoffzufuhr die Ausbleichung der Plastiden fördern oder hemmen können. Unter bestimmten Bedingungen sind die Mutanten gleich vital und grün wie die Ausgangsform. Dazu gehören auch solche Mutanten, die mehr Chlorophyll führen als der Normaltypus (vgl. [128, 129, 130], und dort cit. Lit.). Diese Veränderungen der Reaktionsnorm unter „normalen" Umweltbedingungen gleichen in gewissem Sinn der künstlich erzeugten Chlorose oder dem Etiolement ursprünglich voll entwickelter Plastiden. Dabei ist wichtig, festzuhalten, dass eine Plastidendegeneration, die einmal ein bestimmtes Stadium überschritten hat, irreversibel ist [37]. Eine vergleichende elektronenmikroskopische und biochemische Untersuchung der vitalen Chlorophyllmutanten und der Chlorose wie des Etiolements wird vor allem den Form- und Stoffwechsel des ausdifferenzierten Chloroplasten beleuchten können.

Bei einem Vergleich der Chlorophyll-Letalen, die durch Faktormutationen

bedingt sind, mit solchen, die einen ausserkaryotischen Erbgang zeigen, sind vor allem zwei Unterschiede beachtenswert. In den hier untersuchten Chlorophyll-Letalen ist ein Block der Plastidenentwicklung feststellbar, d.h. die Chloroplasten erreichen nicht das voll ausdifferenzierte Stadium. Weiter konnte keine Vakuolisierung der Chloroplasten im Endzustand festgestellt werden. Das steht mit lichtmikroskopischen Beobachtungen an anderen Gerstenmutanten in Übereinstimmung [52].

Bei den bisher untersuchten Chlorophylldefekten von *Oenothera*, sog. Plastidommutanten, [151] erreichen die Chloroplasten einen ausdifferenzierten Zustand mit Grana- und Stromalamellen. Erst dann setzt früher oder später in der Pflanzenentwicklung eine Vakuolisierung der Plastiden und eine Zerstörung ihrer Struktur ein. So zeigt eine weisse Mutante des *suaveolens*-Plastidoms die Vakuolisierung bereits früh und sehr extrem, während eine gelbgrüne Mutante der *suaveolens*-Plastiden in dieser Hinsicht gemässigter ist. Offenbar lässt sich diese Vakuolisierung und Zerstörung der Plastiden durch schwache Lichtintensitäten hinauszögern [132]. Da dieser Unterschied der genom- und plasmatisch bedingten Chlorophyll-Letalen vielleicht ein allgemeiner und grundsätzlicher ist, seien einige neuere lichtmikroskopische Strukturanalysen nicht mendelnder Plastidendefekte besprochen.

So ist für nicht mendelnd vererbte Chlorophylldefekte von *Nicotiana* und *Nepeta* eine starke Vakuolisierung der Plastiden charakteristisch [166]. Bei *Chlorophytum comosum* [150] zeigen die blassen Plastiden der albicaten Blattzonen einer albomaculaten Form eine Vakuolisierung, wie sie für *Oenothera* gefunden wurde. Schliesslich wurde dasselbe für albomaculate Formen von *Antirrhinum majus* gezeigt und ausdrücklich betont, dass bei starker Belichtung die Vakuolisierung sehr früh auftritt [93]. Bei letzterem Objekt zeigen die jungen Plastiden in 4 von 5 albomaculaten Fällen eine deutliche Granastruktur und es ist wahrscheinlich, dass gerade wie bei *Oenothera* zunächst normal strukturierte Chloroplasten ausgebildet werden, die dann „degenerieren". Dieser Prozess beginnt zunächst mit dem lichtmikroskopischen Auftreten von unregelmässig grossen „Granen". Im weiteren Verlauf enthalten die Plastiden wenige stark vergrösserte „Granen" und schliesslich bleibt ein einziges riesiges „Granum" übrig. Darauf setzt die vollständige Vakuolisierung ein. Das steht in guter Übereinstimmung mit den elektronenmikroskopischen Befunden bei *Oenothera*. Das Stadium mit den unregelmässig grossen „Grana" entspricht der Abb. 5 bei Stubbe und v. Wettstein. Vereinzelt sind lichtmikroskopisch die wirklichen Grana noch erkennbar, während die sog. „grösseren Grana" die auseinander gesprengten Schichten darstellen. Auch das Stadium mit dem einzigen riesigen „Granum"

kommt. Die Oberflächenasymmetrie der gepaarten Stromalamellen bzw. Stromafeinschichten hat vielleicht etwas mit der räumlichen Trennung von Synthese und Ableitung niedermolekularer Stoffe einerseits und der Speicherung andererseits zu tun. Eine Oberflächenasymmetrie der Chloroplastenlamellen nimmt interessanterweise Calvin [20] zur Verbindung des photochemischen Apparates mit dem Photosynthese-Kohlenstoff-Cyklus und dem Krebs-Cyklus [9, 21] in Anspruch.

Chloroplastenentwicklung

Einen entscheidenden Beitrag zur Frage der Kontinuität der Proplastiden konnte die vorliegende Untersuchung nicht erbringen. In den jüngsten untersuchten Meristemzellen der Gerste konnten die Proplastiden unter den 4 beobachteten Organellen nicht mit Sicherheit identifiziert werden. So bleibt diese Frage einstweilen offen [58, 163].

Bezüglich der Kontinuität des Plastidenzentrums bestehen im Augenblick soviele Auffassungen wie Möglichkeiten, trotz weitgehend übereinstimmender elektronenmikroskopischer Abbildungen. Leyon [88, 90] vertritt die Ansicht, dass den jüngsten Proplastiden das Zentrum fehlt und es im Zuge der Plastidenentwicklung gebildet wird. Zu einer ähnlichen Vorstellung sind Heitz und Maly [68] sowie Düvel [27] auf Grund fluoreszensmikroskopischer Untersuchungen gelangt. Mühlethaler [103] hält einige der stark elektronenstreuenden Organellen („osmiophile Granula") in den jüngsten Meristemzellen für das Plastidenzentrum („primäre Granen") und nimmt die Bildung einer „Stromahülle" um das Plastidenzentrum an. Ein Beweis für diese Auffassung konnte nicht gegeben werden. In einer grossen Zahl von lichtmikroskopischen Untersuchungen haben Strugger und seine Mitarbeiter versucht, den Beweis für die Persistenz des Plastidenzentrums („Primärgranum") zu erbringen (Lit. zusammenstellung bei [150 a]). In den drei letzten vorliegenden Arbeiten wurde danach getrachtet, diese mit Schärfe vertretene Hypothese für *Helianthus* und *Chlorophytum* elektronenmikroskopisch zu unterbauen [150 a, 113, 114]. Bei *Helianthus* werden vorwiegend Proplastiden mit Stärkekörnern abgebildet. In diesen deuten die Autoren bestimmte „osmiophile lamellenartige" Bereiche als Plastidenzentrum. Die stärkeführenden Proplastiden von *Aspidistra* ([88] Abb. 1) und der Gerste können ein Zentrum enthalten, hingegen sind die jüngsten Proplastiden stärkefrei (vgl. auch [150 a], S. 715). Für *Helianthus* wird nur eine stärkefreie Proplastide mit einem „lamellierten Primärgranum" wiedergegeben. Diese Proplastide zeigt ein aufgelockertes „Stroma", wie das zumindest für die jüngsten Proplastiden der Gerste nicht gefunden wurde. Die zu dieser

Frage interessierenden Bilder der Arbeit an *Chlorophytum* ([113], Abb. 1–3) scheinen mir die Persistenz des Plastidenzentrums nicht belegen zu können. Abb. 1 enthält vermutlich eine relativ alte Proplastide, in welchem die das Plastidenzentrum umgebende Grundsubstanz bereits die starke Auflockerung zeigt. Gerade charakteristisch für die jüngsten Plastidenstadien ist aber die ausserordentlich dichte Struktur, wie sie in Abb. 2 und 3 von *Chlorophytum* deutlich zum Ausdruck kommt. Für diese Bilder ist Perner selbst bezüglich der Anwesenheit des „Primärgranums" unsicher. Diese Bilder stehen im übrigen in auffallender Übereinstimmung zu den vermutlich chlorophyllfreien Proplastidenbildern der Gerste (Abb. 24, 26, 31–36, 40). Nach den vorliegenden Bildern der Gerste scheint mir die sekundäre Entstehung des Plastidenzentrums eher richtig als seine Persistenz. Die bezüglich der Entstehung des Zentrums geäusserte Kritik, dass das Fehlen des Plastidenzentrums in den elektronenmikroskopischen Bildern der jüngsten Proplastiden auf schiefer oder einseitiger Schnittführung beruhe, ist nicht stichhaltig. Warum denn sollte es in den älteren Plastiden im Schnitt so viel öfter getroffen werden, wo doch die Aussicht einen Schnitt durch die dann um das Plastidenzentrum breitere und aufgelockerte Grundsubstanz allein zu erhalten, bedeutend grösser ist? Die Frage der Entstehung des Plastidenzentrums wird in laufenden Untersuchungen an *albina*-Mutanten, die einen frühen Block der Plastidenentwicklung besitzen, bearbeitet.

Das zunächst isodiametrische Plastidenzentrum kann eine kristallartige Struktur annehmen [64, 67, 89, 90, 114]. Trotz intensiver Suche konnte bei der Gerste eine solche ausgesprochen kristallartige Struktur bisher nicht gefunden werden. Das zeigt, dass eine Ausfaltung der Chloroplastenschichten nicht unbedingt mit einer „Kristallisation" des Plastidenzentrums verbunden sein muss.

Ob mehr als ein Plastidenzentrum auftreten kann, ist im vorliegenden Material nicht zu klären. Möglicherweise enthalten die Plastiden der Abb. 52 und 57 zwei Plastidenzentren.

Was die weitere Entwicklung der Proplastiden der Gerste betrifft, steht diese in guter Übereinstimmung mit den Befunden an *Aspidistra* [88, 90]. Beim Gerstenchloroplasten erfolgt eine Schichtenausfaltung aus dem Plastidenzentrum und eine nachfolgende lokale Lamellenbildung an voneinander unabhängigen Orten im Chloroplasten. Diese Lamellenstücke verdicken und spalten sich und wachsen in der Fläche bis der Chloroplast einheitlich durchlamelliert ist.

Die Unterschiede zu der Deutung von Strugger und Perner lassen sich teilweise aus der unterschiedlichen Terminologie erklären (vgl. oben). So

dürften die „multigranulären Jungchloroplasten" den Stadien mit der lokalen Lamellenbildung entsprechen. Diese Orte der lokalen Lamellenbildungen erscheinen lichtmikroskopisch als „Grana", obgleich sie diesen nicht direkt homolog sind, und wurden lichtmikroskopisch wohl zuerst von Twiss [154] beim Mais gesehen und abgebildet. Die Grana der ausdifferenzierten Chloroplasten werden erst verhältnismässig spät, nachdem eine durchgehende Lamellierung des Chloroplasten erfolgt ist, aufgebaut. In bestimmten Zellen kann sie, wie beim Mais festgestellt, unterbleiben. Wahrscheinlich enthalten die Orte lokaler Lamellenbildung wie das Plastidenzentrum Chlorophyll und so ist es nicht möglich zu entscheiden, ob Heitz und Maly bzw. Düvel Plastiden im Stadium der Lamellenbildung, solche im Stadium der Granadifferenzierung oder beides beobachtet haben.

Chlorophylldefekte Mutanten und Biochemie der Plastiden

Die genetisch bedingten Chlorophylldefekte umfassen einfarbige und gescheckte, letale und vitale Typen. Trotz morphologischer Ähnlichkeit können sie durch ein stabiles Gen, durch Deficiencies, durch ein labiles Gen, plasmonisch oder plastidomisch bedingt sein.

Die Chloroplasten der vitalen hellgrünen bis gelbgrünen Typen dürften eine normale submikroskopische Struktur erreichen, wie das etwa für eine gelbgrüne Mutante vom Mais festgestellt ist, die sich in ihrer Chloroplastenstruktur elektronenmikroskopisch nicht von den normalen Chloroplasten unterscheiden liess [70]. Hier handelt es sich offenbar um eine quantitative mutative Beeinflussung der Synthese und der Lichtempfindlichkeit des Chlorophylls. Für diese Typen ist charakteristisch, dass Variationen der Temperatur, Lichtintensität und Nährstoffzufuhr die Ausbleichung der Plastiden fördern oder hemmen können. Unter bestimmten Bedingungen sind die Mutanten gleich vital und grün wie die Ausgangsform. Dazu gehören auch solche Mutanten, die mehr Chlorophyll führen als der Normaltypus (vgl. [128, 129, 130], und dort cit. Lit.). Diese Veränderungen der Reaktionsnorm unter „normalen" Umweltbedingungen gleichen in gewissem Sinn der künstlich erzeugten Chlorose oder dem Etiolement ursprünglich voll entwickelter Plastiden. Dabei ist wichtig, festzuhalten, dass eine Plastidendegeneration, die einmal ein bestimmtes Stadium überschritten hat, irreversibel ist [37]. Eine vergleichende elektronenmikroskopische und biochemische Untersuchung der vitalen Chlorophyllmutanten und der Chlorose wie des Etiolements wird vor allem den Form- und Stoffwechsel des ausdifferenzierten Chloroplasten beleuchten können.

Bei einem Vergleich der Chlorophyll-Letalen, die durch Faktormutationen

bedingt sind, mit solchen, die einen ausserkaryotischen Erbgang zeigen, sind vor allem zwei Unterschiede beachtenswert. In den hier untersuchten Chlorophyll-Letalen ist ein Block der Plastidenentwicklung feststellbar, d.h. die Chloroplasten erreichen nicht das voll ausdifferenzierte Stadium. Weiter konnte keine Vakuolisierung der Chloroplasten im Endzustand festgestellt werden. Das steht mit lichtmikroskopischen Beobachtungen an anderen Gerstenmutanten in Übereinstimmung [52].

Bei den bisher untersuchten Chlorophylldefekten von *Oenothera*, sog. Plastidommutanten, [151] erreichen die Chloroplasten einen ausdifferenzierten Zustand mit Grana- und Stromalamellen. Erst dann setzt früher oder später in der Pflanzenentwicklung eine Vakuolisierung der Plastiden und eine Zerstörung ihrer Struktur ein. So zeigt eine weisse Mutante des *suaveolens*-Plastidoms die Vakuolisierung bereits früh und sehr extrem, während eine gelbgrüne Mutante der *suaveolens*-Plastiden in dieser Hinsicht gemässigter ist. Offenbar lässt sich diese Vakuolisierung und Zerstörung der Plastiden durch schwache Lichtintensitäten hinauszögern [132]. Da dieser Unterschied der genom- und plasmatisch bedingten Chlorophyll-Letalen vielleicht ein allgemeiner und grundsätzlicher ist, seien einige neuere lichtmikroskopische Strukturanalysen nicht mendelnder Plastidendefekte besprochen.

So ist für nicht mendelnd vererbte Chlorophylldefekte von *Nicotiana* und *Nepeta* eine starke Vakuolisierung der Plastiden charakteristisch [166]. Bei *Chlorophytum comosum* [150] zeigen die blassen Plastiden der albicaten Blattzonen einer albomaculaten Form eine Vakuolisierung, wie sie für *Oenothera* gefunden wurde. Schliesslich wurde dasselbe für albomaculate Formen von *Antirrhinum majus* gezeigt und ausdrücklich betont, dass bei starker Belichtung die Vakuolisierung sehr früh auftritt [93]. Bei letzterem Objekt zeigen die jungen Plastiden in 4 von 5 albomaculaten Fällen eine deutliche Granastruktur und es ist wahrscheinlich, dass gerade wie bei *Oenothera* zunächst normal strukturierte Chloroplasten ausgebildet werden, die dann „degenerieren". Dieser Prozess beginnt zunächst mit dem lichtmikroskopischen Auftreten von unregelmässig grossen „Granen". Im weiteren Verlauf enthalten die Plastiden wenige stark vergrösserte „Granen" und schliesslich bleibt ein einziges riesiges „Granum" übrig. Darauf setzt die vollständige Vakuolisierung ein. Das steht in guter Übereinstimmung mit den elektronenmikroskopischen Befunden bei *Oenothera*. Das Stadium mit den unregelmässig grossen „Grana" entspricht der Abb. 5 bei Stubbe und v. Wettstein. Vereinzelt sind lichtmikroskopisch die wirklichen Grana noch erkennbar, während die sog. „grösseren Grana" die auseinander gesprengten Schichten darstellen. Auch das Stadium mit dem einzigen riesigen „Granum"

ist aus der *Oenothera*-arbeit, Abb. 4, verständlich. Die noch übrig gebliebenen Schichten und Lamellensysteme bilden einen zusammenhaltenden Kern, um den die gequollene Grundsubstanz und Chloroplastenrandschicht in Form eines Hofes liegt. Es ist durchaus möglich, dass zwei oder drei unabhängige solche Kerne gebildet werden können. Eine Auflösung dieses Kernes in einzelne Schichten und Lamellen wie im Elektronenmikroskop ist lichtmikroskopisch offenbar nicht möglich. Die entwickelte Vorstellung erklärt auch die „multi-" und „unigranulären" Plastiden der albicaten Zone von *Chlorophytum*, obgleich Strugger und Losada-Villasante [150] ihren Befunden die Deutung geben, dass die Plastiden dieser Gewebe kein ausdifferenziertes Entwicklungsstadium erreichen. So halten sie die „multigranulären" Plastiden der Blattbasis für die weiterentwickelten, obgleich allgemein an der Blattbasis die jüngeren Plastidenstadien zu finden sind. Vermutlich entsprechen die „multigranulären" Plastiden von *Chlorophytum* den ersten Degenerationsstadien der anderen eben besprochenen Objekte und die Plastiden mit der normalen ausdifferenzierten Struktur wurden bei *Chlorophytum* nicht erfasst. Die „unigranulären" Plastiden wären demnach die älteren Degenerationsstadien mit dem Kern. Derselbe Entwicklungsprozess wie für *Antirrhinum* und *Oenothera* lässt sich aus den Bildern von *Nepeta* und *Nicotiana* entnehmen. Die lichtmikroskopische Übereinstimmung zwischen diesen Objekten und *Antirrhinum* ist auffallend.

Eine Erklärung der plastidomisch bedingten Schecken ist die Entmischung verschiedener selbständiger Plastidensorten im Laufe der Pflanzenentwicklung [10, 120, 121]. Correns hat zahlreiche kritische Einwände gegen diese Vorstellung vorgebracht und sie abgelehnt [24]. Sie verlangt Mischzellen mit zwei verschiedenen Plastidensorten. Maly und Wild [93] haben für 4 albomaculate *Anthirrhinum*-Typen erkannt, dass solche eventuellen Mischzellen leicht mit „Übergangszellen" verwechselt werden können, d.h. solchen in denen verschiedene Chloroplastenstadien des Degenerationsprozesses gemeinsam in einer Zelle vorliegen, eine Erscheinung, die auch bei *Oenothera* zu beobachten ist. Schliesslich berichten Maly und Wild von einer weiteren albomaculaten Form, in der sie echte Mischzellen gefunden zu haben glauben. Die Chloroplasten dieser Form zeigen lichtmikroskopisch wenige grosse „Grana", also ein für die Degeneration charakteristisches Stadium. Soweit aus der Arbeit ersichtlich, verharren die Plastiden offenbar lange in diesem Stadium, so dass in den hellgefärbten Blattpartien eine grosse Einheitlichkeit der Plastiden in Bezug auf ihre Struktur erreicht wird. Es wird von Interesse sein, ob diese Plastiden in ihrer Entwicklung wie bei den anderen Typen ein normales Chloroplastenstadium mit Stroma- und

Granalamellierung erreichen und die vermeintlichen Mischzellen nicht doch auch Übergangszellen mit noch normal strukturierten Chloroplasten und einem Degenerationsstadium darstellen. Die abweichende Art dieser Übergangszellen dürfte aus einem anderen Entwicklungsrhythmus erklärbar sein.

Wenn, wie es mir gegenwärtig scheint, die nicht mendelnden Chlorophylldefekte allgemein eine sekundäre Degeneration normal ausgebildeter Chloroplasten und nicht eine Entwicklungshemmung der Chloroplasten darstellen, haben die nicht mendelnden Erbfaktoren geringen Einfluss auf die Plastidenentwicklung selbst. Der Aufbau der Chloroplastenstruktur würde allein von Kerngenen bestimmt, deren Ausfall eine Blockade der Plastidenentwicklung bedingt. Durchlaufen die Plastiden der nicht mendelnden Chlorophylldefekte allgemein ein vielleicht zuweilen auch nur kurzes Stadium mit voll ausdifferenzierter Struktur, so dürften auch die Proplastiden strukturell gleich sein und die gleichen Entwicklungspotenzen besitzen. Vielleicht ist dann doch Correns' Auffassung eines labilen Plasmazustandes oder eine Lage nicht mendelnder Erbfaktoren im Plasma richtiger?

In pflanzlichen Organismen besteht ein bedeutender Unterschied bezüglich der Bildung von Chlorophyll im Licht und im Dunkeln. Zahlreiche Algen wie *Chlorella* und *Chlamydomonas* können Chlorophyll im Dunkeln bilden. Ebenfalls ist das für die Kotyledonen der Coniferen [126] bekannt. Die meisten höheren Pflanzen können im Dunkeln kein Chlorophyll oder höchstens Spuren davon bilden [44, 137]. Bei *Chlorella* und *Chlamydomonas* lässt sich dieser Unterschied durch eine einfache Faktormutation erzielen [45, 127]. Diese Mutanten können bei Anzucht im Licht Chlorophyll in normaler Menge synthetisieren und assimilieren. Im Dunkeln gezogen, sind sie dagegen gelb und chlorophyllfrei. Eine solche Mutante von *Chlamydomonas* aus Dunkelkultur wurde elektronenmikroskopisch untersucht und dabei das Fehlen der Lamellierung der Chromatophoren festgestellt. Ebenso zeigen Stämme von *Euglena* und *Poteriochromonas*, denen eine Dunkelsynthese des Chlorophylls nicht möglich ist, bei Dunkelkultur ein Verschwinden der Chromatophorenschichten und Lamellen zusammen mit dem Abbau der Pigmente [164]. Dieser Vorgang ist reversibel. Bereits diese Autoren vermissen eine strikte Parallelität der Chlorophyllsynthese und der Bildung von Chromatophorenlamellen. Zweifellos ist für die Bildung von Chromatophoren- bzw. Chloroplastenlamellen die Anwesenheit von Chlorophyll eine notwendige Voraussetzung. Die Gerstenmutanten und die Chloroplasten der Moossporen zeigen uns, dass aber umgekehrt für die Synthese oder Anwesenheit von Chlorophyll die Lamellenstruktur keine notwendige Voraussetzung ist. Die Mutante *xantha*-3 lehrt weiter, dass die Stabilität

des Chlorophylls (d.h. ein Überwiegen der Synthese gegenüber dem Abbau) in den Chloroplasten der Blätter mit der Anwesenheit von Lamellen verbunden ist. Auf der anderen Seite zeigen die Plastiden in den Moosporen dass das Chlorophyll in ihnen stabil sicher mehr als 10 Jahre erhalten werden kann, ohne dass ausgeprägte Grana- oder Stromalamellen vorhanden sind. Diese Überlegungen führen dazu, dass das Chlorophyll nicht nur in den Granalamellen sondern auch in anderen Chloroplastenstrukturen vorhanden sein dürfte. Die Grana enthalten eine besonders hohe Konzentration fluoreszierenden Chlorophylls. Nach Thomas, Post und Vertregt [153] gibt die Oberfläche der Granalamellen die für Chlorophyll charakteristische Silbernitratreduktion. Ob auch die Stromalamellen Chlorophyll enthalten ist nicht mit Sicherheit bekannt. Hingegen besitzen nach der Mutantenanalyse die Globuli Chlorophyll und vielleicht auch gelbe Pigmente. Es wird von Interesse sein, ob die Globuli Lipoide und Proteine enthalten, also aus einem Lipochromoproteid oder einem Chromolipoid bestehen.

Die Feststellung, dass Chlorophyll in verschiedenen Chloroplastenstrukturen vorhanden ist, aktualisiert die Frage, in welchen Strukturen es möglicherweise in nicht fluoreszierendem Zustand vorkommt. Ein nicht fluoreszierendes Chlorophyll im lebenden Chloroplasten ist diskutiert und gefordert worden [105, 138, 100].

Die Natur der Globuli wurde unterschiedlich bewertet. So werden sie nach Frey-Wyssling [36] als durch „Entmischung entstandene Lipoidtröpfchen" gedeutet, während Steinmann und Sjöstrand [146] in ihnen einen Reservestoff für möglich halten. Die Befunde an der *xantha*-Mutante sind mit einem Entmischungsartefakt schwer vereinbar. Die Globuli sind aber auch die Bausteine der Augenflecke von Flagellaten [164, 127]. Der Augenfleck kann je nach der Art innerhalb des Chromatophors oder ausserhalb von ihm liegen [39]. Die Globuli der Augenflecken in den Flagellaten zeigen die gleiche Grösse wie die Globuli der Gerste oder anderer höherer Pflanzen. Die Carotinoide der Augenflecken sind in Öl gelöst und dürften Chromolipoide darstellen [108, 145]. Solche Globuli kommen vielleicht auch in den Chromoplasten der gelben Kronblätter von z.B. *Ranunculus* [37] vor. Die Ähnlichkeit der Augenfleckenkomponenten und der Globuli in den Chloroplasten unterstützt die in dieser Arbeit dargelegte Auffassung (S. 460), dass die Globuli der Plastiden grüne und gelbe Pigmente wohl in Form eines Chromolipoides enthalten und als Vorstufe oder Reserve funktionieren.

Die Synthese des Chlorophylls wurde mit der Isotopenmethode [42] und mit verschiedenen Mutanten von *Chlorella* [15, 46] studiert. In den höheren Pflanzen wurde das Protochlorophyll als letzte Vorstufe des Chlorophyll *a*

sichergestellt [77, 141, 76, 79, 142, 144, 155, 156]. Die Versuche dieser Autoren, die fast ausschliesslich an Gerste durchgeführt wurden, stimmen darin überein, dass beim Ergrünen etiolierter Keimlinge zunächst ausschliesslich Chlorophyll *a* aus dem im Dunkeln synthetisierten Protochlorophyll gebildet wird und dass Chlorophyll *b* erst sekundär in bedeutendem zeitlichen Abstand auftritt. Das steht im Widerspruch zu den hier mitgeteilten Befunden, dass in der normalen Entwicklung das Chlorophyll *b* zuerst oder zumindest zuerst in grösserer Menge auftritt. In eigenen kürzlich ausgeführten Versuchen konnte papierchromatographisch gefunden werden, dass auch bei der hier verwendeten reinen Gerstenlinie beim Ergrünen etiolierter Keimlinge zunächst Chlorophyll *a* in grösseren Mengen auftritt. Offenbar ist daher der Ergrünungsprozess etiolierter Keimlinge nicht mit der normalen Blatt- und Plastidenentwicklung (durch Testen unterschiedlich alter Blättchen) vergleichbar. In diesem Zusammenhang wird die Plastidenstrukturentwicklung in etiolierten Keimlingen näheren Aufschluss geben können. Die Frage, wann das Chlorophyll in der Plastidenentwicklung gebildet wird, lässt sich auf Grund der *xantha*-3-Mutante einengen. Sie beginnt vor der Ausfaltung der Plastidenschichten und dürfte in der Phase der Schichten- und Lamellenbildung besonders stark sein. Die Isotopenstudien haben ergeben, dass eine Chlorophyllsynthese auch ständig im ausgewachsenen Chloroplasten vor sich geht, da der Chlorophyllgehalt eines Roggenblattes in 24 Std. etwa zur Hälfte erneuert wird [42].

Die ersten biochemischen Untersuchungen an Chlorophyll-Letalen stammen von v. Euler und seinen Mitarbeitern ([32] und dort cit. Lit.). Vor allem konnte eine Beeinflussung der Katalase in *albina*-Mutanten festgestellt werden. Zahlreiche Untersuchungen liegen über den Pigmentgehalt von Chlorophyll-Letalen im Endzustand ihrer Keimlingsentwicklung vor (vgl. z.B. [106]). Die Pigmentausstattung in diesem Endzustand ist stark von Licht- und Temperatureinflüssen abhängig. Aus den Pigmentanalysen der *xantha*-3-Mutante während der Entwicklung geht hervor, dass solche Pigmentanalysen des Endzustandes keine direkte Auffassung über den genetischen Block und die Möglichkeit zur Pigmentbildung vermitteln. In vielen Chlorophyll-Letalen dürften die Umwelteinflüsse nur den Abbau der Pigmente verändern bzw. ihre fortgesetzte Synthese hemmen, nicht aber den genetischen Block modifizieren. So ist auch etwa für die von Highkin [69] beschriebene Gerstenmutante, der Chlorophyll *b* fehlt, nicht erwiesen, ob dieses nicht gebildet wird oder ob es sekundär gänzlich zerstört wird. Zu diesem Mutantentypus gehört auch eine analysierte *albina*-Form vom Mais [78, 79]. In dieser Mutante wird Protochlorophyll im Dunkeln in grösserer

Menge als normal gebildet und bei Belichtung entsteht Chlorophyll *a*, das aber sehr leicht und rasch zerstört wird. In einer weissen Mutante von *Helianthus annuus* [158], die in Bezug auf die Pigmentbildung der eben beschriebenen Maismutante ähnlich ist, konnte eine Erhaltung des Chlorophylls durch extrem niedrige Lichtintensitäten erreicht werden. Hier tritt die Frage scharf hervor, ob es sich um einen unvollständigen Stoffwechselblock handelt, wie er aus der biochemischen Genetik etwa bei den temperaturabhängigen Mutanten von *Neurospora* und anderen niederen Organismen bekannt ist (vgl. [157]).

Während die eben besprochenen Mutanten nicht die Chlorophyllsynthese betreffen, zeigen die Mutanten von Granick an *Chlorella* [15, 45, 46], dass solche Mutanten zu erhalten sind. Eine kürzlich veröffentlichte Untersuchung einer Mutante von *Arabidopsis Thaliana* [124] gibt den ersten Fall für einen genetischen Block der Chlorophyllsynthese höherer Pflanzen. Bei dieser Mutante ist die photochemische und enzymatische Umwandlung von Protochlorophyll in Chlorophyll *a* offenbar vollständig blockiert. Der Block liess sich durch einen Extrakt normaler etiolierter Keimlinge aufheben.

Wenn auch die nähere biochemische Aufklärung der hier untersuchten Chlorophyll-Letalen weiteren Untersuchungen überlassen bleiben muss, so ist die zunehmende biochemische Aufklärung solcher Mutanten zusammen mit einer Analyse des Formwechsels der Plastiden und ihrer submikroskopischen Bausteine ein Weg, die verschiedenen Prozesse der Pigmentbildung, der Photosynthese mit ihren Teilprozessen und des Stoffwechsels der Chloroplasten bestimmten Strukturen makromolekulärer Grösse zuzuordnen. Dabei wird die Lokalisation der Pigmente, Proteine und Lipoide im Chloroplasten das nächste Ziel sein. Dadurch wird vielleicht letztlich ein Verständnis des uns gerade erst bekanntgewordenen komplizierten submikroskopischen Baues der Chloroplasten möglich. Es ist besonders erfreulich, dass gleichzeitig die Wirkung einzelner Gene in der untersten Domäne der Morphologie erfasst werden kann. Wenn wir bedenken, dass 250–300 Loci Chlorophyllmutationen bei der Gerste geben können, besteht die Aussicht, eine bedeutende Zahl verschiedener Stufen in der synthetischen Kette, die zur Bildung der Plastidenbestandteile führt, zu erfassen. Ein solches Material gibt reiche Möglichkeit, die Fragen biochemischer und struktureller Pleiotropie der Genwirkung an höheren Pflanzen erneut in Angriff zu nehmen. Nicht zuletzt gibt uns die biochemische und submikroskopische Analyse der Chlorophyll-Letalen ein neues Handwerkzeug für die Abgrenzung der Wirkung der Gene und der plasmatischen Erbfaktoren auf die Entwicklung und Funktion der Plastiden.

Der elektronenmikroskopische Teil der vorliegenden Arbeit ist im Biochemischen Institut der Universität Uppsala durchgeführt worden, und es ist mir ein besonderes Bedürfnis, dem Direktor dieses Institutes, Herrn Professor A. Tiselius meinen verbindlichsten Dank für die grosszügig gewährten Arbeitsmöglichkeiten und sein stetiges Interesse auszusprechen. Die Untersuchungen wurden in Zusammenarbeit mit anderen Mitgliedern der schwedischen „Arbeitsgruppe für theoretische und angewandte Mutationsforschung an Pflanzen" durchgeführt. Herr Professor Å. Gustafsson unterstützte mich mit Rat, Tat und Kritik und ich möchte nicht nur dafür dankbar sein sondern auch für die Gabe, das Experimentieren in seinem Arbeitskreise zu einem Genuss werden zu lassen. Herr Dr. N. Nybom hat die Pigmentanalysen gefördert und Herr Dr. H. Leyon war auch diesmal ein besonders wertvoller Freund im Laufe der Untersuchungen. Der Landwirtschafts-Forschungsrat und die schwedische Akademie der Wissenschaften („Lars-Hiertas-minne-fond", „Hahnska donationen" und „Hierta Retzius' fond för vetenskaplig forskning") haben die finanzielle Grundlage geschaffen.

SUMMARY

Considerable knowledge of the physiology of gene action in morphological and biochemical mutants of different organisms has been gained in recent years. The present investigation deals with the gene action on the submicroscopic structure of the plastids, employing chlorophyll lethals of barley.

The submicroscopic structure of the fullgrown chloroplast in barley leaves, as seen in the electronmicroscope, can be traced in Figs. 1 and 2. Within the laminar system of the stroma the grana appear as sharply defined areas, judged by their heavier contrast and their accentuated parallel lamellation. The stroma- and grana-lamellae are grouped in 6 to 12 layers. The number of grana-lamellae within one layer varies from 2 to 14, with some preponderance for 6 and 8. The thickness of the grana-lamellae was determined at 40 ± 20 Å and that of the stroma-lamellae at 75 ± 25 Å. Both grana- and stroma-lamellae are subdivisible into two fine layers of 10 to 20 Å in diameter. The ratio of stroma- to grana-lamellae as well as that of their fine layers is 1:2. The chloroplast layers are connected by stroma-lamellae, resulting in a network structure. The number of grana per chloroplast was estimated at 160–200. The results of the submicroscopic analysis in the barley chloroplast are summarized schematically in Figs. 22 and 23.

In the youngest meristematic leaf cells, so far investigated, four different organells were found. Their ontogenetic interrelationship and their relationship to plastids and mitochondria is not fully clear. In older meristimatic cells (Fig. 24) the proplastids and mitochondria are to be distinguished by their submicroscopic properties from one another and from other organells.

The development of the barley chloroplast may be summarized as follows (Figs. 46–70):

1. In the undifferentiated proplastid the plastid center is formed.
2. Starch grains accumulate in the proplastids.
3. The material for the formation of the chloroplast layers protrudes radially from the plastid center.
4. Within the chloroplast layers the first pieces of lamellae are formed locally and at mutually independent points.
5. The short lamellae multiply intensively by a process of thickening and splitting.
6. These pieces of lamellae connected in pairs grow radially until they come into contact with one another.
7. The pieces of lamellae fuse and the plastid as a whole becomes transversed by lamellae. The plastid center disappears.
8. The chloroplast layers multiply.
9. The grana are differentiated within certain areas by heterogeneous deposition of material and one further cleavage of the lamellae.
10. Throughout development the globuli are present and show an increase towards the end of the chloroplast differentiation.

Three processes seem necessary, to explain the formation of the chloroplast structure: protrusion of folds, thickening and splitting, fusion and division perpendicular to the plane of the lamellae. It is of special interest that the lamellae transversing the whole chloroplast are formed from parts of macromolecular size.

The *albina* type (Figs. 71–77) investigated shows essentially normal early proplastids enclosed by a double membrane. The plastid center as well as some globuli are formed. There is no differentiation of ordered layers, lamellae, nor of grana. Thus the differentiation does not proceed beyond the earliest stages. However, the plastid increases considerably in size, almost reaching that of a fullgrown chloroplast. The gene change has blocked the development of the submicroscopic chloroplast structure at an early stage but not the growth of the plastid as a whole.

The yellow-green mutant *xantha*-3 (Figs. 78–85) is blocked at a later intermediate stage of chloroplast development. There is a normal formation of the plastid center and some layers are even produced out of the center. The differentiation of lamellae cannot be accomplished in this mutant. Instead of the formation of lamellae, the globuli accumulate in large masses

gradually filling up the interior of the plastids. As a consequence of the gene change their further functioning seems to be arrested. It is a block mutant which has lost the ability to perform a step in the biosynthetic chain leading to the chloroplast structure.

In older stages of the plastids in this mutant the globuli are broken down, and although the plastids still increase in size their inner structure ends in a disordered state.

With the aim of studying the biochemical nature of the block in mutant *xantha*-3, pigment analyses were performed in different developmental stages. The contents of chlorophyll *a* and *b* and the yellow pigments in developing plastids of the normal barley strain increase up to a certain level, whereafter they remain constant. This level is reached independently by the different pigments. In contrast to this normal development the pigment content of *xantha*-3 shows a typical optimum curve. At the optimum coinciding with the large accumulations of globuli in the plastids, higher contents of pigments are found than are normally present in corresponding stages of plastid development. In addition there is more chlorophyll *b* than in any investigated normal chloroplast. This strongly suggests that chlorophyll *b*, and probably all pigments, are located in the globuli. Parallel to the morphological destruction of the globuli the pigment content diminishes, chlorophyll *b* suffering most. The mutant thus shows no genetical block of pigment synthesis. Knowledge of the submicroscopic and chemical pattern of chlorophyll lethals greatly facilitates a better understanding of the developmental processes in the plastids and provides a means of localizing substances in specific submicroscopic structures.

Some results concerning plastids in spores of the moss, *Funaria*, are reported. They do not lend support to the view of a direct morphological and genetical continuity of the grana structure that is held by some authors.

Some other organells in the cytoplasm, including mitochondria of barley, the moss *Funaria* and the brown alga *Fucus* are described.

The discussion centers upon the problem of the effect of mendelian and non-mendelian factors producing chlorophyll defects in plants. Judging from the studies on barley and *Oenothera* as well as from recent light-microscopic analyses in other objects, the difference between gene or factor mutations and plastidom mutations is as follows: In the plastidom mutants the plastids reach a completely differentiated chloroplast structure and are secondarily destroyed by a process of swelling and vacuolization. Hence the "plastidom" does not seem to determine the formation of the chloroplast structure at all. The gene mutations (in a wide sense) resulting

in chlorophyll lethals are primarily concerned with blocks in the development of the submicroscopic chloroplast structure. This is not necessarily connected with a block in the chlorophyll synthesis.

LITERATUR

1. Afzelius, B., *Exptl. Cell Research* **10**, 257 (1956).
2. —— *ibid.* **11**, 67 (1956).
3. Bahr, G. F., *ibid.* **5**, 551 (1953).
4. —— *ibid.* **7**, 457 (1954).
5. —— *ibid.* **9**, 277 (1955).
6. Bahr, G. F. und Moberger, G., *ibid.* **6**, 506 (1954).
7. Bairati, A. und Lehmann, F. E., *ibid.* **5**, 220 (1953).
8. Bartels, F., *Planta* **45**, 426 (1955).
9. Bassham, J. H., Shibata, K., Steenberg, K., Bourdon, J. und Calvin, M., *J. Am. Chem. Soc.* **78**, 4120 (1956).
10. Baur, E., *Z. ind. Abst. Vererbungslehre* **1**, 330 (1909).
11. Beadle, G. W., *Chem. Rev.* **37**, 15 (1945).
12. Beadle, G. W. und Tatum, E. L., *Proc. Natl. Acad. Sci. U.S.A.* **27**, 499 (1941).
13. Beams, H. W. und Tahmisian, T. N., *Exptl. Cell Research* **6**, 87 (1954).
14. Beauverie, J., *Rev. Cytol. et Cytophysiol. végétales* **3**, 80 (1938).
15. Bogorad, L. und Granick, S., *Proc. Natl. Acad. Sci. U.S.A.* **39**, 1176 (1953).
16. Böing, J., *Protoplasma* **45**, 55 (1955).
17. Bünning, E., Entwicklungs- und Bewegungsphysiologie der Pflanze. Springer, Berlin, 539 S., 1953.
18. Butenandt, A., *Naturwissenschaften* **40**, 91 (1953).
19. Butenandt, A., Weidel, W. und Becker, E., *Naturwissenschaften* **28**, 447 (1940).
20. Calvin, M., The photosynthetic cycle. U.S. Atom. Energ. Comm. UCRL-2924, 1955.
21. Calvin, M. und Bassham, J. A., *International Conference on the Peaceful Uses of Atomic Energy* **12**, 347 (1955).
22. Claes, H., *Z. Naturforsch.* **9b**, 461 (1954).
23. Comar, C. L. und Zscheile, F. R., *Plant Physiol.* **17**, 198 (1942).
24. Correns, C. und Wettstein, F. von, Handbuch der Vererbungswissenschaft. Borntraeger, Berlin, **II**. H, 159 S. 1937.
25. Davis, E. A., *Am. J. Bot.* **39**, 535 (1952).
26. Demerec, M., *Cold Spring Harbor Symposia Quant. Biol.* **3** (1935).
27. Düvel, D., *Protoplasma* **44**, 239 (1954).
28. Egle, K., *Naturwissenschaften* **40**, 569 (1953).
29. Ehrenberg, L., *Svensk Kem. Tidskr.* **67**, 207 (1955).
30. Ehrenberg, L., Gustafsson, Å. und Wettstein, D. von, Conference on Chromosomes, Wageningen, April, 1956. Tjeenk Willink, Zwolle, Netherlands.

30 a. Ehrenberg, L. und Wettstein, D. von, Botan. Notiser **108**, 216 (1955).

31. Emerson, R. A., Beadle, G. W. und Frazer, A. C., *Mem. Cornell Agr. Exptl. Stat.* **180** (1935).
32. Euler, H. von, Festschrift der Akademie der Wissenschaften, Göttingen. S. 124, 1951.
33. Euler, H. von und Moritz, H., *Svenska Vetenskapsakad. Arkiv* **A 10**, 11 (1930).
34. Fasse-Franzisket, U., *Protoplasma* **45**, 194 (1955).
35. Frey-Wyssling, A., Submicroscopic Morphology of Protoplasm. Elsevier, Amsterdam und New York, 255 S., 1953.
36. —— Protoplasmologia. Springer, Wien, **II A**, **2**, 244 S. 1955.
37. Frey-Wyssling, A., Ruch, F. und Berger, X., *Protoplasma* **45**, 97 (1955).
38. Geitler, L., *Fortschr. Bot.* **17**, 2 (1955).
39. —— Handbuch der Pflanzenphysiologie. Springer, Berlin, **1**, S. 123, 1955.
40. Godnev, T. N. und Shlik, A. A., *Doklady Akad. Nauk SSSR* **91**, 599 (1953).
41. —— *ibid.* **95**, 301 (1954).
42. —— *International Conference on the Peaceful Uses of Atomic Energy* **12**, 358 (1955).

43. Goodwin, T. W., Moderne Methoden der Pflanzenanalyse. Springer, Berlin, **3**, 272, 1955.
44. Goodwin, R. H. und Owens, O. V. H., *Plant Physiol.* **22**, 197 (1947).
45. Granick, S., *Ann. Rev. Plant Physiol.* **2**, 115 (1951).
46. —— *Rec. Chem. Progr.* **15**, 27 (1954).
47. —— Handbuch der Pflanzenphysiologie. Springer, Berlin, **1**, 507, 1955.
48. Granick, S. und Porter, K. R., *Am. J. Bot.* **25**, 558 (1947).
49. Grave, G., *Protoplasma* **44**, 273 (1954).
50. Gustafsson, Å., *Hereditas* **24**, 33 (1938).
51. —— *Kgl. Fysiograf. Sällskap. Lund Handl.* N.F. **51**, 3 (1940).
52. —— *Hereditas* **28**, 483 (1942).
53. —— *ibid.* **32**, 263 (1946).
54. —— *ibid.* **33**, 573 (1947).
55. —— Procedings from the Radiobiological Symposium in Liège. Butterworth, London, 282, 1955.
56. Gustafsson, Å. und Nybom, N., *Hereditas* **36**, 113 (1950).
57. Gustafsson, Å., Nybom, N. und Wettstein, U. von, *ibid.* **36**, 383 (1950).
58. Gustafsson, Å. und Wettstein, D. von, Handbuch der Pflanzenzüchtung. Parey, Berlin, **1**, 612, 1956.
59. Hadorn, E., Letalfaktoren. Thieme, Stuttgart, 338 S., 1955.
60. Hadorn, E. und Kühn, A., *Z. Naturforsch.* **8b**, 582 (1953).
61. Hadorn, E. und Mitchell, H. K., *Proc. Natl. Acad. Sci. U. S. A.* **37**, 650 (1951).
62. Hadorn, E. und Stumm-Zollinger, E., *Rev. Suisse Zool.* **60**, 506 (1953).
63. Hall, C. E., Jakus, M. A. und Schmitt, F. O., *Biol. Bull.* **90**, 32 (1946).
64. Heitz, E., *Planta* **26**, 134 (1936).
65. —— *Exptl. Cell Research* **7**, 606 (1954).
66. —— *Nova Acta Leopoldina* **17**, 517 (1955).
67. —— *Experientia* **12**, 476 (1956).
68. Heitz, E. und Maly, R., *Z. Naturforsch.* **8b**, 243 (1953).
69. Highkin, R. H., *Plant Physiol.* **25**, 294 (1950).
70. Hodge, A. J., McLean, J. P. und Mercer, F. V., *J. Biophys. and Biochem. Cytol.* **1**, 605 (1955).
71. Holm, G., *Act. Agr. Scand.* **4**, 457 (1954).
72. Horowitz, N. H., *J. Biol. Chem.* **171**, 255 (1947).
73. —— *Advances Genet.* **3**, 33 (1950).
74. Kaja, H., *Ber. deut. botan. Ges.* **47**, 93 (1954).
75. Kausche, G. A. und Ruska, H., *Naturwissenschaften* **28**, 303 (1940).
76. Koski, V. M., *Arch. Biochem.* **29**, 339 (1950).
77. Koski, V. M. und Smith, J. H. C., *J. Am. Chem. Soc.* **70**, 3558 (1948).
78. —— *Arch. Biochem. and Biophys.* **34**, 189 (1951).
79. Koski, V. M., French, C. S. und Smith, J. H. C., *ibid.* **31**, 1 (1951).
80. Kühn, A., *Nachr. Ges. Wiss. Göttingen, Math.-Phys. Kl.* **6**, 231 (1941).
81. —— *Naturwissenschaften* **43**, 25 (1956).
82. Kühn, A. und Berg, B., *Z. ind. Abst. Vererbungslehre* **87**, 25 (1955).
83. Küster, E., *Ber. deut. bot. Ges.* **29**, 9 (1911).
84. Leitgeb, H., Bau und Entwicklung der Sporenhäute. Leuschner und Lubensky, Graz, 1884.
85. Leyon, H., *Exptl. Cell Research* **4**, 371 (1953).
86. —— *ibid.* **5**, 520 (1953).
87. —— *ibid.* **6**, 497 (1954).
88. —— *ibid.* **7**, 265 (1954).
89. —— *ibid.* **7**, 609 (1954).
90. —— *Svensk Kem. Tidskr.* **68**, 70 (1956).
91. Leyon, H. und Wettstein, D. von, *Z. Naturforsch.* **9b**, 471 (1954).
92. Lorch, W., Handbuch der Pflanzenanatomie. Borntraeger, Berlin, **VII/1**, 1931.
93. Maly, R. und Wild, A., *Z. ind. Abst. Vererbungslehre* **87**, 493 (1956).
94. Manton, I., *Proc. Leeds Phil. Lit. Soc. Sci. Sec.* **6**, 306 (1955).
95. McClintock, B., *Genetics* **29**, 478 (1944).
96. Menke, W., *Naturwissenschaften* **28**, 158 (1940).
97. Menke, W. und Koydl, E., *ibid.* **27**, 29 (1939).

98. Menke, W. und Menke, G., *Protoplasma* **46**, 535 (1956).
99. Mercer, F. V., Hodge, A. J., Hope, A. B. und McLean, J. D., *Australian J. Biol. Sci.* **8**, 1 (1955).
100. Metzner, P., *Flora* **142**, 81 (1954).
101. Meyer, A., Das Chlorophyllkorn in chemischer, morphologischer und biologischer Beziehung. Felix, Leipzig, 1883.
102. Mikosch, C., *Österr. Bot. Z.* **2**, 2 (1877).
103. Mühlethaler, K., *Protoplasma* **45**, 264 (1955).
104. —— *Fortschr. Bot.* Bd. **16**, **17**, **18** (1954, 55, 56).
105. Noack, K., *Biochem. Z.* **183**, 135 (1927).
106. Nybom, N., *Hereditas* **41**, 483 (1955).
107. —— *ibid.* **42**, 211 (1956).
108. Paech, K., Biochemie und Physiologie der sekundären Pflanzenstoffe. Springer, Berlin, 268 S. 1950.
109. Palade G. E., *Anat. Rec.* **114**, 427 (1952).
110. —— *J. Histochem. and Cytochem.* **1**, 188 (1953).
111. Pauling, L., Itano, H. A., Singer, S. J. und Wells I. C., *Science* **110**, 543 (1949).
112. Perner, E. S., *Ber. deut. bot. Ges.* **67**, 26 (1954).
113. —— *Z. Naturforsch.* **11b**, 560 (1956).
114. —— *ibid.* **11b**, 567 (1956).
115. Perutz, M. F., Liquori, A. M. und Eirich, F., *Nature* **167**, 929 (1951).
116. Pirson, A., *Fortschr. Bot.* **17**, 529 (1955).
117. Preston, R. D., The Molecular Architecture of Plant Cell Walls. London, 1952.
118. Pringsheim, N., *Jahrb. wiss. Botan.* **12**, 3 (1881).
119. Reinhardt, H., *Protoplasma* **19**, 541 (1933).
120. Renner, O., *Ber. Math. Phys. Kl. Sächs. Akad. Wiss. Leipzig* **86**, 241 (1934).
121. —— *Flora* N. F. **30**, 218 (1936).
122. Rhoades, M. M. und Carvalho, A., *Bull. Torrey Botan. Club* **71**, 335 (1944).
123. Rhodin, J., Thesis, Stockholm, 1954.
124. Röbbelen, G., *Z. ind. Abst. Vererbungsl.* **47**, 532 (1956).
125. Rosa, R. J. Della, Altmann, K. J. und Salomon, K., *J. Biol. Chem.* **202**, 771 (1953).
126. Sachs, J., *Lotos*, Z. f. Naturw. Prag. (1859).
127. Sager, R. und Palade, G. E., *Exptl. Cell Research* **7**, 584 (1954).
128. Sagromsky, H., *Kulturpflanze* **2**, 155 (1954).
129. —— *Z. Naturforsch.* **11b**, 548 (1956).
130. —— *Z. Naturforsch.* **11b**, 554 (1956).
131. Schimper, A. F. W., *Jahrb. wiss. Bot.* **16**, 1 (1885).
132. Schötz, F., *Z. Naturforsch.* **10b**, 100 (1955).
133. Schramm, G., *Z. Naturforsch.* **3b**, 320 (1948).
134. —— Biochemie der Viren. Org. Chem. in Einzeldarst. **5**. Springer, Berlin, 276 S., 1954.
135. Schroeder, W. A., Kay, L. M. und Wells, I. C., *J. Biol. Chem.* **187**, 221 (1950).
136. Senn, G., Die Gestalts- und Lageveränderung der Pflanzenchromatophoren. Engelmann, Lepizig, 1908.
137. Seybold, A., *Planta* **36**, 371 (1948).
138. Seybold, A. und Egle, K., *Bot. Arch.* **41**, 578 (1940).
139. Sjöstrand, F. S. und Hanzon, V., *Exptl. Cell Research* **7**, 393 (1954).
140. Smith, J. H. C., *Chem. Education* **26**, 631 (1949).
141. —— Photosynthesis in Plants. Ames, Iowa, Kap. **9**, 209, 1949.
142. —— Plant Physiol. **29**, 143 (1954).
143. Smith, J. H. C. und Benitez, A., Moderne Methoden der Pflanzenanalyse. Springer, Berlin, **4**, 142, 1955.
144. —— *Plant Physiol.* **29**, 143 (1954).
145. Steffen, K., Handbuch der Pflanzenphysiol. Springer, Berlin, **1**, 574, 1955.
146. Steinmann, E. und Sjöstrand, F. S., *Exptl. Cell Research* **8**, 15 (1955).
147. Stern, C., Analysis of Development. Saunders, U.S.A., S. 151, 1955.
148. Strugger, S., *Protoplasma* **43**, 120 (1954).
149. —— *Ber. deut. bot. Ges.* **69**, 177 (1956).
150. Strugger, S. und Losada-Villasante, M., *Protoplasma* **46**, 540 (1956).

150 a. Strugger, S. und Perner, E., *Protoplasma* **46**, 711 (1956).
151. Stubbe, W. und Wettstein, D. von, *ibid.*, **45**, 241 (1955).
152. Tatum, E. L., Bonner, D. M. und Beadle, G. W., *Arch. Biochem.* **3**, 477 (1944).
153. Thomas, J. B., Post, L. C. und Vertregt, N., *Biochim. et Biophys. Acta* **13**, 20 (1954).
154. Twiss, W. C., *Am. J. Bot.* **6**, 217 (1919).
155. Virgin, H., *Physiol. Plantarum* **8**, 389 (1955).
156. —— *ibid.* **8**, 630 (1955).
157. Wagner, R. P. und Mitchell, H. K., Genetics and Metabolism. Wiley, New York, 443 S., 1955.
158. Wallace, R. H. und Schwarting, A. E., *Plant Physiol.* **29**, 431 (1954).
159. Wettstein, D. von, *Hereditas* **38**, 345 (1952).
160. —— *Act. Agr. Scand.* **4**, 491 (1954).
161. —— *Z. Naturforsch.* **9b**, 476 (1954).
162. —— Symposium on the Fine Structure of Cells, Leiden, 1954. U.I.S.B. Ser. B **21**, Noordhoff, Groningen, S. 55, 1955.
163. —— *Z. Naturforsch.* **10b**, 119 (1955).
164. Wolken, J. J. und Palade, G. E., *Ann. New York Acad. Sci.* **56**, 873 (1953).
165. Wolken, J. J. und Schwertz, F. A., *J. Gen. Physiol.* **37**, 111 (1953).
166. Woods, M. W. und Du Buy, H. G., *Am. J. Bot.* **38**, 419 (1951).
167. Zscheile, F. P., Comar, C. L. und MacKinney, G. *Plant Physiol.* **17**, 666 (1942).

Abb. 1.—Zelle mit Chloroplasten der Gerste. Vergr.: 34000 ×.

Abb. 2.—Gerstenchloroplast mit Stärke. Vergr. 63000 ×.

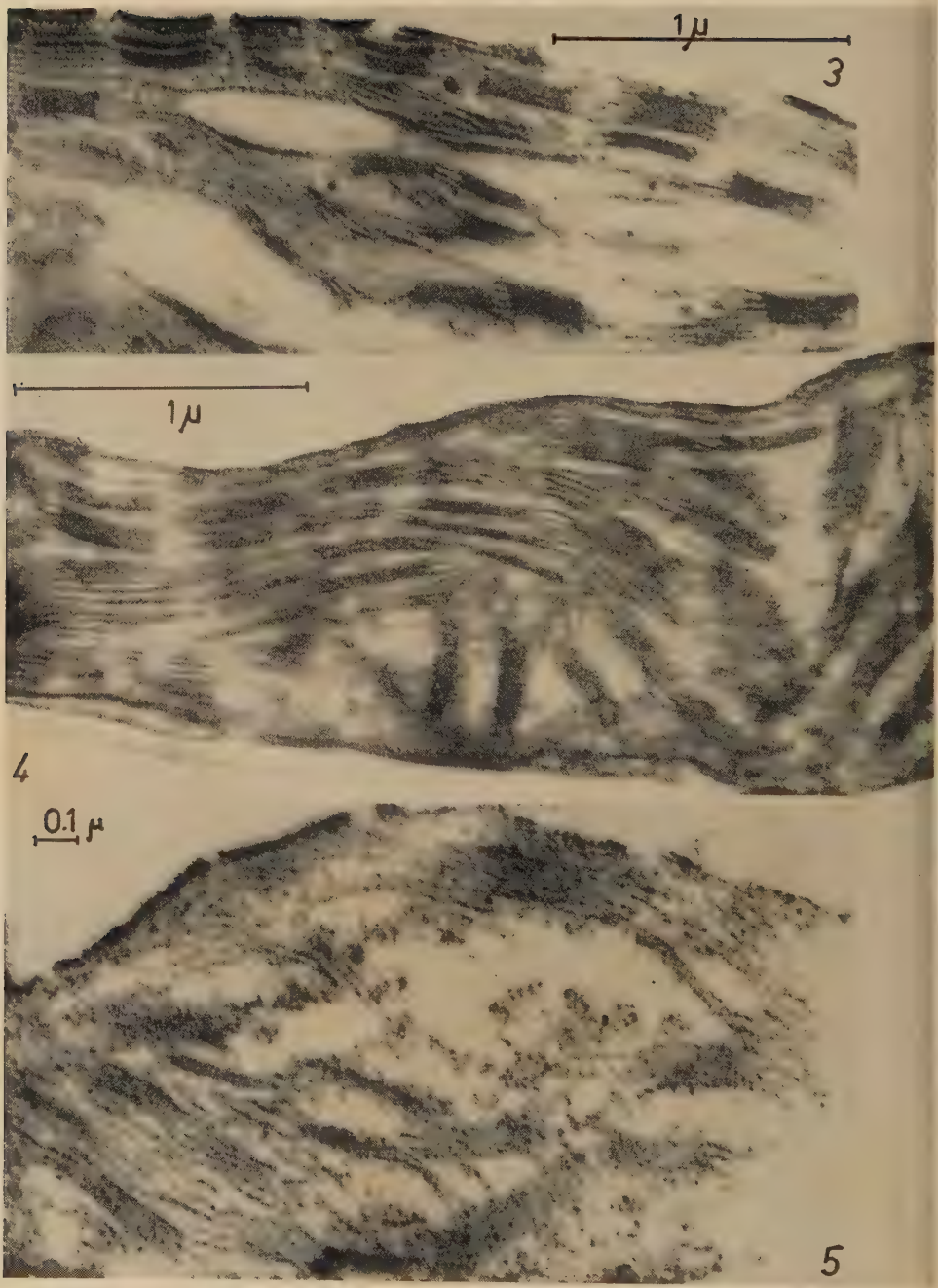

Abb. 3–5.—Die Chroroplastenstrukturen: Schichten, Grana und Stromalamellen. Vergr.: 40000 × und 60000 ×.

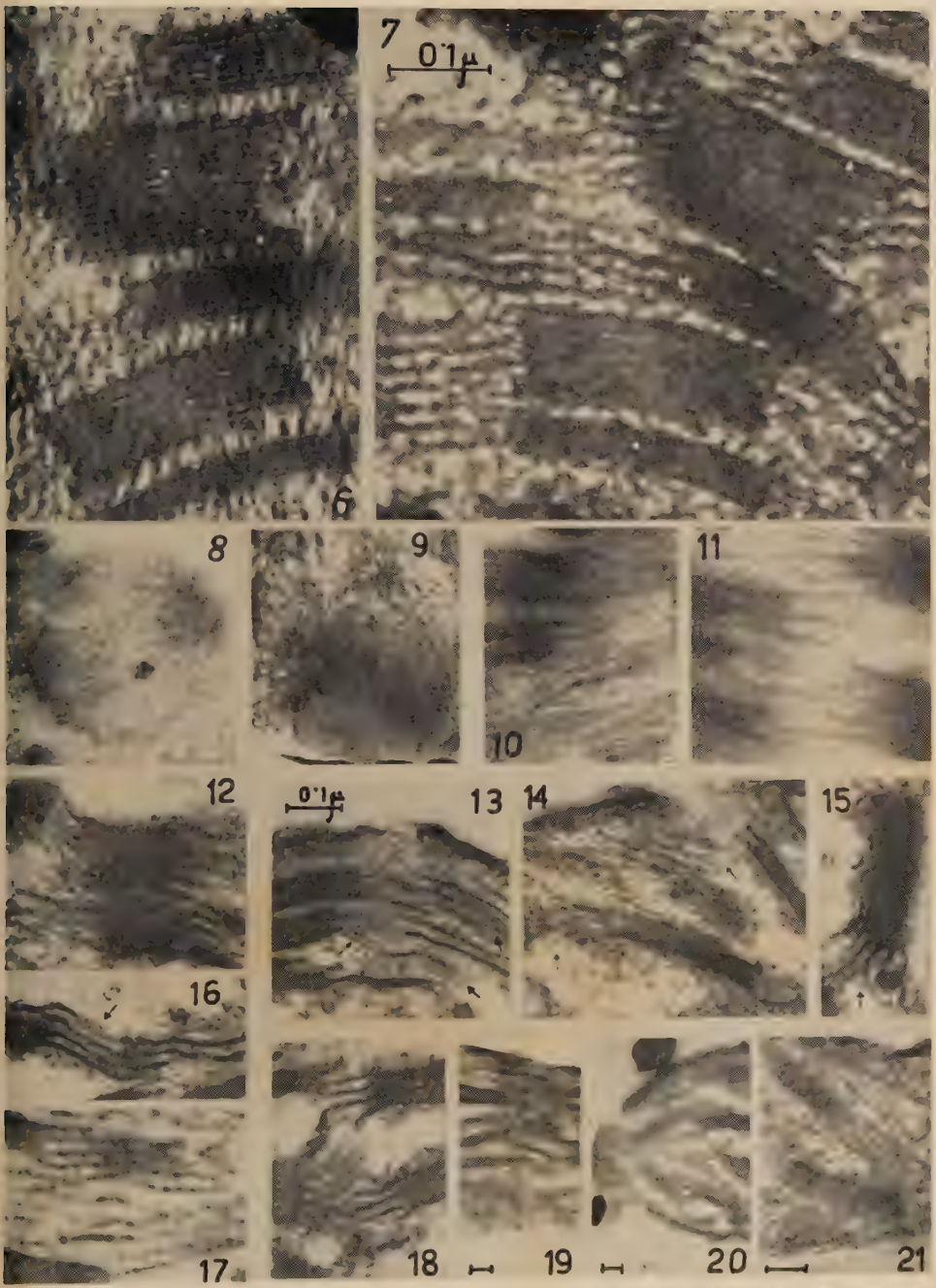

Abb. 6–21. — *6, 7.* Feinstruktur der Grana- und Stromalamellen in verschiedener Focuseinstellung. Vergr.: 136000 ×. *8, 9.* Flächenschnitte einzelner Grana. Vergr. 71000 ×. *10–21.* Feinstrukturen der Grana- und Stromalamellen. Nähere Erklärung siehe Text. Vergr.: 71000 ×, 28000 × und 50000 ×.

Abb. 24–25.—*24.* Ältere Blattmeristemzelle mit 4 verschiedenen Zellorganellen. Nähere Erklärung siehe Text. Vergr.: 17000 ×. *25.* Ausschnitt aus einer jungen Blattmeristemzelle mit Zellwand und Plasma. Vergr.: 28000 ×.

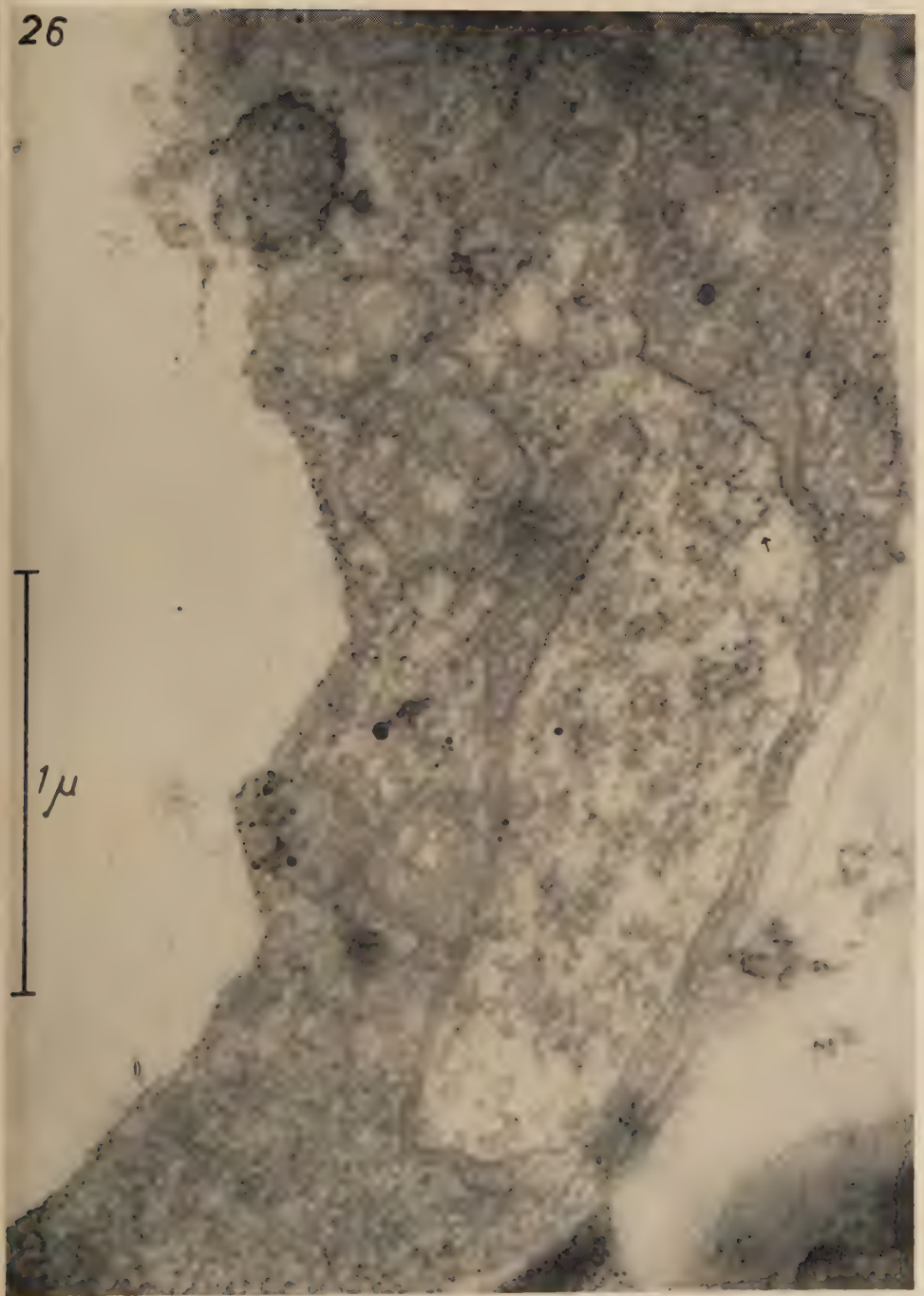

Abb. 26.—Ausschnitt aus einer jungen Blattmeristemzelle mit 3 verschiedenen Zellorganellen. Vergr.: 58000 ×.

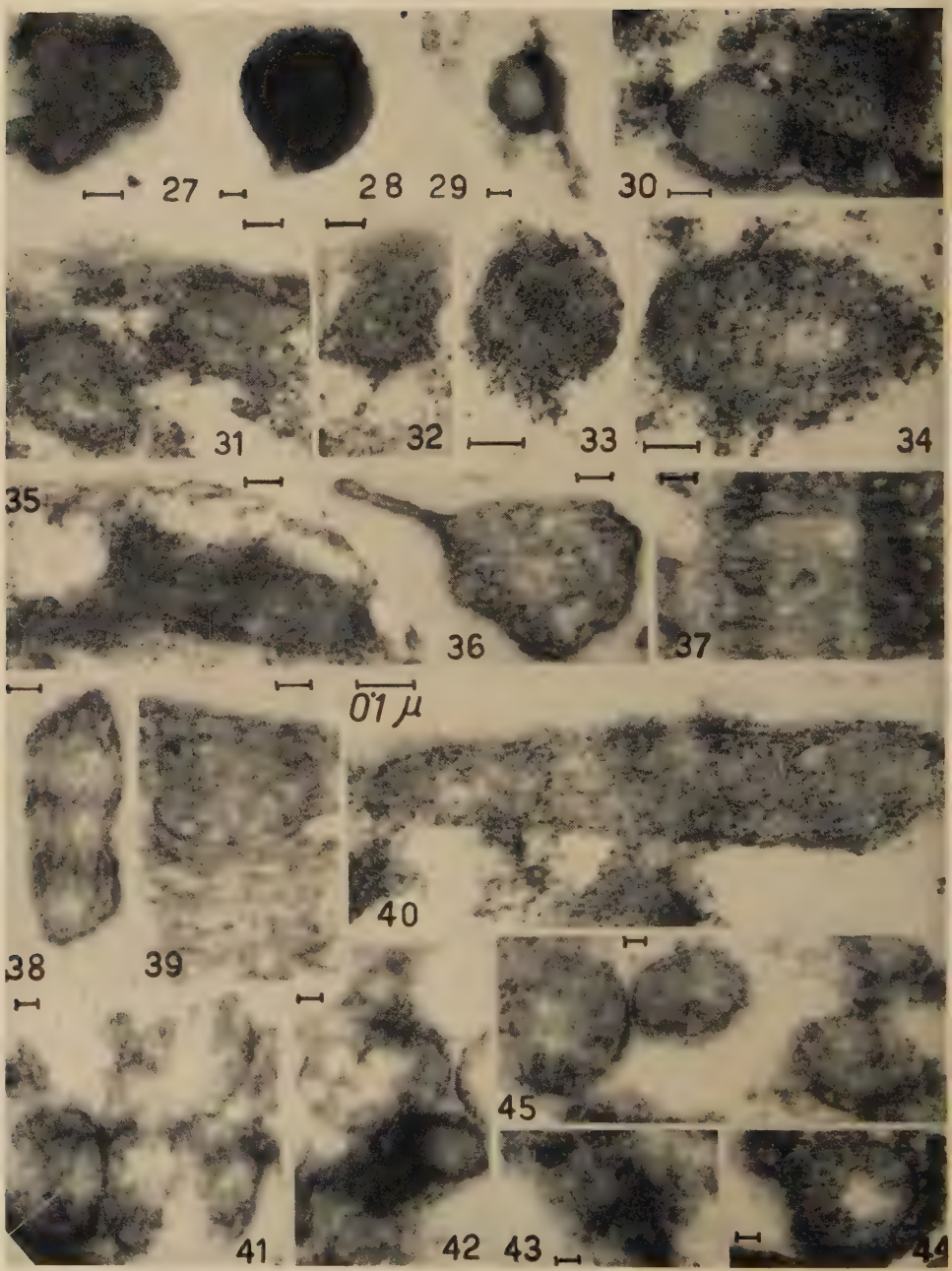

Abb. 27–45.—*27–40.* Zellorganelle aus dem Blattmeristen der Gerste. Abb. 31–36 und 40 vermutlich junge Proplastiden. *41–45.* Mitochondrien der Gerste. Vergr.: 30000 ×.

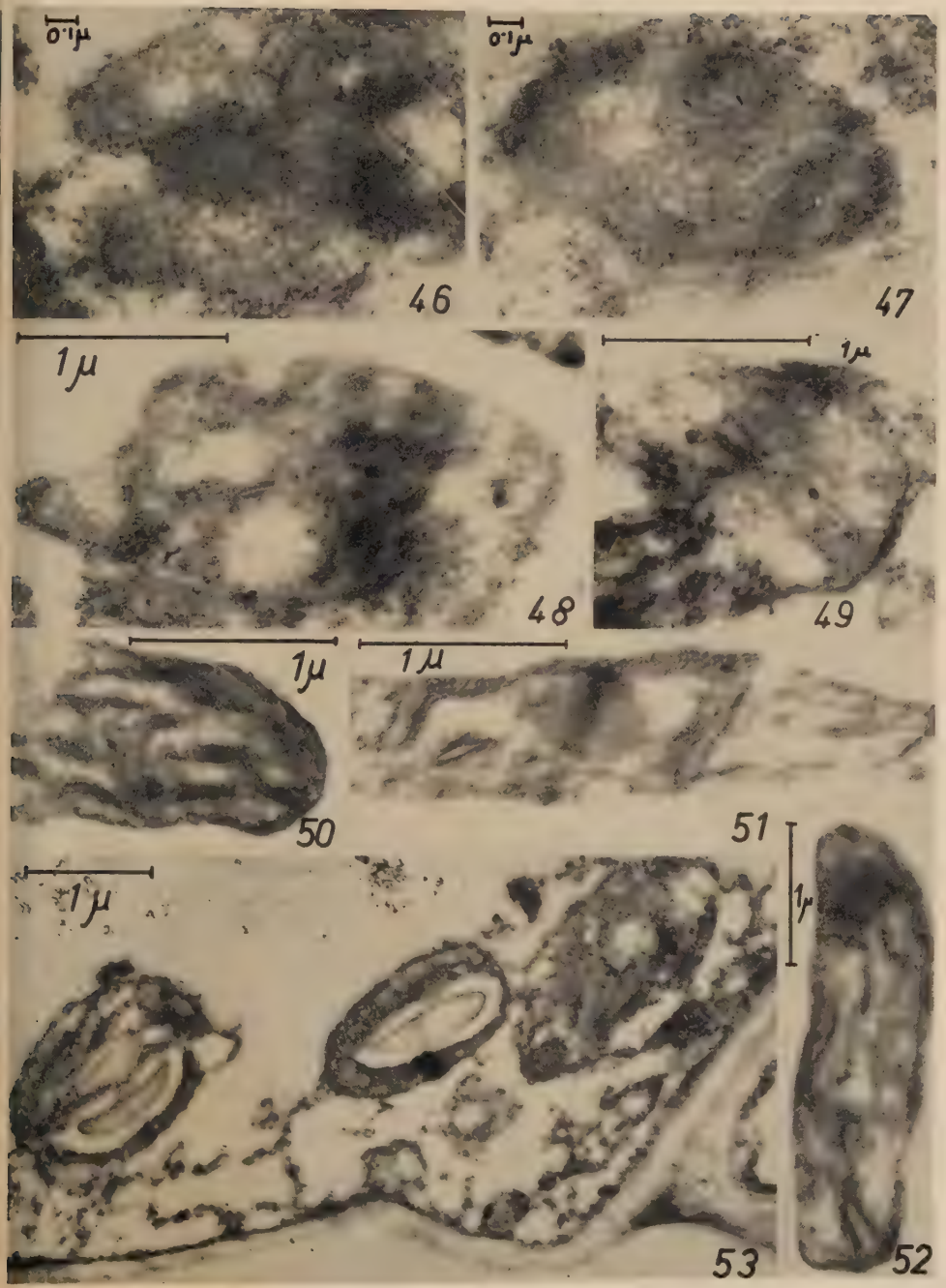

Abb. 46–53.—Verschiedene Stadien der Chloroplastenentwicklung bei der Gerste.

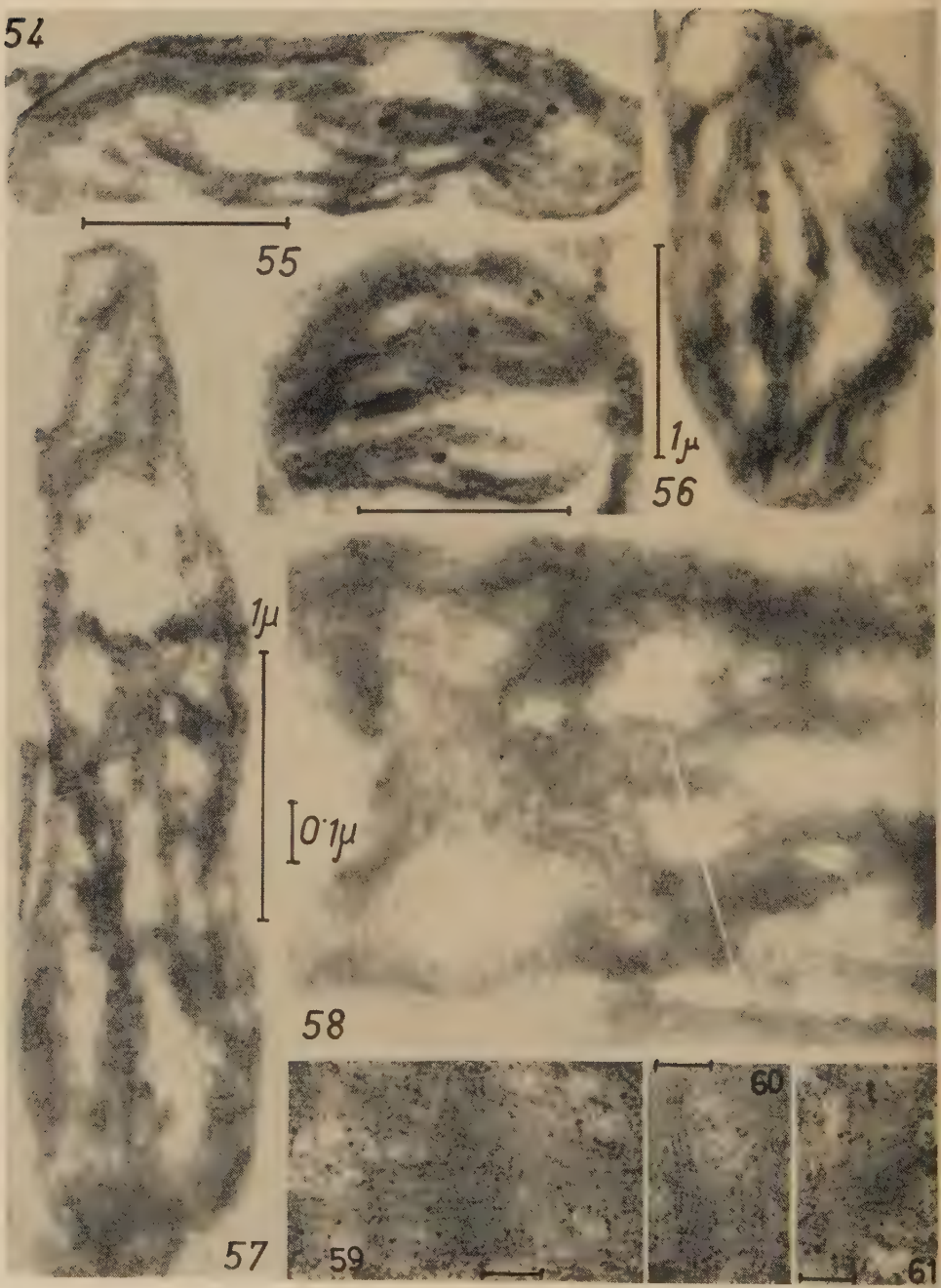

Abb. 54–61.—Stadien der Chloroplastenentwicklung der Gerste. Nähere Erklärung siehe Text.

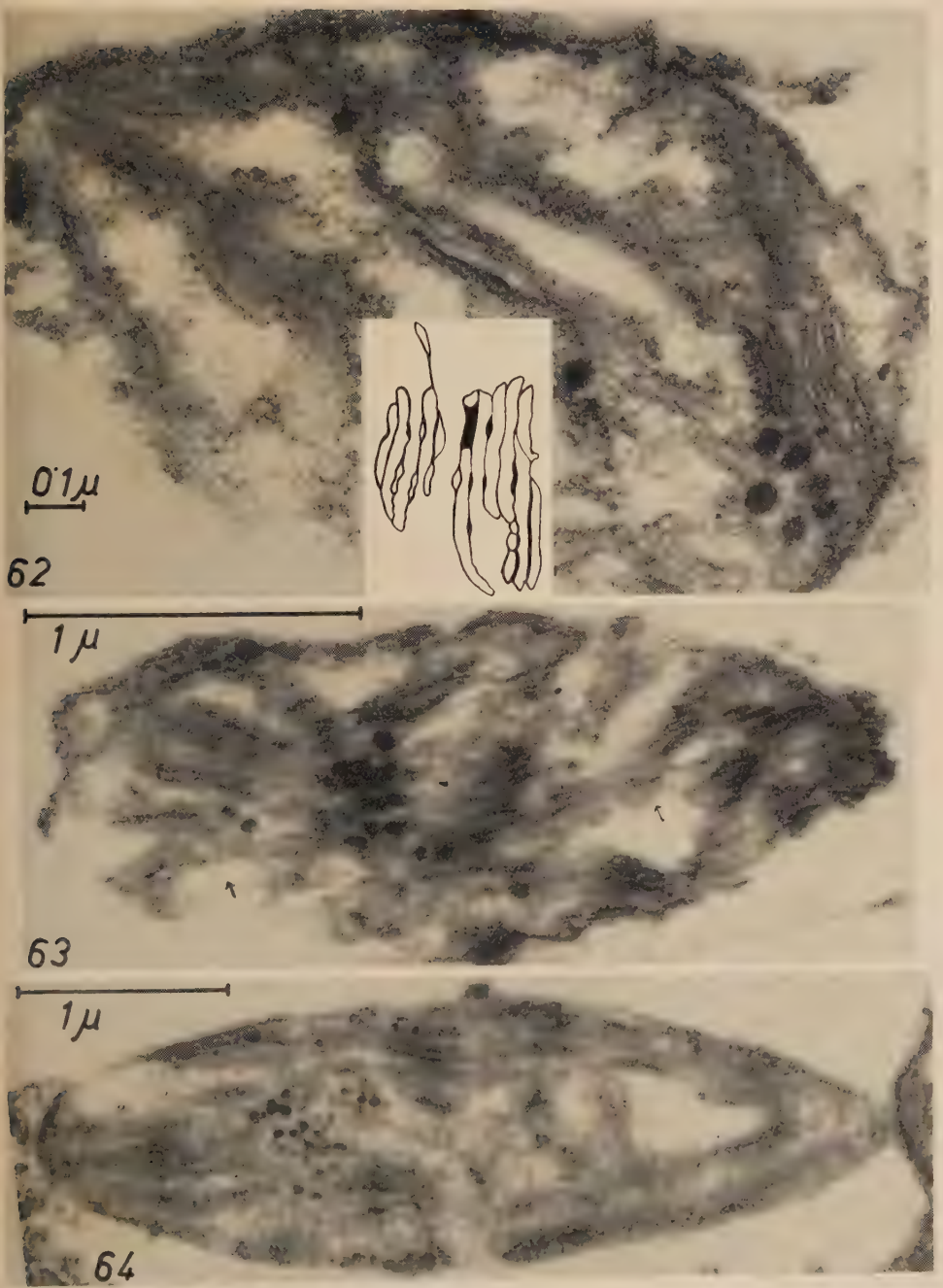

Abb. 62–64.—Entwicklungsstadien des Gerstenchloroplasten. Bildung der Lamellen und der Granastruktur. Vergr.: 75000 ×, 45000 × und 28000 ×.

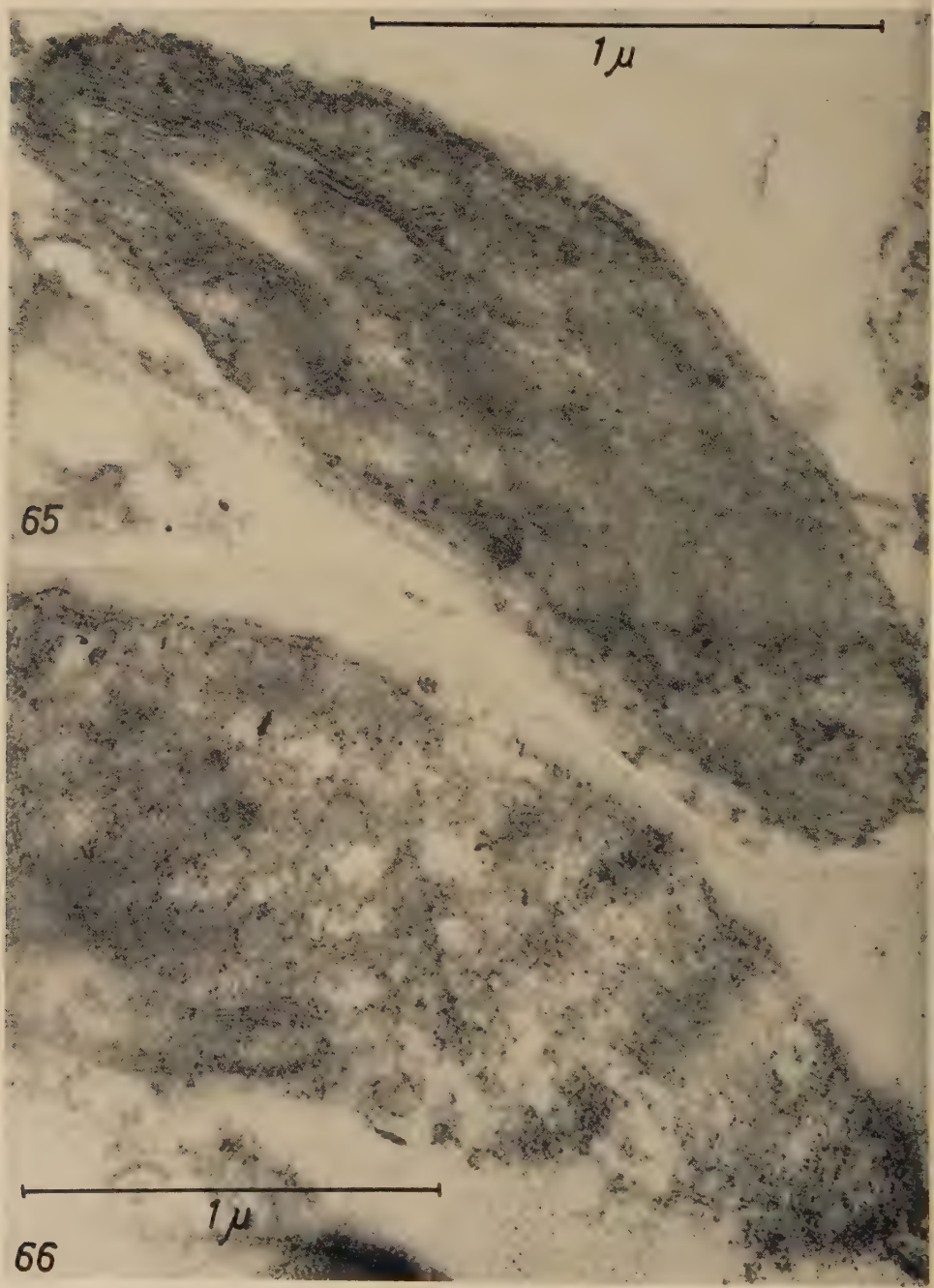

Abb. 65, 66.—Junge Chloroplasten mit durchgehender Lamellenstruktur. Vergr.: 69000 × und 57000 ×.

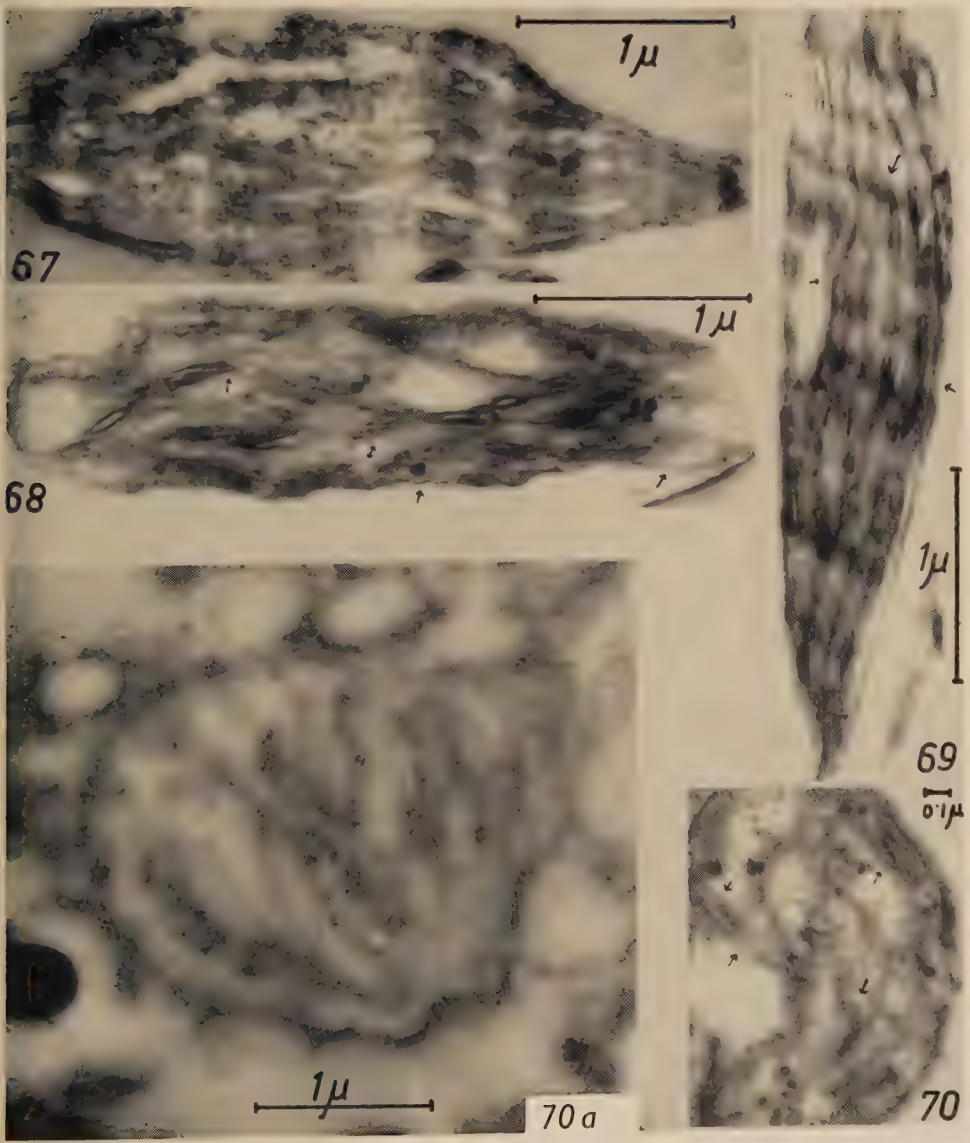

Abb. 67–70a.—*67*. Chloroplast mit durchgehender Schichten- und Lamellenstruktur. Vergr.: 28000 ×. *68*, *70*. Chloroplasten mit beginnender Granadifferenzierung. Vergr.: 28000 ×. *70a*. Plastide in einer Spore von *Funaria hygrometrica*, fixiert in 1 molarer Rohrzuckerlösung. Vergr.: 23000 ×.

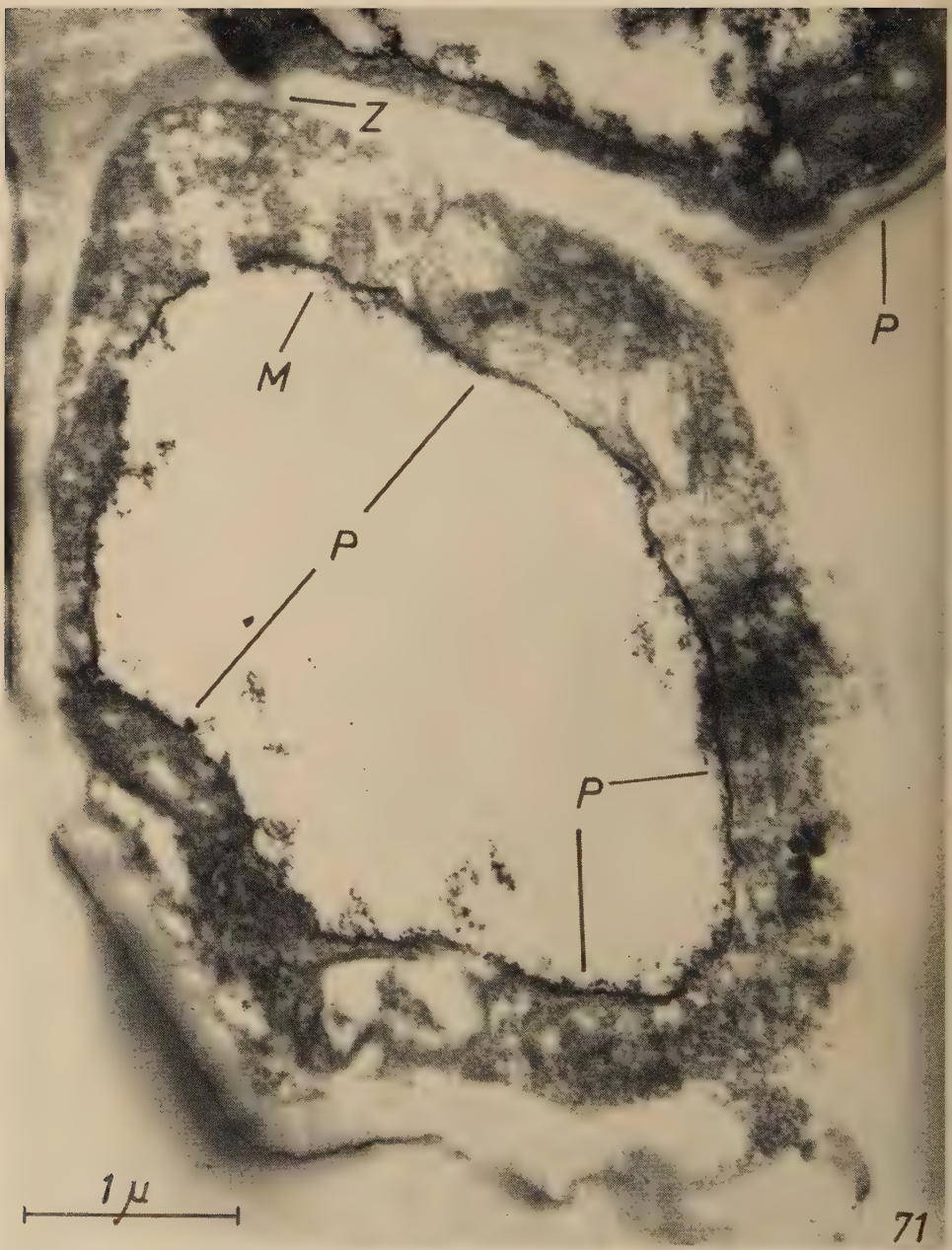

Abb. 71.—Junge Blattzelle einer *albina*-Mutante der Gerste. M = Mitochondrien, P = Plastiden, Z = Zellwand. Vergr.: 28000 ×.

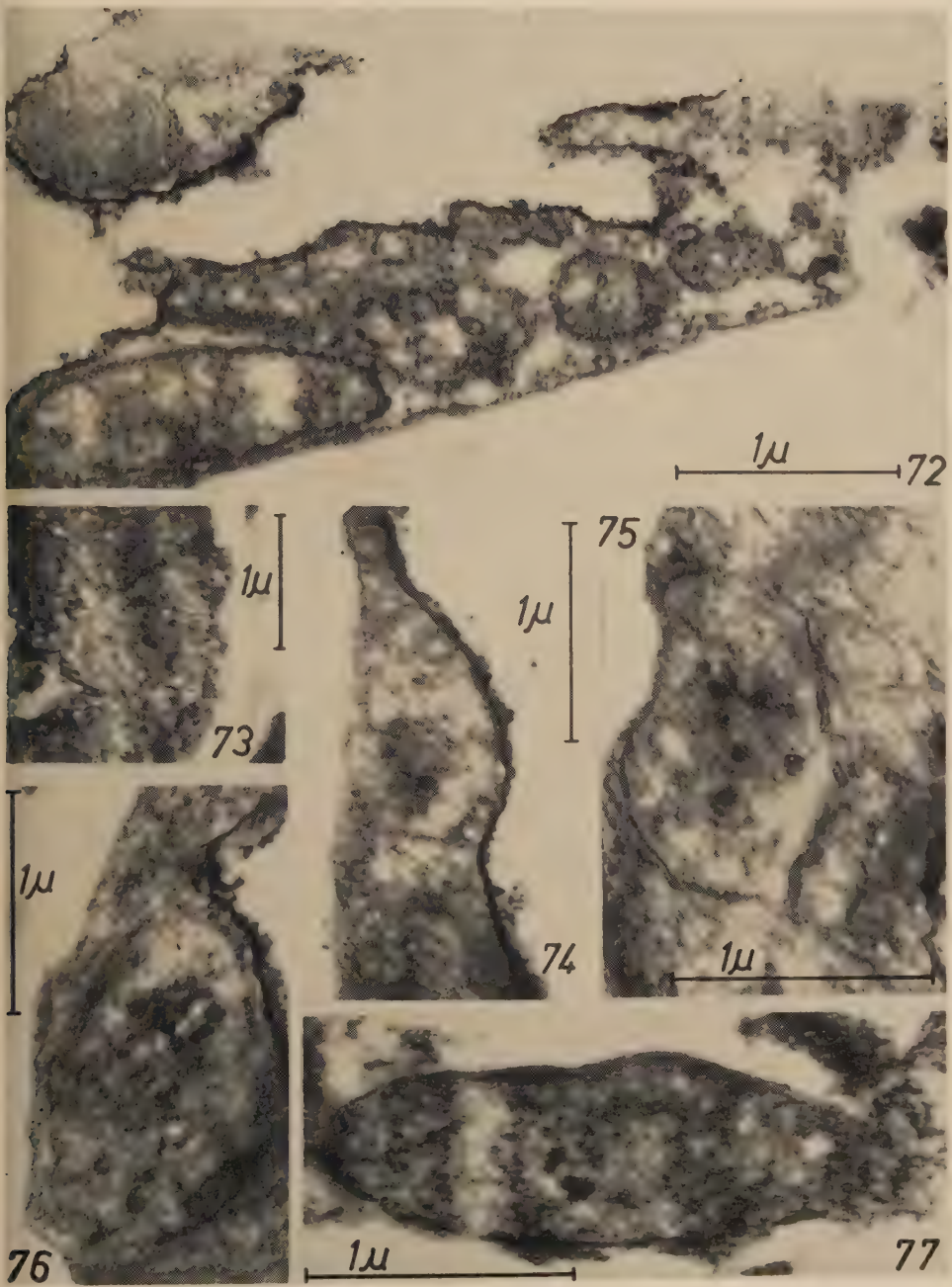

Abb. 72–77.—Plastiden aus einer *albina*-Mutante der Gerste. *72*. Junge Stadien; *77*. Endzustand der Plastiden; die Übrigen: dazwischen liegende Stadien mit Plastidenzentrum.

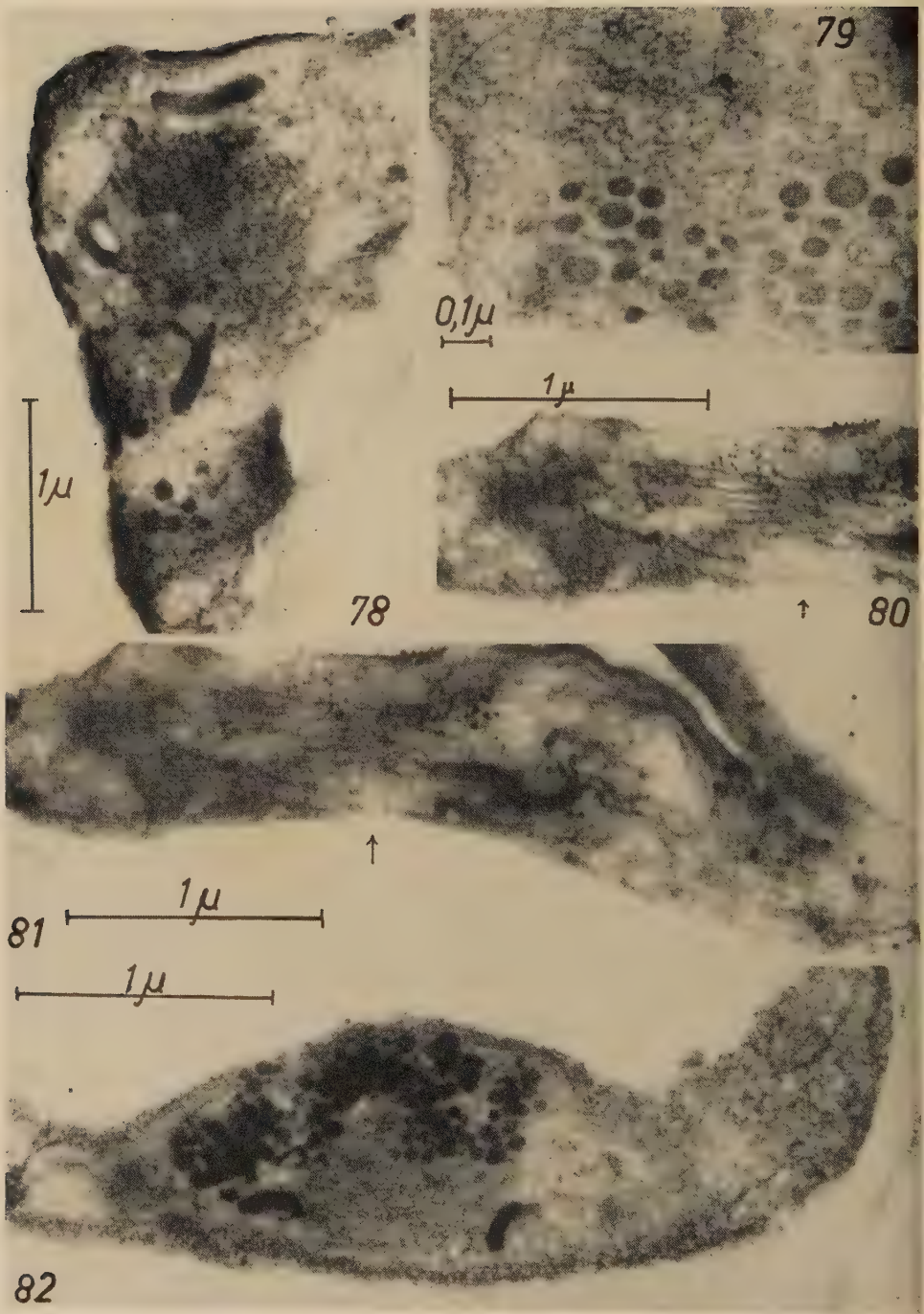

Abb. 78–82.—Verschiedene Entwicklungsstadien der Plastiden aus der *xantha*-3-Mutante .Nähere Erklärung siehe Text. Vergr.: 29000 ×, 35000 × und 70000 ×.

Abb. 83–85.— *83*. Plastide der Mutante *xantha*-3 im Stadium mit den zufolge des genetischen Blockes angehäuften Globuli. Vergr.: 46000 . *84*, *85*. Endzustand der Plastiden in der Mutante *xantha*-3. Vergr.: 24000 × und 29000 ×.

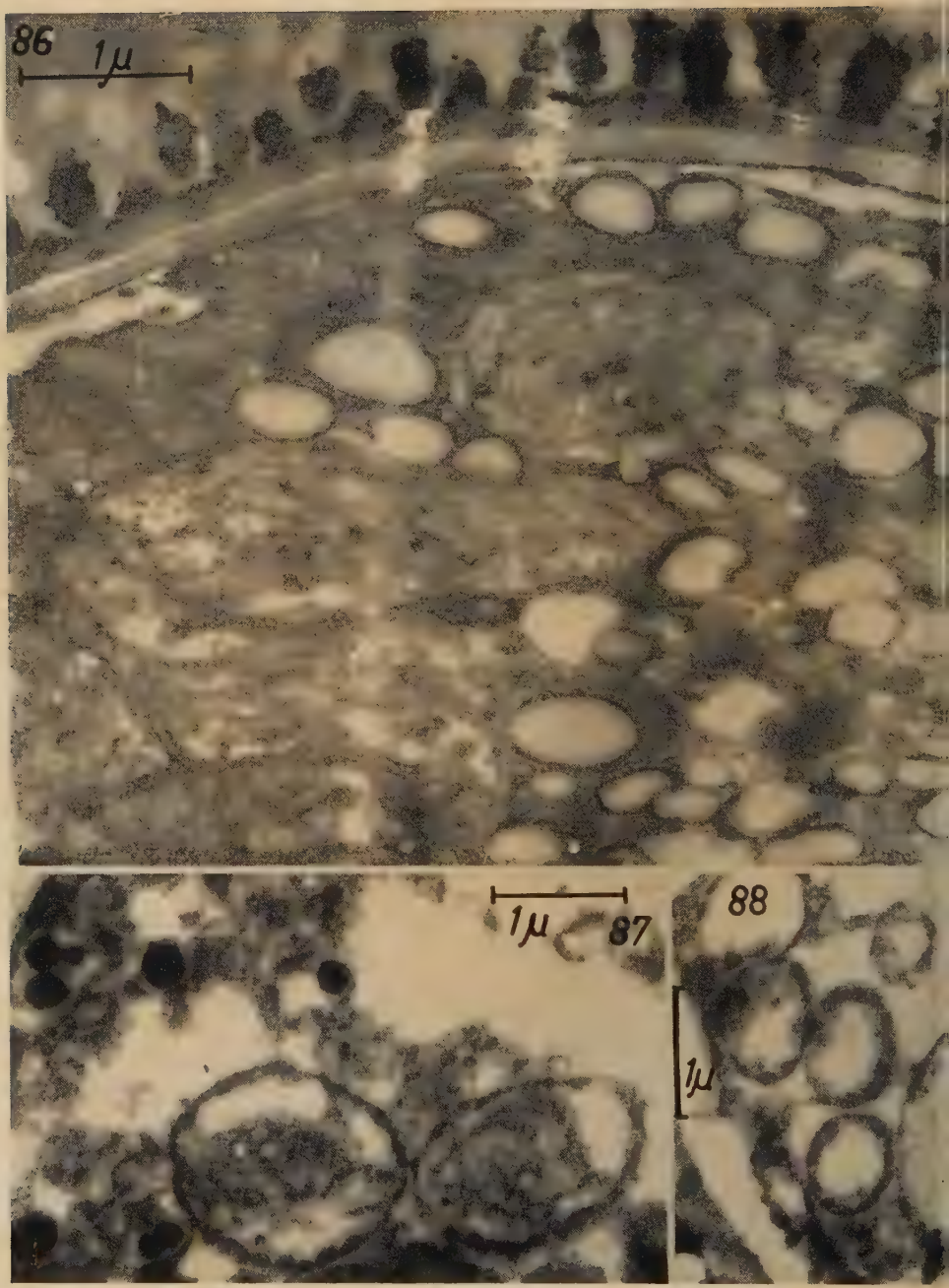

Abb. 86–88.—*86.* Schnitt durch eine Spore des Mooses *Funaria hygrometrica.* Vergr.: 23000 ×
87, 88. Zellorganelle aus der Moosspore. Vergr.: 18000 ×.

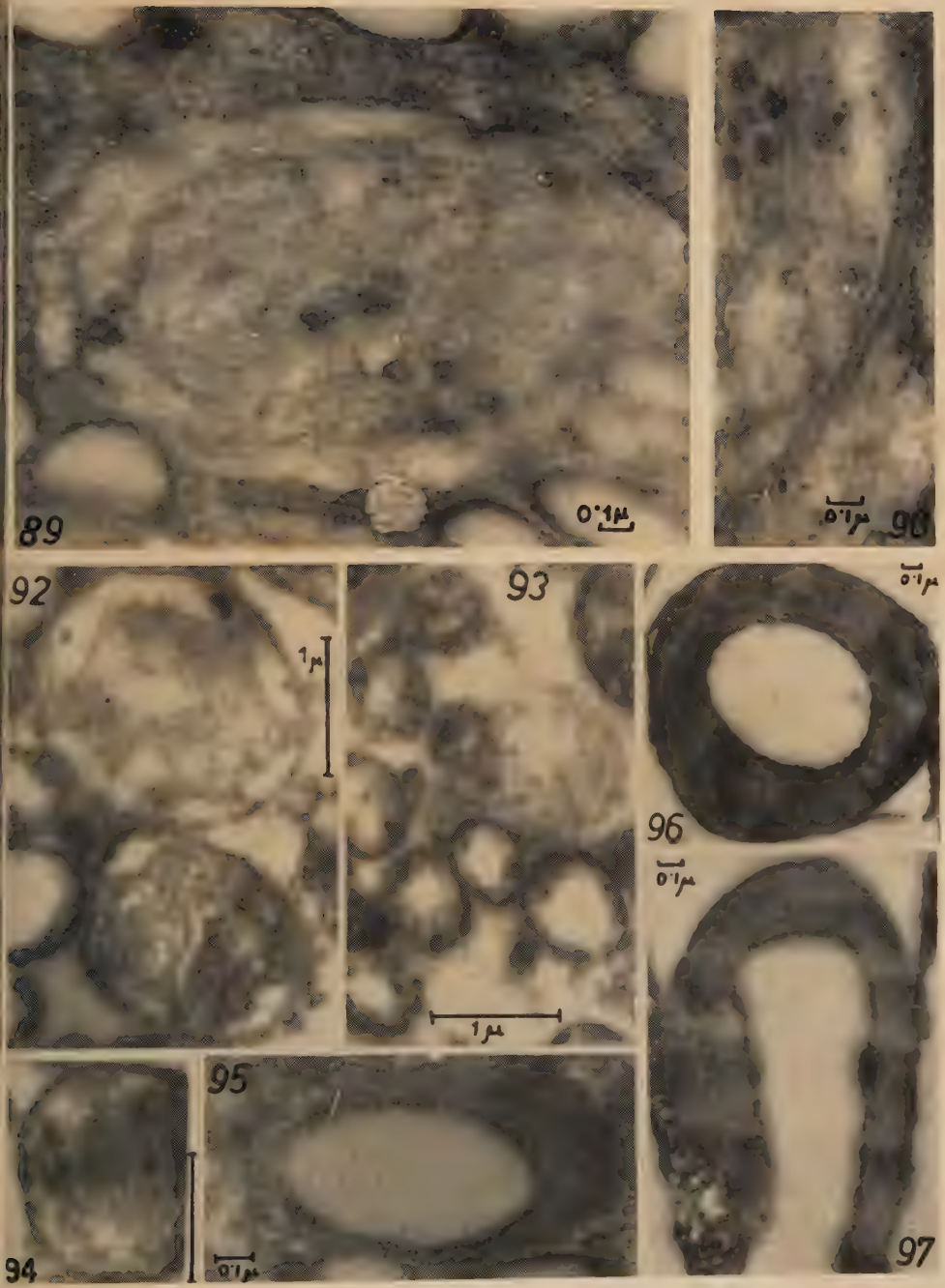

Abb. 89–97.—*89.* Plastide aus einer Moosspore (*Funaria hygrometrica*). Vergr.: 45000 ×. *90.* Plastidenmembran in einer Moosspore. Vergr.: 45000 ×. *92–94.* Organelle aus der Moosspore. Vergr.: 18000 × und 50000 ×. *96, 97.* Bestandteile aus der Eizelle von *Fucus vesiculosus*. Vergr.: 28000 ×.

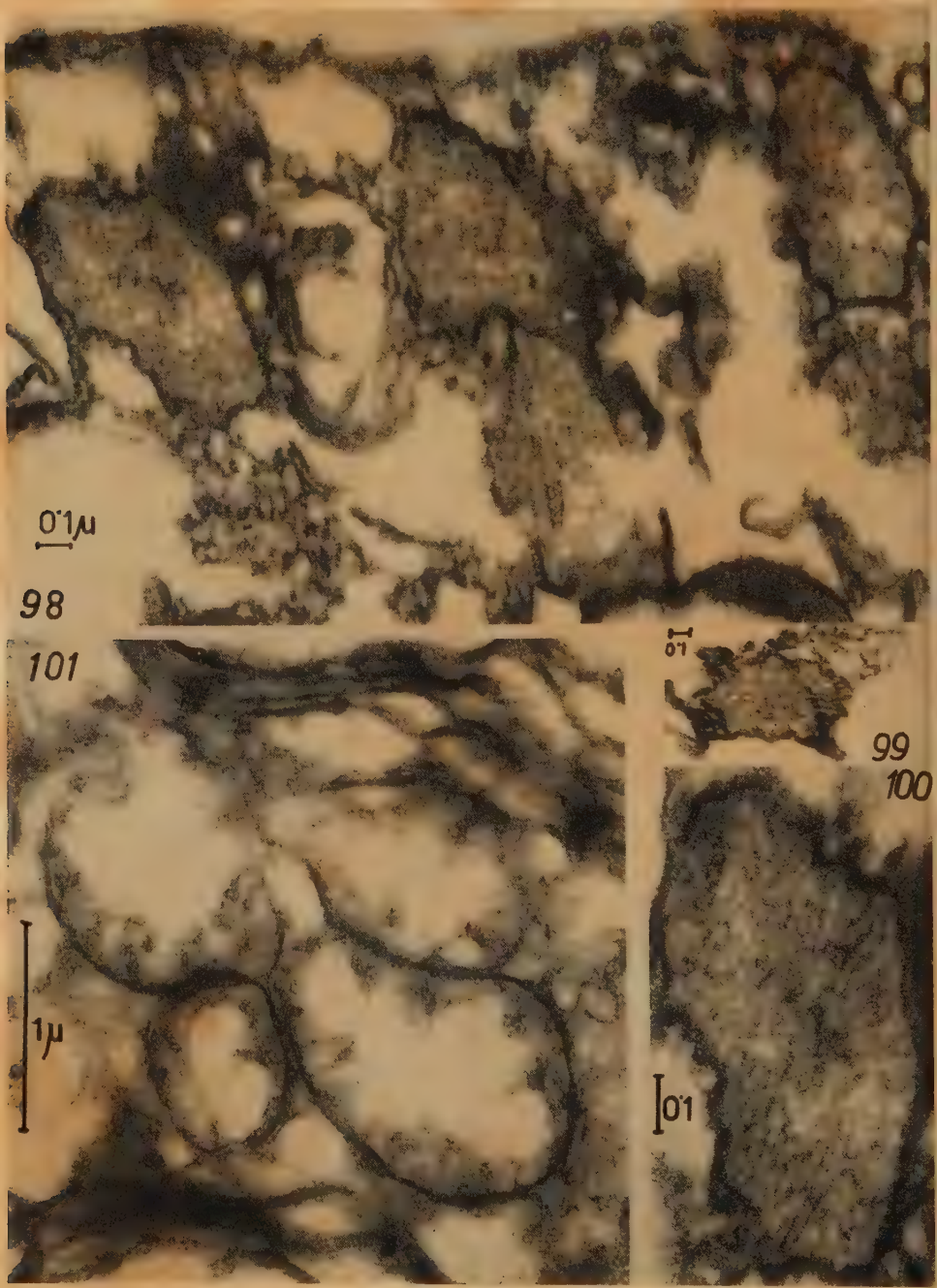

Abb. 98–101.—*98–100.* Mitochondrien aus der Eizelle von *Fucus vesiculosus.* Vergr.: 48000 ×, 28000 × und 75000 ×. *101.* Mitochondrien aus einer älteren Rindenzelle des Thallus von *Fucus vesiculosus.* Vergr.: 28000 ×.

INJURY AND RECOVERY OF *SPIROGYRA* EXPOSED TO ULTRASOUND[1]

D. E. GOLDMAN and W. W. LEPESCHKIN[2]

Naval Medical Research Institute, Bethesda, Maryland, U.S.A.

Received October 15, 1956

Living cells have built-in maintenance and repair facilities which can compensate to some extent for deviations of the environment from optimum conditions. When noxious external stimuli are encountered, these internal mechanisms are brought into play to reduce the degree to which the condition of the cells departs from normal. Experimental studies of such systems require that both the environment and the state of the cells be measurable. However, to describe the condition of a cell requires a large number of variables, and the use of a single parameter as an index of cell condition can only be made with great care.

Studies on the time course of the destruction of cells in suspension resulting from exposure to audible sound or ultrasound have shown that the number of intact cells decreases more or less exponentially with time [1, 3, 5, 6]. These results, however, apply to irreversible changes produced by rather intense forces and reveal very little of the cells' homeostatic machinery. It might be expected that the use of more gentle forces and of more subtle, reversible changes in cell state would yield helpful data.

Spirogyra, when exposed to ultrasound or other mechanical forces, has been shown to undergo a characteristic sequence of morphological changes which are readily observed under a microscope [4]. There is first a slight displacement of the chloroplasts and the nucleus. Next there is a definite retraction of chloroplasts. Then the chloroplasts contract and fuse to form droplets; then the protoplasm coagulates; and finally there is complete disintegration of the cell contents. The first two stages are reversible but further changes are not.

Spirogyra is easy to obtain and to handle and the cells are quite uniform. The sequence of morphological changes thus appears to be a useful, if crude, measure of the condition of the cells. Further, as a means of applying force,

[1] The opinions contained in this report are those of the authors. They are not to be construed as necessarily reflecting the views of the Navy Department.

[2] Deceased.

ultrasound is fairly satisfactory. The power density and field characteristics, while difficult to measure in absolute terms, are rather easily reproducible and controllable. It was hoped in this study that examination of the time course of cell injury at various sound intensities would cast some light on the homeostatic mechanisms of the cell.

MATERIAL AND METHODS

Spirogyra used for these experiments were of two species taken from a single culture of rather long filaments. Wherever possible, sections cut from a single filament were used for comparative studies, since the results then obtained were more closely reproducible than if sections from different filaments were used. Sections were cut 1 to 1.5 cm long (50 to 70 cells) and were kept in culture water overnight before being exposed to ultrasound. The sections were mounted in small cages made of coverslip glass and fine glass threads. The cages were mounted in an exposure chamber filled with tap water which had come to equilibrium with room air at room temperature. A standing wave sound field was used; specimens were placed either at nodes or at antinodes. The difference in effect between these two places can be made quantitative [2].

The specimens were removed from the sound field at frequent intervals for study under the microscope and then returned for further exposure. The time out of the field was about 3 to 5 minutes for each examination and stated exposure times include only time in the sound field. Observations on the rate of recovery of reversibly injured cells after removal from the sound field showed that detectable changes could scarcely have occurred during the short time the specimens were out of the field.

The ultrasound, at 400 and 700 kcps. was generated by quartz crystals immersed in oil; these produced a beam passing through the oil into the cylindrical container holding the specimens. Circulation of both oil and aqueous medium was used to maintain temperatures within 2°C. The geometrical arrangement of all objects in and near the sound field was kept fixed throughout the experiments to ensure reproducibility of the field characteristics. The voltage at the plate of the final amplifier stage of the generator system was used as an index of the sound power input. Details of the techniques and equipment have been given elsewhere [2, 4].

Estimates of the condition of the cells were made by counting the number of cells in each stage described above; cells were recorded injured or dead. In a few cases a detailed history was kept of each cell of a filament section throughout the course of an exposure period. The index of injury chosen was the total number (or fraction) of affected cells (both injured and dead) since the grading of degrees of injury was too coarse to justify detailed statements concerning average degree of injury.

RESULTS

When randomly chosen pieces of *Spirogyra* filament were exposed to various fixed ultrasound power input levels, the number of injured cells increased steadily at first and, if the power was high, continued to increase until all

cells were visibly damaged. At lower power inputs the number of injured cells reached a maximum in 5 to 15 minutes and then fell off slightly to a level which was maintained for up to an hour or more. Intermediate cases showed either an injury level which was maintained or which later increased to complete damage (Fig. 1). This was the general pattern in terms of the injury produced. In terms of degree of response to a given power input,

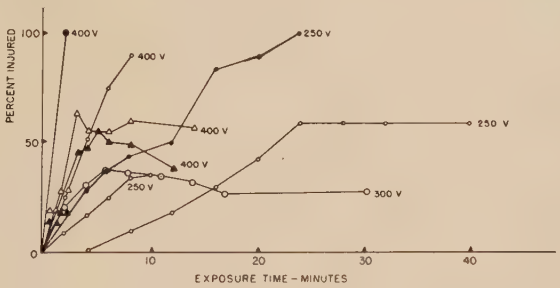

Fig. 1. Time course of injury of *Spirogyra* filaments exposed to ultrasound at 400 kilocycles at room temperature and at input voltages indicated.

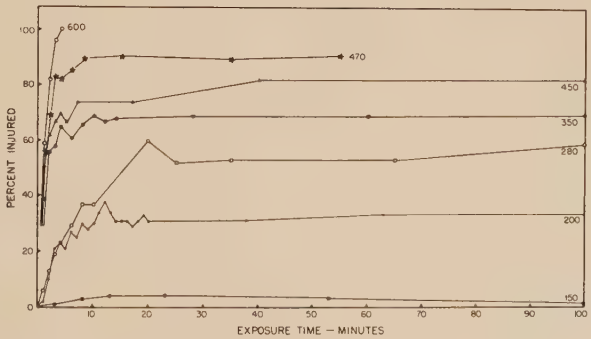

Fig. 2. Time course of injury of sections of a single filament of *Spirogyra* exposed to ultrasound at 400 kilocycles, 24°C and at input voltages indicated.

however, these results were not adequately reproducible and it was necessary to expose sections from a single filament to a graded series of ultrasound power levels. The results of such an experiment (Fig. 2) show the same general pattern of response but it is now evident that both the initial rate of appearance of injury and the final degree of damage reached increase with the applied ultrasound. It can also be seen that at intermediate power values a number of cells appear normal throughout 100 minutes. However, longer exposures do produce gradual further damage (Fig. 3).

Cells embedded in agar gel and placed at a pressure node show a similar time course of injury (Fig. 4). Agar greatly increases the cavitation threshold of an aqueous medium and the placing of the specimen at a pressure node makes the injury a result of some coherent property of the sound field

associated with the particle motion [5]. Evidently the time-injury characteristics are essentially the same whether the injury results from cavitation or from other mechanical forces of an ultrasound field.

The results of a detailed, cell by cell study show several features of interest (Table I). Of a total of 47 cells in one section, 23 showed no visible change during the 53 minutes of exposure. This may be due partly to irregularites

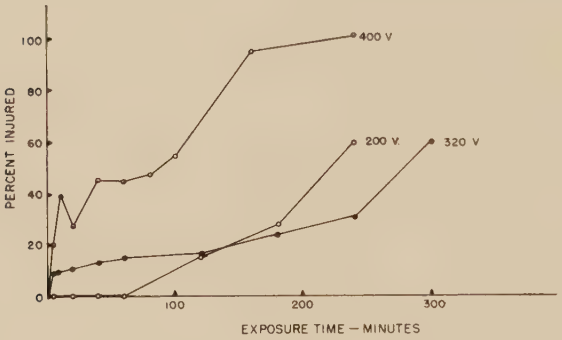

Fig. 3. Time course of injury of *Spirogyra* over a period of 4 hours or more at 400 kilocycles, 24°C, at input voltages indicated.

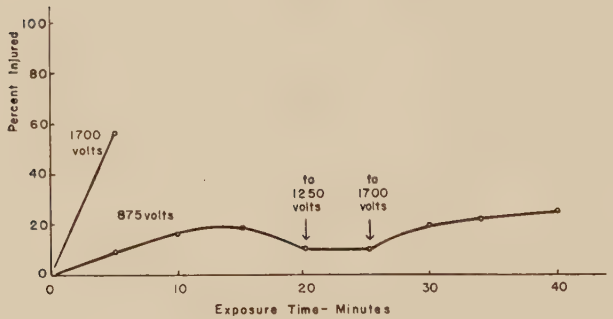

Fig. 4. Time course of injury of *Spirogyra* embedded in 2 per cent agar gel at a pressure node of the sound field (400 kc) at room temperature and at input voltages indicated.

in the sound field distribution and partly to differences in the susceptibility of the cells. In two cells the protoplasm coagulated. Eight of the injured cells recovered by one stage, and 8 cells recovered by two stages at some time during the exposure period. It is occasionally difficult to decide in which of two adjacent stages a cell may be, but differences of two in the stage of injury are unmistakable. The total per cent of affected cells follows the same course as is shown in Fig. 1. Table II shows a less detailed breakdown of the observations of another experiment.

Another way of observing the injury-recovery process in the ultrasound field is to pre-expose pieces of *Spirogyra* filament to a sound power insufficient to produce visible changes and then to re-expose these same pieces, together

TABLE I

Phase of injury of each cell of a section 47 cells long as a function of time during exposure to ultrasound.
Degree of injury indicated as follows:—, normal; 1, slight displacement of chloroplasts; 2, retraction of chloroplasts; 3, fusion of chloroplasts to droplets; 4, protoplasm coagulated.

Cell no.	Time								
	Before	2	4	6	8	11	14	29	53
					minutes				
1	—	1	—	—	—	—	—	—	—
	—	—	—	—	—	—	—	—	—
	—	—	—	—	—	—	—	—	—
	—	—	—	—	—	—	—	—	—
5	—	—	—	—	—	—	—	—	—
	—	—	—	—	—	—	—	—	—
	—	—	—	—	—	—	—	—	—
	—	—	—	—	—	—	—	—	—
	—	—	—	—	—	—	—	—	—
10	—	—	—	—	—	—	—	—	—
	—	—	—	—	—	—	—	—	—
	—	—	—	—	—	—	—	—	—
	—	—	—	—	—	—	—	—	—
	—	—	—	—	—	—	—	1	1
15	—	—	—	—	1	1	1	2	2
	—	—	—	—	—	2	2	2	2
	—	—	—	1	2	2	2	—	—
	—	—	—	2	2	2	1	—	—
	—	—	—	—	—	—	1	—	—
20	—	—	2	2	2	1	—	2	2
	—	—	—	1	2	2	2	1	—
	—	2	2	2	1	—	1	2	2
	—	1	1	1	1	1	1	1	1
	—	2	2	2	2	2	2	1	1
25	—	1	1	2	2	2	2	1	1
	—	2	2	1	2	2	1	2	2
	—	—	1	1	1	2	1	1	1
	—	2	2	2	2	3	3	3	4
	—	—	2	2	2	2	—	—	—
30	—	—	1	2	1	—	—	—	—
	—	2	2	2	1	—	—	—	—
	—	—	1	1	—	—	—	—	—
	—	—	—	—	—	—	—	—	—
	—	—	—	—	—	—	—	—	—
35	—	—	—	—	—	—	—	—	—
	—	—	—	—	—	—	—	—	—

Table I (*cont.*)

Cell no.	Time							
	Before	2	4	6	8	11	14	29	53
					minutes				
	—	—	—	—	—	—	—	—	—
	—	—	—	—	—	—	—	—	—
	—	1	—	—	—	—	—	—	—
40	—	—	—	—	—	—	—	—	—
	—	—	—	—	—	—	—	—	—
	—	—	—	—	—	—	—	—	—
	—	—	—	—	—	—	—	—	—
	—	—	—	—	—	—	—	—	—
45	—	—	—	—	—	—	—	—	—
	—	1	1	1	1	1	1	1	1
	—	1	4	4	4	4	4	4	4
Per cent affected cells		23	30	36	36	32	32	30	28

with non pre-exposed control sections to more intense ultrasound. It was consistently found that the pre-exposure reduced the apparent susceptibility of the cells to further exposure (Fig. 4). The same kind of behavior is indicated by the responses shown in Fig. 5.

Since these partial recovery phenomena presumably depend on metabolic processes of the cell, it is of interest to know how they are affected by such factors as temperature or narcotics. A series of exposures of sections of the same filament to the same power level were carried out at different temperatures (using water saturated at each temperature). It can be seen (Fig. 6) that the degree of injury is the least and the per cent recovery is the greatest at 23°C which is also near the optimum growth temperature of *Spirogyra*. At both higher and lower temperatures the cells fare less well. The temperature

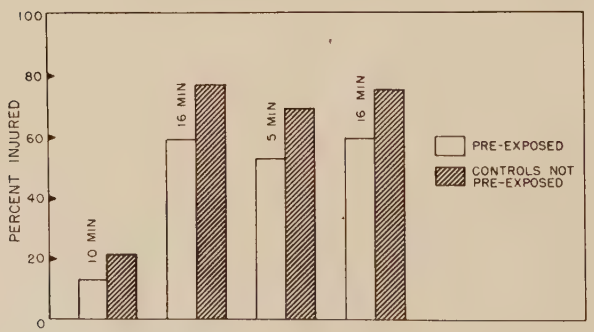

Fig. 5. Injury produced in paired halves of *Spirogyra* filaments, one half pre-exposed to ultrasound (150 volts, 400 kc) for times indicated. Both halves then exposed for 5 minutes at 225–300 volts.

TABLE II

Per cent of cells in each phase of injury of a 65 cell section of *Spirogyra* exposed to ultrasound. Index numbers are the same as in Table I.

Time	Stage of injury					Total
	—	1	2	3	4	
Before	100	0	0	0	0	0
1 min.	98	2	0	0	0	2
2	90	4	6	0	0	10
3	79	15	6	0	0	21
4	77	15	8	0	0	23
5	79	13	8	0	0	21
6	73	19	8	0	0	27
7	75	15	10	0	0	25
8	70	17	13	0	0	30
9	72	15	13	0	0	28
10	70	15	15	0	0	30
11	67	10	23	0	0	33
12	62	19	19	0	0	38
13	66	13	15	4	2	34
14	69	10	15	4	2	31
15	69	8	17	4	2	31
16	69	8	17	4	2	31
17	71	6	17	4	2	29
18	69	4	21	4	2	31
19	67	8	19	4	2	33
20	69	6	19	4	2	31
40	69	6	19	4	2	31

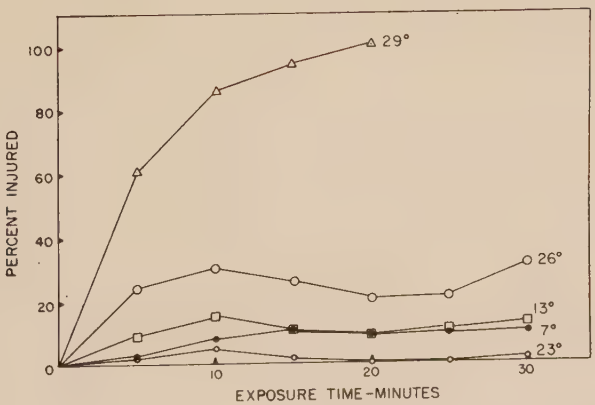

Fig. 6. Time course of injury of sections of single *Spirogyra* filament exposed to ultrasound at 300 volts, 700 kc at indicated temperatures.

effect presents other features of interest and is discussed in more detail elsewhere.

Small amounts of ethyl ether added to the exposure medium produce a definite effect (Fig. 7). The ether appears to reduce the degree of injury

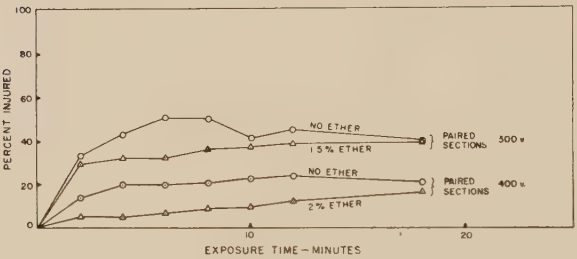

Fig. 7. Time course of injury of section of *Spirogyra* filament exposed at 700 kc with or without ethyl ether added to medium.

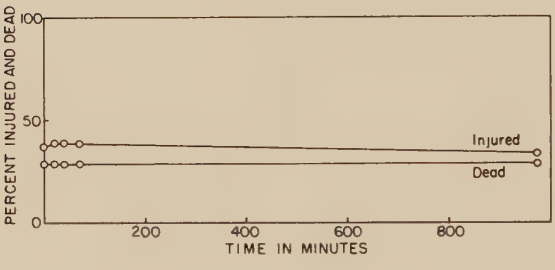

Fig. 8. Time course of condition of *Spirogyra* filamens at 23°C after cessation of exposure to ultrasound at 400 kc, 500 volts for 3 minutes.

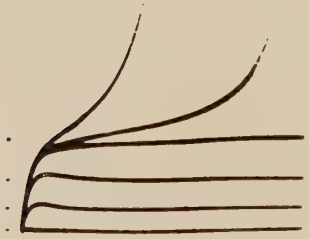

Fig. 9. Oscilloscope trace of injury time curves obtained by solution of differential equation. Abscissa is time and degree of injury is ordinate. Each curve for a strength of noxious stimulus greater than for the one below it. Zero time at beginning of continuous trace.

(possibly because of its effect in reducing cavitation) but the cells then seem less able to recover.

Sections of filament exposed so as to produce a moderate number of injured cells recover very slowly in culture water on removal from the sound field (Fig. 8). This observation justifies to a considerable extent the procedure followed in temporarily removing the specimens from the sound field for observation. However, this does not mean that no changes at all occurred. There may well have been an effect on the precise time course of the injury recovery process, although it is doubtful whether the overall characteristics

of the process were thereby affected. This very slow recovery also raises the question as to whether the same processes are involved in recovery during exposure as after exposure. Possibly the sound field itself releases some of the active recovery factors.

DISCUSSION

The foregoing results provide an interesting example of the way in which the maintenance systems of a cell react protectively to noxious stimuli. The condition of a cell may be described by a large number of variables, each of which has a normal range; the viable state of the cell then corresponds mathematically to a region in an appropriate multidimensional space. The cell prefers, as it were, to remain somewhere near the middle of this region and when external forces drive the cell toward its viability limits, there is an active cell response which resists the displacement or even pushes the cell back toward its normal state. These internal mechanisms require a finite time to act, so that strong forces may succeed in destroying the cell before the maintenance system can be brought into action. Very strong forces overcome these mechanisms completely.

This way of describing active homeostasis suggests the possibility of a somewhat more analytical treatment. We have dealt with a definite noxious force and have risked the characterization of the condition of the cell by a single parameter. The results indicate a rather definite kind of response pattern which we may further attempt to formulate in the following way:

(1) Assume that the displacement of the *Spirogyra* cell from its normal state is representable by a variable, x, at time, t.

(2) Assume that the ultrasound input represents a damaging "force," f.

(3) Assume that the restorative processes of the cell itself can be expressed as a power series in the displacement and that there is both a direct and a cumulative effect.

It is then possible to write a relation,

$$\frac{dx}{dt} = Af + (ax + bx^2 + cx^3 + \cdots) + \int (\varkappa f + px + qx^2 + rx^3 \cdots)\, dt$$

or,

$$\frac{d^2x}{dt^2} = (a + 2bx + 3cx^2 + \cdots)\frac{dx}{dt} + \varkappa f + px + qx^2 + rx^3 + \cdots.$$

It is evident that the system to be described is non linear, and that it has limited stability. The simplest special case of the foregoing equation which is

still capable of describing the behaviour of interest is that in which only terms through the second degree are kept, and in which, $b>0>a$, $q>0>p$, and $a^2+4p>0$. This special case cannot be solved in terms of any known functions, nor is it susceptible to standard analytical methods. However it can be easily solved with an analogue computing machine of suitable design. A sample set of solutions, made with a G. A. Philbrick electronic analogue computer for a suitably chosen set of parameters is shown in Fig. 9. These solutions reproduce certain general characteristics of the system fairly well. However, to compare solutions of this equation with experimental data, a further step is needed. Cells are not identical and a distribution curve for each of the parameters of the equation must be assumed. It is then possible, in principle, to convert from degree of injury of cell to total per cent injured to some specified degree, remembering that once the injury has reached a critical degree no recovery is possible. It is apparent that the general characteristics of the curves are not thereby greatly affected.

The above formulation is clearly only an approximate representation of what must be an extremely complicated mechanism. The possibility that one or more of the equation parameters varies with the sound input cannot be overlooked. Indeed, the recovery rate following interruption of the exposure makes this likely. Other cells and other kinds of noxious stimuli may well produce response patterns of a different detailed kind.

It is interesting to consider the possible kinetic mechanisms of the autosynthetic systems which must underlie the homeostatic behavior of these cells, but obviously this problem cannot be discussed seriously until more detailed information is available. What is greatly to be desired is a more clearly defined and more precisely measurable index of cell condition. Under proper circumstances the electrical impedance of the cell protoplasm, the oxygen consumption rate or the exchange rate of some metabolic product might profitably be used. The foregoing experiments are not satisfactory for detailed analysis but it is to be hoped that the use of better measures of the state of a cell will throw light on the interaction of the various elements of a cell's metabolic maintenance system.

SUMMARY

1. The time course of morphological changes in *Spirogyra* exposed to ultrasound is as follows:

There is an initial rate of appearance of injury which increases with ultrasound power input.

At relatively low power inputs the degree of injury reaches a maximum within 5 to 15 minutes and there is then a partial recovery to a level which is maintained for an hour or more. Eventually further damage may occur.

At high power inputs there is no maximum and all cells are irreversibly injured or killed within a short time.

2. Pre-exposure of *Spirogyra* specimens to a level of ultrasound which produces no visible change has a marked inhibiting effect on the production of injury by a subsequent exposure to more intense ultrasound.

3. Recovery of reversibly damaged cells removed from the ultrasound field is very slow compared with changes occurring during exposure.

4. Near 23°C, the injury produced by a given sound field is a minimum and the partial recovery during exposure is a maximum. At higher and lower temperatures, the cells are less resistant to injury and recover less.

5. Ethyl ether added to the exchange medium in small amounts reduces both the degree of damage and the degree of partial recovery.

6. A discussion of the general characteristics of injury and recovery of cells under the influence of noxious stimuli leads to a formulation of the processes in terms of a second order, non-linear differential equation the solution of which reproduces certain general characteristics of the system fairly well.

REFERENCES

1. Chambers, L. A. and Gaines, N., *J. Cellular Comp. Physiol.* **1**, 451 (1932–1933).
2. Goldman, D. E. and Lepeschkin, W. W., *J. Cellular Comp. Physiol.* **40**, 255 (1952).
3. Le Galley, D. P. and Pattersen, G. W., *Am. J. Pharm.* **112**, 373 (1940).
4. Lepeschkin, W. W. and Goldman, D. E., *J. Cellular Comp. Physiol.* **40**, 383 (1952).
5. Morrow, P. L., Bierman, H. R. and Jenkins, R., *J. Natl. Cancer Inst.* **10**, 843 (1950).
6. Williams, O. B. and Gaines, N., *J. Infectious Diseases* **47**, 485 (1930).

THE METABOLIC UTILIZATION OF C^{14}-FORMATE IN SEA URCHIN EMBRYOS

T. HULTIN

The Wenner-Gren Institute for Experimental Biology, University of Stockholm, Sweden

Received October 15, 1956

In previous communications a number of experiments have been described pertaining to the metabolic utilization of labeled metabolites in sea urchin embryos at different stages of development (for references, see [11]). These investigations showed that pronounced alterations in the metabolic pattern of the embryos occur at two particular periods of the early development, at the blastula stage, and during gastrulation.

At the blastula stage, simultaneously with the period of primary determination, a dramatic rise was observed in the incorporation of N^{15}-ammonia and C^{14}-carbon dioxide into purines and pyrimidines, in the acid soluble fraction of the embryos as well as in the ribonucleic acid [12, 15]. At the same time the incorporation of labeled amino acids into structural proteins became strikingly intensified. A particularly rapid incorporation was found in the proteins of the "microsome" fraction [14].

From the initial stages of gastrulation new possibilities for the utilization of labeled metabolites became apparent in the embryos. C^{14}-acetate gradually became more readily utilized as a metabolic fuel [15]. Amino acids were increasingly synthesized from N^{15}-ammonia [13]. Labeled amino acids were more rapidly incorporated into the proteins of the mitochondrial fraction and into the soluble proteins of the cell fluid [10, 14]. The increased range of metabolic capacity may be correlated with a rapid development of the mitochondrial system, which has been observed during this period [8, 9].

EXPERIMENTAL

Material.—Embryos of the sea urchin species *Psammechinus miliaris* (Gmelin), and *Paracentrotus lividus* (LM.) were used in the experiments. Dilute suspensions of eggs were fertilized and allowed to develop at 18–19°C in motor-driven, rocking glass-trays.

In the experiments with *Psammechinus* embryos equal samples were taken from the homogeneous suspensions at the following stages of development: (1) Before the

first cleavage (30 minutes), (2) at the 64-cell stage (3¼ hours), (3) early blastula stage (6 hours), (4) swimming blastulae (10¾ hours), and (5) gastrula stage (20–21 hours). The samples were washed by gentle centrifugation and were transferred to fresh sea water containing 0.07 μCs of C^{14}-formate per ml (1.7 mCs per m*M*). Approximately 15 ml of isotope solution were used per mg of total egg nitrogen. A further sample, similar to the samples 1–5, was taken from the egg suspensions soon after fertilization. This sample was allowed to develop in sea water containing 5.5×10^{-4} *M* *o*-iodosobenzoate (IBA). Like sample 3, it was treated with C^{14}-formate at the blastula stage.

The embryos were kept in the isotopic medium for 2½ hours. They were afterwards collected by centrifugation and preserved at −20°C. Small control samples of the IBA-treated embryos were allowed to develop in fresh sea water after the isotope incubation. These embryos became pronouncedly animalized [20].

Eight independent developmental series of the kind just described were performed with *Psammechinus* embryos. Before the chemical fractionation of the material these series were brought together four and four. The two series with combined material thus obtained were then worked up independently.

The *Paracentrotus* embryos were incubated with C^{14}-formate for 3 hours during the stages of mesenchyme blastulae and early gastrulation. The isotope incubations were performed in approximately the same way as in the case of the *Psammechnius* material. The incubation suspensions, however, were more dilute, about 50 ml of isotope solution being used per mg of total egg nitrogen. Four embryo suspensions were incubated independently. The samples were afterwards fractionated together.

The acid-soluble fraction.—The combined samples were suspended in ice-water. One ml of *N* formic acid was added for the purpose of isotope dilution, followed by ice-cold trichloroacetic acid (TCA) to a final concentration of 10 per cent. The suspensions were centrifuged at low temperature, and the precipitates were repeatedly washed with cold 5 per cent TCA.

The TCA was removed from the extracts by treatment with ether in a liquid extractor. The extracts were then concentrated *in vacuo* and fractionated by ion exchange chromatography (Dowex 50, 300 mesh, H^+ form). The following major fractions were collected: uridylic acid, inosine, hypoxanthine, and guanine. The uridylic acid was digested with *N* HCl at 120°C for 150 hours. The HCl was removed *in vacuo*, and uracil was isolated by ion exchange chromatography (Dowex 50). The inosine and hypoxanthine fractions were combined. They were treated with *N* HCl at 100°C for 75 minutes.

On the basis of the ultraviolet absorption curves of the collected fractions the uracil, hypoxanthine and guanine were diluted with appropriate amounts of the corresponding non-labeled compounds. The purines were precipitated with $CuSO_4 + NaHSO_3$ [17]. The uracil and purine samples were combusted, and the specific acitivities of the $BaCO_3$ obtained was determined by using a thin mica window counter.

Paracentrotus embryos contain considerable amounts of picolinic acid methyl betaine [16]. This compound was isolated from the acid soluble fraction of the *Paracentrotus* material by chromatography. The betaine was precipitated from the eluate as periodate. The oily precipitate was dissolved in ethanol, and the betaine was precipitated from this solution with ethanolic $HgCl_2$. The specific activity of the dry precipitate was determined after combustion to $BaCO_3$.

The lipid fraction.—The insoluble residues after the extraction of the embryos with cold TCA were washed with ethanol and thoroughly extracted with ethanol and ether. These extracts were combined and evaporated. The phospholipids were dissolved in petroleum ether, and choline was liberated and precipitated as reineckate according to the method of Entenman *et al.* [5].

The ribonucleic acid extracts.—Ribonucleic acid (RNA) nucleotides were extracted from the lipid-free embryos by fractionated treatment with cold *N* $HClO_4$ [19, 12]. The extracts were neutralized with KOH, and the $KClO_4$ precipitates were removed by centrifugation. The solutions were concentrated *in vacuo*, and the nucleotides were isolated by ion exchange chromatography [12].

The guanylic and adenylic acids were hydrolyzed with *N* HCl for 75 minutes at 100°C, and diluted, on the basis of the ultraviolet absorption curves, with appropriate amounts of unlabeled guanine and adenine. The purines were precipitated with $CuSO_4$ + $NaHSO_3$, and the precipitates were combusted to $BaCO_3$. The pyrimidine nucleotides were treated with *N* HCl at 120°C for 150 hours, and the uracil obtained was isolated by chromatography (Dowex 50). The uracil samples were diluted in known proportions with uracil carrier, and were then combusted to $BaCO_3$.

The protein fraction.—The material, which had been extracted with cold perchloric acid, was treated with 5 per cent TCA at 90°C for 20 minutes, and the residues were washed in the same medium. Minor parts of the protein samples were used for the determination of the specific activities of the total proteins (Fig. 3). The main part of the protein material (approximately 300 mg per sample) was hydrolyzed for 10 hours in 10 per cent HCl at 120°C. The hydrolyzates were evaporated *in vacuo*, and the HCl was largely removed by repeated evaporations with small volumes of water. The amino acid solutions were added to columns of the anion exchanger Amerlite IR 4B (30 cm × 0.65 cm^2). The basic and neutral amino acids were eluted from the columns with water, while the acid amino acids were eluted with 2 *N* acetic acid. The separation was controlled with ninhydrin tests. After evaporation both amino acid fractions were transferred to separate columns of the kation exchanger Dowex 50 (145 cm × 1.6 cm^2). The columns were provided with water jackets, which were kept at a constant temperature of 45°C. The amino acids were eluted with HCl in continuously increasing concentrations (0.5–2.5 *N*). The eluates were tested by ninhydrin spot tests, and the amino acid fractions were identified by paper chromatography.

Of the neutral amino acids serine, threonine, glycine, alanine, valine, proline, methionine, leucine + isoleucine and tyrosine were collected. The β-carbon of serine was isolated as formaldehyde by periodate oxidation according to Nicolet and Shinn [18], and was precipitated from the aerated samples by condensation with dimedone. The dimedone derivative was combusted to $BaCO_3$, and the specific activities were corrected for the isotope dilution involved in the precipitation procedure. The alanine was decarboxylated with ninhydrin. The carboxyl carbon was directly recovered as $BaCO_3$. The acetaldehyde, originating from the α-and β-carbon atoms, was oxidized with chromic acid. The acetic acid obtained was isolated by steam distillation, and combusted in the form of sodium acetate. The other neutral amino acids had very low specific activities, and combustion to $BaCO_3$ therefore seemed undesirable. They were counted without combustion, the amounts of the amino acid in the counted samples being determined by quantitative paper chromatography [1].

The glutamic and aspartic acids were isolated from separate Dowex 50 columns.

The glutamic acid was crystallized from saturated hydrochloric acid at 0°C. The aspartic acid was precipitated and recrystallized as copper aspartate. The acids were combusted to $BaCO_3$.

RESULTS

The rate of incorporation of C^{14}-formate into purines was rather low during the first hours of development, but rapidly increased during the early blastula stage (Figs. 1, 2). From the mesenchyme blastula stage it gradually

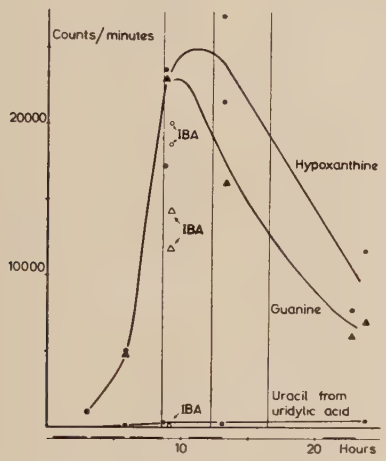

Fig. 1.

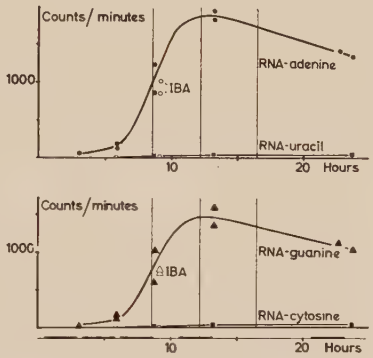

Fig. 2.

Fig. 1. *Psammechinus* embryos at different stages of development maintained for $2\frac{1}{2}$ hours in sea water containing C^{14}-formate. Specific activities (counts per minute per 16 mg $BaCO_3$ per cm^2) of nucleotide bases isolated from TCA extracts of the embryos. Values obtained from embryos treated with *o*-iodosobenzoic acid (IBA) are indicated by open signs. Vertical lines indicate hatching, appearance of mesenchyme cells, and start of invagination. The periods of isotope incubation are indicated by horizontal lines at the bottom of the figure.

Fig. 2. The same material as in Fig. 1. Isotope incorporation into purines and pyrimidines from ribonucleic acid.

decreased again. The purines isolated from RNA followed the acid soluble purines fairly closely. Probably, however, the culmination of the RNA purines occurred in these experiments slightly later than the culmination of the acid soluble purines. The general level of isotope incorporation was much higher in the acid soluble purines, suggesting more frequent interactions between them and the intermediary nucleotide metabolites. They may very well have been directly related to the low-molecular RNA precursors.

The isotope content of the protein fraction (Fig. 3) was concentrated to the serine, of which the β-carbon had a relatively high specific activity. The

carboxyl carbon, on the other hand, contained very small amounts of isotope. Some activity was observed in alanine (Fig. 3), probably also in this case concentrated to the β-carbon. The carboxyl carbon of alanine contained only insignificant amounts of isotope, activity values of 0, 1, 3, 5, and 18 counts

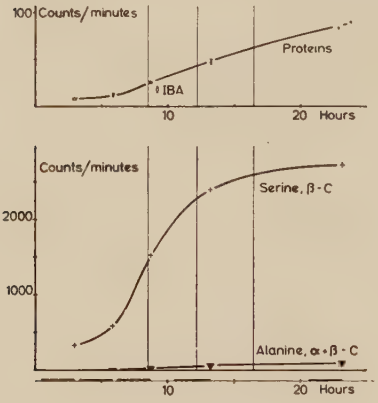

Fig. 3. The same material as in Fig. 1. Isotope incorporation into proteins and into serine and alanine isolated from proteins.

TABLE I

Incorporation of C^{14}-formate into early *Paracentrotus* gastrulae. Counts per minute per 16 mg $BaCO_3$ per cm^2.

The samples with an asterisk were counted without combustion and recalculated to $BaCO_3$-standard on the basis of an empirical activity saturation curve.

TCA-soluble fraction	
Guanine	82,000
Uracil from uridylic acid	800
Picolinic acid methyl betain	20
RNA fraction	
Adenine	2,140
Guanine	2,600
Lipid fraction	
Choline*	50
Protein fraction	
Serine, β-carbon	9,000
Alanine, α- and β-carbon	300
Alanine, carboxyl carbon	30
Methionine*	95
Glutamic acid	45
Aspartic acid	40
Tyrosine*	35
Threonine*, glycine*, valine*, proline*, leucine*	5–25

per minute being observed at the five developmental stages investigated. Of the other amino acids only methionine showed an appreciable incorporation. The specific activities of methionine (recalculated as $BaCO_2$) were at the same stages: 12, 13, 14, 37 and 56 counts per minute. The isotope contents of glutamic and aspartic acids did not reach 10 counts per minute until the last stages. The specific activities of threonine, glycine, valine, proline, leucine, isoleucine and tyrosine were still smaller.

Low incorporation values (10–50 counts per minute) were observed also in choline.

The experiments with *Paracentrotus* embryos were performed mainly in order to measure the incorporation of C^{14}-formate into the picolinic acid methyl betaine (homarine), a compound which occurs in considerable amounts in the embryos of this species [16]. As a consequence of the larger amounts of isotope added to the *Paracentrotus* embryos the incorporation values were in general higher in this material (Table I). The specific activity of the betaine, however, was very low.

DISCUSSION

As is well known, the first period of development in the sea urchin embryo is characterized by a series of rapid cell divisions. The deoxyribonucleic acid (DNA) involved in this mitotic activity may possibly be furnished to some extent from preexistent complex precursors stored in the cytoplasm [cf. 3, 24]. Fairly soon, however, the total amounts of DNA in the embryos begin to successively increase [22, 4]. The intensified incorporation of C^{14}-formate into the purines of the acid-soluble cell constituents at the early blastula stage may be indicative of an increased demand for DNA metabolites during this period of rapid DNA production.

The increased nucleotide metabolism during the blastula stage is not confined, however, to the production of DNA. The labeled formate was rapidly incorporated also into the RNA purines (Fig. 2). Contrary to DNA, the total amounts of RNA in the sea urchin embryo only moderately fluctuates during the early development [22, 4]. The rapid incorporation of C^{14}-formate into RNA during the blastula stage may imply a rapid reconstitution of RNA units during this period. The reconstitution seems to be rather fundamental, since besides C^{14}-formate also other simple nucleotide metabolites (N^{15}-ammonia [12], C^{14}-carbon dioxide [15]) are readily introduced into the new RNA units.

As was mentioned in the introduction, the incorporation of labeled amino acids into proteins is particularly concentrated to the submicroscopic cell

structures during the blastula stage [14]. It seems very likely that the primary determination is attended with a rapid outgrowth of submicroscopic structural elements, characterized by a high content of RNA. It seemed possible that a treatment of the embryos with *o*-iodosobenzoic acid (IBA), a powerful animalizing agent [20], might accentuate the increased RNA metabolism during the determination period [cf. 11]. The embryos treated with IBA, however, did not show any specific effects of that kind. On the contrary, a generally diminished metabolic activity was indicated (Figs. 1–3).

Correlated with the sharp increase in purine metabolism during the blastula stage there was a rapid incorporation of C^{14}-formate into the β-carbon of serine [cf. 21]. This is consistent with the close interrelationship between the metabolism of serine and the introduction of formate into purine ribotides, which has been observed in other systems [2, 7, 23]. In such systems serine can function as a donor of hydroxymethyl groups, which after condensation with tetrahydrofolic acid and oxidation may be introduced into positions 2 and 8 of nucleotide purines. The rapid incorporation in the present experiments of C^{14}-formate into serine makes it very likely that this enzymatic mechanism operates with high efficiency also in sea urchin embryos. The experiments suggest a twofold function in purine metabolism of the large amounts of glycine accumulated in the sea urchin eggs. Besides being a key metabolite in the formation of glycineamideribotide [6], glycine may function as a secondary carrier of C_1 units, by which the folic acid system, during the period of rapid reconstitution of nucleotides, may be drained and replenished without loss of ATP energy.

The experiments indicate a fairly rapid conversion of serine to alanine. For the formation of other amino acids the labeled formate was very slightly utilized. This utilization, though still insignificant, increased somewhat at the gastrula stage, as a consequence, probably, of a more rapid formation of labeled carbon dioxide or carbohydrate metabolites from formic acid after that period.

The small utilization of C^{14}-formate in the formation of methyl groups (methionine, choline, picolinic acid methyl betaine) was unexpected, and this metabolic deficiency cannot be properly interpreted at present.

SUMMARY

C^{14}-formate was readily incorporated into the purines of sea urchin embryos. The incorporation into both acid-soluble and RNA-bound purines

increased rapidly during the blastula stage, simultaneously with the period of primary determination.

The incorporation of C^{14}-formate into protein-bound serine (β-carbon) appeared to be correlated with the incorporation into purines. Of the other investigated amino acids only alanine contained any considerable amounts of isotope.

The incorporation into methionine, choline and picolinic acid methyl betaine was relatively small.

The work was supported by a grant from the Swedish Natural Science Research Council. The author wishes to express his gratitude to Mrs. Kerstin Litzén and Mrs. Gunilla Beskow for skilful technical assistance, and to Fil. mag. B. Markman for a preparation of labeled *Paracentrotus* material. He is much indebted to Professor J. Runnström and to Dr. G. Gustafsson, the Zoological Station of Kristineberg, for working facilities and material.

REFERENCES

1. Awapara, J., *J. Biol. Chem.* **178**, 113 (1949).
2. Buchanan, J. M., Levenberg, B., Flaks, J. G., and Gladner, J. A., *in* Amino Acid Metabolism. McElroy, W. D. and Glass, B., eds., p. 743. Baltimore, 1955.
3. Elson, D. and Chargaff, E., *Experientia* **8**, 143 (1952).
4. Elson, D., Gustafson, T., and Chargaff, E., *J. Biol. Chem.* **209**, 285 (1954).
5. Entenman, C., Taurog, A., and Chaikoff, I. L., *J. Biol. Chem.* **155**, 13 (1944).
6. Goldthwait, D. A., Greenberg, G. R., and Peabody, R. A., *Biochim. et Biophys. Acta* **18**, 148 (1955).
7. Goldthwait, D. A., Peabody, R. A., and Greenberg, G. R., *in* Amino Acid Metabolism. McElroy, W. D. and Glass, B., eds., p. 765, Baltimore, 1955.
8. Gustafson, T. and Hasselberg, I., *Exptl. Cell Research* **2**, 642 (1951).
9. Gustafson, T. and Lenicque, P., *Exptl. Cell Research* **3**, 251 (1952).
10. Hultin, T., *Exptl. Cell Research* **3**, 494 (1952).
11. —— Studies on the structural and metabolic background of fertilization and development, Stockholm, 1953.
12. —— *Arkiv Kemi* **5**, 267 (1953).
13. —— *ibid.* **5**, 543 (1953).
14. —— *ibid.* **5**, 559 (1953).
15. —— *ibid.* **6**, 195 (1953).
16. Hultin, T., Lindvall, S., and Gustafsson, K., *Arkiv Kemi* **6**, 477 (1953).
17. Krüger, M. and Schmied, J., *Z. physiol. Chem.* **45**, 1 (1905).
18. Nicolet, B. H. and Shinn, L. A., *J. Biol. Chem.* **139**, 687 (1941).
19. Ogur, M. and Rosen, G., *Arch. Biochem.* **25**, 262 (1950).
20. Runnström, J. and Kriszat, G., *Exptl. Cell Research* **3**, 497 (1952).
21. Sakami, W., *J. Biol. Chem.* **176**, 995 (1948).
22. Villee, C. A., Lowens, M., Gordon, M., Leonard, E., and Rich, A., *J. Cellular Comp. Physiol.* **33**, 93 (1949).
23. Warren, L. and Flaks, J. G., *Federation Proc.* **15**, 379 (1956).
24. Zeuthen, E., *Arch. Néerland. Zool.* Suppl. **1**, 31 (1953).

THE SOLIDIFYING EFFECT OF CERTAIN OXIDATION-REDUCTION INDICATORS ON THE SURFACE OF THE UNFERTILIZED SEA URCHIN EGG

J. RUNNSTRÖM and G. KRISZAT

The Wenner-Gren Institute for Experimental Biology, University of Stockholm, Sweden

Received October 15, 1956

In a preceding paper [13] the senior writer demonstrated that two oxidation-reduction indicators, porphyrindin and porphyrexid, exert a strongly inhibitory effect on the fertilization of the sea urchin egg. It seemed probable that the action resided in the solidification of the surface layers of the egg as a consequence of the oxidation of some of their components.

In further experiments the solidification was directly demonstrated by aid of centrifugation of the egg.

Moreover, it was shown that a preceding treatment of the eggs with trypsin may neutralize the effect of the indicators, at least to some extent. On the other hand, pretreatment with the indicators was found to protect the egg surface against trypsin. These results will be described and discussed below.

MATERIAL AND METHODS

For these experiments the gametes of *Paracentrotus lividus* and particularly of *Psammechinus miliaris* were used. The first-mentioned species was provided at the Stazione Zoologica, Naples, the latter at Kristineberg Zool. Station at the west coast of Sweden. The material was treated in the customary way, cf. for example [4]. The oxidation-reduction indicator preferentially used in these experiments was porphyrindin [10] which Dr. Hans Bielig (Heidelberg) very kindly put at our disposal. The cryst. trypsin used was that of Worthington Chem. Corporation, Lot T 519. In the centrifugation experiments the centrifuge-microscope of E. N. Harvey and Loomis [7] was used. In the tables n designates the number of eggs counted in each series.

RESULTS

Centrifugation of Eggs Subjected to Porphyrindin

The centrifuge experiments were carried out in a way similar to that introduced by E. N. Harvey [6] and E. B. Harvey [5]. The eggs were suspended in microcuvettes on the border between sea water and an isotonic cane sugar

solution. From the moment the centrifuge had reached the speed giving an acceleration of 4350 *g* the elongation of the egg was measured each minute by means of an ocular micrometer according to the procedure adopted by Kriszat [9].

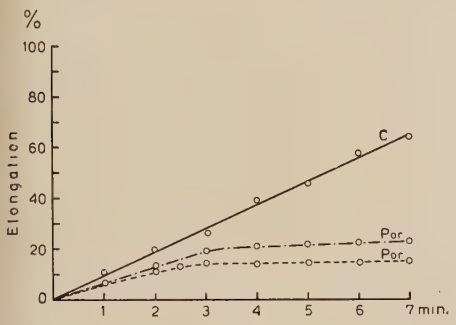

Fig. 1.

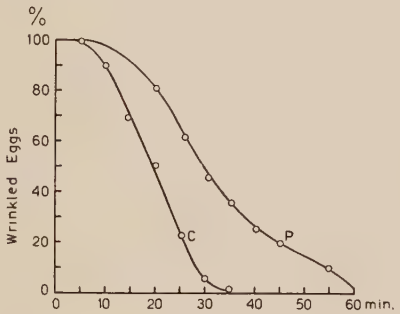

Fig. 2.

Fig. 1. *C*, the elongation of unfertilized eggs of *Psammechinus miliaris* in sea water. *Por*, elongation of eggs of the same species which had been subjected for 30 minutes to 5×10^{-4} *M* (upper *Por*-curve) and 10^{-3} *M* porphyrindin (lower *Por*-curve).
Fig. 2. The smoothening of eggs of *Psammechinus miliaris* in a hypertonic solution. *C*, control eggs. *P*, eggs which had been pretreated for 30 minutes with 5×10^{-4} *M* porphyrindin.

In Fig. 1 curve *C* gives the elongation in the control eggs. The rate of elongation is here 9–10 per cent per minute. In the particular experiment reproduced in Fig. 1 equilibrium was not definitely reached during the time of observation, although in general the rate of elongation begins to decrease after 5–6 minutes in control eggs. In parallel tests the eggs were subjected to 5×10^{-4} and 10^{-3} *M* porphyrindin for 30 minutes and thereafter transferred to the microcuvettes of the centrifuge microscope. The rate was below the value of the control. Particularly it is obvious that an equilibrium is approached already after about 3 minutes. In the porphyrindin-treated eggs the final values of elongation were only ca. 30 per cent of those observed in the control. A considerable increase of the "rigidity" of the surface layer occurs thus when the eggs are subjected to the porphyrindin solution.

In parallel series the eggs were centrifuged on the border between sea water and a 20 per cent gum arabic solution. Here no gradient arises and the eggs remain spherical or almost spherical. In such eggs it was easier to observe and compare the inner stratification. There was no difference in the rate of stratification between control eggs and eggs subjected to porphyrindin. This shows that the difference which appears in the eggs suspended on the border between sea water and sucrose solution was entirely due to differences in rigidity of the egg cortex.

The Porphyrindin-Treated Eggs in Hypertonic Solution

Parallel to the centrifugation experiments the behavior of eggs of *Psammechinus miliaris* was observed while they underwent plasmolysis in a hypertonic solution. When unfertilized eggs have reached their minimum size after immersion in a hypertonic medium (2 ml sea water + 0.6 2.5 *M* NaCl solution) the surface becomes wrinkled. After some time the wrinkles disappear. The rate of disappearance of the wrinkles seems to be an indicator of the rigidity of the surface layer. In a typical experiment the eggs were exposed to 5×10^{-4} *M* porphyrindin for 30 minutes. Thereafter the eggs were brought into hypertonic solutions still containing porphyrindin. After 2–3 minutes the wrinkling appeared; thereafter the number of still wrinkled eggs was followed by counting 75–100 eggs each time. The curves in Fig. 2 give a typical result. The smoothing is more rapid and more uniform in the control eggs than in those subjected to porphyrindin. The form of the curves tends to indicate that one group of the eggs was more strongly affected by the indicator than the remainder.

The Effect of Pretreatment with Crystalline Trypsin on the Action of Porphyrindin

Eggs of *Psammechinus miliaris* were first pretreated with trypsin 0.003 per cent. Thereafter the eggs were washed and transferred to different porphyrindin solutions and finally washed again in sea water and inseminated in this medium. The trypsin pretreatment lasted for 15 minutes: the eggs were then subjected to different concentrations of porphyrindin for 30 minutes and finally washed in normal sea water and inseminated here. Five hours later the counts were made which are represented in Fig. 3.

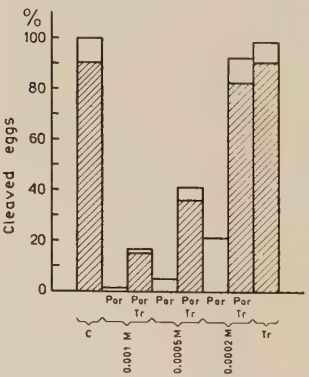

Fig. 3. Eggs of *Psammechinus miliaris* were exposed to porphyrindin 0.0002, 0.0005, 0.001 *M* for 30 minutes and thereafter transferred to normal sea water and fertilized there. The eggs had been pretreated with 0.003 per cent trypsin (*Tr*) or had not undergone any pretreatment with trypsin. *C* (on the left end), eggs not pretreated with either trypsin or porphyrindin. *Tr.* (on the right end), eggs pretreated only with trypsin. The hatched parts of the columns indicate the percentage of divided eggs, the non-hatched that of non-divided, fertilized eggs. The counts were made 5 hours after fertilization, about 300 eggs being counted each time.

In the following experiment with *Psammechinus miliaris* parallel observations were carried out on eggs which were subjected to porphyrindin and then fertilized in normal sea water and eggs which were inseminated in the presence of porphyrindin. Moreover, eggs were used which had or had not received a pretreatment with 0.002 per cent trypsin.

1A. The following gives a survey of the treatment of the egg in this experiment:

a	Sea water control	Not pretreated with trypsin.
b	10^{-4} *M* porphyrindin in sea water	
c	,, ,, ,, ,, ,,	
d	Sea water control	Pretreated for 30 minutes with 0.002 per cent trypsin.
e	10^{-4} *M* porphyrindin in sea water	
f	,, ,, ,, ,, ,,	

After 30 minutes:

a, *b*, *d*, *e*, eggs transferred to normal sea water and inseminated here.

After 35 minutes:

c, *f*, eggs inseminated in the porphyrindin solution.

After 2 hours, 45 minutes:

c, *f*, eggs transferred to normal sea water and reinseminated here.

In *a* and *d* 100 per cent fertilization, in *a* with membrane elevation and in *d* without; in *b* there is 100 per cent fertilization but strong contractions are observed and the membrane is in general only locally elevated, cf [13]. In *e* 100 per cent fertilization, no contractions of the egg surface but a certain tendency to polyspermy which was not quantitatively evaluated. In *c* no fertilization followed the first insemination although spermatozoa seem to stick to the egg surface. In *f* about 2 per cent of the eggs were fertilized at the first insemination. Clear bulges were sometimes observed on the surface of the eggs even if they were otherwise not fertilized. They resembled entrance cones.

a, *b*, *d*, *e* were examined 6 hours and 40 minutes after insemination. The following gives a survey of the state of the eggs in the different tests.

	Non-divided eggs per cent	Cleavage stages and partially developed blastulae per cent	Blastulae per cent	*n*
a	—	—	100	>200
b	61	—	39	228
d	—	—	100	>200
e	17	16	67	286

Only some few of the blastulae had hatched in *a*, in *b* the outline of the blastocoel was very irregular; in *e* as well as in *a* the blastocoel is larger and with an even outline. Evidently the secretion of the content of the blastocoel is retarded in *b*, but is more advanced in *a* and *e*.

6–7 hours after the reinsemination, cf. above, *c* and *f* were examined:

c: 7 per cent were not fertilized, 93 per cent fertilized ($n = 137$), no cleavage, membrane low and very often corrugated with at most local smoothening and elevation.

f: A high percentage of eggs developed into blastulae as shown by the following counts.

Non-divided eggs, mostly fertilized	Partially developed blastulae	Blastulae	*n*
14 per cent	21 per cent	65 per cent	218

The prolonged treatment with porphyrindin (2 hours, 45 minutes) had brought about a complete suppression of cleavage in the eggs not pretrated with trypsin (*c*). The development capacity was thus considerably lowered as compared with the eggs subjected to porphyrindin for only 30 minutes (*b*).

Conversely following pretreatment with trypsin there was no significant difference between the eggs subjected to porphyrindin for 30 minutes or for two hours and 40 minutes, as the counts demonstrate (*e*, *f*). The blastulae were however slightly more irregular in *f* than in *e*. Moreover, the cells had a stronger tendency to dissociation in *f*.

One group of embryos was distinguished as partially developed blastulae. This means that about half the egg underwent cleavage whereas the rest remained non-divided. No doubt such half blastulae originated from eggs in which the fertilization impulse had covered only about half the surface of the egg. As shown previously the impulse often subsides after pretreatment with porphyrindin [13].

The Action of Trypsin on Eggs Pretreated with Porphyrindin

In some experiments the order of treatment was reversed as compared with that adopted in the experiment previously described. The eggs were first pretreated with porphyrindin and only after this they were subjected to trypsin. It was demonstrated in this way that the porphyrindin pretreatment brings about a decrease in the sensitivity of the eggs to trypsin. The extent of the effect depends on the concentration of the porphyrindin and the duration of treatment.

2A. The following gives a survey of the treatment of the eggs in this experiment:

a	Sea water.	
a'	Sea water. 85 minutes after suspension in sea water, subjected to trypsin 0.0025 per cent for 30 minutes. Thereafter the trypsin concentration was lowered about 10 times.	
b	10^{-4} *M* porphyrindin in sea water for 30 minutes.	—
c	As above.	Subjected to trypsin as in *a'*.

d	As above.	Subjected to trypsin as in *a'*.
e	2.5×10^{-4} *M* porphyrindin in sea water for 30 minutes.	—
f	As above.	Subjected to trypsin like in *a'*.
g	As above.	Subjected to trypsin like in *a'*.

The tests *a*, *b*, and *e* were inseminated 70 minutes after final transfer to normal sea water (*N.B.* no trypsin treatment).

In these fertilization occurred but cleavage was not frequent in the eggs pretreated with porphyrindin. Counts were made 6 hours 30 minutes after fertilization:

	Non-fertilized eggs per cent	Non-divided eggs fertilized per cent	Blastulae per cent	*n*
a	—	—	100	~200
b	2	73	25	232
e	—	82	18	202

The tests *a'*, *c* and *f* were inseminated 15 minutes after transfer from the trypsin solution to normal sea water. The treatment with trypsin brought about a considerable lowering of the fertilizability of the eggs in *a'*, which had been subjected to trypsin without previous porphyrindin pretreatment. There is a high percentage of fertilization in *c*, *f*, as shown in the following survey.

60–70 minutes after fertilization:

	Non-fertilized eggs per cent	Non-divided fertilized eggs per cent	2-cell stages per cent	*n*
a'	58	0.5[1]	41[1]	232
c	7	12[2]	81[1]	195
f	—	78[3]	12[3]	90

[1] Without fertilization membrane.

[2] With tight membrane, some of the eggs were incompletely cleaved into two cells.

[3] All the non-divided eggs had a fertilization membrane which was not or was only incompletely elevated. About half the number of divided eggs in *f* had an elevated membrane.

6 hours, 15 minutes after fertilization the eggs were examined again and the result was now the following:

	Non-developed eggs, non-fertilized or blocked in early cleavage stages per cent	Blastulae with large blastocoel per cent	*n*
a'	71	29	166
c	17	83	265
f	100	—	~200

The tests *d* and *g* were inseminated 2 hours after dilution of the trypsin to about 1/10. At the same time untreated control eggs from the same female were inseminated (*a''*).

After 3 hours and 15 minutes the situation was the following:

	Non-divided eggs per cent	Divided eggs with blastocoel per cent	*n*
a''	—	100	~200
d	63[1]	37	259
g	25[2]	75	216

[1] The majority not fertilized.

[2] The majority fertilized.

Only in the control fertilization membranes were formed.

The prolonged treatment with diluted trypsin has suppressed the capacity of normal membrane formation both in *d* and *g*. In *d* the percentage of inhibited eggs approaches that found in *a'*, but in *g* the pretreatment with 2.5×10^{-4} *M* porphyrindin has brought about a considerable protection.

In other experiments a more thorough washing was carried out after the treatment for 30 minutes with 0.0025 per cent trypsin. This interrupted more efficiently the continued action of trypsin which can be distinguished in the experiment 2 A, but otherwise the type of result was the same. A pretreatment with 2.5×10^{-4} *M* porphyrindin for 30 minutes rather efficiently inhibited the dissolution of the membrane. This, on the other hand, arrested the majority of eggs in an early stage.

DISCUSSION

This paper brings data which are in agreement with the conclusions which were formulated in the preceding paper [13]. The centrifugation experiments indicate a high rigidity of the surface of eggs which are exposed to porphyrindin, whereas the rigidity of the endoplasm is not different from that found in non-treated control eggs. The hypertonicity test also indicates a higher rigidity of the surface than in the control.

The experiments with eggs pretreated with trypsin demonstrate that the effect of pretreatment with porphyrindin is much less inhibitory in these than in eggs not pretreated with trypsin. The material in the egg surface which is attacked by trypsin seems to be identical with that which is preferably in-

fluenced by pretreatment with porphyrindin. This material corresponds mainly to a metaplasmatic structure in the egg surface which appropriately should be designated as vitelline membrane.

The existence of this membrane in our material, *Psammechinus miliaris*, has been proved by Afzelius [1] in an electron microscopic study, cf. also [13]. One should expect that the vitelline membrane would be absent when the eggs had been subjected to treatment with trypsin before fixation. However, the electron microscopic picture still shows a vitelline membrane. Trypsin does not break down the membrane completely but attacks only certain peptide bonds. This does not change the morphological picture of the membrane [2]. Yet this is now rather a mosaic of adjacent sheets than a continuous membrane. It is no longer capable of serving as a support for the cortical granules which normally merge with the membrane. After previous trypsin treatment such fenestrated membranes may at most arise as those described by Minganti [10].

In the presence of porphyrindin in low concentrations the fertilization is inhibited even if the eggs have been pretreated with trypsin. This confirms that the indicator is able to change the cytoplasmic cortex. Provided the concentration of the indicator has not been too high the action on the cytoplasm is reversible owing to the metabolism which is able to convert the porphyrindin into its harmless reduced form. The change of the metaplasmatic structures under the action of the indicator is more irreversible owing to the absence of a metabolism in these structures. This is the same conclusion which was formulated already on the basis of the data presented in the preceding paper [13]. The data submitted in the present paper seem appropriate to give a definition of metaplasmatic structures which distinguishes them from the metabolically active cytoplasm. The primary action of the trypsin or the porphyrindin on metaplasm or cytoplasm is alike. The difference resides in the incapacity of the metaplasm to restore the changes brought about by the agents, whereas the metabolism of the cytoplasm removes their effect.

The order of treatment has been reversed in certain experiments. The eggs were first exposed to porphyrindin and only thereafter to trypsin. The pretreatment with the high potential indicator proved to protect the surface structures against the action of trypsin. Different degrees of protection were found according to concentration of the indicator and duration of exposure to this latter. It is evident that the oxidation of the surface structures renders them less accessible to the action of trypsin.

In the first place the vitelline membrane becomes resistant—a change

which resembles that occurring normally in the elevated membrane. During its elevation the membrane is extremely senstitive to proteolytic enzymes. In connection with the toughening of the membrane, however, it becomes very resistant to these enzymes [8]. It is tempting to infer that the natural toughening is due to an oxidation process caused by a substance analogous to porphyrindin. Observations carried out by our colleague Markman do not speak in favor of this contention. He added porphyrindin to eggs in which the fertilization membrane was under formation but failed to recognize any premature toughening of the membrane under the action of the oxidizing reagent.

In one experiment reported above (2A) the trypsin has damaged the cytoplasmic surface to such extent that the percentage of eggs capable of fertilization was definitely reduced (*a'*). Under the given experimental conditions the pretreatment with porphyrindin did not suffice to protect the vitelline membrane against the action of trypsin but, on the other hand, it protected against the breakdown of the fertilizing capacity of the egg (*g*). The fact that trypsin is able under certain conditions to render the eggs non-fertilizable has been reported earlier [3, 12].

Probably studies with combined action of the high potential indicators and trypsin would contribute to the analysis of the important phenomenon of the inactivation of the eggs through trypsin.

In the preceding paper [13] an experiment was described in which eggs were kept in sea water for 25 hours. In these eggs no membrane appeared upon fertilization. It must be concluded that the vitelline membrane had been broken down by enzymic activity emanating either from the egg or from bacteria of the medium. The latter possibility is less probable. From the concentration 3.6×10^{-5} *M* porphyrindin on the eggs were protected against the breakdown of the vitelline membrane, as here a rather tight membrane appeared upon fertilization. This observation is in keeping with the results obtained following combined treatment with indicator and trypsin.

It is of some interest to note that even subsequent to trypsin treatment a temporary treatment with porphyrindin may cause a partial development of the egg, cf. 1A, *f*. This is due, no doubt, to a decrement in the propagation of the activation impulse or "fertilization wave" (Yamamoto; for references see [14]), so that only the part of the egg surface adjacent to the site of sperm entry has been covered by the activation impulse. The oxidation-reduction state in the cortex may be involved in the propagation of the impulse.

SUMMARY

Further studies have been carried out on the effect of porphyrindin on the egg of the sea urchin, *Psammechinus miliaris*. To a smaller extent also eggs of *Paracentrotus lividus* were studied.

Eggs suspended on the border between sea water and isotonic sucrose solution were centrifuged under certain standard conditions. Following treatment with porphyrindin the eggs elongated very slightly and an equilibrium state was soon attained. The elongation was stronger in the control eggs and the equilibrium was attained only after a longer interval of time. Conversely, the stratification in the interior was alike in control eggs and those subjected to porphyrindin. The results indicate that the rigidity of the egg surface but not that of the interior of the egg is increased subsequent to the treatment with porphyrindin. Observations on the plasmolysis of eggs in a hypertonic solution also pointed to an increased rigidity of the surface in eggs subjected to porphyrindin as compared with control eggs.

Pretreatment of unfertilized eggs with crystalline trypsin removed to a considerable extent the effect of a temporary exposure to porphyrindin. If such eggs were fertilized a much higher percentage developed into blastulae of normal type than when the eggs had been subjected to porphyrindin without pretreatment with trypsin. Both trypsin and porphyrindin attack in an irreversible way metaplasmatic structures in the surface of the unfertilized egg, particularly the vitelline membrane. If this membrane has been removed by trypsin treatment the direct effect of porphyrindin is on the cytoplasmatic cortex but this effect is reversible at least to a certain extent depending on concentration of porphyrindin and duration of the exposure. Even a temporary exposure of trypsin-pretreated eggs to porphyrindin was sometimes observed to impair the propagation of the impulse of activation. Partially developed eggs and blastulae then resulted. The possibility is considered that the oxidation-reduction state is involved in the propagation of the impulse. When insemination was carried out in the presence of porphyrindin, fertilization was inhibited also in eggs pretreated with trypsin.

In certain experiments unfertilized eggs were first pretreated with porphyrindin and only afterwards subjected to trypsin. The treatment with porphyrindin protects the egg surface against the action of trypsin. Under these conditions the vitelline membrane may resist the trypsin treatment whereas it is broken up by trypsin in non-porphyrindin-pretreated eggs.

Sometimes the trypsin treatment deprives the egg of the capacity of being fertilized. Porphyrindin may protect against this effect of trypsin.

The financial support of the Swedish Natural Science Research Council and the Swedish Cancer Society is gratefully acknowledged.

We are greatly indebted to Dr. Peter Dohrn and to Dr. Gunnar Gustafsson for their ready helpfulness during our sojourns at the Zoological Station, Naples, and at Kristinebergs Zoological Station.

We are much obliged to Dr. H.-J. Bielig, Heidelberg, for his kindness of providing the porphyrindin used in our experiments.

REFERENCES

1. Afzelius, B. A., *Exptl. Cell Research* **10**, 257 (1956).
2. Afzelius, B. A. and Minganti, A., personal communication.
3. Bohus-Jensen, A., *Exptl. Cell Research* **4**, 60 (1953).
4. Harding, C. V., *Exptl. Cell Research* **2**, 403 (1951).
5. Harvey, E. B., *Biol. Bull.* **62**, 155 (1932).
6. Harvey, E. N., *Biol. Bull.* **61**, 273 (1931).
7. Harvey, E. N. and Loomis, A. L., *Science* **72**, 42 (1930).
8. Kopac, M. J., *J. Cellular Comp. Physiol.* **18**, 215 (1941).
9. Kriszat, G., *Exptl. Cell Research* **7**, 103 (1954).
10. Kuhn, R. and Franke, W., *Ber. Deutsch. Chem. Ges.* **68 B**, 1528 (1935).
11. Minganti, A., *Exptl. Cell Research* **7**, 1 (1954).
12. Runnström, J., *Arkiv Zool.* **40 A**, Nr. 17 (1948).
13. ——— *Exptl. Cell Research* **12**, 374 (1957).
14. Yamamoto, T., *Exptl. Cell Research* **10**, 387 (1956).

Experimental Cell Research **12**, *537–545 (1957)*

THE INTRACELLULAR DISTRIBUTION OF LIVER GLYCOGEN[1]

J. SACKS, P. M. JOHNSTON, JO H. MORTON and JAQUELIN A. N. HARVEY

Departments of Chemistry and Zoology, University of Arkansas, Fayetteville, Ark., U.S.A.

Received October 16, 1956

The finding of Lazarow [8] that glycogen is present in the liver in the form of aggregates of submicroscopic particles not associated with protein, has been confirmed by other users of the technique of differential centrifugation [1, 3]. Lazarow obtained this particulate glycogen as a compact mass by centrifugation at approximately 12,000 *g* after a preliminary centrifugation at lower speed to remove nuclei and mitochondria from the homogenate. This glycogen sedimented together with reddish submicroscopic particles composed of lipoprotein. These particles could easily be separated from the compact mass of glycogen by gentle swirling with saline solution. The glycogen so obtained was found to be insoluble in water, but could readily be converted to the ordinary type by several treatments which would not be expected to cause any hydrolytic change.

The existence of this particulate, insoluble, glycogen raises some questions. The most obvious one is whether all the glycogen present in the liver of the fed animal is in this particulate form, and if not, what fraction of the total glycogen content is so represented. Another question is with respect to the possible presence of glycogen within the organelles of liver as ordinarily obtained by differential centrifugation. Practically all investigators using this technique for enzyme or nucleic acid studies, use fasted animals, with livers essentially devoid of glycogen. The experiments described below were undertaken to obtain answers to these two questions. It has been found that the particulate glycogen isolated by essentially the method of Lazarow accounts for a relatively small fraction of the total glycogen that can be demonstrated in the liver of the fed rat by ordinary techniques, and that mitochondria and microsomes, as well as the particles sedimented at 12,000 *g*, also contain glycogen demonstrable by both chemical and histological tech-

[1] Work performed under contract AT-(40-1) 1521 between the U.S. Atomic Energy Commission and the University of Arkansas.

niques. A considerable portion of the total glycogen content is present in the supernatant solution remaining after sedimentation of the major portion of the microsomes. It has also been found that considerable glycogenolysis takes place when the particulate fractions of liver are isolated by the standard conditions of the technique.

EXPERIMENTAL

The experiments were carried out on female rats of the Wistar strain which were allowed free access to food and water. All operations up to the point at which enzymatic activity was stopped by the addition of trichloroacetic acid were carried out in a cold room maintained at 1 2°C, or in a refrigerated centrifuge operating at this temperature.

The livers were removed under pentobarbital anesthesia, weighed rapidly, and a small piece removed and placed in fixing solution for histological examination. The liver was then immediately dropped into a beaker containing a fairly large volume of 0.25 *M* sucrose solution, and cut into small pieces. These were washed several times with the cold sucrose solution, to remove as many erythrocytes as possible, then homogenized in a Potter–Elvehjem homogenizer with Teflon pestle. The subsequent treatment, which is based on the procedures of Hogeboom *et al.* [7], Lazarow [8], and Smellie *et al.* [10] is indicated in the flow diagram.

The sediment obtained by centrifugation at 600 *g* contained nuclei, unbroken cells, erythrocytes, connective tissue, some cell debris, and mitochondria. These latter were demonstrated by staining with Janus Green B [4]. The treatment with citric acid dissolved the erythrocytes, mitochondria, and cell debris.

The sediment obtained from the centrifugation at 13,000 *g* was easily separated into the two portions described by Lazarow [8]: a reddish part that could easily be suspended by swirling with sucrose solution, which is referred to below as the poorly sedimentable fraction, and a compact translucent mass which was difficult to re-suspend. A similar separation into two portions was obtained with the mitochondrial fraction in one case and with the microsome fraction in two cases. These observations tend to confirm the finding by Claude [3] that the aggregates of particulate glycogen are not uniform in size.

The original sucrose washings and aliquots of both the citric acid extract and the final supernatant fluid representing the cytoplasmic soluble fraction were treated with zinc sulfate and barium hydroxide solutions, the reagents used by Nelson [9] for deproteinization and removal of non-sugar reducing substances. Reducing sugar was then determined on the filtrates by the method of Nelson. Total nitrogen was determined on aliquots of all the sediments, the citric acid washings, and the cytoplasmic soluble fraction, by the standard micro-Kjeldahl procedure.

Chemical determination of glycogen.—Aliquots of the suspensions of the sediments, the citric acid washings, and the final supernatant liquid were treated with equal volumes of 20 per cent trichloroacetic acid solution, the protein precipitates removed by filtration, and glycogen precipitated from a measured volume of the filtrate by the addition of 1.5 volumes of ethanol, essentially the method of Good *et al.* [6].

Flow sheet for isolation of particulate fractions

Liver chilled and minced in 0.25 *M* sucrose, washed to remove erythrocytes, homogenized 2 minutes, centrifuged 10 min. at 600 *g*. Sediment suspended in 0.25 *M* sucrose, homogenized 15 seconds. Mixed with supernatant, and the whole layered over 0.34 *M* sucrose, centrifuged 10 min. at 600 *g*, washed once with 0.25 *M* sucrose.

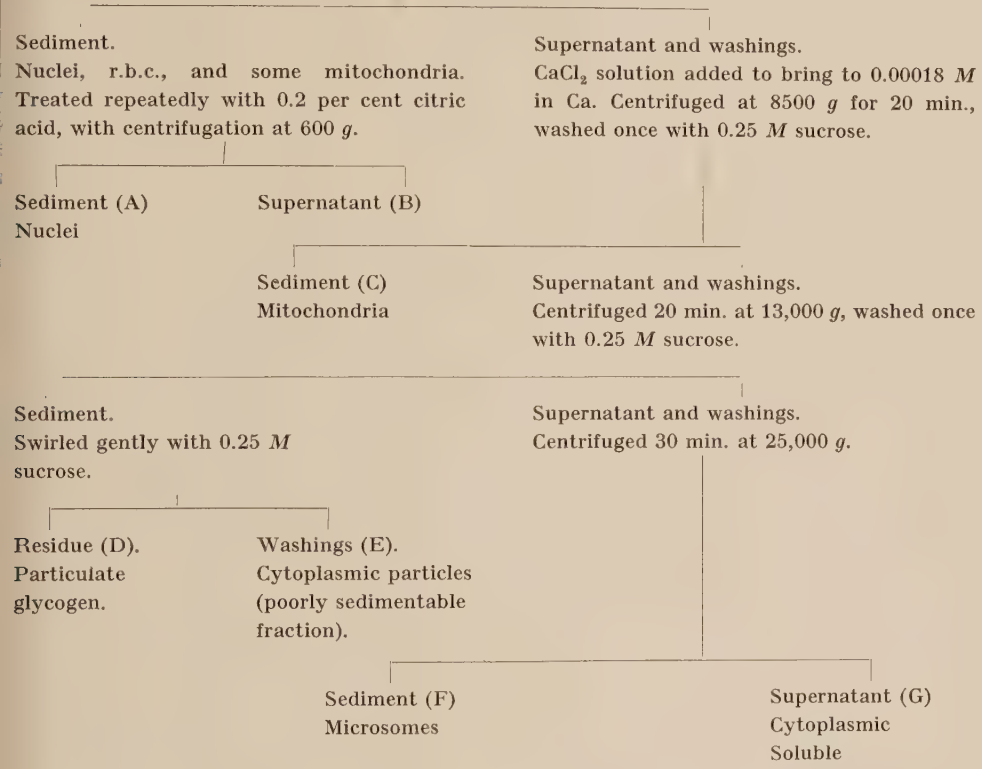
Sediment.
Nuclei, r.b.c., and some mitochondria. Treated repeatedly with 0.2 per cent citric acid, with centrifugation at 600 g.
Supernatant and washings.
CaCl2 solution added to bring to 0.00018 M in Ca. Centrifuged at 8500 g for 20 min., washed once with 0.25 M sucrose.
Sediment (A)
Nuclei
Supernatant (B)
Sediment (C)
Mitochondria
Supernatant and washings.
Centrifuged 20 min. at 13,000 g, washed once with 0.25 M sucrose.
Sediment.
Swirled gently with 0.25 M sucrose.
Supernatant and washings.
Centrifuged 30 min. at 25,000 g.
Residue (D).
Particulate glycogen.
Washings (E).
Cytoplasmic particles (poorly sedimentable fraction).
Sediment (F)
Microsomes
Supernatant (G)
Cytoplasmic
Soluble

All sediments and solutions denoted by letters made up to volume and aliquots taken for determination of glycogen and total N. Sediments A, C, D, E, and F examined histologically.

The precipitates were let stand overnight in the cold, centrifuged, and washed three times with 60 per cent ethanol saturated with sodium sulfate. The supernatant fluids from the final washing were tested for the presence of sucrose by the anthrone reagent. A negative reaction was always obtained, but to make sure that the glycogen values would be valid, an additional washing with the ethanol solution was made. The precipitated glycogen was then dissolved in water, the solutions made up to volume, and aliquots taken for determination by the anthrone [11] method, using pure glycogen from rabbit liver as a standard.

In some experiments, aliquots of the mitochondria, microsomes, and the poorly sedimentable fraction from the centrifugation at 13,000 *g* were treated with KOH solution for glycogen determination, in the attempt to localize the glycogen which Bloom *et al.* [2] found not to be extracted from liver by trichloroacetic acid. In no case was the glycogen value obtained by the KOH treatment higher than that obtained on the trichloroacetic acid filtrate from the same particulate fraction.

Histochemical methods.—The small portion of liver was fixed for 24 hours in either cold absolute alcohol or a mixture of 9 parts of absolute alcohol and 1 part of formalin. The tissue was then rinsed in absolute alcohol, cleared in xylol, infiltrated in 52–54° tissuemat, and embedded. Sections were cut at 5 micra and stained for glycogen by either the Bauer–Feulgen [5] technique or with Best's Carmine [5]. Controls were prepared using salivary digestion. Sections adjacent to those treated as above were stained for polysaccharides by the Hotchkiss [5] technique. Controls on this technique were made by salivary digestion.

Smears were made on dry slides without fixative, of sediments A, C, E, and F, representing respectively the nuclei, mitochondria, poorly sedimented particulates, and microsomes. These were allowed to stand in the cold room for 1 or 2 hours, then fixed in the 9:1 mixture of absolute alcohol and formalin for 24 hours. After the fixation, the smears were stained as described above. Control smears were processed after salivary digestion.

Attempts to obtain stainable smears of the particulate glycogen fraction in this way were unsuccessful, on account of the failure of the glycogen to adhere to the slide. When slides prepared with albumin–glycerin fixative were used, it was possible to obtain stainable smears, although a portion of the material washed off even under these conditions. Salivary digestion controls were run on these smears also.

In order to check for contamination during the separation procedure, fresh preparations of the nuclear, mitochondrial, poorly sedimentable, and microsomal fractions were treated with Janus Green B [4]. These showed that complete or nearly complete separations were accomplished.

RESULTS AND DISCUSSION

Histochemical

The tissue sections were used only to ascertain grossly that glycogen was present in the liver being fractionated, and to verify that all the intracellular polysaccharide present was glycogen. Sections stained according to the Bauer–Feulgen, Best's Carmine, and Hotchkiss methods were all strongly positive. The glycogen was present either as finely divided particles or as large particulates, distributed fairly uniformly throughout the cytoplasm. Sections stained by the Hotchkiss method after treatment with saliva showed no intracellular PAS-positive substances, and it was therefore concluded that the material staining with Best's Carmine and according to the Bauer–Feulgen method was glycogen.

No glycogen was found in the smears of the nuclear fraction except that present in the occasional cell which failed to be disrupted during the homogenization. Many investigators have found no evidence that liver cell nuclei contain glycogen.

The smears of the mitochondrial, microsomal, and poorly sedimented fractions, and of the albumin-glycerin-fixed particulate glycogen, were all uniformly positive. The distribution of the PAS-positive material in the smears of the mitochondrial fraction was quite comparable to that of the Janus Green B-positive material. In the smears of the microsomal and poorly sedimentable fractions also, the PAS-positive material was generally distributed, so that the distribution of this material in each of the organelle fractions was comparable to that in the albumin-glycerin-fixed smears of the particulate glycogen. Since the particulate glycogen itself did not adhere to a dry slide, it is reasonable to assume that the PAS-positive material in the organelle fractions represents glycogen contained within these particles, rather than some particulate glycogen that failed to become part of the compact mass formed in the centrifugation.

Chemical

Glycogenolysis.—Even though all the operations were carried out at 1–2°, determinations of reducing sugar showed that considerable glycogenolysis had taken place. Since liver contains no enzyme capable of hydrolyzing the sucrose of the homogenizing medium, it is evident that the reducing sugar found must have arisen from enzymatic degradation of the glycogen during the course of the separation of the particulate fractions. The reducing sugar, calculated as glycogen, amounted to 16 to 69 per cent of the total glycogen, with an average of 45 per cent. Of this, approximately 10 per cent was found in the sucrose washings to remove erythrocytes, approximately 5 per cent in the citric acid washings of the 600 *g* sediment, and the remainder in the supernatant from the centrifugation at 25,000 *g*. The values for total glycogen, 2.25 to 4.1 per cent, are within the range found in this laboratory for the whole liver of rats in the same nutritional condition and under the same experimental conditions as those of the present experiments.

Glycogen distribution.—The distribution found in the separate experiments was quite variable. The nuclear fraction contained only a few tenths of one per cent of the total glycogen, and the histochemical findings indicate that this should be assigned to the unbroken cells present in this material. The citric acid washings contained from 3 to 6.6 per cent of the total glycogen. Part of this was present as reducing sugar. Since this fraction contained

mitochondria, it is reasonable to assign at least a part of the glycogen content to these organelles.

Complete data for two of the experiments are given in Tables I and II. These are illustrative of the variability found in the whole group of experiments. One point that is shown by these tables is that the use of calcium chloride to agglutinate the mitochondria does not appear to have any effect on the distribution of the glycogen between mitochondria, on the one hand, and the poorly sedimentable and microsomal fractions, on the other. This despite the observation by Hogeboom *et al.* [7] that some microsomes are carried down with the mitochondria in the presence of calcium ion. These tables also show that the effect of the calcium on nitrogen distribution, discussed below, is not accompanied by any effect of glycogen distribution.

It is quite probable that centrifugation at 25,000 *g* does not sediment all the microsomes. However, this limitation, imposed by the equipment available, would not appear to be too formidable. In three of the six experiments, much more glycogen was found as such in the supernatant fluid than in the microsome sediment, and in the other three the glycogen content of the supernatant fluid from the centrifugation at 25,000 *g* was equal to that found in the microsome sediment.

The mitochondrial fraction contained from 7.5 to 16.9 per cent of the total glycogen, the poorly sedimentable fractions from 3.2 to 9.0 per cent, and the microsomes from 4.1 to 12.2 per cent. The supernatant contained from 38.3 to 81.7 per cent of the total, of which the major portion was in the form of reducing sugar. However, in each experiment glycogen was present as such in this solution.

The particulate glycogen described by Lazarow [8] was found in five of the six experiments. The fraction of the total glycogen content present in this form was quite variable, ranging from 3.3 to 20.0 per cent in these five. In addition to this particulate glycogen sedimenting at 13,000 *g*, two livers showed some of this material in the 25,000 *g* sediments, and one of these showed some in the 8500 *g* sediment. These additional portions of particulate glycogen were present where the fraction of total accounted for Lazarow's particulate glycogen were present where the fraction of total accounted for by Lazarow's particulate glycogen was the highest.

Nitrogen distribution.—The nuclear fraction accounted for about one-twelfth of the total nitrogen, the citrate washings for approximately the same fraction, and the mitochondria for 40 to 50 per cent of the total N when $CaCl_2$ was added to agglutinate the mitochondria. The calcium was omitted in two experiments, and in these the mitochondrial fraction accounted

TABLE I

Distribution of nitrogen and glycogen among fractions of rat liver obtained by differential centrifugation.

Mitochondria agglutinated by $CaCl_2$ in final concentration of 0.00018 *M*.

Fraction	Nitrogen		Glycogen		Mg glycogen per mg nitrogen
	Amount (mg)	Per cent of total	Amount (mg)	Per cent of total	
Nuclei	13.8	9.6	0.4	0.15	0.028
Citrate washings	8.9	6.2	11.8*	4.5	1.52
Mitochondria	58.0	40.3	27.3	10.5	0.47
Poorly sedimented fraction from 13,000 *g* ppt.	5.1	3.5	14.4	5.5	2.83
Particulate glycogen from 13,00 *g* ppt.	0.7	0.4	40.6	15.6	55.6
Microsomes	3.0	2.1	24.7	9.5	8.22
Particulate glycogen from 25,000 *g* ppt.	0.04	0.02	33.6	13.0	965
Supernatant	54.4	37.8	87.7*	33.7	1.58
Sucrose washings			20.1*	7.7	
Total	144.2		260.2		

* Includes reducing sugar.

TABLE II

Distribution of nitrogen and glycogen among fractions of rat liver obtained by differential centrifugation.

No $CaCl_2$ used to agglutinate mitochondria.

Fraction	Nitrogen		Glycogen		Mg glycogen per mg nitrogen
	Amount (mg)	Per cent of total	Amount (mg)	Per cent of total	
Nuclei	16.2	8.5	3.6	1.8	0.22
Citrate washings	28.9	15.2	13.0*	6.6	0.45
Mitochondria	44.4	23.4	18.4	9.4	0.41
Poorly sedimented fraction from 13,000 *g* ppt.	8.0	4.2	7.8	7.6	0.98
Particulate glycogen from 13,000 *g* ppt.	1.5	0.8	7.6	3.9	5.1
Microsomes	8.4	4.4	8.1	4.1	0.96
Supernatant	82.5	43.4	128.3*	65.6	1.56
Sucrose washings			8.9*	4.5	
Total	189,9		195.7		

* Includes reducing sugar.

for 20.8 and 23.0 per cent of the total N. The fraction of the total glycogen present in the mitochondria was of the same order in these two experiments as in the four in which calcium was added. In these two cases, the nitrogen content of the final supernatant accounted for the major part of that which came down with the mitochondria when calcium was used.

The poorly sedimentable fraction and the microsomes each accounted for less than 5 per cent of the total N, without regard to the presence of calcium ion. The particulate glycogen fraction, as was to be expected, contained only a small amount of nitrogen. The poorly sedimentable fraction and the microsomes contained relatively more glycogen in proportion to their nitrogen content than did the mitochondria. The average ratios of mg glycogen per mg total N was 0.44 for mitochondria, 2.0 for the poorly sedimentable fraction, and 4.4 for the microsomes.

The use of calcium to agglutinate the mitochondria appeared to have some effect on the glycogen to nitrogen ratios of the poorly sedimentable and microsome fractions. In the two experiments in which calcium was not used, the same glycogen to nitrogen ratio was found in these two fractions. When calcium was used, the microsomes showed a considerably higher glycogen to nitrogen ratio than did the poorly sedimentable fraction. The most reasonable interpretation is that the addition of calcium ion results in the agglutination of some of the soluble proteins into aggregates large enough to be sedimented with the mitochondrial and poorly sedimentable fractions. These agglutinated proteins would not stain with the Janus Green, so that their presence would not necessarily be observed under the microscope.

SUMMARY

1. A study has been made of the histochemically demonstrable glycogen of rat liver particulate fractions obtained by differential centrifugation of sucrose homogenates.

2. Histochemically demonstrable glycogen was found in mitochondria, microsomes, a poorly sedimentable fraction of proteinaceous material isolated by centrifugation at 13,000 *g*, and as particulate glycogen not associated with proteinaceous material. No glycogen could be demonstrated histochemically in isolated nuclei.

3. Quantitative chemical determinations of glycogen on these fractions were in general agreement with the histochemical findings.

4. In terms of ratio of glycogen to nitrogen contents of the particulate fractions, microsomes were highest, and mitochondria lowest.

5. The use of calcium ion to agglutinate mitochondria resulted in the carrying down of a markedly increased fraction of the total nitrogen of the homogenate, without any increase in the fraction of total glycogen in these particulates.

6. Despite the carrying out of all operations in the cold room, a very large fraction of the total glycogen initially present in the liver was found as reducing sugar.

7. The occurrence in liver of particulate glycogen not associated with protein, first reported by Lazarow, is confirmed.

8. An appreciable fraction of the total glycogen content of liver is present in solution in the cytoplasm.

REFERENCES

1. Barton, A. D., *Federation Proc.* **15**, 10 (1956).
2. Bloom, W. L., Lewis, G. T., Shumpert, M. Z., and Shen, T.-M., *J. Biol. Chem.* **188**, 631 (1951).
3. Claude, A., *J. Exptl. Med.* **84**, 61 (1946).
4. Gatenby, J. B. and Beams, H. W., The Microtomist's Vade Mecum. 11th ed., pp. 258 and 300. J. and A. Churchill, Ltd., London, 1950.
5. Glick, D., Techniques of Histo- and Cytochemistry, pp. 44, 48. Interscience Publishers, New York, 1949.
6. Good, C. A., Kramer, H., and Somogyi, M., *J. Biol. Chem.* **100**, 485 (1933).
7. Hogeboom, G. H., Schneider, W. C., and Striebich, M. J., *J. Biol. Chem.* **196**, 111 (1952).
8. Lazarow, A., *Anat. Rec.* **84**, 31 (1942).
9. Nelson, N., *J. Biol. Chem.* **153**, 375 (1944).
10. Smellie, R. M. S., McIndoe, W. M., Logan, R., Davidson, J. N., and Dawson, I. M., *Biochem. J.* **54**, 280 (1953).
11. Viles, F. J., Jr. and Silverman, L., *Anal. Chem.* **21**, 950 (1949).

CHANGES IN THE ULTRAVIOLET ABSORPTION SPECTRUM OF PARTS OF LIVING CELLS FOLLOWING IRRADIATION WITH AN ULTRAVIOLET MICROBEAM

R. P. PERRY[1]

Committee on Biophysics, University of Chicago, Chicago, Ill., U.S.A.

Received October 16, 1956

Recently some interesting effects of ultraviolet radiation on living cells have been reported by Zirkle, Bloom, and Uretz [1, 2, 17, 19]. When a spot of ultraviolet radiation a few microns in diameter[2] is focused on a chromosome (or group of chromosomes) of a single cell in mitosis, it is found that the irradiated part of the chromosome(s) "pales", i.e., it loses its dark appearance as viewed with medium dark phase contrast optics. This indicates that the index of refraction gradient between the chromosome and its surroundings has undergone a change at the site of irradiation. It is also found that the pale area sometimes increases in size for a period of up to 30 minutes following irradiation, and that there is less paling when the irradiation area is increased while maintaining constant flux and exposure. Interphase nuclei which appear dark relative to the cytoplasm with medium dark phase contrast optics are also susceptible to paling by exposures that produce the effect in metaphase and prophase chromosomes.

An attempt to relate this morphological change to a molecular change was made by employing standard histochemical procedures [1]. After Zenker-formol fixation and Feulgen staining, a discontinuity was found in the Feulgen positive chromosome at the irradiated site, there being either no

[1] Present address: Biology Division, Oak Ridge National Laboratory, Oak Ridge, Tennessee.

[2] The ultraviolet microbeam is achieved by means of a reflecting objective (0.56 N.A.) which serves to view the specimen and to simultaneously focus onto a particular part of the cell a demagnified image of a pinhole on which there is a real image of an ultraviolet source. Hence the beam is in the form of a hollow cone converging at an angle of 52° to a spot a few microns in diameter. The cells are growing in tissue cultures made from newt heart fragments.

Fig. 1. (*a*) (Phase contrast) Interphase nucleus before irradiation. (*b*) (Phase contrast) Same cell as (*a*) after irradiation with 8 μ diameter microspot. Paled area indicated by arrow. (*c*) (260 mμ) Interphase nucleus before irradiation. (*d*) (260 mμ) Same cell as (*c*) after irradiation with 8 μ diameter microspot. Area of decreased absorption shown by arrow. (*e*) (Phase contrast) Prophase before irradiation. (*f*) (Phase contrast) Same cell as (*e*) after irradiation with a 4 μ diameter microspot. Paled area indicated by arrow.

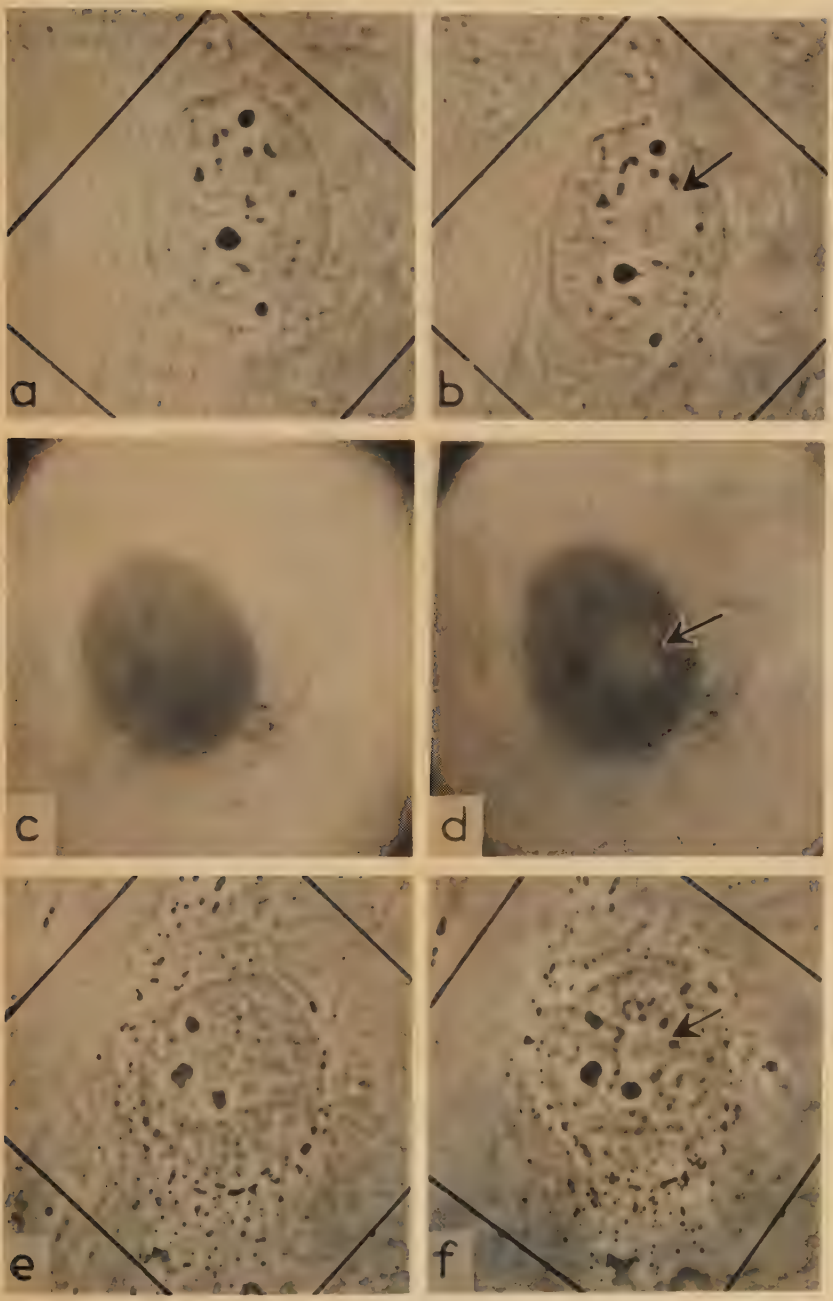
a
b
c
d
e
f

stain in this area or a diffuse stain of much lower density. On the basis of the Feulgen specificity for desoxyribose nucleic acid and an assumption that there is no pertinent molecular change upon fixation one might infer that either the DNA loses its specificity for Feulgen reagent or else is lost from the chromosome during the paling process.

Another method which also enables one to follow molecular changes, but at the same time eliminates the possibility of a molecular redistribution due to the fixation process, is ultraviolet microspectrography of living cells. It is the purpose of this paper to discuss ultraviolet absorption measurements made on chromosomes and interphase nuclei which were irradiated over small areas by an ultraviolet microbeam.

PROCEDURE

The cells used were cultured from fragments of heart of adult newt (*Triturus viridescens*) by a procedure outlined previously [2].

The microbeam was essentially that described previously [17] with the following modifications: a phase contrast system was incorporated for viewing the objects during irradiation; the 100 w source was replaced by a 1000 w water cooled high pressure capillary mercury arc (G.E. AH6) which puts out a continuous spectrum beginning at 226 mμ except for a self-reversal minimum around 257 mμ; and the water cell was replaced by a 5 cm filter of $CoSO_4$–$NiSO_4$ solution which removes most of the radiation above 330 mμ. The integrated flux of radiation below 300 mμ per unit area at the microspot as measured by a calibrated photomultiplier was approximately 0.15 ergs μ^{-2} sec^{-1}. With 15 seconds exposure the energy is sufficient to give a paling reaction which is already visible upon completion of bombardment and is well developed in five minutes.

The microspectrographic apparatus was of the photographic variety, consisting of an AH6 source, a grating monochromator, a microscope optical system, and a 35 mm camera. A pair of reflecting-refracting lenses (Grey V) were used as objective and condenser. The objective N.A. was 0.72 while the condenser N.A. was stopped down to 0.44. The spectral band width of radiation was approximately 3.7 mμ. A circular area of film 0.14 mm in diameter, corresponding to a circle of 0.84 μ diameter in the cell, was scanned with a densitometer.

The energy per unit area delivered to the cell in taking a spectral series, one picture each at 310, 300, 280, 260, and 240 mμ, was approximately 0.016 ergs/μ^2. The effect on the ultraviolet absorption due to this amount of ultraviolet exposure

---

Fig. 1 (*continued*). (*g*) (260 mμ) Same cell as (*e*) after irradiation. (*h*) (310 mμ) Same cell as (*e*) after irradiation. (*i*) (Phase contrast) Metaphase before irradiation. Dotted circle (arrow) shows size of 4 μ diameter microspot. (*j*) (Phase contrast) Same cell as (*i*) after irradiation with 4 μ diameter microspot. Paled chromosome indicated by arrow. (*k*) (260 mμ) Same cell as (*i*) after irradiation. (*l*) (310 mμ) Same cell as (*i*) after irradiation.

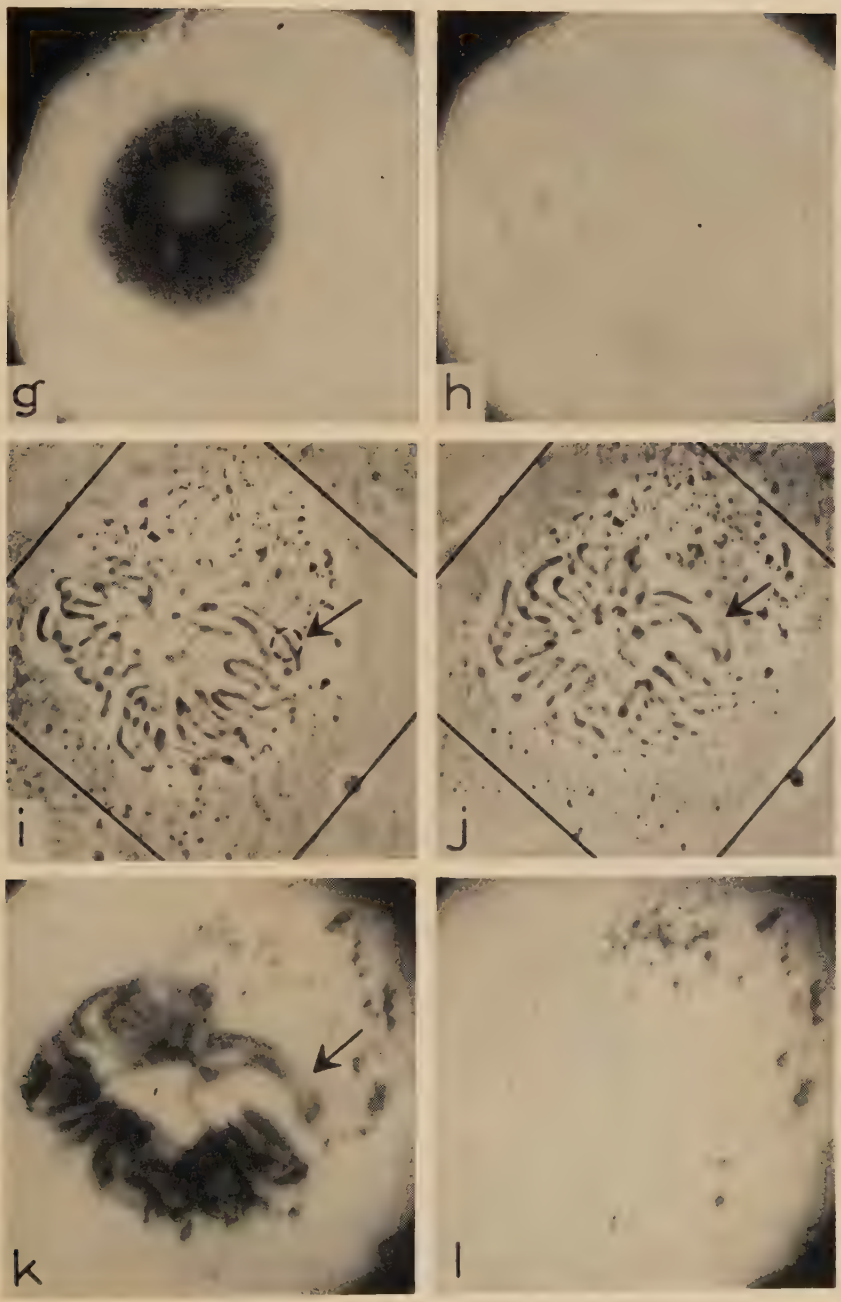
g
h
i
j
k
l

was tested by taking two series of ultraviolet photographs spaced five minutes apart. With both chromosomes and interphase nuclei the absorption of the first set was identical with that of the second set within the experimental error. This does not imply, however, that there is no effect on the cell. If cells in metaphase were observed under the phase microscope for 30–60 minutes following the taking of an absorption series, effects described previously [2, 19], such as spindle collapse, were seen to occur. Interphase nuclei may round up after about 15 minutes.

Errors owing to the treatment of the film and errors such as lens glare, which were introduced from the microscope optical system of the microspectrographic apparatus but which were not due to the small size of the objects, were estimated to be about 3 per cent. This value was obtained by a comparison of the spectral curve of a sheet of mica, 5 μ thick, measured in the microspectrographic apparatus with a curve measured photometrically outside the apparatus.

The errors related to object size (e.g. scattering) were estimated by looking at the range of absorbance (optical density) values for chromosomes and nucleoli at nonabsorbing wavelengths throughout the course of the experiment. These values were found to be always less than 10 per cent of the maximum absorbance at 260 mμ.

Accordingly, the overall accuracy of the absorbance measurements was of the order of 10 per cent.

The general procedure then was as follows: a flat newt cell in tissue culture was chosen; a photograph was taken with phase contrast optics; the cell was moved by means of a locator plate to the ultraviolet microbeam apparatus, and an appropriate part was exposed for 15 seconds; the cell was returned to the phase microscope, and at plus four minutes from bombardment another phase picture was taken; the cell was taken quickly to the microspectrographic apparatus, focused, and an absorption series taken, this taking from two to three minutes; finally it was returned to the phase microscope, and a last photograph was taken. In a few cases an absorption series was also taken previous to microbeam bombardment. Over fifty cells were thus studied.

RESULTS AND DISCUSSION

Figs. 1 and 2 are some examples of the phase and absorption photography. The phase pictures are framed by diagonal crosshairs. The absorption pictures shown are at the peak absorption wavelength of nuclear material, 260 mμ, and at a nonabsorbing wavelength, 310 mμ. The absence of an image in the 310 mμ pictures illustrates the degree to which refraction, scattering, and "out-of-focus" phase effects have been eliminated and thus to a certain extent the degree to which the 260 mμ picture represents true

Fig. 2. (*a*) (260 mμ) Metaphase chromosomes after irradiation with 4 μ diameter microspot. Arrow indicates dark spot. Triangular clump of fat droplets at bottom. (*b*) (310 mμ) Exactly as in (*a*). (*c*) (260 mμ) Metaphase chromosomes after irradiation with 4 μ diameter microspot. Arrow shows irradiation site. (*d*) (310 mμ) Exactly as in (*c*). (*e*) (Phase contrast) Metaphase before irradiation. Dotted circle (arrow) shows size of 10 μ diameter microspot. (*f*) (Phase contrast) Same cell as (*e*) 4½ min. after irradiation with 10 μ diameter microspot.

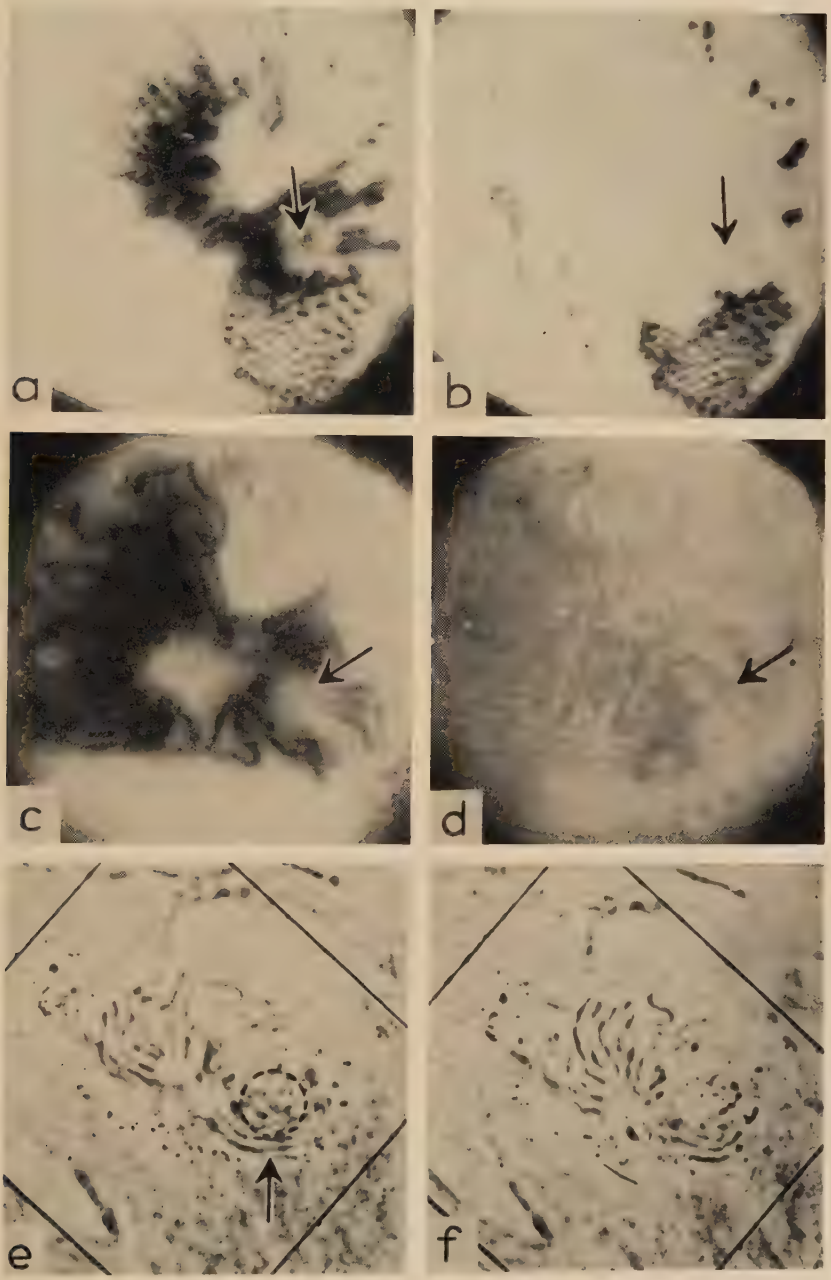
a
b
c
d
e
f

absorption. Because of anomalous dispersion the index of refraction gradient between the chromosome and its surroundings may be greater at 260 mμ than at 310 mμ and consequently the scattering and phase effect larger at the former wavelength. However, there are several arguments [5, 12, 15] which lead one to believe that this effect will be small in the case of living

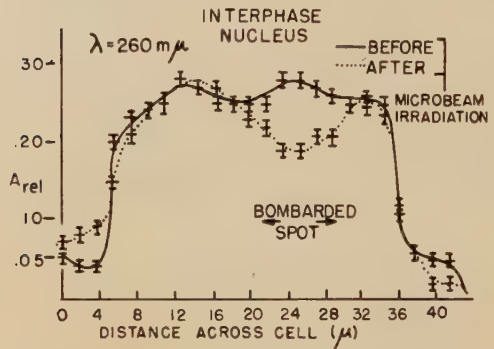

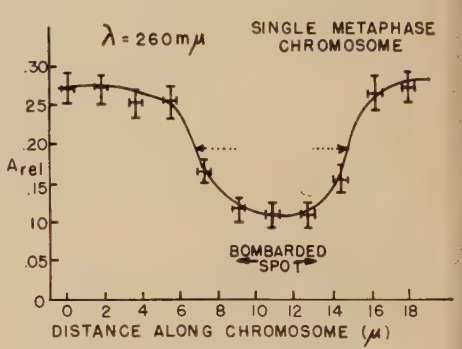

Fig. 3 (left). Trace across interphase nucleus (1 *c*, *d*) at 260 mμ.
Fig. 4 (right). Trace across single paled metaphase chromosome (1 *i–l*) at 260 mμ.

systems where index of refraction differences are of the order of 0.01, and hence such effects are neglected here.

Figs. 1 *a*, *b* show the paling effect of a microspot 8 μ in diameter on an interphase nucleus as seen by phase contrast. Figs. 1 *c*, *d* are 260 mμ photographs of a similar nucleus before and after bombardment. They clearly show the drop in absorption in the irradiated area. Densitometric traces through the target area before and after irradiation with the microbeam give curves shown in Fig. 3. A_{rel} is the absorbance of the nuclear material minus the absorbance of the surrounding cytoplasm. If a strip is chosen which does not include the target area, the before and after curves are identical except in a few cases where the nucleus rounded up, causing an increase in absorption; such determinations were discarded. An early prophase such as that pictured in Figs. 1 *e–h* gives results similar to the interphase nucleus with a markedly greater optical density difference between irradiated and unirradiated material.

Fig. 2 (*continued*). (*g*) (Phase contrast) Same cell as (*e*) 10 min. after irradiation. (*h*) (260 mμ) Same cell as (*e*) 5 min. after irradiation. (*i*) (Phase contrast) Metaphase before irradiation. Dotted circle (arrow) shows size of 20 μ diameter microspot. (*j*) (Phase contrast) Same cell as (*i*) 4½ min. after irradiation with 20 μ diameter microspot. (*k*) (Phase contrast) Same cell as (*i*) 10 min. after irradiation. (*l*) (260 mμ) Same cell as (*i*) 5 min. after irradiation.

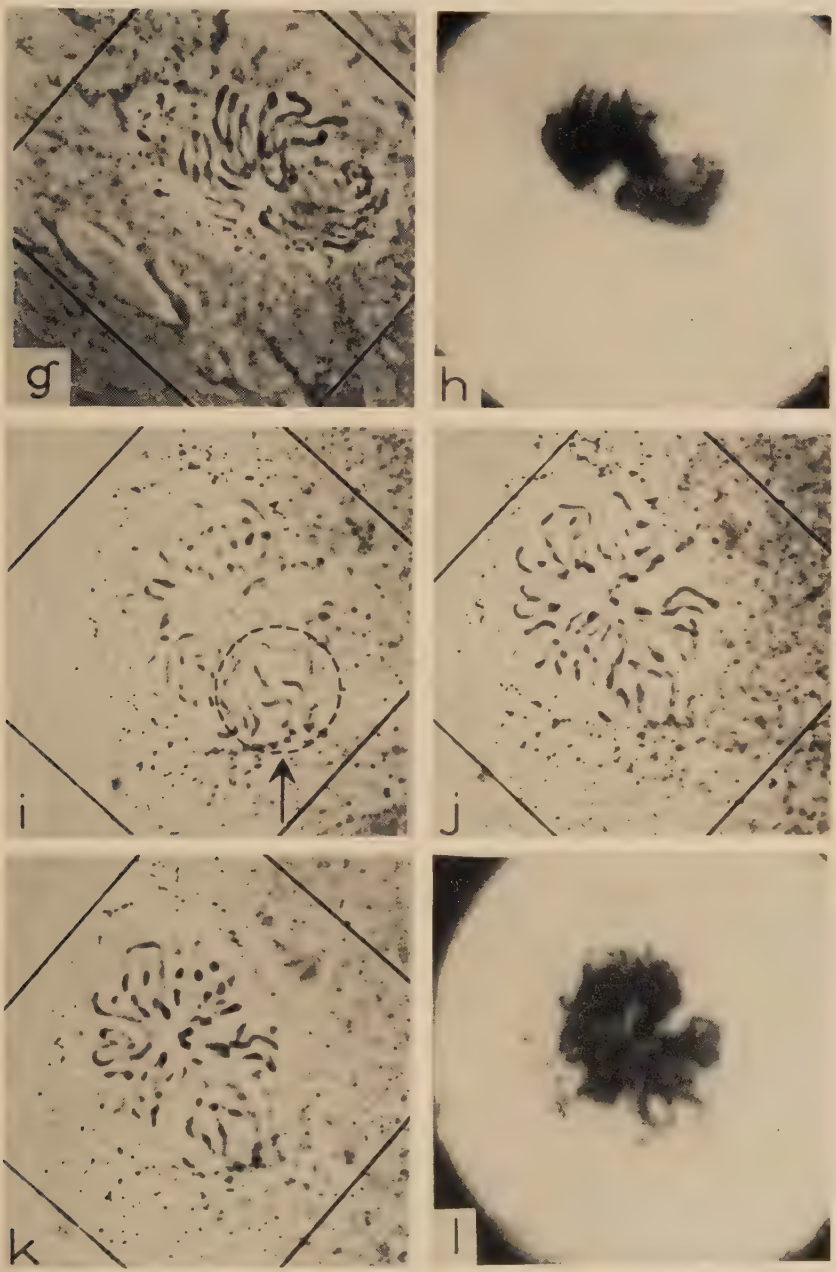
g
h
i
j
k
l

The effect on metaphase chromosomes is illustrated by Figs. 1 *i–l*, 2 *a*, *b*, and 2 *c*, *d*. With a 4 μ diameter spot individual chromosomes may be made pale along a fraction of their length (Figs. 1 *i–l*). A trace along the chromosome length results in the curve in Fig. 4. The growth of the pale area beyond the size of the original irradiated spot in the five minutes between microbeaming and absorption measurements is clearly evident from this curve. The width

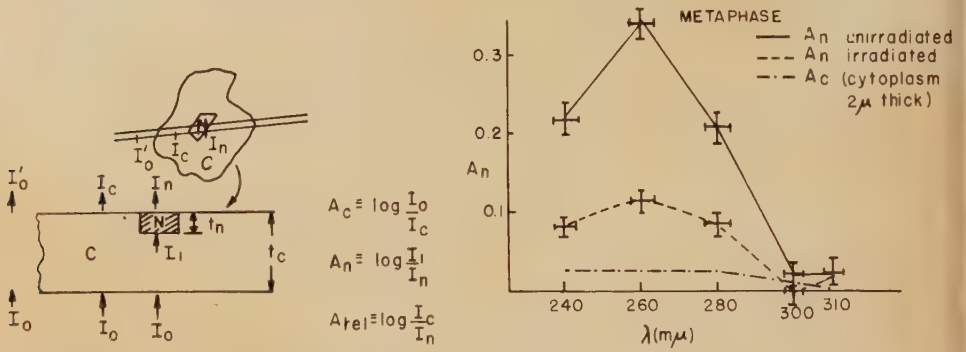

Fig. 5 (left). Absorbance definitions. See text.
Fig. 6 (right). Spectral curves for metaphase chromosomes (2*c*, *d*).

of the curve at one half the maximum extinction difference is 8 μ or twice the diameter of the ultraviolet microbeam.

If one makes a densitometric trace of a strip of nonchromosomal material, i.e. spindle or cytoplasm, which contains an irradiated portion, one finds no detectable difference in absorbance between the irradiated and unirradiated areas. Since a microspot diameter of 4 μ is at least twice the width of a chromosome these measurements are most easily made by taking a strip adjacent to an irradiated chromosome.

Sometimes when a group of chromosomes are microbeamed and observed under the phase microscope there appears in the center of the paled area a dark spot. Figs. 2 *a*, *b* are photographs at 260 mμ and 310 mμ of such an event. It is seen by the photographs and substantiated by densitometry that the dark spot like the fat droplets has the same optical density at all wavelengths. From this fact it is concluded that its origin is purely refractive and not due to any absorptive change.

If we are only interested in measuring the change in absorbance of the nuclear material, ΔA, which was produced by the microbeam irradiation, it is arbitrary to express absorbance in terms of A_{rel} (Fig. 5). Since

$$\Delta A = A_{rel_2} - A_{rel_1} = \log (I_c/I_{n_2}) - \log (I_c/I_{n_1}) = \log (I_{n_1}/I_{n_2}),$$

one need only measure the ratio of transmissions of unirradiated (n_2) and irradiated (n_1) material. If, however, we are interested in the percentage decrease, as for instance in comparing absorption at different wavelengths, the true absorbance of the nuclear material, A_n, should be measured. To measure A_n the following considerations apply. Given a hypothetical cell, C (Fig. 5), of thickness t_c, which contains nuclear material, N, of thickness t_n, we put light of intensity I_0 in and measure the emerging intensities, I_0' (clear area), I_c (cytoplasm), and I_n (nuclear material plus overlying and underlying cytoplasm). Setting $I_0' = I_0$ and assuming a homogeneous concentration of material in the cytoplasm, it may be shown that

$$A_n = A_{\text{rel}} + (1 - f_t)\, A_c, \qquad f_t = (t_c - t_n)/t_c.$$

For a chromosome 2 μ thick in an average cell ≥ 8 μ thick, $f_t \geq \frac{3}{4}$, the true absorbance is greater than the relative absorbance by a factor $\leq A_c/4$. Corrections are made where this value is significant. The spectral curves for the cell in Figs. 2*c*, *d* are shown in Fig. 6. The A_n for the irradiated material which is used is the minimum A_n obtained in a scan through the irradiated area. Besides the curves for irradiated and unirradiated chromosome a curve for a 2 μ thick slice of cytoplasm, estimated as $A_c/4$, is included for comparison.

One should also keep in mind that if a comparison of the percentage decrease in absorbance, $\Delta A/A_n$, at different wavelengths is to be used to determine the degree of involvement of various chromophoric species it must be assumed that $\Delta A \sim A_n$, or that the over-all process is first order for any chromophoric species. ΔA is found to be proportional to A_n with the following conditions held constant: stage of cell, microbeam flux, size of microspot, and time between irradiation and absorption measurement.

The variation in ΔA for chromosomes as a function of microspot size was also studied. It has been reported previously [1, 19] that the degree of paling, as observed by phase-optics, diminishes as the percentage of chromosomal material irradiated is increased. Qualitatively a similar effect was found in the ultraviolet absorption measurements. ΔA is smaller if larger areas are irradiated. Since more energy is delivered to the cell with larger spots, other effects, such as spindle collapse and rounding up of the cell, may occur along with the paling reaction thus making a quantitative estimation of ultraviolet absorption difficult. The effect is illustrated for a 10 μ diameter spot by the series in Figs. 2*e–h* and for a 20 μ spot by Figs. 2*i–l*. The 260 mμ photographs show very little absorption difference between the irradiated and unirradiated ends of the metaphase plate. A characteristic loss of form

by the chromosomes accompanying slight paling is seen in Fig. 2*g*. It has not been definitely established whether it is the increased amount of irradiated chromosome or rather the increased amount of irradiated chromosome and/or irradiated milieu that is responsible for diminishing the effect. No data for interphase nuclei irradiated with varying spot sizes is available because of their rapid rounding up at high total dose.

The main features of the above results may now be discussed.

Ultraviolet irradiation of small volumes of chromosomes or interphase nuclei results in striking decreases in the 260 mμ ultraviolet absorption of the irradiated sites. This decrease in absorption is a concomitant of paling as observed with the phase microscope. Since in nuclear material, especially chromosomes, the extinction at 260 mμ is to a great extent due to the purine and pyrimidine bases of desoxyribose nucleic acid, one may conclude that at the site of irradiation there is a decrease in the number of intact bases.[1] Whether there is a photochemical change in the aromatic rings at their normal sites or a movement of the molecules from their sites cannot be decided on the basis of this evidence alone. Using the fact that the chromosomes lose most of their Feulgen specificity at the irradiated sites one may extend the conjecture to: either there are caused photochemical changes in the aromatic rings which extend to the pentose components of the DNA molecules or there is a movement of both from their sites on the chromosomes.

It is interesting to note that photochemical disruption by very high ultraviolet doses of the ultraviolet absorption properties of the purines and pyrimidines in all natural forms of combination has been demonstrated *in vitro* with dilute solutions [8, 9, 13, 16], but not with solutions of nucleic acid of $\frac{1}{2}$ per cent or more [9, 13]. The destruction of the pentose fraction with high dose ultraviolet has also been demonstrated *in vitro* [14].

When the decrease in absorption is measured at different wavelengths the percentage decrease in absorbance at one wavelength does not differ appreciably from that at any other wavelength. Because the ultraviolet absorption of chromosomal material is very strongly influenced by the nucleic acids and only weakly influenced by protein it would be difficult with an experimental error of 10 per cent to pick up the variation in $\Delta A/A_n$ as a function of the wavelength even if the nucleic acid were preferentially lost and the protein left completely intact. Thus, although the data show no appreciable $\Delta A/A_n$

[1] A decrease in absorption could also arise if the irradiation causes the bases to become highly oriented and thus give rise to a dichroic effect such as described by Commoner [7]. However, besides being unlikely, such a mechanism may be discounted because it would lower the A_n only to 0.3 whereas the observed decreases are down to about 0.1.

variation with λ, the sensitivity of the experiment prohibits a final conclusion that neither the protein nor nucleic acid is *preferentially* destroyed. An effect on both components is rather plausible however, since the ultraviolet microbeam is heterochromatic.

As the size of the irradiated area is increased, energy per unit area held constant, the decrease in absorption of chromosomes is greatly diminished. This may mean that this decrease is not simply due to a photochemical change of the chromophoric groups at their sites, but to migration away of intact chromophores, and that when large areas are irradiated there is a greater impeding of diffusion because of some overall gelation of the chromosome milieu. Alternatively, larger area irradiation may cause the appearance of an antagonistic factor or the absence of a necessary factor for photochemical change.

The decreasing ΔA with increasing irradiation area is undoubtedly a reason why previous workers studying ultraviolet effects on the absorption of living cells have not observed this striking phenomenon. These workers were primarily interested in how the ultraviolet used in their absorption measurements influenced subsequent absorption measurements [3, 4, 6, 11, 18]. Such studies have always (*a*) dealt with the results of total cell irradiation, (*b*) considered quantitatively only the absorption changes in interphase nuclei, and (*c*) involved dose rates per μ^2 which were from 0.01 to 0.001 that of the microbeam.

Walker and Davies [18], using chick fibroblasts growing in tissue culture, have shown that the observed increase in optical density following ultraviolet irradiation is a result of the rounding up of the cell, and that if the decreased area is taken into account, one actually finds a decrease in total absorption (measured at 260 mμ) of 30 per cent. If the increased thickness of the nucleus were also taken into account the decrease would probably have been greater. A similar decrease in absorption has also been observed for fixed material during prolonged irradiation [6]. Bradfield and Errera [3, 4], making measurements on a variety of fresh specimens, indicate that in most cases in which the change in cell volumes are taken into account a decrease in total absorption is observed. They find no apparent difference between the decrease at 260 mμ and 280 mμ, and argue that the fall in nuclear absorption is primarily due to a depolymerization of nucleoprotein with immediate leakage of the breakdown products through the nuclear membrane. Since depolymerization of nucleic acid *in vitro* leads to an increase in the extinction coefficient of about 30 per cent [10], loss through the membrane is a necessary condition of this hypothesis.

On the basis of the results presented here a general theory for the observed decrease in absorption of nuclear material induced by ultraviolet irradiation would be highly speculative and therefore is not presented. It is not yet clear that both interphase material and chromosomes are paled by the same mechanism. In fact, if a depolymerization-diffusion mechanism is suggested, the efficiency of energy transfer from the aromatic rings to sites of bond breakage would depend on the extent of coiling of both protein and nucleic acid. Further studies with interphase nuclei (at a known stage in the mitotic cycle) in which one measures the spatial distribution of absorbing material as a function of time following microbeam irradiation may lead to a better understanding of the mechanism.

SUMMARY

The effects of ultraviolet irradiation of small areas of chromosomes and interphase nuclei on the ultraviolet absorption characteristics of these components have been studied. When irradiation is confined to an area of 50 μ^2 or less, heterochromatic ultraviolet radiation of the order of 2 ergs/μ^2 causes an appreciable decrease in the absorbance at the site of irradiation. The relation of this absorbance decrease to a change in the chromosomal DNA is discussed. As the irradiation area is increased beyond 50 μ^2, energy per unit area being held constant, the observed decrease in chromosomal absorbance is considerably lessened. The percentage decrease in absorbance is essentially the same at 240, 260, and 280 mμ, measurements being to an accuracy of about 10 per cent.

The author is particularly indebted to Dr. R. B. Uretz for many valuable discussions and suggestions throughout the course of this research. He also wishes to thank Dr. R. E. Zirkle and Dr. W. Bloom for their guidance and encouragement.

Miss T. Panny, Mr. J. Costa, Mr. C. Soderquist, Mr. J. Hanacek, and Mr. G. Gibson have been very generous with their time and technical assistance.

This work was made possible through financial assistance from the U.S. Atomic Energy Commission, the U.S. Public Health Service and the Abbott Memorial Fund of the University of Chicago, and by a predoctoral fellowship from the National Institutes of Health.

REFERENCES

1. Bloom, W. and Leider, R. J., *Radiation Research* **3**, 214 (1955).
2. Bloom, W., Zirkle, R. E., and Uretz, R. B., *Ann. N.Y. Acad. Sci.* **59**, 503 (1955).
3. Bradfield, J. R. G., *Disc. Faraday Soc.* **9**, 481 (1950).
4. Bradfield, J. R. G. and Errera, M., *Nature* **164**, 532 (1949).

5. Caspersson, T. O., Cell Growth and Cell Function. W. W. Norton and Co., New York, 1950.
6. Catchpole, H. R. and Gersh, I., *Disc. Faraday Soc.* **9**, 471 (1950).
7. Commoner, B., *Science* **110**, 31 (1949).
8. Heyroth, F. F. and Loofbourow, J. R., *J. Am. Chem. Soc.* **53**, 3441 (1931).
9. Hollaender, A., *J. Natl. Cancer Inst.* **2**, 23 (1941).
10. Kunitz, M., *J. Gen. Physiol.* **33**, 349 (1950).
11. Mellors, R. C., Berger, R. E., and Streim, H. G., *Science* **111**, 627 (1950).
12. Ornstein, L., *Lab. Invest.* **1**, 83 (1953).
13. Rapport, D. and Canzanelli, A., *Science* **112**, 469 (1950).
14. Rice, E. W., *Science* **115**, 92 (1952).
15. Scott, J. F., *Lab. Invest.* **1**, 73 (1953).
16. Uber, F. M. and Verbrugge, F., *J. Biol. Chem.* **134**, 273 (1940).
17. Uretz, R. B., Bloom, W., and Zirkle, R. E., *Science* **120**, 197 (1954).
18. Walker, P. B. M. and Davies, H. G., *Disc. Faraday Soc.* **9**, 461 (1950).
19. Zirkle, R. E., Bloom, W., and Uretz, R. B., Proceedings of the International Conference on Peaceful Uses of Atomic Energy **11**, p. 273. United Nations, New York, 1956.

QUANTITATIVE CYTOLOGY AND CYTOPATHOLOGY

VI. CHROMOSOMAL MASS IN GERMINAL CELLS AND IN CANCER CELLS OF THE MOUSE

R. C. MELLORS, L. G. ORTEGA, A. STOHOLSKI and J. HLINKA

Division of Pathology, Sloan-Kettering Institute for Cancer Research; Pathology Laboratories, Memorial Center for Cancer and Allied Diseases and Cornell University Medical College, Sloan-Kettering Division, New York, N.Y., U.S.A.

Received October 18, 1956

In this study, one of a series [6–10] dealing with applications of interference microscopy in quantitative cytology, the mass (dry weight, fat-free) of each of the twenty metaphase chromosomes in meiotic cells of mouse testis was estimated and arranged in order of magnitude from largest to smallest. Since each of the meiotic chromosomes is classically regarded as consisting of four components or chromatids, the total number of chromatids contained in the meiotic cells is tetraploid, as would be the case in ordinary somatic metaphase. Utilizing the data of the present and previous work [10], the conclusion is reached that the dry weight per chromatid set is constant, within the limits of error of measurement, during the prophase and the metaphase of meiosis.

The total mass of metaphase chromosomes in mouse tumor cells, comprising several cytologic varieties in the ascites form, was measured in the present investigation. Leukemia 1210 [1], which according to Levan [4] is near diploid (chromosome number = 42), was found to be deficient in chromosomal (or chromatid) mass in comparison with germinal cells; whereas in Ehrlich carcinoma, Krebs-2 carcinoma, and sarcoma 180 studied as ascites tumors, the chromosomal masses were commensurate with the chromosome numbers, known to be near-tetraploid in these cancer cells [3, 5].

MATERIALS AND METHODS

The analytic procedures which utilize a multiple-beam interference microscope and the method of calculation (equation (10) in reference [8]) have been previously described. The cytologic material was fixed in acetic-acid alcohol, dehydrated and defatted in anhydrous alcohol, and mounted in anhydrous glycerin. Testes were obtained from 20–21 week-old Swiss mice at approximately six hours after the

intraperitoneal injection of an LD_{50} dose of trimethylcolchicinic acid [2] to produce metaphase arrest of germinal chromosomes. The ascites tumors, Ehrlich carcinoma, Krebs-2 carcinoma, and sarcoma 180, were serially transferred to Swiss mice by Dr. Sugiura and were sampled on the seventh to ninth days after intraperitoneal inoculation. Leukemia 1210, propagated in ascites form in DBA/2 mice, was obtained from Dr. Charlotte Friend. Standard morphologic studies of the cytologic material were made utilizing routine stains or the phase microscope.

RESULTS

Germinal-cell chromosomes.—The average mass, expressed in $\mu\mu g$ (10^{-12} g), of the twenty metaphase germinal chromosomes in mouse testis are given in Table I, as are also the mass per unit area ($\mu\mu g/\mu^2$), the area (μ^2), and statistical coefficients of variation of the data. The notable features are the two- to three-fold ratios of area and mass that the largest chromosome (i) bears to the smallest (xx) and the relatively slight variation in the mass per unit area in the twenty chromosomes. Since each of the meiotic chromosomes consists of four chromatids, each recorded chromosomal mass is four times the mass of a single chromatid.

The total mass of the twenty meiotic chromosomes, comprising eighty chromatids in all, is 56 $\mu\mu g$. This value is approximately four times the mass, 13 $\mu\mu g$, previously reported [8] for mouse sperm nuclei which presumably contain twenty interphase chromosomes (or chromatids) and is,

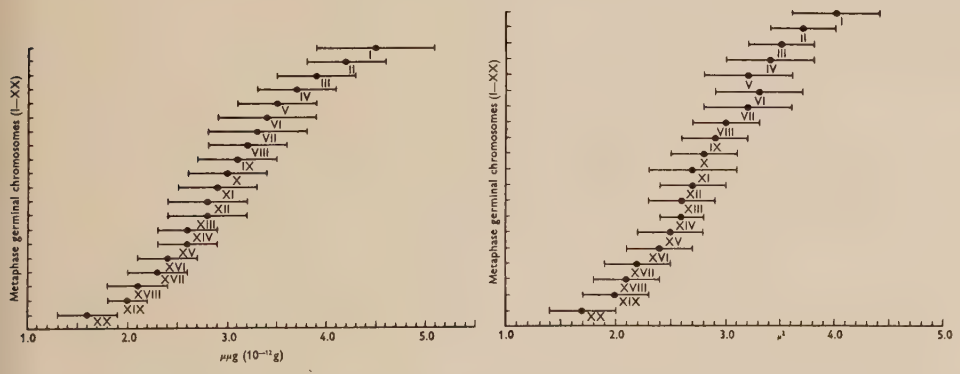

Fig. 1 (left). Mass or dry weight (fat-free) of individual metaphase chromosomes in mouse testicular cells in meiosis. The chromosomes have sequential numbers assigned in the order of decreasing mass. Average values are designated by centered dots and the 95 per cent confidence intervals for the estimate of average by horizontal lines.
Fig. 2 (right). Area of individual metaphase chromosomes in mouse testicular cells in meiosis. The chromosomes have been designated by numbers assigned in the order of decreasing mass (see Fig. 1).

TABLE

Mass or dry weight (fat-free) of individual metaphase germinal chromosomes (four chromatids

Symbols: *AV*, average, the arithmetic mean; *SD*, standard deviation; and *CI*, confidence

Chromosome	Number of measurement	Mass ($\mu\mu$g)				
		AV	*SD*	*SD/AV*	$2SD/\sqrt{N}$	*CI*
i	11	4.5	1.05	0.23	0.63	3.9–5.1
ii	11	4.2	0.75	0.18	0.45	3.8–4.7
iii	11	3.9	0.67	0.17	0.40	3.5–4.3
iv	11	3.7	0.69	0.19	0.41	3.3–4.1
v	11	3.5	0.73	0.21	0.44	3.1–3.9
vi	11	3.4	0.81	0.24	0.49	2.9–3.9
vii	11	3.3	0.77	0.23	0.46	2.8–3.8
viii	11	3.2	0.75	0.23	0.45	2.8–3.7
ix	11	3.1	0.69	0.22	0.41	2.7–35
x	11	3.0	0.71	0.24	0.43	2.6–3.4
xi	11	2.9	0.69	0.24	0.42	2.5–3.3
xii	11	2.8	0.59	0.21	0.35	2.5–3.2
xiii	11	2.7	0.58	0.21	0.35	2.5–3.2
xiv	11	2.6	0.54	0.21	0.33	2.3–2.9
xv	11	2.6	0.57	0.20	0.34	2.3–2.9
xvi	11	2.4	0.51	0.21	0.31	2.1–2.7
xvii	11	2.3	0.43	0.19	0.26	2.0–2.6
xviii	11	2.1	0.49	0.23	0.29	1.8–2.4
xix	11	2.0	0.29	0.15	0.18	1.8–2.2
xx	11	1.6	0.47	0.29	0.28	1.3–1.9
Total (i–xx)	14	56.1	10.8	0.19	5.8	50.3–61.8

within the limits of error of measurement, equal to the mass of an equal number of prophase chromatids [10]. To this demonstration of the constancy of chromatid mass in prophase and metaphase can be added the observation of equipartition of chromosomal mass in anaphase, as measured by microinterferometry on several occasions in our laboratory.

In Fig. 1 the chromosomal masses are arranged in order of magnitude from largest (i) to smallest (xx). The similarity which the array of chromosomal areas (Fig. 2) bears to the array of mass indicates that the area is the principal determinant of mass, the mass per unit area being relatively constant in the several chromosomes.

Cancer-cell chromosomes.—The average mass, expressed in $\mu\mu$g, of metaphase chromosomes in cancer cells of the mouse are given in Table II, as are

I

in each) in the mouse testis, expressed in $\mu\mu$g (10^{-12} g) and measured by microinterferometry. interval, $AV \pm 2SD/\sqrt{N}$, which includes 95 per cent of the estimates of the average.

Mass per unit area ($\mu\mu g/\mu^2$)					Area (μ^2)				
AV	*SD*	*SD/AV*	$2SD/\sqrt{N}$	*CI*	*AV*	*SD*	*SD/AV*	$2SD/\sqrt{N}$	*CI*
1.13	0.24	0.22	0.11	1.0–1.2	4.0	0.72	0.18	0.43	3.6–4.4
1.14	0.23	0.21	0.10	1.0–1.2	3.7	0.54	0.15	0.33	3.4–4.0
1.11	0.21	0.19	0.09	1.0–1.2	3.5	0.55	0.16	0.33	3.2–3.8
1.09	0.24	0.22	0.11	1.0–1.2	3.4	0.63	0.19	0.38	3.0–3.8
1.09	0.23	0.21	0.10	1.0–1.2	3.2	0.59	0.18	0.36	2.8–3.6
1.03	0.29	0.29	0.13	0.9–1.1	3.3	0.63	0.19	0.38	2.9–4.7
1.03	0.23	0.22	0.10	0.9–1.1	3.2	0.70	0.22	0.42	2.8–3.6
1.07	0.23	0.23	0.10	0.9–1.1	3.0	0.47	0.16	0.28	2.7–3.3
1.07	0.23	0.22	0.10	1.0–1.2	2.9	0.41	0.14	0.25	2.6–3.2
1.07	0.26	0.25	0.12	0.9–1.2	2.8	0.47	0.17	0.28	2.5–3.1
1.07	0.20	0.19	0.09	1.0–1.1	2.7	0.47	0.17	0.28	2.4–3.0
1.04	0.26	0.26	0.12	0.9–1.1	2.7	0.46	0.17	0.28	2.4–3.0
1.08	0.27	0.27	0.12	0.9–1.1	2.6	0.48	0.18	0.29	2.3–3.9
1.00	0.24	0.24	0.11	0.9–1.1	2.6	0.36	0.14	0.22	2.4–2.8
1.04	0.29	0.30	0.13	0.8–1.1	2.5	0.45	0.18	0.28	2.2–2.8
1.00	0.29	0.29	0.13	0.9–1.1	2.4	0.44	0.18	0.27	2.1–2.7
1.04	0.26	0.26	0.12	0.9–1.1	2.2	0.49	0.22	0.30	1.9–2.5
1.00	0.27	0.26	0.12	0.9–1.1	2.1	0.43	0.20	0.26	1.8–2.4
1.00	0.33	0.33	0.15	0.9–1.2	2.0	0.54	0.27	0.33	1.7–2.3
0.94	0.16	0.18	0.07	0.8–1.0	1.7	0.41	0.24	0.25	1.5–2.0
1.04	0.20	0.19	0.11	0.93–1.15	54.4	7.4	0.14	4.0	50.0–58.0

also the mass per unit area, the area, and statistical coefficients of variation of the data. Leukemia 1210 studied in the ascites form has a total chromosomal mass of 39 $\mu\mu$g, for which the confidence interval is 33–45 $\mu\mu$g. Known to have a near-diploid chromosome number of 42, leukemia 1210 in metaphase consists provisionally of 84 chromatids, and yet its chromosomal mass is substantially less than that of 80 germinal chromatids, which is 56 $\mu\mu$g, as shown in Table I. The mass per unit area of leukemia-cell chromosomes is 0.74 $\mu\mu g/\mu^2$ which is significantly less than that of germinal chromosomes.

The frequency-distribution of total chromosomal mass as shown in Fig. 3 has a tendency toward a mode in the region of 30–40 $\mu\mu$g and has asymmetry to the right produced by the occurrence of masses in the range of 60–110 $\mu\mu$g.

TABLE II

Mass or dry weight (fat-free) of metaphase chromosomes in cancer cells of the mouse.

Symbols: AV, average, the arithmetic mean; SD, standard deviation; N, number of determinations; CI, confidence interval, $AV \pm 2SD/\sqrt{N}$, which includes 95 per cent of the estimates of the average.

Cancer	AV	SD	N	SD/AV	$2SD/\sqrt{N}$	CI
			Mass ($\mu\mu g$)			
Leukemia 1210	39	17	67	0.44	6	33–45
Ascites tumors*	109	49	169	0.45	8	101–117
			Mass per unit area ($\mu\mu g/\mu^2$)			
Leukemia 1210	0.74	0.17	67	0.23	0.04	0.70–0.78
Ascites tumors*	1.07	0.18	169	0.17	0.03	1.04–1.10
			Area (μ^2)			
Leukemia 1210	51	16	67	0.32	4	47–55
Ascites tumors*	99	45	169	0.45	7	92–106

* Composite data for Ehrlich carcinoma, Krebs-2 carcinoma, and sarcoma 180.

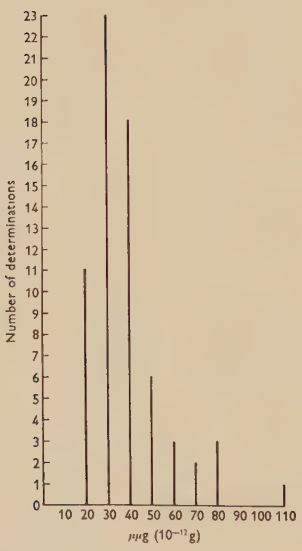

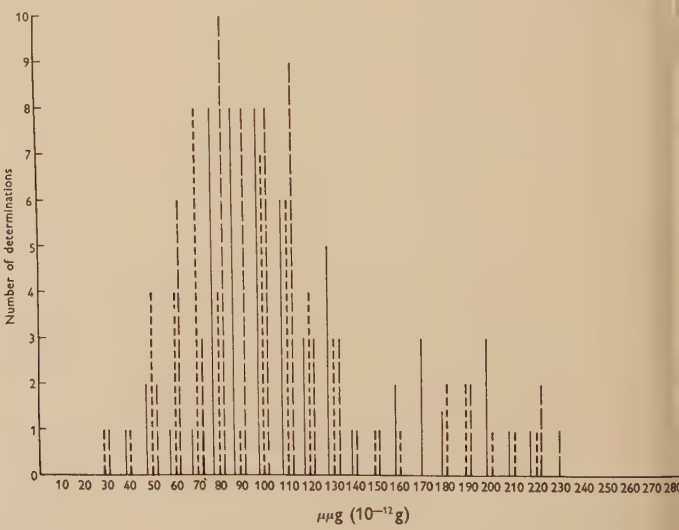

Fig. 3 (left). Frequency-distribution of mass or dry weight (fat-free) of metaphase chromosomes in mouse leukemia 1210, studied in the ascites form.
Fig. 4 (right). Frequency-distribution of total mass or dry weight (fat-free) of metaphase chromosomes in mouse ascites tumors, Ehrlich carcinoma (- - -), Krebs-2 carcinoma (— —), and sarcoma 180 (——).

Ascites-tumor cells, as judged from composite data on nearly equal samples of Ehrlich carcinoma, Krebs-2 carcinoma, and sarcoma 180, have a total chromosomal mass of 109 $\mu\mu$g, for which the confidence interval is 101–117 $\mu\mu$g. Known to have predominantly a near-tetraploid chromosome number and thus in metaphase provisionally to consist of approximately 160 chromatids, the ascites tumors have on the average about twice the mass of 80 germinal chromatids, which is 56 $\mu\mu$g. The total area, but not the mass per unit area, of ascites tumor-cell chromosomes is substantially increased, thus comprising the major explanation for the mass increase.

The frequency-distribution of total chromosomal mass in the ascites tumors, as shown in Fig. 4, displays a tendency toward a more frequent occurrence of values in the region of 70–110 $\mu\mu$g and has asymmetry to the right produced by the occurrence of masses in the region of 160–230 $\mu\mu$g. Several unresolved modes, displaying a tendency toward better resolution when different class-intervals and a semilogarithmic plot are used [6], exist in the tumor-cell population, apparently reflecting the mitotic activity of cells of various orders of ploidy.

Representative interference patterns of chromosomes in unstained cancer cells of the mouse as well as in testicular germinal cells are shown in Fig. 5 (plate).

SUMMARY

In this study the mass (dry weight, fat-free) of each of the twenty metaphase chromosomes in meiotic cells of the mouse testis was estimated by interference microscopy and arranged in order of magnitude from largest to smallest. Utilizing the data of the present and previous work, the conclusion is reached that the total dry weight of chromosomes per chromatid set is constant, within the limits of error of measurement, during the prophase and the metaphase of meiosis.

The total mass of metaphase chromosomes in mouse tumor cells, comprising several cytologic varieties in the ascites form, was measured in the present investigation. Leukemia 1210, near diploid in chromosome number, was found to be deficient in chromosomal (or chromatid) mass in comparison with germinal cells; whereas the chromosomal masses in Ehrlich carcinoma, Krebs-2 carcinoma, and sarcoma 180 were commensurate with the chromosome numbers, known to be predominantly near-tetraploid in these cancer cells.

This investigation was supported in part by research grant C-1345 from the National Cancer Institute of the National Institutes of Health, Public Health

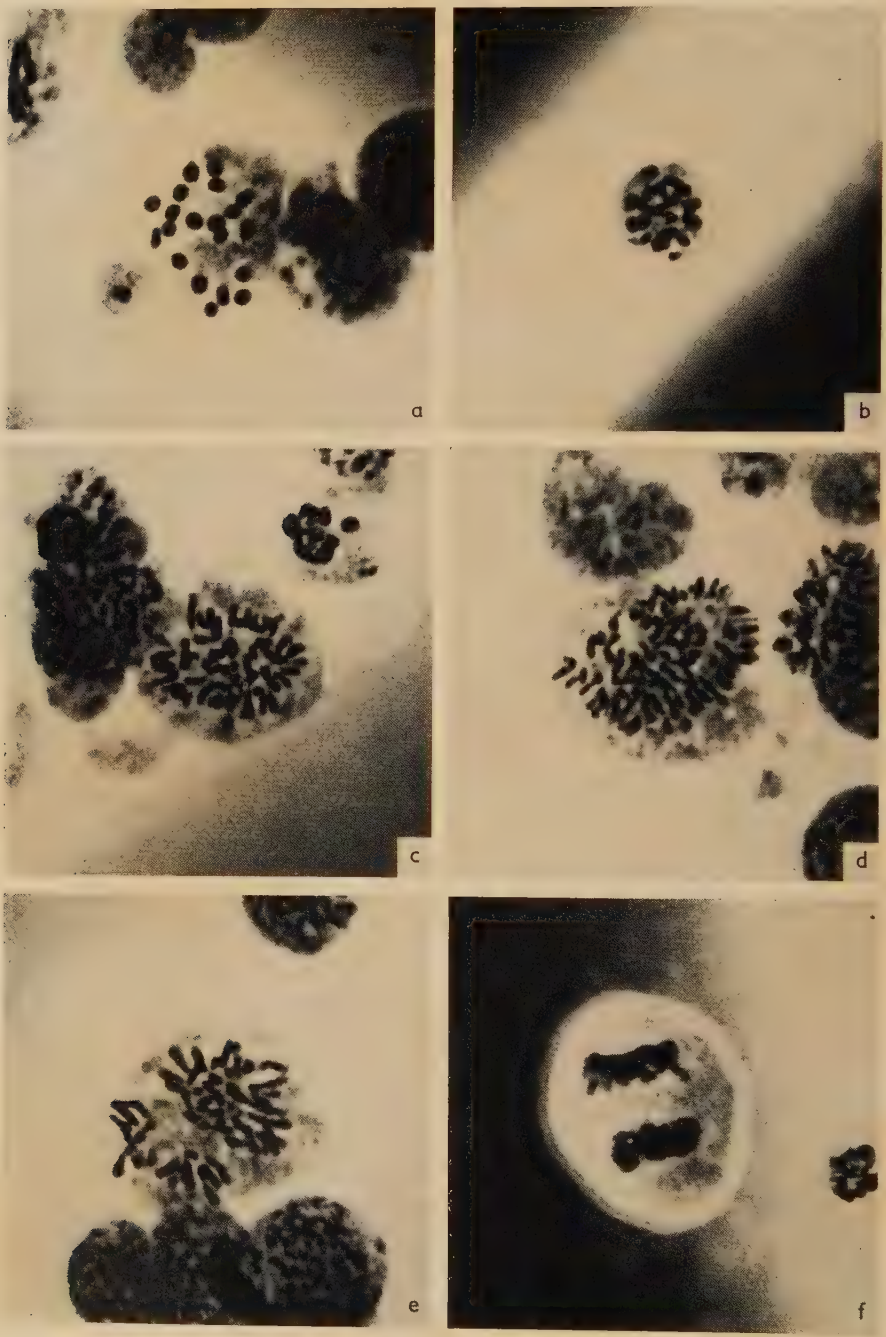
a
b
c
d
e
f

Service, and by grants from the Damon Runyon Memorial Fund, the Elsa U. Pardee Foundation, and the Rippel Foundation.

We acknowledge our indebtedness to Dr. Charlotte Friend and to Dr. Kanematsu Sugiura for the ascites tumors and to Dr. Glenn Ullyot of Smith, Kline, and French Laboratories for the trimethylcolchicinic acid used in this work.

REFERENCES

1. Friend, C. and Yuceoglu, M., *Proc. Am. Ass. Cancer Research* **2**, 106 (1956).
2. Goldberg, B., Ortega, L. G., Goldin, A., Ullyot, G. E., and Schoenbach, E. B., *Cancer* **3**, 124 (1950).
3. Hauschka, T. S. and Levan, A., *Exptl. Cell Research* **4**, 457 (1953).
4. Levan, A., personal communication.
5. Levan, A. and Hauschka, T. S., *J. Natl. Cancer Inst.* **14**, 1 (1953).
6. Mellors, R. C., *Cancer Research* **15**, 557 (1955).
7. —— *Ann. N.Y. Acad Sci.* **63**, 1177 (1956).
8. Mellors, R. C. and Hlinka, J., *Exptl. Cell Research* **9**, 128 (1955).
9. Mellors, R. C., Kupfer, A., and Hollender, A., *Cancer* **6**, 372 (1953).
10. Mellors, R. C., Stoholski, A., and Beyer, H., *Cancer* **7**, 873 (1954).

Fig. 5. Interference patterns of meiotic testicular germinal cells (*a*) and mitotic cancer cells (*b–f*) of the mouse. Metaphase figures (except *f*); tumor cells in ascitic form (except *f*). Acid-alcohol fixation; no staining; glycerin mount. 1000 × (*a*) testis, (*b*) leukemia 1210, (*c*) Ehrlich carcinoma, (*d*) Krebs-2 carcinoma, (*e*) sarcoma 180, (*f*) sarcoma 180, smear of solid tumor, anaphase.

ELECTRON MICROSCOPE STUDY OF THE EXCRETION OF CATHECOL-CONTAINING DROPLETS IN THE ADRENAL MEDULLA[1]

E. DE ROBERTIS[2] and A. VAZ FERREIRA

Departments of Cell Ultrastructure and Electrobiology, Instituto de Investigación de Ciencias Biológicas, Montevideo, Uruguay

Received October 19, 1956

The various histochemical reactions characteristic of the adrenal medulla are due to the strong reducing properties of adrenaline, noradrenaline and other cathecol amines localized in the cell cytoplasm and some of which are excreted into the blood stream [1, 2]. Among these reactions the rapid reduction of osmium tetroxide noted by Plenick in 1902, has been repeatedly used [2] as an indicator of the localization of adrenaline and related compounds in the adrenal medulla. Since fixation with osmium tetroxide has become the standard procedure for the study of tissues with the electron microscope, its use in the adrenal medulla provides a mean for the localization of cathecols at the high resolution level attained by this instrument.

Sjöstrand and Wetzstein [13] have recently demonstrated the presence of cathecol-containing granules with the electron microscope in adrenal cells of the cat, mouse and guinea pig. These granules appeared in the sections as discs with a mean diameter of 138.6 mμ and showed a definite surface membrane and a fine granular structure of high electron density. The authors emphasized the presence of a clear space (Höfe) surrounding most of the granules. This space was interpreted as a result of the dissolution of lipids, although the possibility of being a space of retraction was not discarded. Finally the authors reached the conclusion, previously advanced by Hillarp *et al.* [8], that the cathecol-containing granules should be considered as real cell organoids and not secretion granules.

EXPERIMENTAL AND RESULTS

Our preliminary electron microscope observations deal with adrenal medullae of rabbits in the normal condition, after section of the splachnic

[1] Work supported by a grant of the Rockefeller Foundation.

[2] Present address: Instituto de Anatomía General y Embriología, Facultad de Ciencias Médicas, Buenos Aires, Argentina.

nerve and under stimulation of the nerve with supramaximal rectangular pulses of different frequencies. In all cases the glands were fixed for 2 hours in a cold (4°C) solution of isotonic 1 per cent osmium tetroxide at pH 7.4 by a special modification of the original procedure of Palade [10].

Fig. 1 corresponds to a portion of the cytoplasm of a cell 24 hours after section of the splachnic nerve in which there is a heavy accumulation of cathecol-containing droplets (granules). A similar accumulation of droplets although less marked is found in normal glands (Fig. 3). The cathecol-containing droplets are easily recognized and differentiated from mitochondria by their smaller diameter, very high electron density and entirely different internal structure (Fig. 1). Confirming the observations of Sjöstrand and Wetzstein [13] we do not find any morphological analogy between mitochondria and the cathecol-containing droplets as was suggested by Hillarp *et al.* [8] on the basis of histochemical studies.

The sections of the droplets are circular with a mean diameter of about 160 mμ in Fig. 1 and with a wide range of measurements between 87 and 230 mμ. The observation of numerous electron micrographs of normal specimens shows the presence of smaller droplets which may reach 40 mμ or less. Between these small droplets and the large ones there are all gradations of sizes. Even the smallest droplets show the same fundamental structure with a limiting surface membrane and the internal deposit of reduced osmium. In the larger droplets shown in Fig. 1 one may recognize a single surface membrane of the order of 30 Å separated from the main mass of the osmium deposit by a space of lower electron density of about 100–120 Å.

The inner region of the droplets is occupied by the deposit of reduced osmium which may appear homogeneously distributed but in most cases is in a granular form. The presence of a definite surface membrane in the cathecol-containing droplets agrees with the known physico-chemical properties of isolated elements which suggested the existence of a semipermeable surface membrane. This membrane can be easily altered by different physical, chemical or enzymatic agents [8, 9]. In our preparations of normal animals we have been unable to observe the presence of the large clear spaces (Höfe) indicated by Sjöstrand and Wetzstein [13]. Only in specimens where the fixation was not appropriate or in thick sections subjected to electron bombardment did similar spaces appear. In the case of the normal rabbit cell we consider this space to be an artefact of retraction.[1]

[1] In the adrenal cells of the rabbit in addition to the most common type of cathecol-containing droplets just described there is another more complex one which will be described in another note [7].

The structure of mitochondria will not be described because it corresponds to that well known in other cell types. In addition to these cell components small regions of the cytoplasm with the structure of the Golgi complex and cell membranes studded with the dense granules of Palade [11] can be recognized.

A full description of the submicroscopic organization of the adrenal cell will be published elsewhere. Here we want to call attention mainly to the changes that the cathecol-containing droplets undergo with stimulation of the splachnic nerve. Figs. 2, 4 and 5 correspond to glands continuously stimulated with supramaximal stimuli (8 volts) of 1 ms duration and a frequency of 100 pulses per second during ten minutes. This frequency of stimulus was chosen because Rapela and Covián [12] reported a maximal excretion of cathecols from the adrenal of the dog with 40 to 100 pulses per second.

Comparing Fig. 2 with Fig. 1 the intense changes that have occurred are clearly observed. The cathecol-containing droplets show a great reduction in the osmic reaction not only in intensity but also in cross section as if most of the content had been excreted. The limiting membranes are very conspicuous and with a tendency to become irregularly folded. The clear space below the membrane has increased considerably and several empty droplets can be recognized. This may be the result of sections passing through the clear space but the large number of them and other details, as observed in Fig. 5, indicate that the content of the droplets may be entirely evacuated after stimulation of the splachnic nerve.

Different stages of the process of excretion are illustrated in Figs. 4 and 5 as compared with a normal gland (Fig. 3). All these figures correspond to cathecol-containing droplets lying in the vicinity of the cell membrane. In Fig. 4 there is an apparent increase in size of the droplets with diminution of electron density and a conspicuous attachment of many of them to the cell membrane (marked with arrows). This process of attachment can be

---

Fig. 1. Electron micrograph of a portion of cytoplasm of a cell from the adrenal medulla of the rabbit, 24 hours after section of the splachnic nerve. The field is loaded with cathecol-containing droplets (*cd*); *mi*, mitochondria with double limiting membranes and internal lamellar structure; *cm*, cell membrane. Arrows indicate *cd* in which the limiting membrane is more clearly visible. (See further description in the text.) × 41,700.

Fig. 2. Electron micrograph from an adrenal cell of a rabbit with stimulation of the splachnic nerve for 10 minutes with supra-maximal pulses at a frequency of 100 per second. The section is thought to be tangential to the surface of a thin expansion of cytoplasm limited by the cell membrane (*cm*). Cathecol-containing droplets in different stages of excretion (*cd*) and some empty membranes remaining from the cathecol excretion (*ed*) are shown. (See further description in the text.) × 41,700.

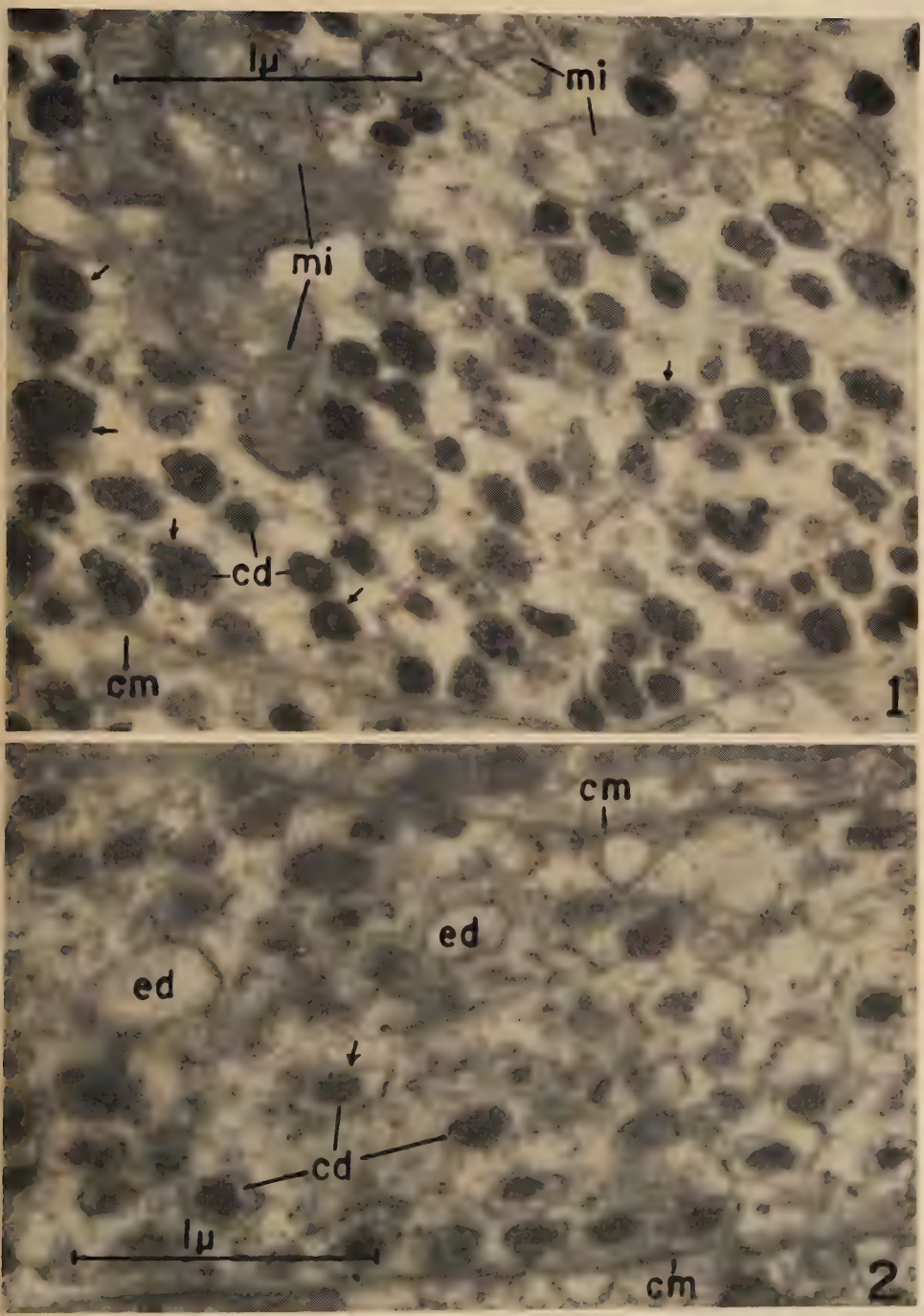
1μ
mi
mi
cd
cm
1
cm
ed
ed
cd
1μ
cm
2

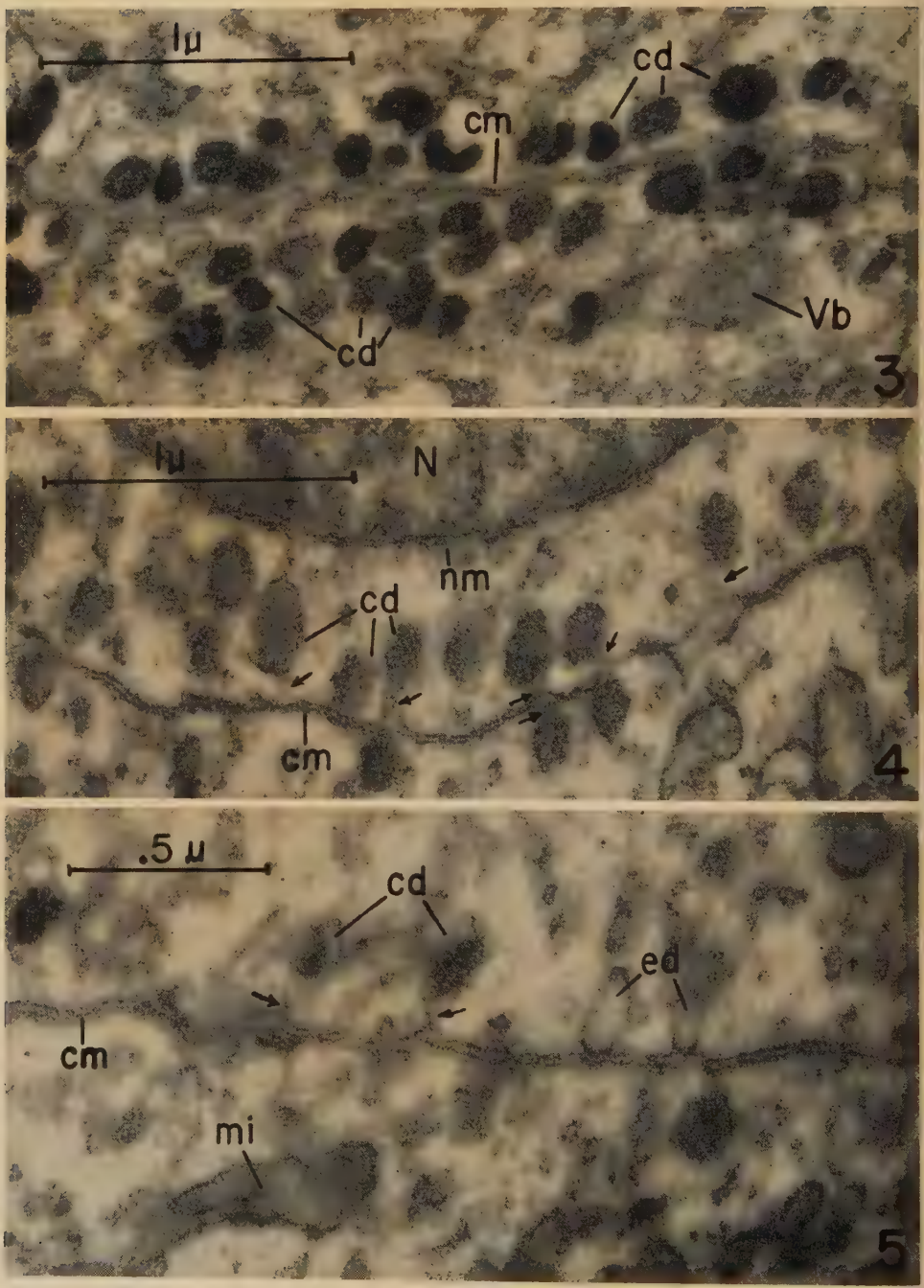
1μ
cd
cm
cd
Vb
3
1μ
N
nm
cd
cm
4
.5 μ
cd
ed
cm
mi
5

observed also in normal glands but it is less frequent. At the same time there is an elongation of the droplets normally with respect to the cell membrane that seems to be independent of the direction of the plane of section. In Fig. 5, at higher magnification, a later stage of excretion is observed, in which irregular droplets in addition to completely empty membranes are present. This process, in its highest degree, leads to the complete excretion of cathecols leaving only the membrane.[1]

DISCUSSION

The observations described cannot be interpreted within the hypothesis postulated by Hillarp *et al.* [8] and Sjöstrand and Wetzstein [13] that the cathecol-containing granules are real cell organoids. In fact, at least for the stimulated glands of the rabbit it can be demonstrated that in certain cells the cathecol droplets may disappear entirely after evacuation of the content or may leave empty membranes.

We are inclined to believe that the cathecol-containing droplets (granules) are secretory inclusions that start as a small vesicle surrounded by a membrane and grow within the cell cytoplasm until finally they excrete their contents at the cell surface. We think that the process of excretion of the cathecol-containing droplets can be interpreted in accordance with the concepts on membrane flow and vesiculation for active transport within the cell, recently postulated by Bennett [3]. A similar mechanism for the excretion of the synaptic vesicles at the synaptic ending was previously postulated by De Robertis and Bennett [5]. By this mechanism acetylcholine, adrenaline, noradrenaline or other active humoral agents may be synthesized by the cell while enclosed within a membrane and then they may be moved and discharged instantly at the surface membrane when the appropriate stimulus is acting.

[1] This process of excretion of the cathecol at the cell surfaces seems to be the most frequent in stimulated glands. More seldom one may find droplets that seem to undergo loss of cathecol content while in the interior of the cytoplasm.

Fig. 3. Electron micrograph of an adrenal cell from a normal rabbit (see description in the text). *Vb* is a typical multivesicular body [7]. × 41,700.

Fig. 4. Electron micrograph of a material similar to that of Fig. 2. The cathecol-containing droplets (*cd*) have increased in size and have lower electron density. Several droplets are shown attached to the cell membrane (marked with arrows). *N*, nucleus; *nm*, nuclear membrane. (See further description in the text.) × 41,700.

Fig. 5. Electron micrograph from the same stimulated material as in Fig. 2. The process of excretion of cathecol is more advanced. Arrows indicate the attachment of the cathecol-containing droplets (*cd*) to the cell membrane (*cm*); *ed*, excreted droplets. The cell membrane with a thickness of about 50–60 Å shows a double osmiophilic layer limiting a central layer of lower density. *mi*, mitochondria. (See further description in the text.) × 54,800.

SUMMARY

The most common cathecol-containing droplets (granules) are described in the normal adrenal medulla of the rabbit and after section of the splachnic nerve. These secretory droplets are spherical with cross sections varying in diameter between 87 and 230 mμ and with a mean of 160 mμ. Smaller droplets (ca. 40 mμ) are also found and there are all gradations in size up to the larger ones. The droplets have a single limiting membrane of about 30 Å and are filled with an internal homogeneous or granular deposit of reduced osmium. Between the membrane and the osmium deposit there is a space of lower electron density of about 100–120 Å.

Under electrical stimulation of the splachnic nerve intense changes occur in the cathecol-containing droplets. First there is an apparent increase in size with diminution in electron density of the droplets and the attachment of many of them to the cell membrane. Then a great loss of the content of the droplets occurs that may reach to the complete evacuation of cathecols and may leave a folded membrane attached to the cell surface. It is concluded that the cathecol-containing droplets are secretion inclusions and not cell organoids. A mechanism of membrane flow is proposed for the excretion of most cathecol-containing droplets.

REFERENCES

1. Bachmann, Handbuch der mikroskopischen Anatomie des Menschen. Bd. 6, 5. Teil. Springer-Verlag, Berlin, 1954.
2. Bennett, H. S., *Am. J. Anat.* **69**, 333 (1941).
3. —— *in* Arden House Symposium on "Tissue Fine Structure" (in press) 1956.
4. Cramer, W., Fever, Heat Regulation, Climate, and the Thyroid-Adrenal Apparatus. Longmans, Green and Co. London, 1928.
5. De Robertis, E. and Bennett, H. S., *Federation Proc.* **13**, 35 (1954).
6. —— *J. Biophys. Biochem. Cytol.* **1**, 47 (1955).
7. De Robertis, E. and Vaz Ferreira, A., *Exptl. Cell Research* **12**, 575 (1957).
8. Hillarp, N. Å., Hökfelt, B., and Nilson, B., *Acta Anat.* **21**, 155 (1954).
9. Hillarp, N. Å. and Nilson, B., *Acta Physiol. Scand.* **31**, Suppl. **113**, 79 (1954).
10. Palade, G. E., *J. Exptl. Med.* **95**, 285 (1952).
11. —— *J. Biophys. Biochem. Cytol.* **1**, 59 (1955).
12. Rapela, C. E. and Covian, M. R., *Rev. Soc. Arg. Biol.* **30**, 157 (1954).
13. Sjöstrand, F. S. and Wetzstein, R., *Experientia* **12**, 196 (1956).

Experimental Cell Research **12**, *575–581 (1957)*

A MULTIVESICULAR CATHECOL-CONTAINING BODY OF THE ADRENAL MEDULLA OF THE RABBIT[1]

E. DE ROBERTIS[2] and A. VAZ FERREIRA

Departments of Cell Ultrastructure and Electrobiology, Instituto de Investigación de Ciencias Biológicas, Montevideo, Uruguay

Received October 19, 1956

In a previous preliminary paper [2] we described with the electron microscope the cathecol-containing droplets of the adrenal medulla of the rabbit. This study was done in normal glands and in glands after section or stimulation of the splachnic nerve and led to the postulation of a mechanism for the excretion of cathecol amines from the cells.

In this paper we want to call attention to a second and different type of cathecol-containing body found in the same material of rabbit's adrenal. Before starting our description it is important to stress that the cathecol-containing droplets, similar to those previously observed by Sjöstrand and Wetzstein [11] in the cat, mouse and guinea pig, are by far the most frequent secretory components. The elements that will be described here are extremely scarce although they have been observed in several specimens under normal conditions, after section of the splachnic nerve and with nerve stimulation. Only in one specimen stimulated for 10 minutes with supramaximal pulses at a frequency of 100 per second were these bodies more conspicuous and our description will be mainly illustrated with this material.

EXPERIMENTAL AND RESULTS

Some of the most important characteristics of these bodies are shown at low magnification in Fig. 1. Parts of the cytoplasms of several adrenal cells in the neighborhood of a venous sinus are observed. Within them, in addition to mitochondria and other vacuolar or particulate components, four large bodies constituted by the aggregation of a small vesicular material are found.

[1] Work supported by a grant of the Rockefeller Foundation.

[2] Present address: Instituto de Anatomía General y Embriología, Facultad de Ciencias Médicas, Buenos Aires, Argentina.

In the interior of many of the individual vesicles (Figs. 2 and 3) there is a black deposit of reduced osmium with an electron density equivalent to or higher than that present in the regular cathecol-containing droplets [2], (Fig. 1). For this and other reasons we consider these vesicles as also containing reducing cathecol amines and we propose to call the entire structure the *multivesicular cathecol-containing body* (*Vcb*). The *Vcb* starts as an intracellular body resulting from a circumscribed conglomeration of vesicles in the midst of the cytoplasm, and frequently in the vicinity of the nucleus. This body is spherical or ovoidal in shape and may vary in size from less than 500 mμ to 2000 mμ or more (Fig. 1). This *intracellular multivesicular cathecol-containing body* (*Ivcb*) becomes surrounded and segregated from the rest of the cytoplasm by a double membrane and, by a process of flow, is displaced toward the intercellular spaces and especially into the subendothelial spaces of the venous sinuses (Figs. 1, 2 and 3). The actual process of flow can be deduced from the observation of sequences in many electron micrographs. Particularly convincing are some showing round *Ivcb* with long processes directed toward the periphery and reaching the subendothelial space. When this material occupies an extracellular position it is called *extracellular multivesicular cathecol-containing body* (*Evcb*).

In the smaller *Ivcb* the double surface membrane is less conspicuous or incomplete. Frequently mitochondria are found near the surface or in contact with the *Ivcb*. When the double membrane is completely formed it is constituted by two layers of about 50–60 Å and separated by a space of 120–170 Å. Of these two membranes one can be considered as belonging to the *Ivcb* proper and the other to the cell cytoplasm. Inside the multivesicular body the vesicles are very densely packed. They are round or ovoidal and with diameters ranging between 240 and 1300 Å with a mean of 590 Å. As can be observed in Figs. 2 and 3 only part of the vesicles contain the osmium deposit. The proportion of cathecol-containing vesicles apparently varies considerably from one *Vcb* to another (see Figs. 1 and 2). The osmium deposit is round-shaped and occupies only a portion of the vesicle. It may be situated either in the middle or near one side of the membrane (Fig. 3).

All figures (1 to 3) are electron micrographs of cells of the adrenal medulla of a rabbit whose splachnic nerve was stimulated for 10 minutes with supramaximal pulses at a frequency of 100 per second.

Fig. 1. Low power micrograph showing *intracellular multivesicular cathecol-containing bodies* (*Ivcb*) and *extracellular multivesicular cathecol-containing bodies* (*Evcb*), some of the latter lying in the subendothelial space. (See description in the text.) *N*, nucleus; *mi*, mitochondria; *cm*, cell membrane; *cd*, cathecol droplets; *E*, endothelium, *VS*, venous sinus. × 21,000.

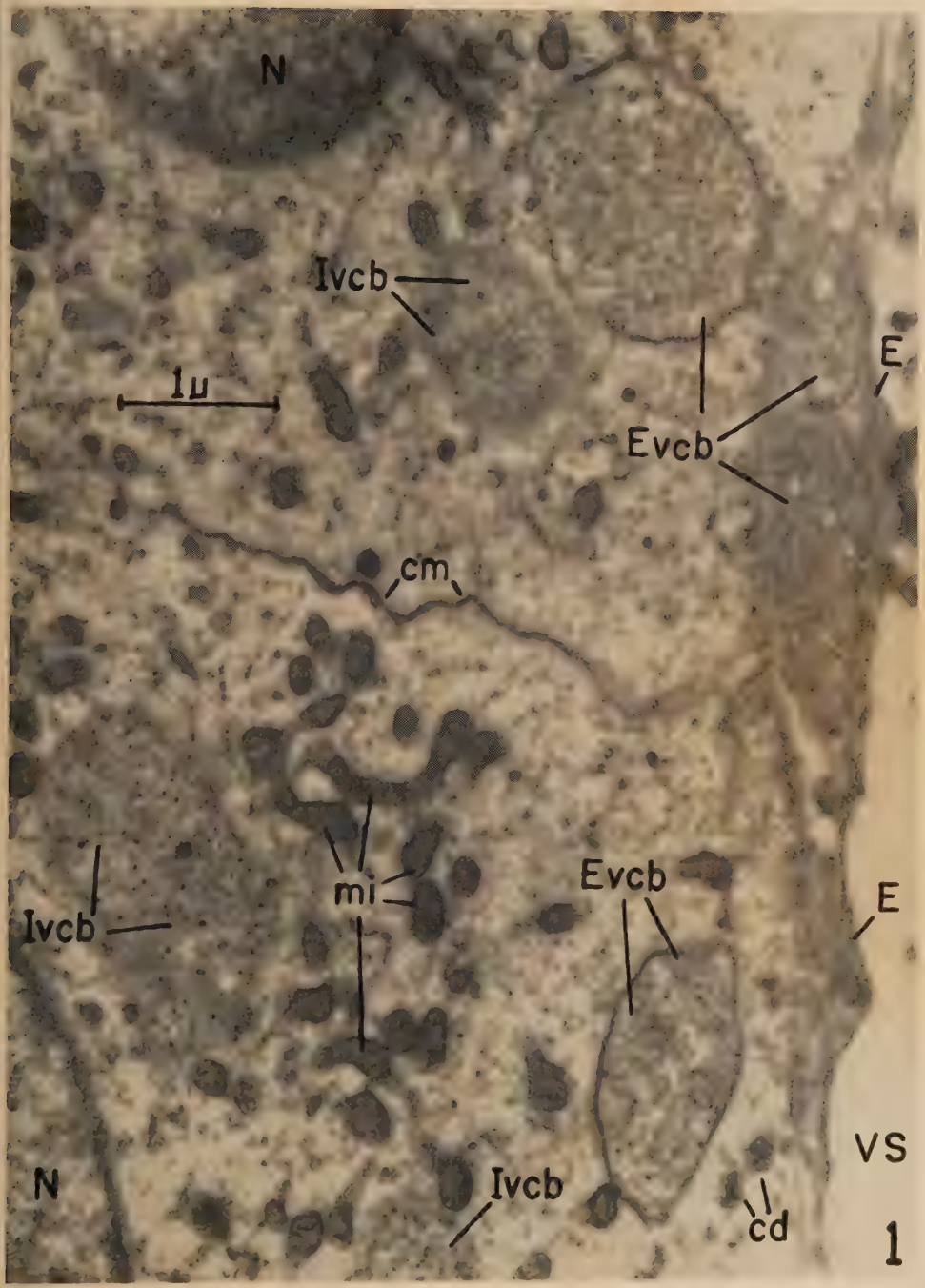
N
Ivcb
1μ
E
Evcb
cm
mi
Evcb
E
Ivcb
N
Ivcb
cd
VS
1

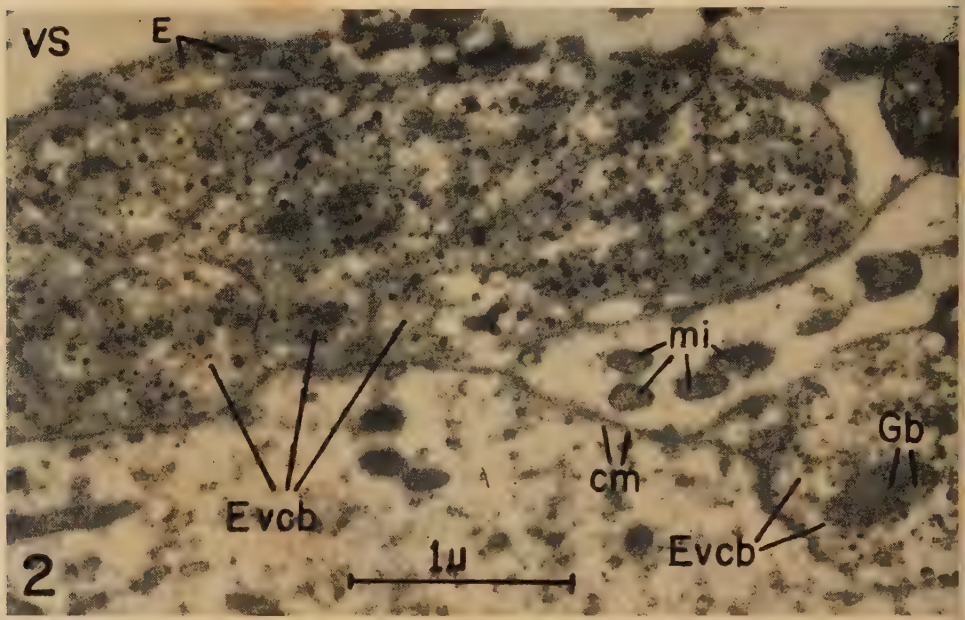
VS
E
mi
Gb
cm
Evcb
Evcb
1μ
2

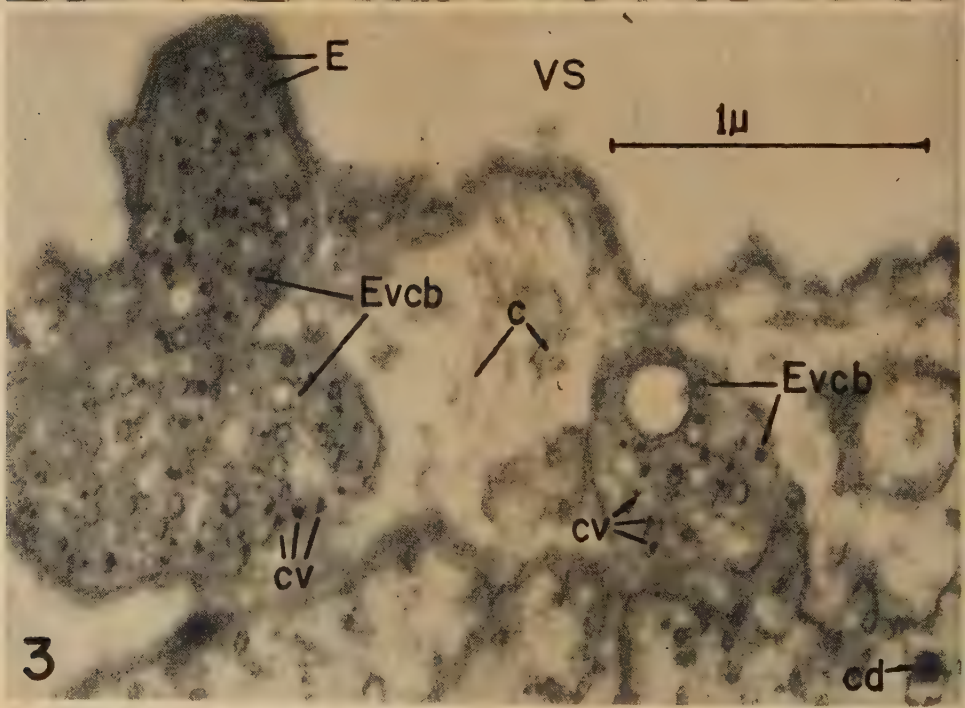
E
VS
1μ
Evcb
c
Evcb
cv
cv
3
cd

Measurements of the diameter of these osmium deposits give a mean of 150 Å and range from 65 to 260 Å.

In addition to the regular vesicular component in the *Vcb* it is possible to find larger clear vacuoles that may reach a considerable size and have a content of very low electron density (Fig. 3). Although nothing definite can be said regarding the significance of these clear vacuoles it is interesting to note that they are more frequently found in the *Ecvb* situated in the subendothelial space where the excretion of cathecol can be expected to occur.

Another component that is found within the *Vcb* is constituted by dense ovoidal or rod-shaped bodies that have a granular structure (*Gb* in Fig. 2). At closer examination these bodies appear to be made up of the close packing of dense granules or small vesicles. The interpretation of this component is not clear either, but since there are many intermediate forms between them and the regular or the cathecol-containing vesicles, the possibility exists that they may be centers in which the vesicular elements are being formed.

The subendothelial spaces of the venous sinuses are frequently packed with *Evcb* that are separated by collagen fibers and the connective tissue space. In this situation the *Ecvb* are surrounded by a single membrane. From the blood stream these *Evcb* are only separated by a very thin layer of endothelium which may be pushed in some places by the cathecol-containing body (Fig. 3).

At the present time it is too early to establish with certainty whether this kind of cathecol-containing body is produced by a special cell type or if the same adrenal cell is capable of synthesizing both the common cathecol containing droplets and the *Ivcb*. So far, the observations tend to show that cells that have *Ivcb* do not contain cathecol droplets or have very few of them (Fig. 1). This would indicate that at least on a time basis there may be a certain cell specificity in secretion.

DISCUSSION

Present studies are too preliminary to permit any interpretation of these two different types of cathecol-containing secretory inclusions in the adrenal

Fig. 2. Extracellular multivesicular cathecol-containing bodies (*Evcb*) localized in the subendothelial space. *Gb* is a granular body frequently found within the *Vcb*. See description in the text. × 28,200.

Fig. 3. Extracellular multivesicular cathecol-containing bodies (*Evcb*). One of them is pushing the endothelium (*E*) into the venous sinus (*VS*). Inside the *Evcb* there are some clear vacuoles. The cathecol-containing vesicles (*cv*) are very conspicuous. Note that the *Evcb* has only one limiting membrane. *c*, collagen fibers (see further description in the text). × 40,800.

cells and nothing can be said yet about their physiological or chemical significance. From the histochemical viewpoint the problem of cell specificity has been raised in recent years with the postulation, in several species, of two types of cells in relation to the production and storage of adrenaline and noradrenaline [3, 4, 5]. In the case of the rabbit's adrenal medulla the content of noradrenaline is very low or non-existent in normal conditions [7] but it appears in the blood after stimulation of the splachnic nerve [12].

The multivesicular cathecol-containing bodies described in this paper are large structures that should be easily resolved with the optical microscope—in contrast with the cathecol droplets, most of which are of submicroscopic dimensions [2]. In the histological literature there are some references that may be related to our findings such as the presence of coarse secretion granules and the presence of positive cathecol reactions in the subendothelial spaces and intercellular clefts, precisely in the region where the *Evcb* are most abundant [6, 1].

From the submicroscopic viewpoint, to our knowledge, multivesicular bodies containing cathecol have not yet been described. However, structures surrounded by a membrane and comprising the aggregation of vesicular or vacuolar material have been observed in different cells.

Sotelo and Porter [9] have observed intracellular bodies limited by a single membrane and containing vesicular material, the so-called *multivesicular bodies* in rat ovocytes and fertilized eggs. Furthermore Sotelo *et al.* [10] have demonstrated the wide occurrence of multivesicular bodies with a single or multiple membrane in invertebrate ovocytes and other cell types. In the epithelial cells of the mouse jejunum Zetterquist [13] describes a vacuole-containing body that is limited by a single membrane, and similar observations have been made by Rhodin and Dalhamn [8] in tracheal epithelium.

The multivesicular body described in this paper, in addition to its content in cathecol amines, differs in that it becomes very early surrounded by a double membrane and is thus segregated from the cell cytoplasm. From its intracellular original position (*Ivcb*) the multivesicular body flows toward the intercellular and subendothelial spaces (*Ecvb*) retaining only its innermost membrane. We have to suppose that in the process of segregation and excretion of the *Ivcb* the outer membrane becomes continuous and incorporated into the membrane of the cell. This would be another interesting example of the role played by membranes in the active transport of material within the cell [2].

SUMMARY

In addition to the most common cathecol-containing droplets [2], in some cells of the adrenal medulla of the rabbit there are multivesicular bodies that also give the osmic reaction for cathecols. These multivesicular bodies are at the beginning intracellular (*Ivcb*) and are formed by the conglomeration of densely packed vesicles some of which contain the osmium deposit. These *Ivcb* become surrounded by a double membrane and by a process of flow are displaced into the intercellular clefts and subendothelial spaces of the venous sinuses. At this moment they may be called *extracellular multivesicular cathecol-containing bodies* (*Evcb*) and are surrounded by a single membrane.

Inside the multivesicular bodies the vesicles vary in diameter between 240 and 1300 Å with a mean of 590 Å. A variable number of vesicles contain a round deposit of osmium (cathecol) with a mean diameter of 150 Å. In the *Evcb* there are larger clear vacuoles that appear to be more frequent in the subendothelial bodies where the excretion of cathecol can be expected to occur. Inside the *Vcb* there is also another component constituted by ovoidal or rod-shaped bodies having a granular structure. These bodies are made of the closed packed aggregation of granules and small vesicles and may represent centers for the formation of vesicular elements.

The segregation and excretion of the multivesicular body is another example of the role played by membrane flow in the transport of material within the cell.

REFERENCES

1. Bennett, H. S., *Am. J. Anat.* **69**, 333 (1941).
2. De Robertis, E. and Vaz Ferreira, A., *Exptl. Cell Research* **12**, 568 (1957).
3. Eränkö, O., *Nature* **168**, 250 (1951).
4. —— *Ibid.* **175**, 88 (1955).
5. Hillarp, N. Å. and Hökfelt, B., *Acta Physiol. Scand.* **30**, 55 (1953).
6. Hillarp, N. Å., Hökfelt, B., and Nilson, B., *Acta Anat.* **21**, 155 (1954).
7. Holtz, P. and Schümann, H. J., *Nature* **165**, 683 (1950).
8. Rhodin, J. and Dalhamn, T., *Z. Zellforsch.* **44**, 345 (1956).
9. Sotelo, J. R. and Porter, K. R. (cited by Palade, G. E., *J. Biophys. Biochem. Cytol.* **1**, 567 (1955)).
10. Sotelo, J. R. *et al.*, 1956 (to be published).
11. Sjöstrand, F. S. and Wetzstein, R., *Experientia* **12**, 196 (1956).
12. West, G. B., *Brit. J. Pharmacol. Chemother.* **5**, 542 (1950).
13. Zetterquist, H., The Ultrastructural Organization of the Columnar Absorbing Cells of the Mouse Jejenum. Stockholm, 1956.

THE DNA CONTENT OF CELLS IN THE ROOT OF *VICIA FABA*

E. M. DEELEY, H. G. DAVIES and J. CHAYEN[1]

Wheatstone Physics Laboratory and Medical Research Council Biophysics Research Unit, King's College, London, England

Received October 23, 1956

The technique of measuring the amount of Feulgen stain in individual cell nuclei, and hence the relative amount of DNA (deoxyribose nucleic acid), has recently been improved by the introduction of a photoelectric scanning method [2] and a technique of cell crushing [1]. The accuracy and rapidity obtained by using these two methods together has already been demonstrated in measurements on certain animal cells [3]. Recently Holmes, Mee, Hornsey and Gray [7] have studied by biochemical methods the average DNA content per nucleus in four segments (cf. Fig. 1) of the root of *Vicia faba* grown under standard conditions. The aim of the present investigation is to study by cytochemical methods the DNA content of individual nuclei in similar root segments.

MATERIAL AND METHODS

The roots were grown under the same standard conditions as those used for the biochemical experiments [7]. The segments into which the main roots were cut (Fig. 1) have been described [7] as follows:

"*Segment A* (PQ) 0–2 mm. Apart from a small number of differentiated epidermal cells, all cells in this segment are meristematic in appearance. The mitotic index of these cells in this culture is known to be around 15–20 per cent. It is customarily assumed that in this region both daughter cells from any given division will divide again, but there is no positive evidence that this is so in all cases."

"*Segment B* (QR) 2–4 mm. Cells in this segment are of two types, mixed in unknown proportions, viz. (*a*) cells which will undergo one (or, rarely more than one) division before commencing to form part of the differentiated root structure, and (*b*) cells which have already commenced to differentiate."

"*Segment C* (RS) 4–8 mm. Predominantly cortical cells and some vascular cells in process of active elongation, but containing cells of meristematic appearance, the two types being present in a roughly known proportion."

"*Segment D* (TU) 12–20 mm. Predominantly cortical cells which have completed

[1] Wheatstone Physics Laboratory and Dept. of Cell Biology, John Innes Horticultural Institution, Herts., England.

the process of elongation, and vascular cells, but mixed with a roughly known proportion of cells of meristematic appearance."

A more detailed morphological study of the first three millimetres of the main root of *V. faba* has been made recently by Jensen [10].

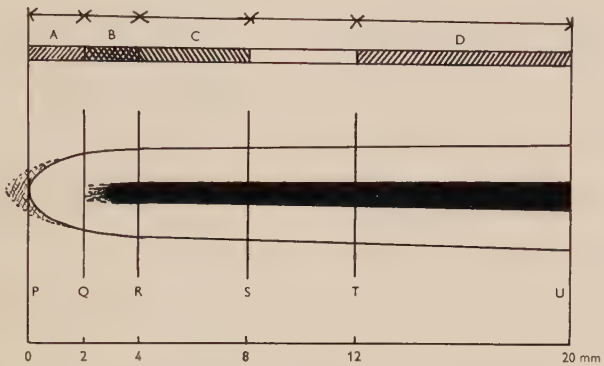

Fig. 1. Segments into which the root tip of *Vicia faba* is divided for measurement; root cap (cross hatched), cortex (unshaded), central cylinder (black), and meristem (unshaded). See also text. *Abscissae:* distance from the root tip in mm.

In order that the segments *A–D* could be directly compared, they were treated together as follows. The segments were fixed for 18 hours in acetic alcohol, hydrolysed in 1 *N* hydrochloric acid at 60° for 6 minutes, stained in the Feulgen reagent for 1½ hours and washed in SO_2 water (three changes).

In the stained segments *B*, *C* and *D* of the root two clearly distinguishable regions are present. These are the heavily stained central cylinder containing the developing vascular system, and the apparently more lightly stained sheath mainly composed of cortical cells which we designate the cortical region. This appearance is largely due to the difference in cell number per unit volume. Preparations have been made of segments *B*, *C* and *D* in which these two regions have been separated by microdissection, as well as of whole segments *A* to *D*. Each stained root segment was macerated and mixed in glycerol on a coverslip, and then a cellophane sheet (approximately 25 microns thick) placed underneath for cell crushing. (For details see [1].) Nuclei were measured at sites scattered over the entire area of the preparation in an attempt to obtain a random sample.

RESULTS

Fig. 2 shows the histograms obtained from segment *A* and from each of the two regions of segments *B–D* described above, taken from one root. These histograms relate the nuclear stain content (and hence relative DNA content) to the number of nuclei.

The mean DNA content of all nuclei measured in the metaphase stage is termed the 4C value, and hence that for each of the two anaphase groups resulting from division has the value 2C. From the measurements on mitotic stages (shaded in Fig. 2) it can be seen that in segment *A* the great majority of DNA contents lie on or between these two values. The proportion of nuclei

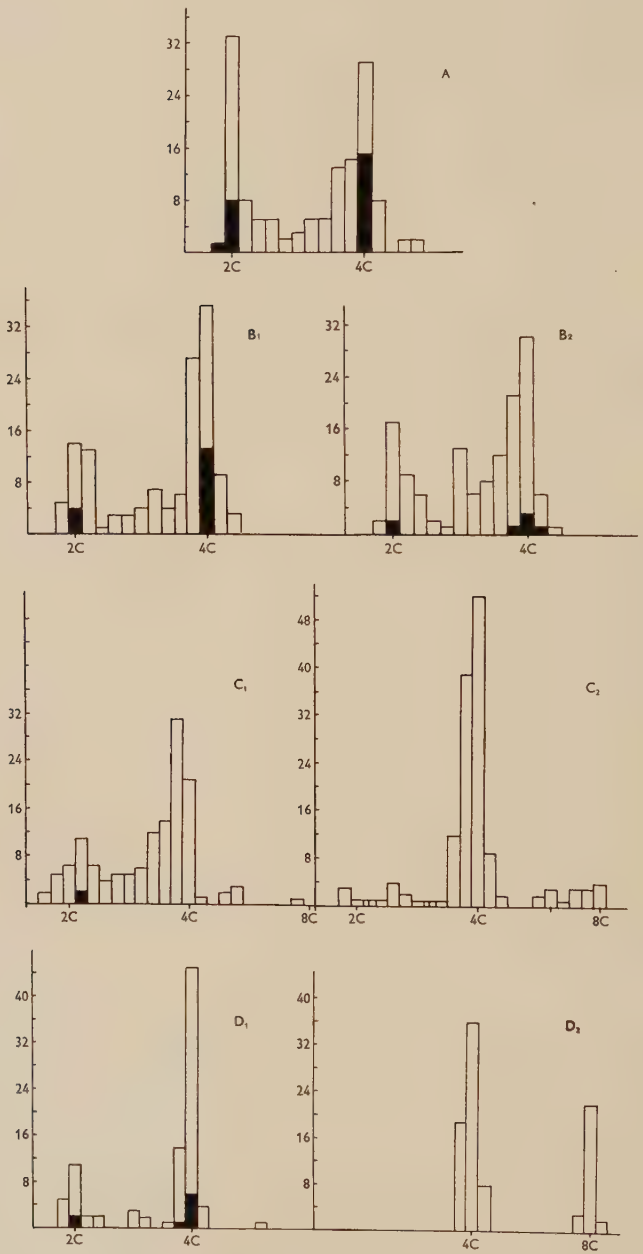

Fig. 2. Histograms relating cell number (ordinates) and Feulgen stain content per nucleus in log arb. units (abscissae), in segments *A*, *B*, *C*, *D*. Affix 1 denotes central cylinder; affix 2 denotes cortex. Cells in mitotic division (black).

TABLE I

DNA content in individual mitotic figures in one root meristem of *Vicia faba*.

Prophase	Metaphase	Anaphase	Telephase
215	216	106	106
210	220	109	109
216	217	108	107
227	219	108	104
221	220	109	107
213	221	108	108
217	220		107
Means 217	217	108	107

with higher values of DNA (4C and above) increases with distance from the root tip, as seen from the other histograms, the proportion being highest in the cortical regions. Cells with DNA values intermediate between 2C and 4C, and 4C and 8C are to be found even in regions of the root where there is no mitotic activity (see Fig. 2, C_1, C_2). The fraction of cells with intermediate values has fallen to a minimum in segment *D*. In three separate experiments on different material, essentially similar results were obtained, although there were small variations in the heights of the 2C, 4C and 8C maxima. Table I gives typical values of DNA content for the individual stages of mitosis.

In two other experiments, preparations were measured and a slightly wider spread of results was found in each segment. This resulted in a somewhat greater proportion of values lying outside the 2C to 4C range, and a wider spread of values for mitotic figures about the two modes. In one preparation the maximum difference between the values of telophase nuclei, for example, was 20 per cent with a mean variation of 4 per cent about the arithmetic average, compared with corresponding figures of 8 and 2 per cent for the preparation used for the histograms shown in Fig. 2. The average values for the different groups of mitotic figures were, however, similar to those given in Table I.

Measurements were also made on preparations of whole segments so as to enable the average amount of DNA per cell in each segment to be calculated. A random sample of 135 nuclei was taken from each segment. The results of four such experiments performed over a period of about two years are shown in Table II, which also includes the values obtained by the biochemical method [7].

Table II

Average nuclear DNA content in each of four root segments, segment *A* being taken as unity. Results for four separate experiments are compared with average biochemical results [7].

Segment	Expt. 1 (18.3.54)	Expt. 2 (24.2.55)	Expt. 3 (6.5.55)	Expt. 4 (19.1.56)	Biochemical
A	1.00	1.00	1.00	1.00	1.00
B	1.20	1.08	1.10	1.02	1.12
C	1.36	1.22	1.23	1.21	1.28
D	1.51	1.48	1.36	1.43	1.32

CALCULATION AND DISCUSSION

The histograms obtained, e.g. those illustrated in Fig. 2, give information concerning the time of onset and rate of synthesis of DNA during the cell cycle in the root meristem (segment *A*) and, though with less accuracy, in the elongation segments.

DNA synthesis in the root meristem (Segment A)

The doubling of the amount of DNA per cell owing to synthesis during interphase is well established [9, 14, 16]. It might therefore be argued that the DNA content of one cell is unlikely to alter during mitotic division since this process merely ensures the equal distribution of chromosomal material to the daughter cells. Table I indeed shows that the *average* DNA value per cell in each of the stages of division is nearly constant, the maximum difference being no more than 1–2 per cent. Hence it may be concluded that there is no change in the DNA content of each *individual* cell during division. This result is in agreement with that found earlier in onion. (Added to proof in Patau and Swift [12].)

A method of deriving the DNA synthesis curve for a cell from the DNA histogram of a population of dividing cells has been given by Walker [15]. Time is expressed as a fraction of the generation time (i.e. the time between exactly similar stages in the cycle) and the cell population must obey the following conditions:

(i) The increase in nuclear DNA content from the 2C to the 4C value with respect to time (as defined above) must be identical in all cells in the population; thus the cell number increases exponentially with time;

(ii) The growth and division of cells in the population must not be syn-

chronised. This can be tested by fixing roots at different times and observing the measured histograms.

At first sight it might appear that a method applicable to a population in which the cell number is increasing exponentially, would not be applicable to the root meristem (i.e. segment *A* in Fig. 1) in which the total population of dividing cells remains constant. The method can be applied, however,

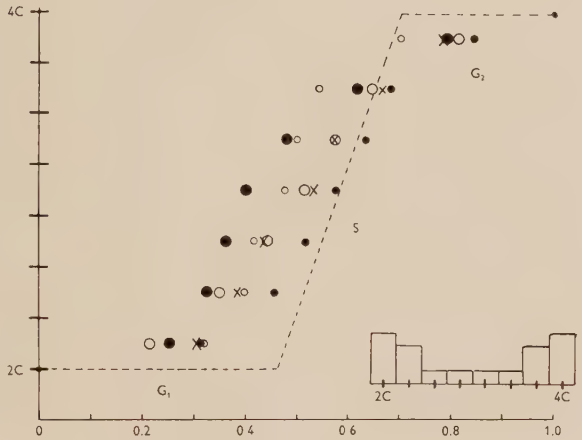

Fig. 3. Data on DNA synthesis deduced by theory from histograms of segment *A*, on five separate occasions; each experiment is denoted by a different symbol. Ordinate: Average nuclear DNA content (non-log. arb. units). Abscissae: fraction of interphase time (*T*). The dotted line shows the synthesis curve derived by the P^{32} method [8], G_1 ($0 \rightarrow 0.47\,T$), $S(0.475 \rightarrow 0.71\,T)$ $G_2(0 \rightarrow 1.0\,T)$. The inset diagram shows a schematic histogram, the abscissae of which correspond to the ordinates in the main figure.

since the measurements are restricted to a root segment which contains only cells which will divide again (cf. the description of segment *A*).

The cell population in segment A departs (see discussion in [7]) from the ideal one envisaged by the theory [15]. Thus there is an unknown proportion of cells which will not divide again (cf. condition (i)). This number is kept small by excluding the root cap from segment *A* and by restricting it to that part of the root where the mitotic index is highest and where no cell elongation is visible. Even so, a few per cent of differentiated epidermal cells are present. Moreover, the first condition may not hold exactly, and it may be assumed that the method when applied will give an average synthesis curve.

To take into account the inevitable spread of values due to experimental error, we have adopted a somewhat different method of plotting the histogram from that used previously [15]. The lowest and highest histogram intervals have been chosen with *average* DNA values of 2C and 4C respectively; the number of (equal) histogram intervals has been arbitrarily chosen as eight (Fig. 3). It is probable that most of the cells in the lowest histogram

group will have the 2C DNA value. The fractional number will of course depend on the relative values of the histogram interval chosen and the spread due to the random experimental errors. Hence, for most of the time deduced by theory from the fractional number of cells in the lowest group, the average cell will have the 2C value of DNA. The way in which DNA value and fractional time have been related will become apparent by examining Fig. 3 (and also [15]) which shows the results of five experiments together with the results of the P^{32} autoradiographic method of Howard and Pelc [8]. The time interval from prophase to telophase has been omitted in Fig. 3. The derived data depend somewhat on the choice of histogram interval.

The time intervals G_1, S and G_2 (Fig. 3) of the autoradiographic method are 12, 6 and 8 hours respectively, the accuracy of S and G_2 probably being about $\pm$ 1 hour. The interval G_1, however, is found by subtraction of S and G_2 from the total interphase time (given as 26 hours) which is subject to a larger uncertainty [13]. For example, if an interphase time of 20 hours is used [5], G_1 would be reduced to 6 hours. In practice G_1 probably lies somewhere between 6 and 12 hours. A reduction in G_1 would bring the autoradiographic results into closer agreement with that of the cytochemical method.

Our results on segment A indicate that DNA synthesis occurs during the middle third of interphase and takes about eight hours. These results differ from those of Grundmann and Marquardt [6], who claim that in the outer periblem cells of *Vicia faba*, synthesis is a continuous process beginning at telophase and ending at prophase. The disagreement appears to lie in the shape of the histogram, i.e. in the experimental data, rather than in the method used for deriving the synthesis curve from the histogram.

As has already been mentioned, in some preparations a wider spread of DNA values in the individual mitotic figures of one group (e.g. metaphase) was found than that illustrated in Fig. 2 or Table I. This, however, cannot be taken to imply that the DNA content of a single cell changes during mitosis; in such preparations there is no significant difference between the *average* values for each mitotic stage. The increased spread could be due either to true differences in the 2C and 4C values of DNA in the cells of the population, for example owing to variation in chromosome number, or to a non-proportionality between the measured amount of stain and the DNA content. Variations in stainability owing to position are unlikely, however, since closely adjacent mitotic figures show as large differences as widely separated ones. This variable behaviour is not peculiar to *Vicia faba* and has been observed in other plant roots [11]. An extreme example of the effect is found in the root cells of *Trillium grandiflorum*. In some, but not all roots of this

plant there is a very large spread of values outside the 2C and 4C range, as is illustrated in Fig. 4 which shows histograms of mitotic figures and a random sample of interphase nuclei. It may be noted that such variations are apparently not accompanied by abnormal chromosome numbers as shown by chromosome counts and hence imply variations in the amount of DNA per chromosome. These observations need elucidation.

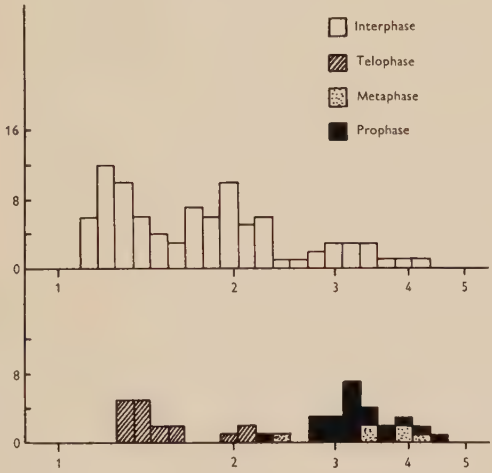

Fig. 4. Histograms of interphase and mitotic cells shown separately, but from the same root meristem of *Trillium grandiflorum*. Ordinates: cell number; abscissae, cellular DNA content in log. arb. units. It is not possible to assign a 2C or 4C value.

We consider that the increased spread of DNA values sometimes found in root cells of *Vicia faba* does not vitiate the general conclusions given in the summary.

DNA synthesis in the elongation segments

The biochemical results of Holmes *et al.* [7] have shown that between about three and twelve millimetres from the root tip there is a progressive increase in the average amount of DNA per cell (Table II). With some variation in the results obtained from different roots, the cytochemical results confirm this general average trend and yield further information as to how DNA increases in the cortex and central cylinder.

The cortical region.—In the cortical region of segment *D* the cells have completed the process of elongation and no mitotic figures are visible. All the DNA values are concentrated around the 4C and 8C values, with no intermediate values present, indicating that the synthesis of DNA is complete. Thus, in *Vicia faba* the differentiated cells of the cortex have at least the 4C value of DNA and in this respect the plant differs markedly from some other

plants studied (*Paris polyphylla, Fritillaria pallidiflora, Scilla campanulata, Scilla sibirica* and *Trillium grandiflorum*), in which the great majority of such differentiated cells have the 2C value of DNA [11]. Root hair cells, for example, in *Vicia faba* have the 4C value of DNA.

In the cortical regions of segment *B* and *C* a proportion of nuclei are present with DNA contents intermediate between the 2C, 4C and 8C values. The mitotic index in the cortex of segment *B* is low and in segment *C* is zero, so that these intermediate values are due mainly to cells which are synthesizing DNA up to the 4C (or 8C) value, but which will not divide again. According to Gray and Scholes [5], the process of root elongation takes approximately 20 hours, which is of the same order as the generation time for dividing cells.

To determine the rate of nuclear DNA synthesis in the elongation segments to an accuracy which approaches that for dividing cells, it would be necessary to study the progressive change in the shapes of histograms derived from a large number of (say) 0.5 mm serial sections throughout the elongating zone of the root. From the present data, therefore, it is not possible to decide whether there is any significant difference between the rate of synthesis for cells in the elongation segment and in the meristem and dividing cells, or whether that for cells in the elongation segments is dependent on distance from the root tip. It appears, however, that synthesis in the cells in the zone of elongation takes less than about 20 hours.

The central cylinder.—In the central cylinder there is a somewhat larger fraction of mitotic cells than in the cortex. The dividing cells in segment D are presumably associated with cambial activity (see [4]). Thus, although it can be seen (Fig. 2) that the DNA content of cells in the zone of elongation increases from the 2C to the 4C value without subsequent division, as in the meristem, it is not possible to compare the rate of increase with that in the cortex. It would appear that DNA values of 8C are more prevalent in the cortical cells in the fully elongated zone than in the cells of the central cylinder.

SUMMARY

The DNA content of individual cells in the root tip of *Vicia faba* has been measured by a cytochemical method. Roots were grown under standard conditions and divided into segments 0–2, 2–4, 4–8 and 12–20 mm behind the root cap, as in the biochemical experiments of Holmes *et al.* [7].

From the measurements on meristematic cells (0–2 mm) synthesis curves for DNA (from the 2C to the 4C value) are derived which are in broad

agreement with that found earlier by the P^{32} autoradiographic method [8]. Our results indicate that DNA synthesis occurs approximately during the middle third of interphase. Our results also indicate that there is negligible change in the total amount of DNA during the division of a cell.

Measurements of the average DNA content per cell in each segment show an increase with distance from the root tip similar to that found by the biochemical method [7]. Cells in the elongation zone of the root appear to synthesise DNA from the 2C to the 4C value and from the 4C to the 8C value, without subsequent cell division.

We would like to thank Professor J. T. Randall, F.R.S., for his continued encouragement, and Dr. B. E. Holmes, Miss L. Mee, Mrs. S. Hornsey and Dr. L. H. Gray for discussion. We are indebted to Mrs. S. Hornsey for supplying the roots. One of us (E. M. D.) receives a Fellowship from the Nuffield Foundation.

REFERENCES

1. Davies, H. G., Wilkins, M. H. F., and Boddy, R. G. H. B., *Exptl. Cell Research* **6**, 550 (1954).
2. Deeley, E. M., *J. Sci. Instr.* **32**, 263 (1955).
3. Deeley, E. M., Richards, B. M., Walker, P. M. B., and Davies, H. G., *Exptl. Cell Research*, **6**, 569 (1954).
4. Eames, A. J. and MacDaniels, L. H., An Introduction to Plant Anatomy. 2nd ed. Chap. X. McGraw-Hill, 1947.
5. Gray, L. H. and Scholes, M. E., *Brit. J. Radiol.* **XXIV**, 82 (1956).
6. Grundmann, E. and Marquardt, H., *Chromosoma* **6**, 115 (1953).
7. Holmes, B. E., Mee, L. K., Hornsey, S., and Gray, L. H., *Exptl. Cell Research* **8**, 101 (1955).
8. Howard, A. and Pelc, S. R., *Heredity* **6**, 261 (1953).
9. —— *Exptl. Cell Research* **2**, 178 (1951).
10. Jensen, W. A., *Exptl. Cell Research* **8**, 506 (1955).
11. La Cour, L. F., Deeley, E. M., and Chayen, J., unpublished.
12. Patau, K. and Swift, H., *Chromosoma* **6**, 149 (1953).
13. Pelc, S. R., private communication.
14. Swift, H. H., *Physiol. Zool.* **23**, 169 (1950).
15. Walker, P. M. B., *J. Exptl. Biol.* **31**, 8 (1954).
16. Walker, P. M. B. and Yates, H. B., *Proc. Roy. Soc. B* **140**, 274 (1952).

Experimental Cell Research **12**, *592–598 (1957)*

DETERMINATION OF STRONTIUM AND CALCIUM IN BONE BY X-RAY ABSORPTIOMETRY

A. ENGSTRÖM, C. LAGERGREN and B. LUNDBERG

Department of Medical Physics, Karolinska Institutet, Stockholm, Sweden

Received November 15, 1956

The characteristic absorption edges in the X-ray absorption spectrum of the elements can be utilized for quantitative elementary analysis. This X-absorptiometric technique was developed on the ultramicroscale by Engström 1946 [2] (see also [3]) in such a way that two X-ray microradiograms were recorded with monochromatic X-rays of wavelengths situated on the top and at the bottom of the absorption discontinuity. Photometry of corresponding points in these images made it possible to calculate the amounts of the element present. The total amounts determined in this way are in the order of 10^{-10}–10^{-12} g (ultramicroscale), but the technique is complicated and time-consuming. In our current studies of bone tissue, it has appeared of great interest to determine the amounts of strontium and calcium in this type of tissue on the microscale (10^{-3}–10^{-6} g). It seems possible that X-ray absorptiometry could be adopted with advantage to the solution of these problems, which are of considerable importance in connection with the osseous metabolism of strontium, one of the main fission products in nuclear reactions for military and peaceful purposes.

Two types of X-ray absorptiometry for studying the amounts of calcium and strontium in bone specimen will be described in this paper. The possibilities to use X-ray crystallographic and X-ray fluorometric procedures for this type of analysis will be reported later. Also, the application of the point focus X-ray tube for the elementary analysis of bone tissue will be described separately.

Theory of Analysis of Strontium and Calcium in Bone by X-Ray Absorptiometry

The mass absorption coefficient $(\mu/\varrho)_m$ of a composite sample can be written

$$\left(\frac{\mu}{\varrho}\right)_m = W_A \left(\frac{\mu}{\varrho}\right)_A + W_r \left(\frac{\mu}{\varrho}\right)_r , \qquad (1)$$

where W denotes weight fraction, and the subscripts m, A and r denote the mixture of elements in the sample, element A to be determined and r the remaining elements in the specimen. In general the intensity of an X-ray beam I transmitted can be written

$$I = I_0 \cdot e^{-(\frac{\mu}{\varrho})_m \varrho_m t}, \tag{2}$$

where I_0 is the incident X-ray energy and m and t the specific gravity and thickness of the specimen. For two wavelengths situated on either side and close to the absorption edge, we can write [1, 2, 3]

$$I_1 = I_0 \cdot e^{-[W_A (\frac{\mu}{\varrho})_{A_1} + W_r (\frac{\mu}{\varrho})_r] \varrho_m t}, \tag{3a}$$

$$I_2 = I_0 \cdot e^{-[W_A (\frac{\mu}{\varrho})_{A_2} + W_r (\frac{\mu}{\varrho})_r] \varrho_m t}, \tag{3b}$$

where A_1 and A_2 are the subscripts for the mass absorption coefficients of element A on the short and long wavelength side of and close to the edge.

Thus we obtain

$$\frac{I_2}{I_1} = e^{W_A \varrho_m t [(\frac{\mu}{\varrho})_{A_1} - (\frac{\mu}{\varrho})_{A_2}]}. \tag{4}$$

If the difference between the mass absorption coefficients $(\mu/\varrho)_{A_1} - (\mu/\varrho)_{A_2}$ is denoted K_A and $\varrho_m t = M_m$, we get

$$\log_e \frac{I_2}{I_1} = W_A \cdot M_m \cdot K_A. \tag{5}$$

M_m varies with W_A for samples of constant thickness and we get

$$W_A \cdot M_m = M_A,$$

M_A being the mass of element per unit area of sample. In this connection it is of interest to consider what thickness of absorber ought to be used in order to obtain a maximum intensity difference of the absorption edge, when the intensity of the radiation incident to the absorber is kept constant. The intensity difference S can be written

$$S = I_0 \left[e^{-(\frac{\mu}{\varrho})_{A_2} \varrho t} - e^{-(\frac{\mu}{\varrho})_{A_1} \varrho t} \right] \tag{7}$$

which has a maximum for

$$t = \frac{\log_e \mu_{A_1} - \log_e \mu_{A_2}}{\mu_{A_1} - \mu_{A_2}}, \tag{8}$$

where μ denotes the linear absorption coefficients, $(\mu/\varrho)\,\varrho = \mu$.

It should be noted that this calculation considers a finite value of I_0 corresponding to a certain value of the density of the photographic emulsion. The calculation thus refers to the possibility of *measuring* I_0, either by photometry of photographic emulsion or direct X-ray intensity measurements. It is obvious that for the visual contrast between the two X-ray wavelengths maximum contrast is obtained at infinite sample thickness, but in this case no quantitative estimation is possible as I_0 is infinitely large in such a case.

Determination of Strontium

A Philips stabilized high voltage X-ray source PW 1010 was used in connection with a precision goniometer type PW 1050. A calcite crystal was inserted at the position, where the powder sample is normally placed (Fig. 1). The sample, which was a powder of calcium and strontium apatite with known composition, was placed immediately in front of the entrance slit to the Geiger counter. The crystal and sample was moved, so that the continuous spectrum from the X-ray tube covered the absorption edge for

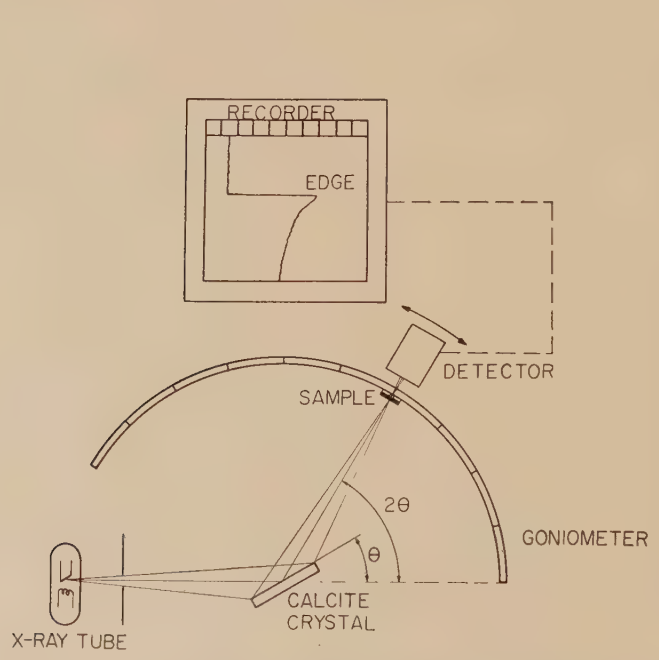

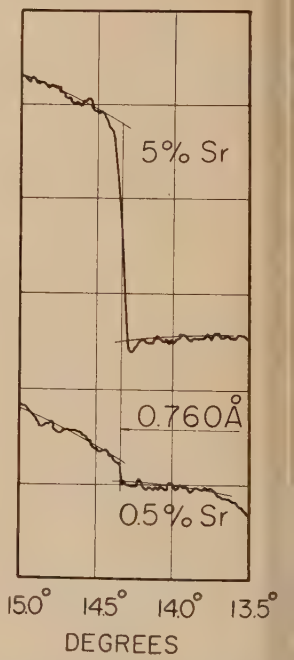

Fig. 1 (left). Principle of elementary analysis by absorption using the X-ray diffractometer.
Fig. 2 (right). K-absorption edges of strontium in strontiumapatite mixed with hydroxylapatite.

strontium. The K-absorption edge for strontium has the wavelength 0.760 Å. The results of this type of analysis are shown in Fig. 2, where two curves have been recorded across the K-absorption edge for strontium in samples containing 5 per cent and 0.5 per cent strontium in a 0.5 mm thick layer over an area of a few mm². It appears that the method is capable of detecting and measuring as small amounts of strontium in bone as a few tenths of a

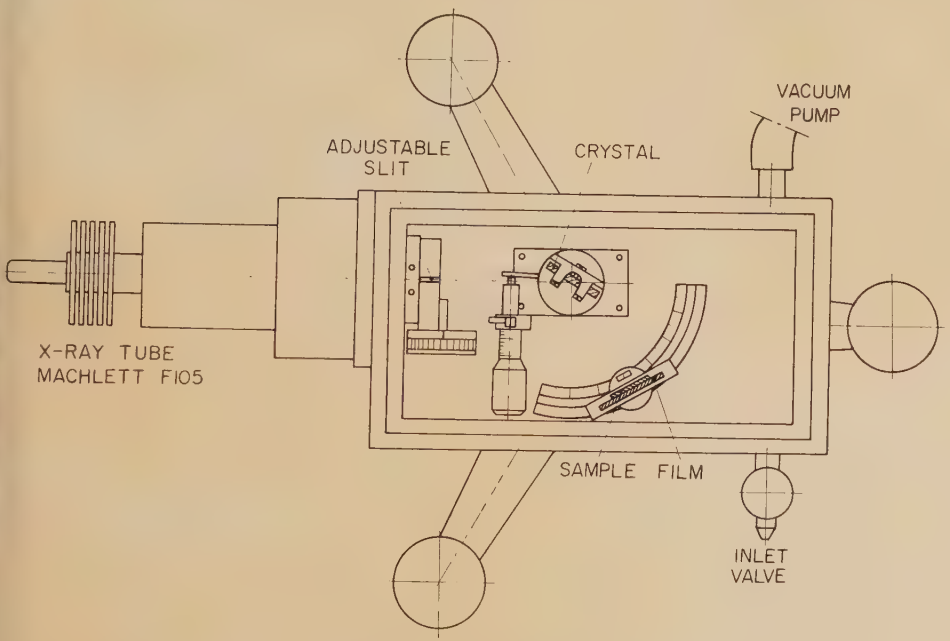

Fig. 3. Equipment for microradiography with a dispersed, continuous X-ray spectrum.

per cent in about 1 mm thick layers. The total mass, therefore, which is analyzed, is relatively large (about 10^{-5} g). Consequently, for the determinations of extremely small total amounts other types of equipment have to be used.

Determination of Calcium in Thin Bone Specimen

The same type of equipment as described in Fig. 1 can also be used for determination of calcium in an intact bone specimen. However, in order to reduce the area measured, another principle was adopted, and Fig. 3 shows schematically this type of analytical procedure. A continuous X-ray spectrum is generated in a small X-ray tube (Machlett Type F 105) with a tungsten

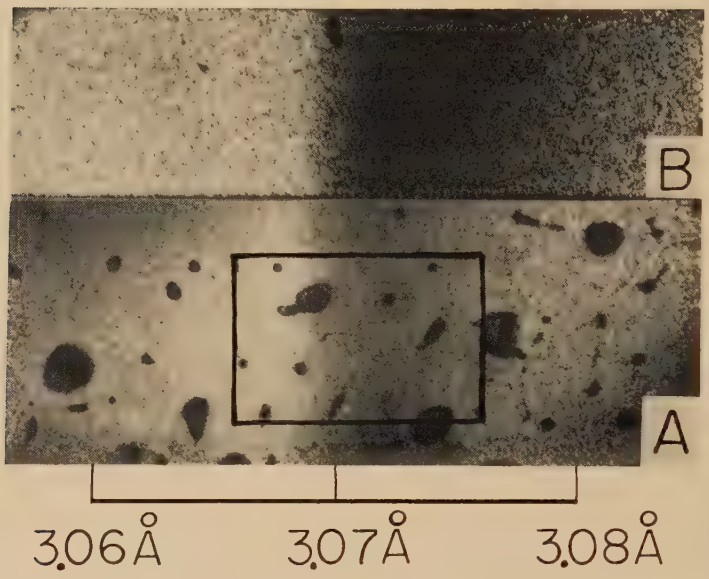

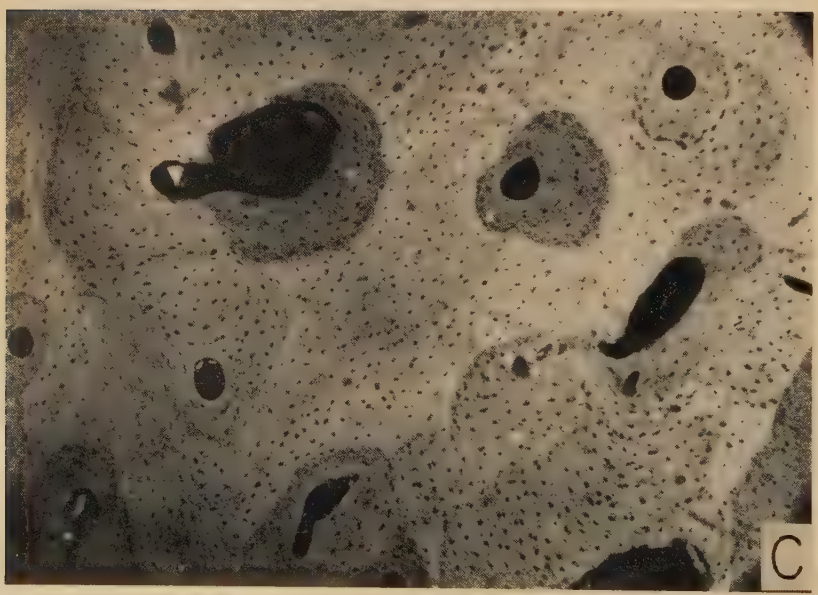

Fig. 4. (*A*) and (*B*). Absorption discontinuities produced by a 50 μ thick section of bone and a thin leaflet of gypsum. Mag. × 24. (*C*) Microradiogram of the enclosed area in *A* showing the evenness of specimen. The difference in mineralization is clearly seen. Mag. × 80.

target. A rock salt crystal is adjusted in such a way, that a small portion of the continuous X-ray spectrum is reflected. This small wavelength range is chosen to cover the K-absorption edge of calcium, which has the wavelength 3.070 Å. Thus a microradiogram of the thin bone specimen is taken with this radiation projected through the specimen. In the image of the specimen, there will appear a discontinuity due to the effect of the absorption edge. Photometry across this discontinuity will give the amounts of calcium present. Fig. 4, *A* and *B*, shows two such microradiograms taken with a dispersed, continuous spectrum covering the K-absorption edge of calcium. Fig. 4*B* shows a thin section of a gypsum crystal and Fig. 4*A* a 50 micron thick specimen of bone tissue. The area in the bone tissue indicated by a square is shown in Fig. 4*C*. This picture was registered directly with the total radiation from the tube and was taken under conditions for maximum contrast, to be able to detect small differences in mineralization. The suitable potential V in volts over the X-ray tube for this type of microradiography can be calculated from Eq. (8) which can be written

$$V \cong 5 \times 10^4 \cdot \sqrt[3]{\varrho \cdot t}, \qquad (9)$$

where t is the thickness in cm and ϱ its weight per unit volume ($g \times cm^{-3}$). For a 50 μ thick section of a fully mineralized tissue ($\varrho = 2$) the voltage is ~ 10 kV.

Fig. 4*C* shows the general distribution of the total amount of mineral salts and the pictures taken with spectrally dispersed radiation allows the quantitative estimation of *calcium* within the various structures. Thus by this technique small amounts of elements can be determined within an area of about 0.1 mm^2 and in the actual case not more than 10^{-3} milligrams of calcium were determined, within a localized structure. It appears that this technique is capable of measuring as small amounts of calcium as 10^{-5} milligrams.

SUMMARY

The use of the X-ray diffractometer for the determination of Sr in the presence of Ca is described. The X-ray absorptiometric technique permits the determination of as small concentrations of Sr as a few tenths of a per cent. A method for microradiography with a dispersed, continuous spectrum covering the absorption edge has been developed and 10^{-6}–10^{-8} g of Ca can readily be determined.

This work has been performed under contract AF 61 (514)-861, European Office, Air Research and Development Command, U.S. Air Force.

REFERENCES

1. Cullity, B. D., Elements of X-ray diffraction. Addison-Wesley Publ., Mass., 1956.
2. Engström, A., *Acta Radiol. Suppl.* **63**, Stockholm, 1946.
3. Lindström, B., *Acta Radiol. Suppl.* **125**, Stockholm, 1955.

NUCLEAR SWELLING IN *ASTERIAS* EGGS AND ITS RELATION TO THE PASSAGE OF MATERIALS INTO AND OUT OF NUCLEI[1]

ALFRED MARSHAK[2]

Marine Biological Laboratory, Woods Hole, Mass., U.S.A.

Received November 19, 1957

The manner in which the movement of substances through the nuclear surface is controlled is of obvious importance in relation to the problem of the genic control of cellular reactions, but the existing experimental evidence on the nature of the controlling mechanism is meager and some of the conclusions which have been reached appear to be conflicting. A series of investigations have shown that under some conditions the nucleus behaves like a simple osmometer [4, 5, 6, 8, 24]. On the other hand, experiments with radioactive tracers have shown that relatively large molecules such as ribonucleic acid may pass from the nucleus to the cytoplasm [16–20] and that desoxyribonucleic acid may pass from the cytoplasm to the nucleus [21]. It has been reported that substances other than nucleic acids of molecular weight as great as 700,000 will enter into the interior of isolated nuclei and this observation has been taken as evidence that the nuclear envelope is freely permeable to large molecules [2]. The possibility which suggests itself is that isolated nuclei may behave differently from those left *in situ*. That this is the case is demonstrated by the experiments to be described. They also provide evidence that the movement of some kinds of molecules into the nucleus of the *Asterias* egg is controlled not by the nuclear membrane alone but by some mechanism which requires the combined activity of the nuclear surface and the contiguous cytoplasm.

METHODS

Each lobe of the gonad of a ripe female *Asterias* was cut into sections approximately 1 cm long while still in the body cavity. Each section was then rinsed in 50

[1] Supported by a grant from the American Cancer Society. A preliminary abstract of some of this work has been published [15].

[2] With the assistance of Robert Marcus.

ml of the solution to be tested and then placed in another beaker containing 50 ml of the same solution which was gently stirred with a glass rod. After 5–10 minutes an aliquot of the suspension of cells and nuclei released from the ovary was put on a slide with a concave polished depression and enclosed with a coverslip. At recorded time intervals measurements were taken of the diameters of 10–25 cells and their included nuclei and of a comparable number of extruded nuclei. Measurements were made with an ocular micrometer at a magnification such that one division on the micrometer scale was equivalent to 7.14 μ except in those experiments in which the pH of the test solutions was varied. In the latter experiments the magnification was such that one micrometer scale division was equal to 11.0 μ. Two sets of measurements were taken, one at 0.5–1.0 hours after immersion of the gonad and the other after 4–5 hours. Measurements made at the end of the experimental period were compared with measurements on eggs which had remained in the beakers. There were no significant differences between the cells and nuclei taken from the beakers and those which had been in the depression slides. In the case of the butane tetrol solutions, appreciable amounts of an unidentified crystalline compound were found to have been deposited by sublimation onto the walls of the beakers and the surfaces of the slides after two hours. With this compound, therefore, observations were not extended beyond two hours. This sublimation did not occur with distilled water solutions of the butane tetrol or with such solutions to which fresh rat liver slices had been added. The nature of the reaction involved has not been determined. As controls in all experiments, sections of the lobes of the gonad of the same experimental animals were placed in filtered sea water, were handled in the same way, and measurements of the nuclear and cell diameters taken each time the eggs in the test solutions were examined. There were no detectible changes in the control cells in sea water during the experimental periods other than the breakdown of the germinal vesicle which occurs normally in a variable percentage of these eggs when they are immersed in sea water. Except where indicated, all of the compounds tested were in solution in distilled water which had not been made carbonate-free. The pH of these unbuffered solutions as measured with a glass electrode was in the range 5.5–6.0. All observations were made at room temperature which varied from 23°C to 27°C. In the experiments on the rate of swelling of cells and nuclei, the temperature variation in the course of each experiment was less than 2°C. The standard errors of the nuclear diameters fell in the range 0.02–0.13 micrometer units, the larger values being obtained in those solutions in which the nuclei showed maximal swelling. In the study of nuclear swelling in glycerol solutions as a function of pH, the individual standard errors are given in Table III.

Fig. 3.—Egg in 0.9 *M* 1,2-ethane diol (ethylene glycol) after 3 hours. Note concavity in cytoplasm separated from nuclear surface. Photomicrograph in phase contrast without fixation.
Fig. 4—Eggs in sea water in depression on microscope slide. Taken after 6 hours in this solution near the periphery of the depression. Note vacuoles and unswollen nuclei. In some cells the nucleus is above or below the vacuole and cannot be distinguished in the photograph. Photomicrograph in phase contrast without fixation.

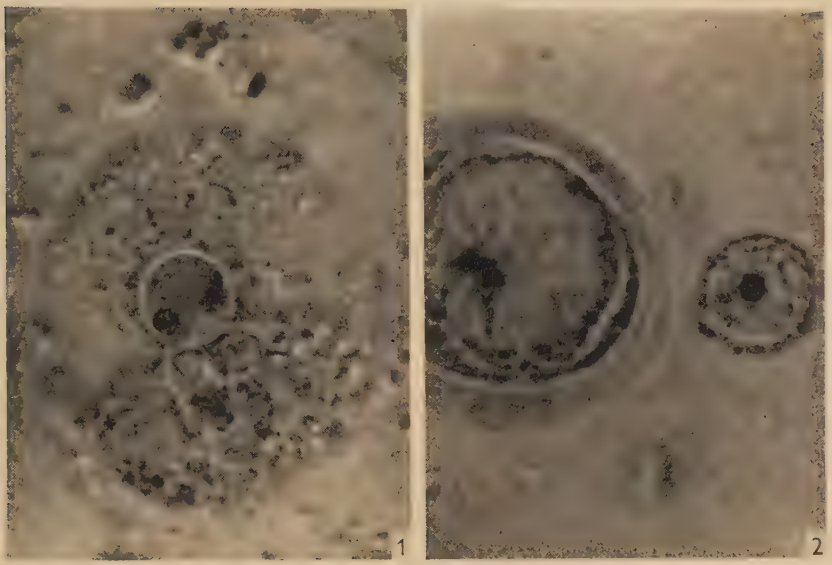

Fig. 1.—Egg swollen in distilled water. The nucleus which is not swollen is in focus. The cell boundary which is not in focus extends beyond the boundaries of this photograph. Photomicrograph in phase contrast of unfixed cell.
Fig. 2.—Egg in 4.8 *M* 1,2,3-propane triol (glycerol) after 5 hours. At the left is a cell with a much swollen nucleus. Most of the cell is out of focus. At the right is a free nucleus which is not swollen. Photomicrograph in phase contrast without fixation.

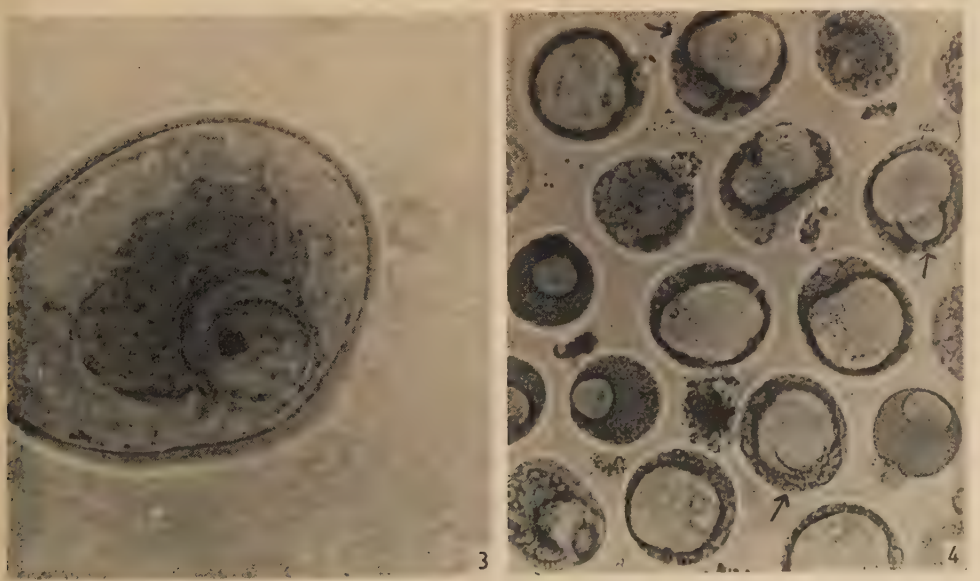

TABLE I

Swelling in hypotonic sucrose and glycerol solutions.

Diameters in ocular micrometer units after 0.5–1.0 hours.

	Sucrose			Glycerol		
M	Cell	Ni	No	Cell	Ni	No
0	43.0	10.2	9.3	49.8	10.1	9.7
0.1	39.6	10.5	10.6	47.9	9.3	8.7
0.15	41.5	10.2	9.7	56.8	9.4	9.0
0.2	34.1	9.9	9.6	49.0	9.5	9.0
0.25	40.2	10.1	9.9	40.7	9.5	8.7
0.35	42.2	10.7	10.4	41.7	8.5	9.3
0.5	36.5	9.9	9.8	36.4	10.2	10.7
Sea	20.8	9.3		21.0	9.1	

M = Molar concentration. Ni = Nuclei inside cells. No = Nuclei outside cells having no attached cytoplasm.

Each value is the mean of measurements on 10 cells or nuclei. One ocular micrometer unit = 7.14 μ.

RESULTS

Hypotonic Solutions

By the methods just described, cells were suspended in distilled water and in a series of solutions of sucrose and of glycerol at concentrations of 0.1, 0.15, 0.2, 0.25, 0.35, and 0.5 molar. In all of these solutions there was prompt and marked increase in the diameters of the cells. Many nuclei were found to have been extruded from the cells and were "clean" in the sense that they usually did not have microscopically visible portions of the cytoplasm to their surfaces. Ten to twenty-five cells and a similar number of extruded and retained nuclei were measured in each case. The mean diameters of both the free and the intracellular nuclei when measured at 0.5–1.0 hours after immersion were either slightly greater than those of the controls, i.e., on the borderline of statistical significance, or the same as the controls. Table I shows the data obtained at 0.5–1.0 hours. Those obtained at 4–5 hours are omitted since they are no different from those of the earlier period.

Isotonic and Hypertonic Solutions

Cell response.—Distilled water solutions of the following compounds were used: 1,2-ethane diol (glycol), 1,2-propane diol (propylene glycol), 1,3-propane diol (trimethylene glycol), 1,2,3-propane triol (glycerol), 1,2,3,4-butane tetrol (erythritol), and sucrose. The concentrations used were 0.75,

0.9, 1.0, 1.5, 2.0, 2.5, 3.0, 3.5, 4.0, 4.8, and 5.0 molar with the exception of erythritol where the maximum concentration was 4.0 molar and sucrose for which the maximum was 2.5 molar. At the 1 molar concentration of the triol, the tetrol and of the sucrose there was no change in the cell diameter, during the first 0.5–2.0 hours. In the solutions at the higher as well as lower concentrations of these compounds there was significant cellular swelling with the exception of the sucrose and the tetrol solutions where no change was observed at concentrations as low as 0.75 *M*. From these results as well as those of previous investigators it was concluded that the osmotic pressure of these cells is equivalent approximately to a one-molar solution of a non electrolyte. The possible significance of the difference in behavior toward the triol where there was pronounced swelling at 0.75 and 0.9 *M* and the tetrol and the sucrose, where no swelling occurred at these concentrations, was not investigated.

The propane diols produced prompt cellular swelling at all concentrations from 0.75 to 5.0 molar, the maximum cell enlargement being found at 1 molar. Similar enlargement was found in all of the ethane diol solutions in this range of concentrations with the exception of the 1.0 and 1.5 molar solutions where almost all of the cells were found to have been denuded of both the vitelline and plasma membranes and no cellular swelling was found. From these results it seems evident that the permeability or solvent action or both of the diols differs from that of the triol and the tetrol.

Nuclear Response

Extrusion.—In the hypotonic solutions of all of the polyhydric alcohols tested and in the hypotonic sucrose solutions, nuclei were extruded from a considerable proportion of the cells. In some cases (0.5 *M* and 0.75 *M* 1,2-propane diol) extrusion of nuclei was so common that only about 5 per cent of the treated cells were found to have retained their nuclei.

In some of the hypertonic solutions extrusion of nuclei was common but in others occurred very infrequently or not at all. In the ethane diol and the 1,2-propane diol solutions, nuclear extrusion was frequent in the isotonic and all of the hypertonic solutions. However, in the 1,3-propane diol solutions, nuclear extrusion was infrequent ($< 5/200$) at concentrations greater than 2.0 *M*, while in the 1,2,3-propane triol solutions this infrequency of extrusion was found in the lower concentration range (0.9–2.5 *M*). Extrusion was infrequent in the isotonic and all of the hypertonic solutions of the tetrol and of sucrose. The significance of these differences in response to concentration and molecular configuration are not known. However, it should be

noted that with respect to nuclear extrusion the response to 1,3-propane diol differed from that toward the other two diols, a difference which was also found in the study of nuclear swelling to be described, but was not found in the cellular swelling.

Loss of the cell membrane did not necessarily result in liberation of the nuclei. In some solutions such as 0.5 *M* ethane diol, where the cells characteristically lost their membranes, very few nuclei were extruded.

The nuclear extrusion process was followed microscopically in hypotonic sucrose solutions (0.25 *M* and 0.34 *M*) and in hypertonic propane triol solutions (1.5 *M* and 4.8 *M*). In both types of solutions the sequence of visually observed events was similar. At first the appearance of the cells was indistinguishable from those in sea water. Then a clear vesicle appeared beneath the cell membrane after which a wave of vesiculation travelled rapidly beneath the membrane and throughout the cytoplasm. While these changes were taking place the nucleus frequently moved to the periphery of the cell, coming to lie beneath the cell membrane. Where extrusion occurred, the cell membrane ruptured and the nucleus along with some of the cytoplasm streamed out of the cell through the opening formed.

Swelling

Although in the hypotonic solutions and in distilled water, the cells were markedly swollen there was very little or no swelling of the nuclei (Fig. 1). In some of the hypertonic solutions, however, pronounced nuclear swelling did occur (Fig. 2). However, in these solutions only those nuclei which remained in contact with the cytoplasm became enlarged, the free nuclei did not. This observation was made repeatedly and no exceptions were found. Frequently in the 3.5–4.8 *M* triol solutions, nuclei were found with $\frac{1}{2}$–$\frac{3}{4}$ of the nuclear surface free, the cytoplasm being still attached to the remainder. These nuclei were seen to swell although nuclei in the same solutions with no cytoplasm attached did not swell. In experiments to be described in a subsequent section of this paper nuclei attached to cytoplasm and those completely free were observed continuously in the same microscope field and in no case did the free nuclei swell.

Table II gives the mean nuclear diameters in ocular micrometer scale units of intracellular nuclei at 0.5–1.0 hours and 4–5 hours after immersion in the test solutions. The data on the extracellular nuclei are omitted from Table II for the sake of clarity. In no case did the mean diameter of these nuclei exceed the diameter of the nuclei in the control cells.

None of the ethane diol or 1,2-propane diol solutions produced nuclear

TABLE II

Swelling of nuclei in polyhydric alcohol and sucrose solutions.[1]

0.5–1.0 hours						4–5 hours				
1,2-thane diol	1,2-Propane diol	1,3-Propane diol	1,2,3-Propane triol	1,2,3,4-Butane tetrol	Sucrose	1,2-Ethane diol	1,2-Propane diol	1,3-Propane diol	1,2,3-Propane triol	Sucrose
9.5	8.8	8.6	10.8	10.4	9.2	9.0	8.3	7.7	9.8	9.0
9.4	8.9	10.1	9.6	—	8.8	8.9	9.0	8.0	9.7	8.5
9.0	9.4	13.3	9.2	10.2	9.1	8.7	9.1	11.3	7.7	13.0
8.5	9.4	11.9	9.0	9.7	11.7	8.9	9.3	9.3	7.9	15.8
8.8	9.0	9.6	9.0	9.7	10.6	9.1	9.0	7.8	8.6	13.3
9.6	10.0	7.4	8.5	13.6	9.5	8.5	9.2	7.5	9.3	9.7
9.0	—	8.9	10.2	13.6	—	8.6	—	6.9	11.3	—
8.9	9.7	7.6	15.7	14.9	—	8.9	9.2	6.7	17.7	—
9.4	9.8	—[3]	15.0	14.2	—	8.5	9.6	—[3]	18.2	—
8.6	9.3	—[3]	16.1	—	—	8.6	7.7	—[3]	19.6	—
9.1	8.0	—[3]	13.7	—	—	8.3	8.6	—[3]	14.4	—
9.5	9.4	9.9	9.3	10.2	9.4	9.6	9.4	9.8	9.2	9.6

[1] The measurements are of nuclear diameters in ocular micrometer scale units. One micrometer scale unit is equal to 7.14 μ. Each value in the table is the mean of 12–25 measurements.
[2] M = Molar concentration.
[3] Nuclei were not discernible in the coagulated cytoplasm.

enlargement. In the 1,3-propane diol solutions there was significant swelling at 1.0–1.5 M but the swelling did not continue after the first hour. In some of the 1,3-propane diol solutions the mean diameter of the intracellular nuclei was significantly reduced. In the sucrose solutions there was slight swelling at 1.5–2.0 M during the first hour which became more pronounced after four hours. In the triol and tetrol solutions the swelling was both prompt and progressive in the sense that the mean nuclear diameters continued to increase after the first hour and in the triol solutions reached maximal values at 4–5 hours after immersion. In the triol solutions nuclear swelling was found at concentrations greater than 3 M while in the tetrol swelling began at 2.5 M. In those triol solutions where nuclear swelling did occur, 5–10 per cent of the cells contained nuclei which remained unswollen even after 5 hours. This phenomenon will be treated in more detail in a subsequent section of this paper.

The cells treated with the hypertonic ethane diol solutions characteristically had a cytoplasmic coagulum containing a large concavity in which the nucleus rested, but the walls of the nucleus were separated from the walls

of the concavity by a considerable distance (Fig. 3). This condition was also found in the other diol and triol solutions in those cells where nuclear swelling did not occur. It is mentioned because of its possible relation to the conclusion to be made on other evidence that nuclear swelling is dependent upon the maintenance of the integrity of a mechanism involving the nuclear and cytoplasmic interfaces at least over a portion of the nuclear surface.

Rates of Swelling

To determine the rate of swelling of cells and nuclei in 4.8 *M* glycerol, gonads were cut into 1 cm pieces in the test solution which was then briefly stirred and aliquots of the suspension of liberated cells and nuclei transferred to depression slides. Before beginning measurements, an area on the slide was located which contained a cell denuded of its plasma and vitelline membranes. Measurements were then made on this and on adjacent cells which had retained their membranes, and also on nearby free nuclei which had been ejected from their cells. The first measurement in all cases was made 3–6 minutes after immersion of the gonad and measurements on the same cells and nuclei were repeated at recorded intervals of 3–5 minutes.

None of the 10 free nuclei in this series showed any increase in size. All of the 4 nuclei of the denuded cells increased in size to an extent as great as that of the nuclei in the cells which had retained their membranes. An example of the increase in nuclear volume as a function of time is given in Fig. 5. The values plotted are $V_x - V_0$, where V_0 is the mean volume of the nuclei of control cells in sea water and V_x is the nuclear volume in the test solution at any given time. The curve, which was fitted graphically, shows an approximately linear increase in volume with time. Six of the nuclei gave data which fitted straight lines during the entire experimental period as in Fig. 5. In two there was deviation from a straight line at 30 minutes and in 5 at 15 minutes. Similar curves were plotted for cell volumes as a function of time. Of the 9 such curves obtained, none were straight lines throughout the entire period of examination. However, they were in all instances straight lines for the first 20 minutes.

The mean increase in cell volume calculated from the slopes of the linear portions of the curves was $15.2 \pm 1.3 \times 10^4$ μ^3/minute. The mean increase in nuclear volume similarly calculated was $18.0 \pm 1.5 \times 10^3$ μ^3/minute. If the surface areas of the cells and nuclei at the beginning of the experiment are used in the computation, the calculated rates of increase per unit surface area obtained are 2.2 μ^3/μ^2/minute for the cells and 1.2 μ^3/μ^2/minute for the nuclei. Making the computation using the mean surface area attained at 20 minutes,

the rate of increment for cells is 0.8 μ^3/μ^2/minute and for nuclei 0.5 μ^3/μ^2/minute. Thus the true rate lies between 0.8–2.2 μ^3/μ^2/minute for the cells and 0.5–1.0 μ^3/μ^2/minute for the nuclei.

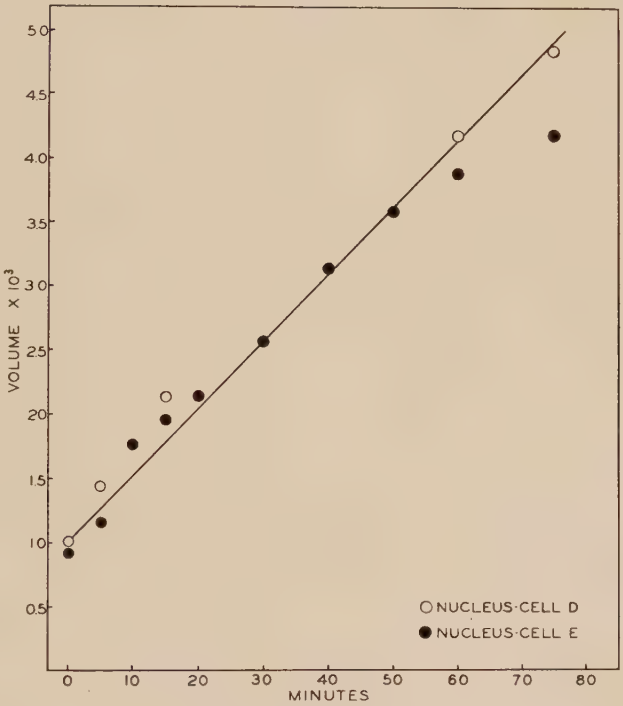

Fig. 5.—Nuclear volume as a function of time in 4.8 *M* 1,2,3-propane triol. Two nuclei showing approximately linear volume increase during the first 60–70 minutes. Zero minutes on the abscissa is 3 minutes after immersion of the gonad into the solution.

Four of the 13 cells in this series had lost their membranes and none of these showed any increase in the volume of the cytoplasm. The cytoplasm of the remaining 9 increased markedly in volume. The cytoplasmic volume increment was greater than the volume increment of the nuclei of the corresponding cells.

The increment in cytoplasmic volume (I_{cy}) was computed from the increments obtained for each cell (I_c) and its nucleus (I_n):—

$$I_{cy} = I_c - I_n.$$

The absolute volume increments of nuclei and cytoplasts were then converted to relative volume increments, (V_r):—

$$V_r = \frac{V_f}{V_i},$$

where V_f is the volume at the end of 75 minutes and V_i is the initial volume.

TABLE III

Nuclear swelling in 4.8 M glycerol as a function of pH.

Solution	$\bar{d}$	$\sigma_{\bar{d}}$	n	% $d \leq 6.5$	% $d = 7$–9
Sea water	*5.84*	*0.081*	*24*	*100.0*	
4.8 *M* glycerol	10.86	0.322	51	9.8	11.8
(no buffer)	*9.90*	*0.341*	*21*	*7.7*	*23.0*
4.8 *M* glycerol					
pH 6.92–6.85	10.21	0.507	46	17.4	26.1
7.00–6.85	*10.66*	*0.260*	*50*	*4.0*	*18.0*
7.10–7.05	8.72	0.392	55	25.4	38.2
7.15–7.00	*8.74*	*0.321*	*50*	*22.0*	*36.0*
7.35–7.30	8.20	0.367	63	44.4	22.2
7.38–7.32	*7.79*	*0.343*	*50*	*48.0*	*30.0*
7.49–7.45	*12.32*	*0.409*	*51*	*5.9*	*11.8*
7.61–7.60	*12.70*	*0.380*	*47*	*6.4*	*10.6*
7.76–7.71	*11.05*	*0.411*	*50*	*18.0*	*8.0*
7.80–7.76	*9.54*	*0.519*	*41*	*26.8*	*26.8*
8.00–7.95	*8.95*	*0.500*	*50*	*36.0*	*20.0*

$\bar{d}$ = nuclear diameter in micrometer scale units after 5–7 hours. One unit = 11.0 μ.
$\sigma_{\bar{d}}$ = standard error of the mean diameter.
n = number of measurements.
pH = reading with a glass electrode pH-meter. The first value is that obtained immediately after the cells were immersed and the second is that obtained at the end of the experiment.

The mean cytoplasmic relative volume increment, excluding the 4 denuded cells was 2.1 ± 0.2 and that for the nuclei was 5.0 ± 0.4. In other words, while the cytoplasmic volume was approximately doubled the nuclear volume was augmented on the average by a factor of 5. In each cell examined the relative nuclear increment was greater than that of the cytoplasm.

Nuclear Swelling in Relation to pH

Because the nuclei swelled when the cells were immersed in solutions which were strongly hypertonic, it seemed unlikely that the phenomenon observed was due to osmosis. To explore the problem further nuclear swelling was measured in buffered solutions of 4.8 *M* glycerol. As mentioned previously the unbuffered solutions had a pH of approximately 5–6 as measured with a glass electrode. When the pH was adjusted to values lower than this the nuclei coagulated. At pH 8.0 and higher there were visible indications of dissolution of nuclear as well as cytoplasmic constituents. In the range pH 7.0–7.4,

0.06 *M* MacIlvaine's buffer was used. In the range pH 7.5–7.8, the buffer was 0.03 *M* veronal and at pH 8.00 the buffer was 0.06 *M* veronal. It should be emphasized that the term pH as it is used here refers only to the value obtained when the solutions were measured with a glass electrode and not to the actual concentration of hydrogen ions in these solutions. These values are considered adequate for the comparative use made of them. Since previous experiments showed that nuclear swelling reached a maximum by 5 hours after treatment all measurements were made at 5–7 hours after immersion in the test solutions.

As shown in Table III there was marked variation in the mean nuclear diameter with pH. The mean nuclear diameter decreased to a minimum at pH 7.38–7.30 and then rose again sharply at pH 7.49–7.45 and then fell off again at pH 7.8. The difference between the mean at pH 7.38–7.30 and that at pH 7.49–7.45 was about 8 times its standard deviation and was clearly significant statistically. The difference between the mean at pH 7.15–7.00 and that at pH 7.38–7.30 was only 1.3 times its standard deviation and hence may not be significant statistically. However, the consistency in the values obtained in duplicate determinations suggests that the differences in the means was nevertheless real. A more striking index of the response to variation of the pH than the mean nuclear diameter was the percentage of nuclei whose diameters remained the same as those of the controls in sea water (Table II, column 5). This percentage rose from about 10 in the unbuffered glycerol solution to a maximum of about 45 at pH 7.38–7.30 and then fell off again very sharply. Both these criteria agree in indicating a sharp turning point at pH 7.38–7.30. The increase in the percentage of nuclei which failed to swell in solutions with pH greater than 7.8 is probably related to the dissolution of nuclear and cytoplasmic constituents detected visually in this pH range and should for this reason be differentiated from the failure to swell in the solutions buffered at about pH 7.4.

DISCUSSION

Previous investigators have reported that the contents of *Asterias* and *Arbacia* eggs have an osmotic pressure of 22–23 atmosphers or the equivalent of a 0.9–1.0 molar solution of a non-electrolyte [4, 8, 10, 12, 13, 22]. In the present experiments 0.9–1.0 molar solutions of glycerol, erythritol, and sucrose were found to be isosmotic with the *Asterias* eggs. Solutions of the ethane and propane diols at these concentrations produced early dissolution or swelling of cytoplasmic constituents of the *Asterias* eggs. These observa-

tions suggest a rapid penetration into the cytoplasm by the diols and a slow penetration or failure to penetrate by the triol, the tetrol, or the sucrose at this concentration. The difference in cellular response to 1,3-propane diol and 1,2,3-propane triol is surprising because of the similarity in both the dimensions and chemical properties of these two compounds. Previous investigators have reported that glucose does not penetrate the *Arbacia* egg and that with reference to the rate of penetration the polyhydric alcohols may be placed in the following order, ethylene glycol > propylene glycol > glycerol [10, 14].

With respect to the response of the nuclei, the 1,3-propane diol differed both from the two diols and the triol and tetrol. The 1,2-diols produced no nuclear swelling, the triol and tetrol produced nuclear swelling only at concentrations greater than 2 *M*, while the 1,3-diol produced maximal nuclear swelling at the 1 *M* concentration but the amount of swelling was much less and did not continue beyond 1 hour. Instead, the data showed a diminution in the mean nuclear diameter by 4–5 hours. In the 1,3-diol solutions at concentrations greater than 2 *M* there was significant reduction in the mean diameter of the nuclei as compared with those of the controls. The observations suggest a removal of nuclear material by extraction in these solutions.

Some observations which may be irrelevant to the main points of this paper seem worthwhile recording here. It was found by previous investigators that echinoderm eggs contract when placed in hypertonic salt solutions [4, 8, 10, 12, 14]. However, quite a different result was obtained when suspensions of *Asterias* eggs in sea water were left at room temperature in depression slides covered with a glass coverslip. After 7 hours, by which time salt crystals had appeared under the coverglass but not in the depression, the cells in the center of the depression were normal in appearance and equal in size to controls kept in covered beakers. However, the cells near the periphery of the depression had developed vacuoles which eventually occupied more than half the cell volume (Fig. 4). With time, vacuolization gradually spread to the cells nearer the center of the depression. It would seem from this observation that *Asterias* eggs may respond to an increased solute concentration in the external solution not only by contraction but by a cytoplasmic reorganization to form one or several compartments or vacuoles and that this kind of response is more likely to occur when the external concentration is changed at a rate slow enough for this adjustment to be made. Whether or not such adjustment to hypertonic solutions of electrolytes is in any way related to the cytoplasmic "vesiculation process" in the hypertonic solutions of nonelectrolytes described earlier is of course questionable, but the similarities are suggestive. In any case, it should be emphasized that the

cellular phenomenon observed in these experiments differs from that studied by previous investigators in that it is a cellular swelling in hypertonic solution rather than one of shrinkage.

The present experiments seem to be interpretable only in terms of a mechanism regulating the flow of materials into and out of the nucleus which requires the preservation of some though not all of the nuclear connections with the cytoplasm. This suggests a structure which is not a membrane in the usual sense, but one through which nucleoplasm and cytoplasm are joined in such a manner that they may act in unison. Recent electron microscope studies describe the nucleus as leaving a definite membrane with regions which have the appearance of pores. The material within the nuclear "pores" is either more osmophilic or intrinsically more dense than other portions of the nuclear membrane and it is not clear whether there is a single or double membrane within the pore or any at all [1, 11, 24, 28]. In the various species examined, including echinoderms, the diameters of these nuclear "pores" are in the range 200–400 Å, a size much too large to prevent the penetration of a molecule as small as glycerol. The fact that the *Asterias* nucleus can discriminate between 1,3-propane diol, and 1,2,3-propane triol suggests that passage of these molecules through the nuclear envelope is not accomplished by a process of filtration through a porous material.

The variation of the capacity of nuclei to swell in glycerol with change in pH does suggest that the swelling may be associated with an electrokinetic phenomenon, particularly with an electroosmotic effect. If the capacity for nuclear swelling were reduced or eliminated when the external pH was made equal to the intranuclear pH a possible electrical potential difference between the interior of the nucleus and the exterior might thereby be removed. Chambers and Pollack [7] found by injecting indicator dyes into the *Asterias* egg nucleus and into the cytoplasm that the nuclear contents had a pH of 7.5 ± 0.1 and that the pH of the cytoplasm was 6.7 ± 0.1. In the present experiments the tendency for nuclei to swell was reduced to a minimum in buffers with an initial pH of 7.38 which on standing with the cells fell to pH 7.32. This is close to the range 7.4–7.6 found by Chambers and Pollack for the nuclear pH. Colorimetric methods as applied to single cells and portions of cells are subject to appreciable error and since corrections to a true hydrogen ion concentration were not made by Chambers and Pollack or in the present experiments the values, pH 7.4 and 7.5 cannot be considered to be significantly different. The observations are therefore best accounted for by the hypothesis that nuclear swelling in 4.8 *M* glycerol occurs by electroosmosis. But, this hypothesis is applicable only if it is assumed that

when cells are immersed in the buffered glycerol solutions the pH of the cytoplasm is shifted to that of the external medium. We have no experimental evidence that this does in fact occur although the microscopic observations suggest massive penetration of the external solution. However, the failure of such adjustment in the cytoplasmic pH to that of the medium in about 50 per cent of the cells would account for the 50 per cent of the cells in the solutions at pH 7.4 which do swell. Although the electroosmosis hypothesis is the only one which at present seems to fit the observations more experimental evidence is needed to establish this point. In any case, if it is an electroosmotic effect, it is one which involves not just the nuclear membrane but requires that the nucleus and cytoplasm retain contact or connection over at least a portion of the nuclear surface.

The conditions under which massive swelling of the *Asterias* nucleus was produced in these experiments are of course abnormal. However, within the cell under normal circumstances the existence of a considerable pH difference between the nuclear interior and the cytoplasm provides a condition which makes electroosmotic flow between the nucleus and cytoplasm possible. Whether such flow actually does occur in the normal development of the egg remains to be demonstrated, but the observations suggest that this may be at least one of the phenomena involved in the tremendous growth in size of the nucleus during the development of the egg. It may also account for a condition frequently observed in tumor cells in which the nucleus enlarges to many times its normal size and almost entirely fills the cell.

Anderson [2] has reported that isolated mammalian nuclei seem to be permeable to molecules with a molecular weight as large as 700,000. On the other hand, the work of a number of other investigators, previously cited, has shown that nuclei of a variety of different species of plants and animals *in situ* within their cells are clearly "semipermeable". The present experiments show that the behavior of the nucleus in contact with its cytoplasm cannot be inferred from the behavior of isolated nuclei.

Afzelius [1] has found that the surface of the sea urchin oocyte nucleus is wrinkled or folded and has suggested that the capacity of the nucleus to swell may reside in the folding of the surface. Some preliminary examinations of sections of osmic acid-fixed *Asterias* eggs have been made. In the controls in sea water, the nuclear "pores" had diameters of approximately 400 Å and were separated by about 2900 Å from center to center. In nuclei which had been swollen in 4.8 *M* glycerol, the approximate dimensions were 1300 Å and 6000 Å for pore diameter and separation respectively. The number of measurements in each case, 3–4, is too small to consider these

values as definitive, but since there was no overlap in the range of values, they are enough to indicate that there was considerable stretching of both the intrapore and interpore portions of the nuclear surface. Apparently the swelling of the nucleus is not limited to the gain in volume possible through the opening out of the surface folds, since the material of the nuclear envelope appears to have the capacity for considerable expansion.

SUMMARY

1. Asterias eggs in the germinal vesicle stage swelled in hypotonic solutions of polyhydric alcohols and of sucrose but their nuclei did not swell.

2. In hypertonic solutions of these alcohols and of sucrose, the cytoplasm of these eggs swelled. The nuclei also swelled in hypertonic propane triol, butane tetrol, and sucrose solutions but not in solutions of the ethane or propane diols.

3. Loss of the vitelline and plasma membranes resulted in failure of the cytoplasm to swell in 4.8 *M* propane triol solutions but the nuclei of these denuded cells swelled at about the same rate as did those of cells which had retained their membranes.

4. In order for nuclear swelling to occur it was necessary that the nucleus retain its connection with the contiguous cytoplasm over a portion but not all of its surface. Nuclei extruded from the cells so that they were no longer in contact with cytoplasm invariably failed to swell.

5. The rate of penetration of fluid into the eggs from 4.8 *M* propane triol was found to be much greater than the rates obtained by other investigators for the entry of water by osmosis into these and other echinoderm eggs. The rate of entry of fluid per square micron of surface was greater for the cytoplasm than for the nucleus. However, the relative volume increment of the nucleus was greater than that of the cytoplasm.

6. The capacity of the nuclei to swell in buffered 4.8 *M* propane triol solutions varied with the pH of the solution. At approximately pH 7.4 there was a sharp minimum in the mean nuclear diameter and in the percentage of nuclei with diameters significantly greater than controls in sea water. This pH corresponds approximately with the value obtained by previous investigators for the intranuclear pH by micrurgical colorimetric methods.

7. It is deduced from these observations that the swelling of the nuclei in 4.8 *M* propane triol is produced by an electroosmotic process which requires the coordinated interaction of the material of the nuclear surface and the contiguous cytoplasmic substance.

8. Preliminary data are presented which indicate that the *Asterias* egg nucleus may enlarge in size not only by opening up of folds in the nuclear membrane but also by extension of both the intrapore and interpore portions of the nuclear envelope.

9. Because of the difference in behavior of the free nuclei and those retaining some contact with the cytoplasm, it is considered that the properties of nuclei as determined from the behavior of isolated nuclei are not necessarily representative of nuclei *in situ.*

10. It is concluded that in the normal egg the movement of some substances between nucleoplasm and cytoplasm is governed not by the nuclear membrane alone but by the coordinated activity of the nuclear envelope and cytoplasmic components contiguous to or connected with it.

REFERENCES

1. Afzelius, B. A., *Exptl. Cell Research* **8**, 147 (1955).
2. Anderson, N. G., *Science* **117**, 517 (1953).
3. Bärlund, H., *Acta Botan. Fennica* **5**, 1 (1929).
4. Beck, L. V. and Shapiro, H., *Proc. Soc. Exptl Biol. and Med.* **34**, 170 (1937).
5. Buck, J. B. and Boche, R. D., *Biol. Bull.* **75**, 344 (1938).
6. Callan, H. G., *Symposia Soc. Exptl. Biol.* **6**, 243 (1952).
7. Chambers, R. and Pollack, H., *J. Gen. Physiol.* **10**, 739 (1927).
8. Churney, L., *Biol. Bull.* **82**, 52 (1942).
9. Hamburger, H. J., Osmotischer Druck und Ionenlehre in den medicinischen Wissenschaften, Bd. 3. Wiesbaden, 1904.
10. Jacobs, M. H. and Stewart, D. R., *J. Cellular Comp. Physiol.* **1**, 71 (1932).
11. Kautz, J. and De Marsh, Q. B., *Exptl. Cell Research* **8**, 394 (1955).
12. Lillie, R. S., *Am. J. Physiol.* **40**, 249 (1916).
13. Lucke, B., Hartline, H. K. and McCutcheon, M., *J. Gen. Physiol.* **14**, 405 (1930–31).
14. Lucke, B., Hartline, H. J. and Ricca, R. A., *J. Cellular Comp. Physiol.* **14**, 237 (1939).
15. Marshak, A., *Biol. Bull.* **109**, 348 (1955).
16. —— *J. Cellular Comp. Physiol.* **32**, 381 (1948).
17. —— *J. Biol. Chem.* **189**, 607 (1951).
18. Marshak, A. and Calvet, F., *J. Cellular Comp. Physiol.* **34**, 451 (1949).
19. Marshak, A. and Fresco, J., *J. Biol. Chem.* **205**, 585 (1953).
20. Marshak, A. and Vogel, H. J., *J. Cellular Comp. Physiol.* **36**, 97 (1950).
21. Marshak, A. and Walker, A., *Am. J. Physiol.* **143**, 235 (1946).
22. McCutcheon, M. and Lucke, B., *J. Gen. Physiol.* **12**, 129 (1928).
23. McCutcheon, M., Lucke, B. and Hartline, H. K., *J. Gen. Physiol.* **14**, 393 (1930–1931).
24. Pollister, A. W., Gettner, M. and Ward, R., *Science* **120**, 789 (1954) (abstract).
25. Shinke, N., *Cytologia. Fujii Jubelaei Volumen*, 449 (1937).
26. Stewart, D. R. and Jacobs, M. H., *J. Cellular Comp. Physiol.* **1**, 83 (1932).
27. —— *J. Cellular Comp. Physiol.* **7**, 333 (1936).
28. Watson, M. L., *J. Biophys. Biochem. Cytol.* **1**, 257 (1955).

Experimental Cell Research 12, 615–625 (1957)

THE DENSITY OF SEA URCHIN EGGS, EMBRYOS AND LARVAE

E. A. SALZEN

Department of Zoology, University of Edinburgh, and Marine Station, Millport, Scotland

Received November 28, 1956

Changes in density of developing eggs may be due to physico-chemical changes of the egg constituents and to the transference of material between the egg and its environment. The former instance occurs in the transformation of "heavy" yolk to "lighter" protoplasm, a change which Needham [15] suggested was the cause of the continuous density decrease in teleost eggs. Transference of materials between the egg and its environment occurs in the respiration processes of all developing eggs and in the development of cleidoic eggs which absorb water and inorganic salts from their environment. The quantity of materials involved in these changes may be considerable, as, for example, in the development of many insect eggs [18]. In amphibia the density of the egg reflects an uptake of water and the formation and subsequent collapse of the blastocoel and archenteron [1]. It can be seen, therefore, that measurements of the density of developing eggs, if carefully interpreted, may provide information on the metabolic and morphogenetic events of embryonic life.

The density gradient method of Linderstrøm-Lang [8] can be used for continuous and accurate measurement of the density of individual eggs. This method was employed in an attempt to detect volume changes during cleavage of sea urchin eggs and the measurements were extended to embryos and larvae since previous work on density changes during echinoderm development has given conflicting results [12, 13].

METHODS

The gradient tube method has been fully described by Linderstrøm-Lang, Jacobsen and Johansen [9], Linderstrøm-Lang and Lanz [10] and Løvtrup [11]. A thorotrast/artificial sea water medium was used as described in a previous paper [16]. The accuracy of the measurements was limited to that of the standards, i.e. ± 0.0005 g/ml. The specimens (eggs, embryos or larvae) to be measured were put into the gradient as a batch of about twelve and they fell, and tended to remain, as a group.

The position of one specimen in each batch was measured at suitable intervals fro the time of entry into the gradient. In this way any irregularity in the movemer of the specimens could be detected. The positions of all the specimens were dete mined at suitable intervals for a period of up to six hours. These measurements wer usually sufficient for an estimate to be made of the definitive position of eac specimen in the gradient (the position at which the specimen and the medium hav the same density), since the rate of movement of the specimen is zero at this position

Preliminary measurements were made on unfertilized eggs of *Echinus esculentu* in May while the rest of the work was done using *Psammechinus miliaris* in th following July. The eggs of a single urchin were used for each determination anc except where stated to the contrary, the jelly was removed by washing in sea wate and the fertilization membranes removed by passing the eggs through bolting silk Observations of the effect of the gradient medium and of the artificial sea water o the egg were made at the temperatures of both the room and the gradient (22° 0.01°C). Measurements of the diameters of the egg and fertilization membranes wer also made.

RESULTS

Echinus esculentus Unfertilized Egg Without Jelly Coat

The gradient was a thorotrast/sea water mixture kept at a temperatur of 20° ± 0.01°C. Measurements of single eggs showed that they fell in th gradient in a normal manner, i.e. with a constant deceleration, reaching a steady position within thirty minutes (Fig. 1). In one case the eggs remaine in the same positions for three hours and there was very little change 2 hours later. Results of the measurements are given in Table I. If all th results are taken together, the density of the unfertilized egg may be sai to be 1.068 g/ml with a standard error of 0.001.

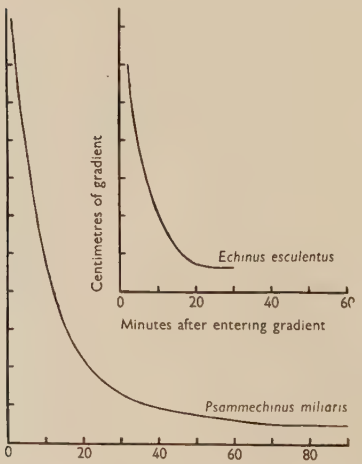

Fig. 1. Graph showing the fall of sea urchin eggs thorotrast/saline gradient.

TABLE I

Density of the unfertilized, dejellied egg of *Echinus esculentus*.

Batch No.	No. of eggs	Mean density (g/ml)	Standard error
1	10	1.0685	0.0004
2	5	1.0675	0.0044
3	10	1.0685	0.0010
Total	25	1.0681	0.0010

Psammechinus miliaris Eggs, Embryos and Larvae

The rates of fall of the eggs were much lower than those of *Echinus* eggs and they took more than one hour to come to rest. Fig. 1 shows, however, that although movement of the eggs was slow it was not irregular. Eggs with fertilization membranes intact behaved abnormally by slowly rising after having been in the gradient for about 1½ hours. Advanced embryos and the larval stages fell even more slowly than the eggs. After periods of 4–5 hours in the gradient the positions of eggs and cleavage stages were mostly unchanged, but the blastulae and gastrulae tended to rise and the prism larvae tended to fall slowly. All the material remained in surprisingly good condition in the gradient, especially in view of the high temperature, abnormal chemical conditions and absence of fertilization membranes. Although the artificial sea water was made with sodium and potassium chlorides only, the embryos did not fall to pieces. The embryonic stages did not disintegrate and the fertilization membranes, when present, did not collapse. The post-embryonic stages were anaesthetised with urethane and they tended to crumple and finally to disintegrate and sink to the bottom of the gradient.

Observations were made, at room temperature, on the effect of the gradient medium on the development of eggs with and without fertilization membranes. After three hours eggs in thorotrast had not developed beyond the four-cell stage and after 24 hours they had begun to disintegrate. Other eggs in sea water reached the blastula stage within 3 hours and became gastrulae within 24 hours. Fertilized eggs in the gradient at 22°C failed to cleave, so that no changes in density could be observed. The effect of thorotrast at room temperature on anaesthetised gastrulae was also observed. After 3 hours they showed signs of deteriorating, but could recover in sea water. After 6 hours they were irreversibly disintegrating. Anaesthetised gastrulae were able to recover within one hour when placed in sea water.

TABLE II

Density of eggs, embryos and larvae of *Psammechinus miliaris*.

Parent urchin	Developmental stage	Time from fertilization	No. of eggs measured	Mean density (g/ml)	Standard error
A	Unfertilized dejellied egg	–	11	1.088	0.0010
B	Fertilized egg with fert. membrane	–	8	1.069–1.074	0.0005
B	Fertilized egg minus fert. membrane	–	10	1.091	0.0005
C	Fertilized egg with fert. membrane	30 min.	10	1.074–1.076	0.0005
C	Fertilized egg minus fert. membrane	30 min.	12	1.093	0.0020
C	Two cells	1½ hr.	6	1.094	0.0015
D	Four cells	2 hr.	12	1.091	0.00075
D	Eight cells	2½ hr.	12	1.091	0.0075
E	Late cleavage	4 hr.	14	1.095	0.0010
E	Early blastula	6 hr.	12	1.095	0.0010
F	Blastula	12 hr.	19	1.084	0.0015
F	Early gastrula	24 hr.	27	1.085	0.0070
G	Gastrula	32 hr.	31	1.087	0.0025
F	Prism larva	40 hr.	19	1.088–1.096	0.0065
G	Pluteus larva	3 days	6	>1.095	–

The stages measured and the results are given in Table II. Since all the measurements were not made on eggs from the same urchin (cf. Table II) it is difficult to know whether the observed density differences were due to constitutional differences in the eggs or to developmental events. The time taken for each determination was too long for eggs from the same parent to be used throughout their development and shortage of material and time prevented the use of mixed batches of eggs from several parents for each stage or the replication of measurements using different parent urchins. The conclusions that can be drawn from the results are therefore tentative and involve a consideration of the different urchins used. The values for fertilized eggs from two urchins (B and C, Table II) suggest that the difference (0.002) due to the use of eggs from separate urchins is comparable with the standard errors of the measurements (0.002 for C, Table II). Results for the cleavage stages show no differences between eggs from the same urchins, but differences of up to 0.004 between eggs from different urchins. It seems unlikely

herefore, that there are any large scale permanent changes in density luring cleavage. Similarly, the suggested difference between the unfertilized nd fertilized eggs (without fertilization membranes) can be considered only s a possibility of a slight increase in density. The results for the intact ertilized egg are uncertain since the eggs were never at rest in the gradient, nd subsequent discussion will show that they cannot be considered as epresentative values. Finally, the results for the gastrulae and larvae are ncertain because their movements in the gradient tended to be irregular nd some were at rest for relatively short periods only. However, the differnces between the embryonic and free-swimming stages are large enough o be real, and the later larvae were undoubtedly denser than the blastulae. t may be said, therefore, that the early free-swimming stages are less dense han the cleavage stages and that there is a steady increase in density during arval development. This final increase in density is accompanied by the ppearance of the larval skeletal spicules.

The measurements from above of the diameters of the egg and fertilization nembrane gave mean values of 110 and 107 $\pm$ 3 μ for the egg and 150 and 120 $\pm$ 3 μ for the fertilization membrane. No significant difference could be letected between the diameters of the unfertilized egg and the fertilized egg within the fertilization membrane. The eggs were approximately spherical nd the fertilization membrane had the form of a prolate spheroid. Assuming hese shapes, the volumes of the fertilized egg with and without the fertilizaion membrane will be 1.13 and 0.67 μl respectively. The volume of the perivitelline fluid is therefore equal to two fifths of the volume of the intact ertilized egg.

DISCUSSION

Density Changes During Morphogenesis

The only previous measurements of the density of sea urchin eggs and mbryos are those of Lowndes who used his displacement weighing method or eggs of *Psammechinus miliaris* and *Echinus esculentus*, and Lyon who used the method of centrifuging eggs in gum arabic solutions of different density for *Arbacia punctulata* and other marine invertebrates. Lowndes found a continuous increase, and Lyon a decrease, in density during development. Table III shows their results compared as far as possible with those given in this paper. It can be seen that the two sets of values for *Psammechinus* do not correspond very closely except for the larval stages. In contrast to Lowndes' results the present work has shown that the density is more or

TABLE III

Density (g/ml) of sea urchin eggs, embryos and larvae.

Stage	*Psammechinus miliaris*		*Arbacia punctulata*
	Gradient method	Lowndes' displacement weighing	Lyon's centrifuge method
Unfertilized egg	1.088	1.07250	1.081–1.084
Fertilized egg	1.076–1.069	1.07360	–
Fertilized egg minus fert. membrane	1.091–1.093	–	1.081–1.087
2 cells	1.094	–	1.081–1.087
4 cells	1.091	–	–
8 cells	1.091	–	–
16 cells	–	–	1.081–1.087
Late cleavage	1.095	–	–
Early blastula	1.095	1.07582	1.024–1.081
Blastula	1.084	1.07930	1.024–1.081
Early gastrula	1.085	–	–
Gastrula	1.087	1.08390	–
Prism larva	1.088–1.096	1.09626	–
Pluteus larva	>1.095	–	1.055–1.066

less constant during cleavage, decreases in the early free-swimming stages and increases during subsequent larval development. Lyon's results for *Arbacia* are similar in that they show no changes during cleavage and a decrease in density at the blastula stage. They differ in that the pluteus larvae are still considerably less dense than the cleavage stages. In comparing these results it must be remembered that both the centrifuge and displacement weighing methods require large numbers of eggs for any one measurement and give an average value. The accuracy of the centrifuge method depends on the range of solutions of different density employed. The results obtained by the displacement weighing method are of doubtful value because the eggs may be damaged when packed into a specific gravity bottle. The gradient method is capable of measuring single small objects with great accuracy. However, the density values obtained in the present work have standard errors of as much as 0.0075. This large variation represents irregular movement of the eggs in the gradient; such movements suggest that changes were occurring in the eggs, probably as a result of the biologically unsuitable chemical and physical conditions in the gradient.

There is little doubt that the density of the blastula is lower than that of any other stage in development. The work of Briggs, who found a fall in density in the embryo of *Rana pipiens* from fertilization until neurulation has already been mentioned. Tuft (unpublished) has found a similar occurrence in the eggs of *Xenopus laevis* and has shown, by measuring the density of embryos with blastocoel and archenteron opened up, that most of this decrease in density is due to the formation of the blastocoel and archenteron from water taken in by the embryo. It is likely, therefore, that in the sea urchin also the formation of the blastocoel is responsible for the decrease in density. The blastula is the first free-swimming stage and being spherical has the minimum ciliated surface area and hence the smallest swimming power; it is interesting to note, therefore, that its density is lower than that of any other stage in development. When gastrulation takes place and skeletal material appears the density increases and at the same time the swimming power increases by the formation of the ciliated bands of the pluteus larva. Subsequent larval development involving further elaboration of the skeletal system is accompanied by a steady increase in density and complication of the ciliated bands.

Density During Cleavage

Lyon was unable to detect any rhythms of change in density during cleavage but his method was too insensitive to detect very small transient density differences of the kind which might accompany cleavage. The gradient method is sensitive enough to do this but the gradient medium appears to inhibit cleavage and so no information on the subject was obtained.

The densities of successive cleavage stages were measured and, when differences due to parentage are allowed for, they give no reason to suppose that there are any permanent large-scale changes in density during cleavage (Table II). Lyon's results for *Arbacia* also suggest that there is no change in density during this period of development.

The Density of Eggs and Protoplasm

Estimations of the density of the unfertilized egg of *Arbacia* have been made in the course of work on the viscosity of protoplasm [6] and the tension of the cell membrane [4]. Heilbrunn's value of 1.0485–1.0656 g/ml is lower than, and Harvey's value of 1.081–1.087 g/ml is in close agreement with, the density of 1.081–1.084 determined by Lyon. Other eggs measured by Lyon gave densities of 1.085–1.087 for *Chaetopterus*, 1.085–1.091 for *Phascolosoma* and 1.066–1.071 g/ml for *Asterias*. In addition to the figures

of 1.087–1.089 for *Psammechinus* and 1.067–1.069 for *Echinus* given in this paper, I have found the density of *Calanus* eggs to be 1.072–1.09 g/ml.

It seems, then, that a density of the order of 1.07–1.09 g/ml may be typical not only of echinoderm eggs but also of the eggs of many other marine invertebrates. For eggs considered as relatively alecithic, this density seems high, especially when compared with values for the density of "protoplasm"—1.045 for myxomycetes [7], 1.06 for brain tissue of *Rana palustris* larvae [2], and 1.04 for adult amphibian neural tissues and 1.05–1.07 g/ml for most vertebrate tissues [17].

Similar information for other types of eggs is scarce. Harvey and Frankhauser [5] give the density of the eggs of *Triturus viridescens* as 1.0845 g/ml, Briggs' value for eggs of *Rana pipiens* is 1.1065 g/ml and Tuft has obtained a similar value for eggs of *Xenopus laevis*, using the gradient method. Also with the gradient method I have found a density of 1.12 g/ml for eggs of *Locusta migratoria migratorioides* (unpublished). It is probable that the high density of eggs is the result of a high solid content which in the telolecithal amphibian and insect eggs is due to yolk, and in the alecithal eggs of marine invertebrates such as echinoderms is due to a high protein content [15].

Density Changes at Fertilization

It is not clear from the results (Table II) whether there is a change in the density of the ovum at fertilization. This is because the unfertilized and fertilized eggs measured were from different urchins. However, the values obtained (1.088 g/ml for the unfertilized egg and 1.091 g/ml for the fertilized eggs) suggests that there may be a slight increase in density at this time. Glaser [3] measured eggs of *Arbacia* and *Asterias* and found a decrease of as much as 10 per cent in the diameter of the egg after fertilization. A change of volume of the order represented by this should result in a detectable increase in density, yet Lyon was unable to detect such a change and even thought that there might be a slight decrease in density.

The density of the fertilized egg with the fertilization membrane intact is, of course, very different from that of the unfertilized egg (Table II). Since there is little change in the density of the ovum itself, the new density must be due to the perivitelline fluid.

Density of the Perivitelline Fluid

Lowndes measured the diameter of the ovum and the fertilized egg with and without the fertilization membrane. His results agree with those given here in that they show that the diameter of the ovum is unchanged after ferti-

lization. He calculated that the volume of the perivitelline fluid is approximately half that of the intact fertilized egg. Lowndes assumed the density of the perivitelline fluid to be 1.03 g/ml on the grounds that it would not be very different from sea water and calculated, using the volume estimations, that for an ovum of density 1.07 g/ml the egg with intact membrane should have a density of 1.05 g/ml. His experimentally obtained value for this was 1.0736 g/ml, and so he postulated the intake of Ca^{++} and their deposition in the egg as "crypto-crystalline calcite". Lowndes cited the increase in ash content of the egg, reported by Needham as occurring at fertilization, in support of his postulate.

The results given in this paper also show this lack of correspondence between experimental and theoretical values for the density of the intact fertilized egg. If the respective volumes of the egg and perivitelline fluid are 0.67×10^{-6} ml and 0.46×10^{-6} ml, and their densities are 1.091–5 and 1.024 g/ml (i.e. density of sea water), then the egg with membrane should have a density of 1.063–6 g/ml. The corresponding experimental values are 1.069–1.076 g/ml. Clearly, either the perivitelline fluid has a density greater than that of sea water or the experimental values are wrong. The lowest experimental value (1.069 g/ml) implies a perivitelline fluid of density 1.032 g/ml. Mitchison and Swann [14] have calculated from measurements made with the interference microscope that the perivitelline fluid has a concentration of material in excess of sea water of 0.074 per cent. If this material were solely protein, a density of 1.032 g/ml would imply a value of the order of 4 per cent.

Unlike the other egg stages, the intact fertilized eggs did not come to rest in the gradient. They fell in an apparently normal manner but then began to rise. It is difficult to explain this behaviour. If thorotrast was entering the perivitelline space the eggs would have sunk slowly to the bottom of the gradient. If the perivitelline fluid had been escaping the eggs would have sunk below their true density positions and approached those of eggs lacking membranes. Finally, if the gradient saline had entered the perivitelline space the eggs would have risen. The last process may explain the final rise of the eggs, but one or both of the other processes are required to account for the fact that the eggs fell below their probable true positions before beginning to rise. It seems unlikely, therefore, that the values for the intact fertilized egg are correct. It seems more likely that the density of the perivitelline fluid is not very different from that of sea water, as suggested by the interference microscope measurements, and that the density of these eggs is therefore probably of the order of 1.066 g/ml.

SUMMARY

The Linderstrøm-Lang density gradient has been used to determine the density of sea urchin eggs, embryos and larvae. The unfertilized eggs of *Echinus esculentus* and *Psammechinus miliaris* have densities of 1.068 and 1.088 g/ml respectively. These values are compared with similar information available for other types of eggs and for "protoplasm".

There is a possibility of a slight increase in density of the ovum of *Psammechinus* at fertilization for the zygote and cleavage stages have densities of 1.091–1.095 g/ml. There are no significant differences in the density of the cleavage stages. No information on transient density changes during cleavage could be obtained.

The blastula has a density of 1.084 g/ml and this is the lowest value attained during the development of *Psammechinus*. The decrease in density during blastulation is compared with similar changes which occur in amphibian development. The density increases throughout larval development, with values of 1.087, 1.088–1.096 and 1.095 g/ml for the gastrulae and prism and pluteus larvae respectively. This increase in density is accompanied by the growth of the larval skeleton.

It was not possible to obtain a reliable value for the density of the fertilized egg with fertilization membrane intact, since that obtained (1.069–1.076 g/ml) implies that the perivitelline fluid has a density far greater than that suggested by other evidence.

I wish to thank Professor M. M. Swann and Dr. P. H. Tuft for help and advice on this work which forms part of a series of embryological studies being made by Dr. Tuft with the help of a grant from the Nuffield Foundation. I am indebted to the Director of the Marine Station, Millport, for providing laboratory facilities and to Dr. J. M. Mitchison for advice on the manuscript. This work was done while I was in receipt of a Carnegie Research Scholarship.

REFERENCES

1. Briggs, R. W., *J. Cellular Comp. Physiol.* **13**, 77 (1939).
2. Brown, M. G., Hamburger, V., and Schmitt, F. O., *J. Exptl. Zool.* **88**, 353 (1941).
3. Glaser, O. C., *Biol. Bull.* **26**, 84 (1914).
4. Harvey, E. N., *Biol. Bull.* **61**, 273 (1931).
5. Harvey, E. N. and Frankhauser, G., *J. Cellular Comp. Physiol.* **3**, 463 (1933).
6. Heilbrunn, L. V., *J. Exptl. Zool.* **44**, 255 (1926).
7. Leontjew, H., *Protoplasma* **2**, 59 (1927).
8. Linderstrøm-Lang, K., *Nature* **139**, 713 (1937).

9. Linderstøm-Lang, K., Jacobson, O., and Johansen, G., *Compt. Rend. trav. Lab. Carlsberg. Sér. Chim.* **23**, 3 (1938).
10. Linderstrøm-Lang, K. and Lanz, H., *Compt. Rend. trav. Lab. Carlsberg. Sér. Chim.* **21**, 315 (1938).
11. Løvtrup, S., *Compt. Rend. trav. Lab. Carlsberg. Sér. Chim.* **27**, 8 (1950).
12. Lowndes, A. G., *Nature* **154**, 55 (1944).
13. Lyon, E. P., *Arch. Entwicklungsmech.* **23**, 151 (1907).
14. Mitchison, J. M. and Swann, M. M., *Quart. J. Microscop. Sci.* **94**, 381 (1953).
15. Needham, J., Biochemistry and Morphogenesis. Cambridge University Press, 1942.
16. Salzen, E. A., *J. Marine Biol. Assoc. U.K.* **35**, 549 (1956).
17. Tsai, Chiao and Lin, Chun-Yu, *Chinese J. Physiol.* **14**, 39 (1939).
18. Wigglesworth, V. B., The Principles of Insect Physiology. Methuen, London, 1939.

INTERFEROMETRIC DRY MATTER DETERMINATIONS ON LIVER NUCLEOLI OF PROTEIN-FED, PROTEIN-DEPRIVED, AND THYROID-FED RATS

U. STENRAM

Department of Pathology, University of Lund, Lund, Sweden

Received November 29, 1956

The nucleolus is considered to play a central role in the nucleic acid and protein synthesis of the cell. It is thought to increase in size and nucleic acid content during such synthesis [3]. The chemical composition of and the interactions taking place in the nucleolus are, however, very little known.

Working with the rat liver the present author found that the liver nucleoli of thyroid-fed rats increased in size [13, 17]. The livers of such rats may be presumed to have an increased nucleic acid and protein synthesis. It has further been shown that the nucleoli of protein-deprived rats turn considerably larger than those of protein-fed animals [12, 14, 15, 16, 18]. This is surprising as the livers of protein-deprived rats are thought to have a decreased rate of protein synthesis. The cytochemical and physiological significance of this nucleolar enlargement is not known. Nor is it known if the increase in size represents only a change in hydration or an actual increase in nucleolar substances. The liver nucleoli of protein-fed, protein-deprived, and thyroid-fed rats therefore seem to be suitable objects for examination, in order to elucidate the role of the nucleolus in the metabolism of the liver cell. It is the aim of the present investigation to contribute to the solution of this problem by determining with the interference microscope the dry matter concentration in nucleoli of isolated, unfixed liver nuclei of rats during the experimental conditions mentioned.

MATERIAL AND METHODS

Twenty-four male adult rats of a strain since long bred by the author were employed for the experiments. The individual weight of the rats was about 175 g. The animals were kept in wooden cages with sawdust on the floor. Nine were fed on a 25 per cent casein diet, nine on a 0 per cent casein diet [14], and in six the casein

diet was supplemented with 0.17 per cent desiccated thyroid (containing 0.3 per cent organic iodine; kindly furnished by AB Astra, Sweden) *ad libitum* for 14 days and then sacrificed. During the experimental time each casein-fed animal increased in weight about 15 g, each protein-deprived animal decreased about 35 g, and each thyroid-fed animal decreased about 10 g. All rats were killed between 8.30 and 9.30 a.m.

One piece of the liver was fixed in Susa. Individual nucleolar size was determined as described previously [14, 16].

Liver nuclei were isolated from other parts of the liver by the method of Hogeboom, Schneider and Striebich [5]. No effort was made, however, to obtain a quantitative yield. The nuclei were only sedimented twice. The nuclei were finally suspended in 0.34 *M* sucrose containing 0.00018 *M* $CaCl_2$, mounted on a microscopic slide and examined in a Dyson interference microscope (Cooke, Troughton & Simms, England). Nucleoli, centrally situated in the nuclei, were chosen at random and photographed with interference bands in the field. A 250 watt compact mercury arc lamp (British Thomson Houston) was used. Observations were made in monochromatic light at 546 mμ. An Ilford mercury green filter 807 was employed. The optics were a 95 × immersion objective N.A. 1.3 and a 6 × compensation ocular. The linear magnification on the photographic plates (Gevaert orthochromatic, 9 × 12) was 570 ×. The distance between two dark, adjacent interference lines on the plates was about 40 mm. The blackness of interference lines, nuclei and the centres of the nucleoli were registered along lines perpendicular to the interference bands with transmitted light onto a photographic paper by a recording microdensitometer. The light cone had a cross-section of 0.03 mm^2. This means that the blackness of nucleoli was measured within a central cylinder, the "depth" of which can be presumed to be equal to the diameter of the nucleolus in this dimension. The distance between two dark, adjacent bands on the photographic paper was 283 mm.

The dry matter concentration of structures in water can by interference microscopy be calculated from the formula

$$c = \frac{\phi}{\chi \cdot t},$$

where c = the dry matter concentration of the structure expressed as g/100 ml. ϕ = the optical path difference caused by the object. This figure is measured with the aid of the interference microscope. χ = the specific refractive increment of the object. t = the thickness of the object. For detailed description of interferometry see Barer [1], Davies *et al.* [4] and Osterberg [10].

The aim of the present investigation was to measure the dry matter concentration in the nucleolus. The path difference measured for the nucleolus in the nucleus must therefore be reduced by the path difference caused by the nuclear sap. Furthermore, the effect of the suspension medium must be added to the path difference caused by the nucleolus. Expressed as a formula this becomes:

$$c = \frac{\phi_1 - \phi_2\left(\frac{t-d}{t}\right)}{\chi \cdot d} + \frac{\chi^1 \cdot c^1}{\chi},$$

where c = the dry matter concentration of the nucleolus expressed as g/100 ml.
ϕ_1 = the path difference between the nucleolus and the interference band.
ϕ_2 = the path difference between the nuclear sap immediately surrounding the nucleolus and the interference band.
d = the thickness of the nucleolus, which was assumed to be equal to the least diameter of the nucleolus, as measured on the photographic plate. Using an additional magnification of 2×, the diameters of the nuclei and nucleoli were measured from the photographic plates with an accuracy of 0.1 mm by means of a sliding caliper.
t = the thickness of the nucleus. This was assumed to be equal to the least diameter of the nucleus as measured on the photographic plate.
χ = the specific refractive increment of nuclei and nucleoli. The figure 0.180 was used, as the main dry matter component of these structures are proteins [1, 4].
χ^1 = the specific refractive increment of sucrose solution, the main component of the suspension medium. The figure 0.141 was used [4].
c^1 = the concentration of the sucrose solution.

The dry matter concentration in nuclei was computed from the formula

$$c^2 = \frac{\phi_2}{\chi \cdot t} + \frac{\chi^1 \cdot c^1}{\chi},$$

where c^2 = the dry matter concentration of the nucleus.

Under the experimental conditions described a few inherent errors could not be avoided. An oval nucleolus might give a result much divergent from the mean (without the shape of the nucleolus being known) if the long axis is parallel to the observation line. Irregular masses of nucleolus-associated chromatin, situated along the observation line, might also influence the result. Mellors *et al.* [8] claimed that the nuclei may be flattened by the coverglass so that the estimated nuclear "depth" would be too large. The extent of this possible flattening could not be determined in the present investigation but was probably small as the nuclei appeared spherical as judged from the interference patterns and their diameters did not seem to be abnormally increased as compared to other measurements on unfixed nuclei. The flattening was probably reduced by the presence in the suspension of unbroken cells and heaps of nuclei, which undoubtedly increased the space under the coverglass. Errors might also be introduced by differences in nuclear "depth" at the spots where the nuclear and the nucleolar path changes were measured.

Determinations were made on about 12 nucleoli and nuclei in every animal. To minimize the influence of the above mentioned sources of errors the *median* of the figures for nuclear and nucleolar dry matter concentration was determined for each animal. For each group of animals the mean and the standard error and the standard deviation of the mean were computed from the medians of the individual animals. The experimental error for the individual nucleolus was determined by photographing the same nucleolus in various locations in the interference field. The error, estimated as the standard deviation, was found to be $< \pm 1$ per cent of dry matter concentration.

The t-test was used to establish possible statistical differences between the groups as regards nucleolar volume and nuclear and nucleolar dry matter concentration.

RESULTS

The results are summarized in Table I. The statistical analysis revealed that the nucleolar volume of Susa-fixed slices was significantly larger for non-protein- ($P < 0.001$), and thyroid-fed ($P < 0.001$) animals as compared to the protein-, non-thyroid-fed animals. The non-protein-fed animals had larger nucleoli than the thyroid-fed animals ($P < 0.001$).

TABLE I

Diet	Nucleolar volume in μ^3			Nucleolar dry matter concentration in per cent	
25 per cent casein	0.7 ± 0.04	$s = 0.4$	$n = 80$	38	$n = 14$
	0.8 ± 0.05	$s = 0.4$	$n = 80$	37	$n = 12$
	0.7 ± 0.04	$s = 0.4$	$n = 80$	38	$n = 8$
	0.8 ± 0.04	$s = 0.4$	$n = 80$	34	$n = 11$
	0.9 ± 0.06	$s = 0.5$	$n = 80$	42	$n = 16$
	0.8 ± 0.04	$s = 0.4$	$n = 80$	34	$n = 17$
	0.9 ± 0.05	$s = 0.5$	$n = 80$	32	$n = 14$
	0.8 ± 0.05	$s = 0.4$	$n = 80$	37	$n = 16$
	0.9 ± 0.07	$s = 0.6$	$n = 80$	42	$n = 18$
	$\Sigma 0.8 \pm 0.03$; $s = 0.1$			$\Sigma 37 \pm 1$; $s = 3$	
Non-protein	1.8 ± 0.14	$s = 1.2$	$n = 80$	40	$n = 9$
	1.4 ± 0.11	$s = 1.0$	$n = 80$	40	$n = 11$
	2.0 ± 0.19	$s = 1.7$	$n = 80$	39	$n = 18$
	1.4 ± 0.12	$s = 1.1$	$n = 80$	37	$n = 11$
	1.5 ± 0.12	$s = 1.1$	$n = 80$	34	$n = 12$
	1.5 ± 0.12	$s = 1.0$	$n = 80$	40	$n = 11$
	1.5 ± 0.11	$s = 1.0$	$n = 80$	41	$n = 15$
	1.3 ± 0.09	$s = 0.8$	$n = 80$	42	$n = 11$
	1.7 ± 0.14	$s = 1.2$	$n = 80$	31	$n = 17$
	$\Sigma 1.6 \pm 0.08$; $s = 0.2$***			$\Sigma 38 \pm 1$; $s = 4$	
Desiccated thyroid	1.0 ± 0.08	$s = 0.7$	$n = 80$	37	$n = 14$
	1.2 ± 0.08	$s = 0.7$	$n = 80$	33	$n = 11$
	1.1 ± 0.08	$s = 0.7$	$n = 80$	33	$n = 7$
	1.0 ± 0.07	$s = 0.6$	$n = 80$	33	$n = 15$
	1.2 ± 0.10	$s = 0.9$	$n = 80$	39	$n = 8$
	0.9 ± 0.06	$s = 0.6$	$n = 80$	45	$n = 6$
	$\Sigma 1.1 \pm 0.05$; $s = 0.1$***			$\Sigma 37 \pm 2$; $s = 5$	

*** Signifies a statistical difference of ($P < 0.001$) as compared to the protein-fed animals.
s = the standard deviation of the mean.
n = the number of observations.

There was no difference in nucleolar dry matter concentration between the groups ($P > 0.1$). This indicates that the increase in nucleolar volume during protein depletion, and thyroid feeding as compared to the protein-, non-thyroid-fed animals is caused by an increase in nucleolar substances other than water.

As well as the calculation of nucleolar dry matter concentration, figures were also obtained for the effect of nuclear dry matter. These figures were probably not quite as accurate since the measurements were not always made in the centres of the nuclei (see material and methods). However, it may nevertheless be of interest to mention them. They were for protein-fed animals 17 $\pm$ 0.4 per cent; $s = 1$; for non-protein-fed animals 16 $\pm$ 0.6 per cent; $s = 2$; and for thyroid-fed animals 17 $\pm$ 0.4 per cent; $s = 1$. There was no statistical difference between the groups.

Fig. 1 shows an isolated, unfixed liver nucleus of a protein-fed rat photographed with interference bands in the field. Fig. 2 shows a liver nucleus of a non-protein-fed animal and Fig. 3 a nucleus of a thyroid-fed animal.

DISCUSSION

The larger liver nucleoli, noted here in protein-deprived and in thyroid-fed rats as compared with protein-, non-thyroid-fed rats are in agreement with observations previously made [12–18]. The present figures for non-protein-fed animals are, however, lower than in previous investigations. This may be due to the fact that the experiments were performed in another department with other environments for the animals, etc. Furthermore, these animals were not sacrificed at the same time of the day as the previous animals.

Dry matter concentration was calculated on the assumption that no sucrose entered the nucleoli. If the sucrose concentration was the same inside the nucleoli as outside the nuclei, the nucleolar dry matter concentration should be about 29 per cent. There would still be no difference between the groups.

It seems possible that some substances, especially those of low molecular weight, may be dissolved out from the nucleoli of the isolated nuclei. This is, however, an inherent error that with all probability does not change the result, which is that the various types of nucleoli have the same dry matter concentration.

The literature on nucleolar mass is sparse. The nucleoli of pollen mother cells of *Zea mays* have been studied. The anthers were fixed in Susa. Protein was determined in the section by quantitative use of the Millon reaction. The concentration of protein in the nucleoli was found to be 430 mg/cm^3 [11]. (500 mg/cm^3 corresponds roughly to 40 per cent dry weight calculated as

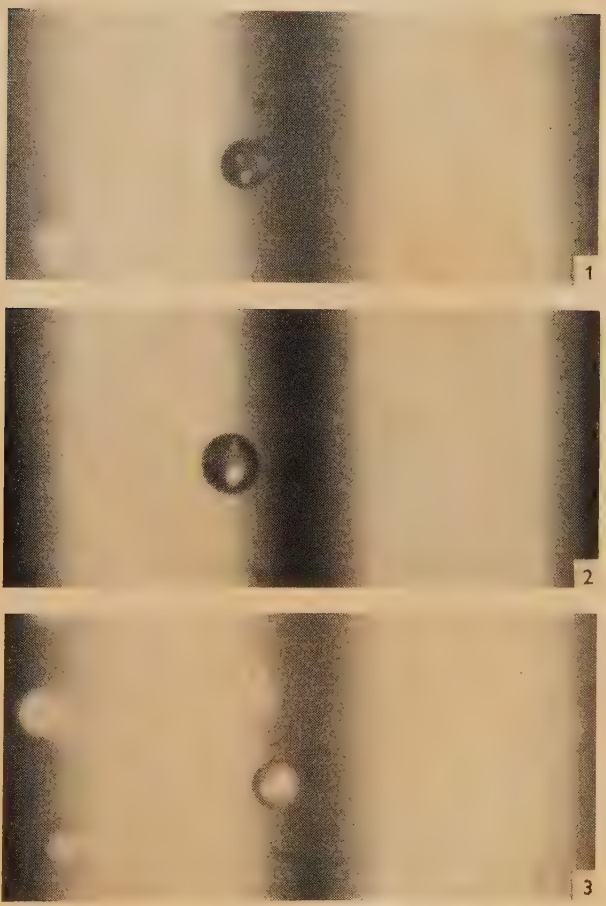

Fig. 1. An isolated, unfixed liver nucleus of a protein-fed rat. Photomicrograph with interference bands in the field. × 570.
Fig. 2. A liver nucleus of a non-protein-fed rat.
Fig. 3. A liver nucleus of a thyroid-fed rat.

protein.) It should, however, be remembered that Susa fixation shrinks nucleoli and probably dissolves some substances. The nucleoli of motor nerve cells in the spinal cord of cat were examined in frozen-dried sections with X-ray and ultraviolet microabsorption technique and found to contain about 70 per cent dry substance [9]. The observations underlying this figure seem to be rather few. In [9] the ratio between dry matter concentration of nuclei and nucleoli was found to be 1:3.0. Other workers found, using the X-ray technique, 500 mg/cm³ in a spinal ganglion cell nucleolus in a frozen-dried section [2]. For further figures on the protein content of nucleoli as measured by ultraviolet absorption technique see Caspersson [3] and Hydén [6, 7]. The dry matter content of starfish oocyte nucleoli isolated in distilled

water was by interferometry found to be maximally 85 per cent, calculated as protein [19].

All studies on various types of nucleoli have shown a high concentration of dry matter. The present study supports these observations. The ratio nuclear : nucleolar dry matter concentration was for the present investigation 1 : 2.3.

SUMMARY

Liver nucleoli of rats fed a non-protein diet or a thyroid-containing diet were considerably larger than those of rats fed a 25 per cent casein diet. The nucleolar dry matter concentration was examined in these three types of nucleoli in isolated, unfixed liver nuclei. The dry matter concentration was found to be 38 ± 1 per cent for protein-deprived animals, 37 ± 2 per cent for thyroid-fed animals, and 37 ± 1 per cent for protein-fed animals. There was no statistical difference between the groups. This indicates that the increase in nucleolar volume during protein deprivation and thyroid feeding signifies an increase in nucleolar substances other than water.

REFERENCES

1. Barer, R., *in* Oster, G. and Pollister, A., Physical Techniques in Biological Research, Vol. **3**, p. 30, 1956.
2. Brattgård, S.-O. and Hydén, H., *Acta Radiol. Suppl.* **94** (1952).
3. Caspersson, T., Cell Growth and Cell Function. New York, 1950.
4. Davies, H. G., Wilkins, M. H. F., Chayen, J. and la Cour, L. F., *Quart. J. Microscop. Sci.* **95**, 271 (1954).
5. Hogeboom, G., Schneider, W. and Striebich, H., *J. Biol. Chem.* **196**, 111 (1952).
6. Hydén, H., *Z. mikroskop.-anat. Forsch.* **54**, 96 (1943).
7. —— *Acta Physiol. scand.* **6**, suppl. 17 (1943).
8. Mellors, R., Hlinka, J., Kupfer, A. and Sugiura, K., *Cancer* **7**, 779 (1954).
9. Nurnberger, J., Engström, A. and Lindström, B., *J. Cellular Comp. Physiol.* **39**, 215 (1952).
10. Osterberg, H., *in* Oster, G. and Pollister, A., Physical Techniques in Biological Research, Vol. **1**, p. 378, 1955.
11. Pollister, A. W. and Ris, H., *Cold Spring Harbor Symposia Quant. Biol.* **12**, 147 (1947).
12. Stenram, U., *Expll. Cell Research* **5**, 539 (1953).
13. —— *Acta Anat.* **22**, 272 (1954).
14. —— *ibid.* **26**, 350 (1956).
15. —— *Acta pathol. microbiol. scand.* **38**, 364 (1956).
16. —— *Kungl. Fysiograf. Sällsk. Lund Förhandl.* **26**, nr 1 (1956).
17. —— *Acta pathol. microbiol. scand.* In press (1957).
18. Stowell, R., *Cancer* **2**, 121 (1949).
19. Vincent, W. S. and Huxley, A. H., *Biol. Bull.* **107**, 290 (1954).

Experimental Cell Research 12, 633–638 (1957)

THE METABOLIC UPTAKE OF SULPHATE IONS BY SKIN

J. C. LAWRENCE and C. R. RICKETTS

Medical Research Council Industrial Injuries and Burns Research Unit, Birmingham Accident Hospital, Birmingham, England

Received December 4, 1956

THE incorporation of ^{35}S into the mucopolysaccharides of connective tissue following the injection of ^{35}S-sulphate in animals has been reported by various authors (e.g. [2]). Experiments with slices of cartilage in tissue culture enabled Boström and Månsson [1] to investigate in detail several factors affecting the uptake of sulphate. The incorporation of sulphate was greatly reduced by pretreatment of the cartilage slices for 30 minutes at temperatures of 40° to 47°C before culture at 37°C. In thermal burns of the skin the earliest changes can be detected in this range of temperatures [6]. Thus it was of interest to see whether skin behaved like cartilage in taking up sulphate ions from the culture medium and whether the incorporation was affected by the same factors as operate for cartilage. Accordingly experiments were made by adding $Na_2{}^{35}SO_4$ to the medium of skin growing in tissue culture in the respirometer as described by Cruickshank [3].

METHOD

For most of the experiments small pieces of skin, 0.1 to 0.2 mm thick were cut from the dorsal surface of guinea-pigs' ears [3]. In other experiments split thickness human skin, surplus to grafting operations, was used so that results could be confirmed for man. Samples of human skin of about the same thickness as the guinea-pig skin were chosen; in general the human skin was thicker, more variable and not so easy to manipulate as guinea-pig skin. To each 20 ml batch of medium [3] 300 μc $Na_2{}^{35}SO_4$ in sterile physiological saline was added. The pieces of skin weighing 5 to 7 mg were grown on 0.5 ml portions of medium at 37°C for 24 hours under sterile conditions. Respiration was measured for selected periods during the 24 hours of culture. At the end of this period the skin cells were killed either by heating to 100°C for 5 minutes or by freezing to −79°C for 30 minutes. Freezing was preferred since it avoided disintegration of the tissue. Inorganic ^{35}S-sulphate was removed by dialysis for 24 hours against three successive 4 ml portions of 0.1 *M* sodium sulphate. The completion of dialysis was demonstrated in a few selected samples by precipitating sulphate from the dialysate and counting. The skin samples were then completely hydrolysed by heating in 1 ml 6 *N* HCl at 100°C for 3 hours. After addition of 4 ml 0.1 *M* Na_2SO_4 as carrier, sulphate was precipitated by addition of 5 ml 0.1 *M* $BaCl_2$ solution. Precipitates were separated by centrifuging, washed with water and acetone,

transferred as suspensions in acetone to planchets and dried under an infra-red lamp. Using a EHM2 mica end-window counter, counts of at least 1000 were made on each sample. A control experiment showed that 100 counts per minute corresponded to 0.18 mμg SO_4^{--} ion.

RESULTS

Preliminary experiments showed that respiring skin took up inorganic sulphate from the medium but skin in which the cells had been killed by heating to 100°C or cooling to −79°C did not do so. The radioactivity rose to about 35 counts per minute after 24 hours and to about 70 counts per minute after 48 hours (Fig. 1). It was convenient to terminate most of the experiments at 24 hours because after this time the rate of respiration tended to fall slightly. In experiments to investigate the effect of pre-treatment at various temperatures the respiration was first measured over a 2 hour period. The skin sample was floated on saline and maintained at the selected temperature for 30 minutes. The sample was then transferred to medium containing $^{35}SO_4^{--}$ ions and incubated at 37°C for 24 hours. During the first three hours and the last three hours respiration was measured. Finally the cells were killed and non-dialysable ^{35}S was determined as described. Fig. 2 shows the respiration of guinea-pig skin initially, immediately after a 30 minute period at the selected temperature and 20 hours later. At 37°C the rate of respiration was steady for the 24 hours' duration of the experiment.

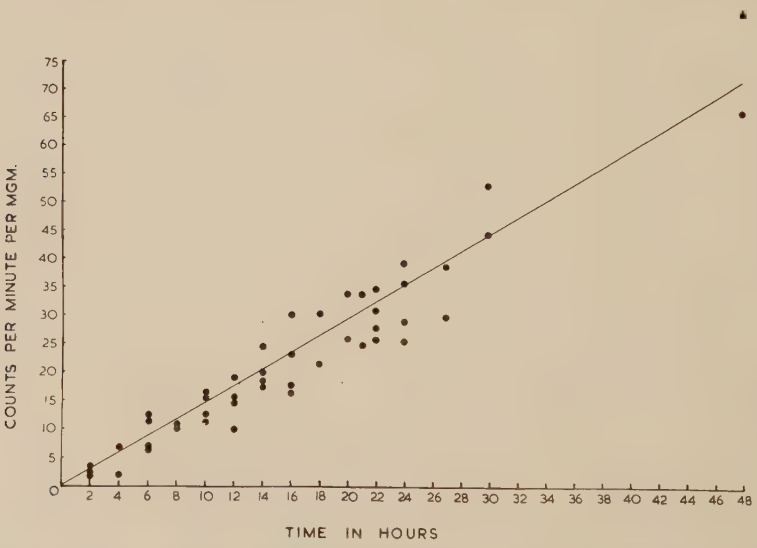

Fig. 1. Showing the rate of uptake of radioactive sulphate by guinea-pig skin in tissue culture.

A 30 minute period at 47°C causes severe damage, respiration falling to 50 per cent of its original rate at 3 hours and to a negligible rate at 21 hours. At 44 and 42°C intermediate results were obtained. At 40°C no effect on respiration was detected. Incorporation of ^{35}S into the guinea-pig skin following

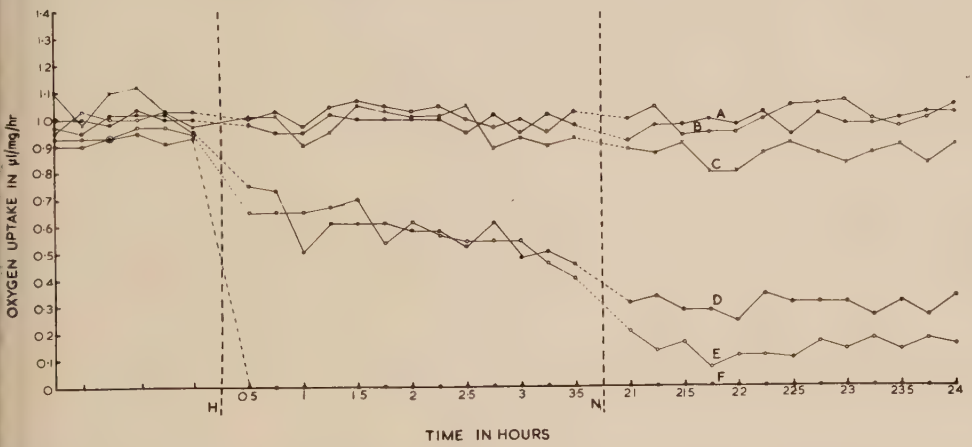

Fig. 2. Showing the effect of heat pretreatment on the respiration of guinea-pig skin. Pretreatment period, *H*, was for 30 minutes —*A* at 37°C, *B* at 40°C, *C* at 42°C, *D* at 44°C and *E* at 47°C; *F* was heated to 100°C for 5 minutes. *N* denotes the overnight period during which observations were discontinued.

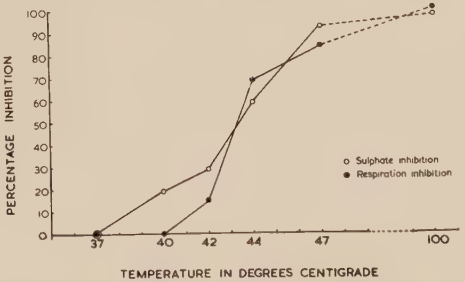

Fig. 3. Comparison of the effect of heat pretreatment on the sulphate metabolism and respiration of guinea-pig skin.

pre-treatment at various temperatures is recorded in Table I. The radioactivity of the sample maintained at 37°C was regarded as maximum uptake, i.e., 0 per cent inhibition. The initial rate of respiration of each skin sample was taken as the normal rate, i.e., 0 per cent inhibition. Fig. 3 shows the inhibition of respiration and of sulphate uptake caused by heating for 30 minutes at various temperatures. Respiration results for human skin, shown in Fig. 4, were less regular, possibly owing to lack of uniformity among the samples. Inhibition of respiration and sulphate uptake, see Table I and Fig. 5, closely resembled the results obtained for guinea-pig skin.

TABLE I

The effect of thermal damage upon respiration and sulphate metabolism of skin.

Pre-treatment temperature °C	Respiration results			Sulphate metabolism			
	μl/mg/hr.						
	Before heating	24 hrs. after heating	Percentage respiration inhibition	No. of cultures	Mean counts per min. per mg	S.E. mean counts	Mean % inhibition SO_4'' uptake
			Guinea-pig skin				
37	1.00	1.00	0	9	37.63	±2.63	0
40	1.00	1.00	0	4	30.50	±2.24	19
42	1.05	0.88	16	8	26.84	±1.22	29
44	1.00	0.31	69	6	15.15	±1.28	60
47	0.95	0.15	84	8	2.71	±0.43	93
Boiled 5 min.	0.93	0.00	100	3	0.65	±0.01	98
−79 ½ hr.	0.96	0.00	100	3	0.65	±0.001	98
			Human skin				
37	0.31	0.32	0	4	23.55	±3.14	0
40	Not measured			4	21.55	±3.48	8
42	0.32	0.28	12	4	16.02	±0.07	32
44	0.29	0.14	52	4	12.25	±1.33	48
47	0.29	0.05	83	4	2.05	±0.13	91
Boiled 5 min.	0.30	0.00	100	2	0.72	±0.004	97
−79 ½ hr.	0.26	0.00	100	2	0.70	±0.01	97

All rates are based upon unit wet weight of skin. Respiration results are quoted from several experiments as insufficient respirometers were available to make all the measurements at any one time.

The effect of a number of inhibitory substances on the uptake of sulphate by guinea-pig skin was as follows: 10^{-4} *M* Na iodoacetate 82 per cent, 10^{-4} *M* cortisone acetate 39 per cent, 3.8×10^{-3} *M* salicylic acid 4 per cent and 100 minimal haemolytic doses per ml of staphylococcus α toxin 82 per cent inhibition.

DISCUSSION

The steady respiration of skin maintained at 37°C (Figs. 2 and 4) together with the uptake of $^{35}SO_4^{--}$ ions (Fig. 1) contrasts with the negligible respiration and very small uptake of sulphate by skin heated to 100°C for 5 minutes or frozen to −79°C for 30 minutes. A graded response to thermal damage

between 37°C and 47°C in respect of both respiration and sulphate uptake was observed. This, together with the effects of the inhibitory substances, serve to confirm the metabolic nature of the uptake of sulphate ions by skin. The shape of the curves relating the temperature of thermal damage and

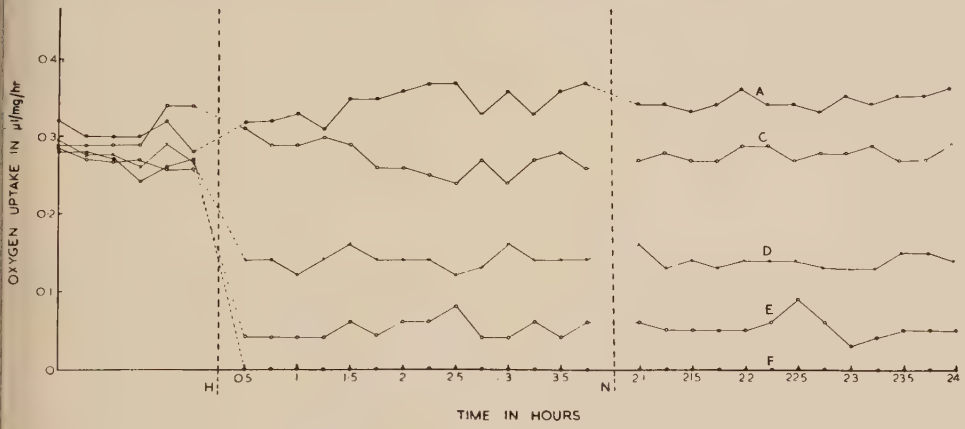

Fig. 4. Showing the effect of heat pretreatment on the respiration of human skin. Pretreatment period, *H*, was for 30 minutes—*A* at 37°C, *C* at 42°C, *D* at 44°C, and *E* at 47°C; *F* was heated to 100°C for 5 minutes. *N* denotes the overnight period during which observations were discontinued.

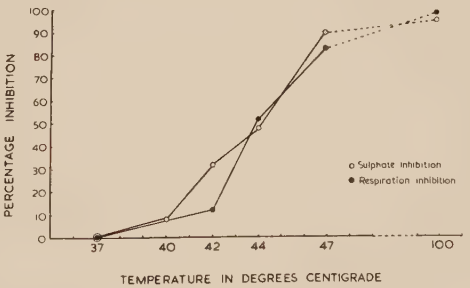

Fig. 5. Comparison of the effect of heat pretreatment on the sulphate metabolism and respiration of human skin.

sulphate uptake (Figs. 3 and 5) closely resembles the curve obtained by Boström and Månsson [1] for cartilage. The effect of inhibitory substances was quantitatively similar for skin and for cartilage. Boström and Månsson's results were based on the radioactivity of isolated chondroitin sulphate. In considering these experiments, based on the total radioactivity of skin, it must be remembered that a different index is being measured. A metachromatic substance free from protein and containing a little ^{35}S was isolated from skin grown in tissue culture. It is hoped to report on the nature of this substance in a future communication. Most of the radioactivity measured is in a chemical form at present unknown but evidently rather resistant to

removal from the skin by diffusion even in the presence of an excess of carrier ions. There is nothing to exclude the view that radioactivity is taken up simply as sulphate ions. However this may be, the sulphate is clearly taken up by a metabolic process subject to graded inhibition in the range of temperature in which the earliest observable changes of burns occur. The first effects of heat upon skin should probably be viewed as a diminution in respiration of the more sensitive members of a population of cells coupled with a decreased availability of sulphate ions for incorporation into the intercellular substances, one of which may be chondroitin sulphate.

SUMMARY

Small pieces of skin were exposed to temperatures between 37° and 47°C for 30 minutes and then grown in tissue culture. Respiration and the metabolic uptake of sulphate ions were diminished. The graded response is viewed as an effect upon a population of cells varying in sensitivity to thermal damage and resulting in decreased availability of sulphate ions for incorporation into intercellular chondroitin sulphate.

Thanks are due to Dr. C. N. D. Cruickshank for advice on the growth of skin in respirometers. The help of Mr. M. Hall, A.I.M.L.T., in the measurements of radioactivity, is gratefully acknowledged.

REFERENCES

1. Boström, H. and Månsson, B., *Arkiv Kemi* **6**, 23 (1953).
2. Boström, H., Odeblad, E., and Friberg, U., *Acta Pathol. Microbiol. Scand.* **32**, 516 (1953).
3. Cruickshank, C. N. D., *Exptl. Cell Research* **7**, 374 (1954).
4. Kodicek, E. and Loewi, G., *Proc. Roy. Soc. B.* **144**, 100 (1955).
5. Pearce, R. H. and Watson, E. M., *Can. J. Research* **27**, 43 (1949).
6. Sevitt, S., *Proc. Roy. Soc. Med.* **47**, 225 (1954).

Experimental Cell Research **12**, *639–648 (1957)*

EFFETS DES RAYONS X SUR *ACETABULARIA MEDITERRANEA*

Z. M. BACQ, F. VANDERHAEGHE, J. DAMBLON, M. ERRERA et A. HERVE

Laboratoire de Pathologie de l'Université de Liège et Laboratoire de Morphologie animale de l'Université de Bruxelles[1], *Belgique*

Reçu le 30 novembre, 1956

Il est important, pour comprendre les effets biologiques des radiations, de connaître la part respective des dommages causés aux divers organites cellulaires. L'utilisation d'un dard ultra-violet avait déjà permis à Schleip [11] en 1923 d'irradier sélectivement le noyau; d'autre part, l'emploi de particules α peu pénétrantes a permis d'irradier le cytoplasme seul [10]. Ces expériences avaient attiré l'attention sur le rôle considérable joué par le noyau : pour obtenir un effet identique (létal par exemple) en irradiant le cytoplasme seul, il fallait mettre en jeu des énergies beaucoup plus grandes. Depuis lors, une série importante d'observations sur les gamètes [1, 16, 14] n'ont fait que confirmer cette manière de voir. Tous les effets génétiques observés ne font évidemment qu'accentuer l'importance des phénomènes nucléaires.

Cependant, ces travaux indiquent tous que l'irradiation du cytoplasme seul produit certainement des effets, mais généralement à la suite de doses extrêmement grandes.

Des expériences de transplantation d'un noyau sain dans du cytoplasme irradié [4, 9] de même que de nombreux travaux utilisant les U.V. (références dans Errera [5]) permettent d'arriver aux mêmes conclusions.

Il nous a donc paru utile de reprendre ce type d'expérience en utilisant comme matériel expérimental l'algue géante *Acetabularia mediterranea* au stade de son cycle biologique où elle est unicellulaire [6], et au cours duquel Brachet et ses collaborateurs [3] ont étudié les relations biochimiques existant entre le noyau et le cytoplasme.

Ce travail a été commencé en 1954 et fut l'objet d'une collaboration étroite entre les laboratoires de Liège et de Bruxelles. Certains résultats ont déjà été publiés sous une forme préliminaire [2].

[1] Travail effectué par le Laboratoire de Recherches pour la Protection des Populations civiles.

Une étude analogue à celle-ci a fait également l'objet de travaux du Laboratoire de Hämmerling qui ont été publiés récemment [7].

Il nous a donc semblé intéressant de décrire nos résultats et de confronter nos conclusions avec celles de Hämmerling.

MATÉRIEL ET MÉTHODES

Les algues employées pour ces expériences proviennent toutes de cultures qu'ont utilisées Brachet, Chantrenne et Vanderhaeghe [3]; les milieux étaient identiques, de même que les conditions dans lesquelles les algues ont été sectionnées. Après l'irradiation les algues sont réparties par lots de 10 dans de petites boîtes de Pétri.

Conditions d'irradiation.—L'irradiation des algues a été réalisée à l'aide d'un appareil à faible tension (tube Machlett A.E.G. 50 ou A.E.G. 60 à fenêtre de Beryllium sans filtre, fonctionnant soit à 40 kV et 25 mA, soit à 30 kV et 30 mA). Dans le premier cas la distance focale utilisée était de 12 cm (env. 14.000 r/min) ou de 20 cm (env. 3.000 r/min); dans le second la distance focale n'était que de 8 cm (env. 30.000 r/min). La couche de demi-absorption dans les tissus est comprise, dans ces conditions, entre 0.7 et 1 mm. Nous avons irradié des algues entières ou des algues partiellement protégées. Dans ce dernier cas, le champ d'irradiation était réduit par un diaphragme métallique de manière à exclure des rayonnements la partie de l'algue désirée; cette partie était en outre recouverte d'un écran de plomb.

D'autre part, nous avons irradié des fragments nucléés et anucléés, sectionnés au 1/3 proximal dans les conditions décrites par Brachet et ses collaborateurs [3].

Les algues étaient étalées dans une boîte de Pétri humidifiée et le champ d'irradiation était contrôlé par un écran radioscopique.

Il faudra tenir compte dans l'interprétation des résultats présentés, de quelques particularités du matériel :

La partie distale de l'algue est un peu plus hydratée que le rhizoïde et la membrane y est plus mince et moins calcifiée. La proportion de Ca recueilli dans les cendres du rhizoïde est environ deux fois plus importante que celle de la tige (20 % et 8 %) tandis que la proportion de Cl est la même dans les deux et que le Si y est indosable.

Au cours de la croissance, le diamètre de l'algue s'accroît et sa membrane s'épaissit.

RÉSULTATS

Aspect morphologique des algues irradiées

Dans une première série d'expériences, l'irradiation totale d'algues entières montre que déjà pour 6000 r on peut observer des lésions cytoplasmiques à l'extrémité de la tige 20 jours après l'irradiation. Ces mêmes lésions apparaissent plus tôt lorsque la dose est plus forte : 2 jours après l'irradiation pour

240.000 r et 720.000 r et 3 jours après pour les doses de 12.000 et 120.000 r. Si les algues sont plus jeunes, les lésions se produisent plus précocement encore.

La plupart des algues irradiées finissent par régénérer totalement ou partiellement, suivant que toute la tige ou une partie seulement est cytolysée. Cependant dans le cas des très fortes irradiations, le rhizoïde reforme une nouvelle tige mais celle-ci présente certaines anomalies à son extrémité : pour des doses dépassant 72.000 r, les verticilles de poils stériles ont un aspect irrégulier et, au-delà de 240.000 r, on n'observe plus de verticilles et l'extrémité de la tige prend une forme de massue. Celles qui survivent finissent néanmoins par former des verticilles, des chapeaux et même des cystes.

Enfin, pour la plus forte dose (750.000 r), le rhizoïde meurt à son tour ou est tout au moins incapable de régénérer.

Dans une seconde série d'expériences, seuls les rhizoïdes ont été irradiés, les tiges étant protégées par du plomb. On observe, au bout de 20 jours, pour des doses comprises entre 24.000 r et 72.000 r, et au bout de 2 jours pour les doses les plus fortes, des lésions du cytoplasme non irradié. Le rhizoïde est toutefois capable de régénération et celle-ci se trouve même accélérée après l'irradiation par 24.000 r plus que pour des doses moindres ou plus fortes. La régénération s'est produite dans toutes les algues, et les chapeaux formés se sont remplis de cystes.

Dans une troisième expérience, les fragments anucléés ont été irradiés par lots de cinq. Les résultats de deux expériences sont consignés dans le tableau I.

TABLEAU I

Irradiation de fragments anucléés[1] (40 kV 25 mA).

Dose en r	Individus morts après		Individus morts après	
	13 jours	20 jours	22 jours	55 jours
0	0	0	0	0
10^3	5	5	2	5
$3 \cdot 10^3$	5	5	5	5
10^4	4	5	1	5
10^5	3	4	1	3

[1] Il s'agit de tiges d'algues adultes légèrement calcifiées.

Nous observons un phénomène particulier : la survie des tiges irradiées à l'aide de 10^3 et $3 \cdot 10^3$ r est moins bonne que celle d'algues ayant subi des doses plus considérables.

De ces premières expériences on peut conclure que la survie de la tige est moins bonne que celle du rhizoïde, celui-ci résiste à de très fortes irradiations et peut régénérer une tige pouvant former un chapeau et des cystes. Quand le rhizoïde seul est irradié, on peut observer certaines lésions cytoplasmiques au niveau de la tige pouvant entraîner la cytolyse de cette dernière. Même pour des doses allant jusqu'à 240.000 r, les rhizoïdes résistent : ils régénèrent des tiges formant des chapeaux pourvus de cystes.

Les fragments anucléés sont très sensibles aux rayons X et des doses de $3 \cdot 10^3$ r semblent être plus néfastes que certaines doses supérieures.

Etude systématique de l'effet des rayons X sur la survie, la croissance et la morphogénèse

Dans le but de reprendre ces observations de manière plus quantitative, des irradiations intéressant un nombre plus important d'algues par lots ont été entreprises et les observations se sont portées sur la *survie* d'algues entières ou de fragments, sur la *croissance des algues entières* ou la *régénération des fragments* et enfin sur la formation des chapeaux, c'est à dire la *morphogénèse*.

Survie.—Comme nous l'avons vu dans les expériences précédentes, dans de très nombreux cas, seule la tige de l'algue entière se cytolyse, alors que le rhizoïde reste robuste et capable de régénérer une nouvelle tige. C'est pourquoi, même si l'irradiation a porté sur des algues entières, il nous a paru utile de noter séparément la survie des tiges et des rhizoïdes *des mêmes algues*.

La fig. 1 (*A* et *B*) montre l'effet de doses croissantes de rayons X sur la survie d'algues irradiées *in toto*. Pour des doses de 10^4 et 10^5 r, il meurt plus de tiges que de rhizoïdes. Ces mêmes doses données à des algues plus âgées (peu de jours avant le début de la morphogénèse) n'ont entraîné la mort d'aucun individu.

La fig. 1 (*C* et *D*) concerne la survie de fragments d'algues cultivées et observées en même temps que celles faisant l'objet de la première expérience (*A* et *B*). Les fragments nucléés résistent mieux que les anucléés même après de fortes doses : les rhizoïdes meurent brusquement entre le 4e et le 6e jour alors que les tiges sont presque toutes cytolysées dès le second jour. Les algues semblent être l'objet d'un phénomène particulier, déjà recontré à l'occasion de l'irradiation de tiges isolées : il semble que la survie soit meilleure après 10^5 r qu'après des doses de l'ordre de 10^4 r.

Croissance ou régénération.—Indépendamment de la survie, on peut chercher à savoir si l'organisme continue à croître après l'irradiation. La *crois-*

vance des algues entières a été appréciée par l'aspect des verticilles qui se forment à la partie distale : leur absence indique un arrêt de croissance.

S'il s'agit de *fragments d'algues*, la *régénération* à partir de l'endroit où s'est faite la section est aisée à observer : la membrane de la partie en régénération est brillante et lisse tandis que celle qui recouvre la partie ancienne

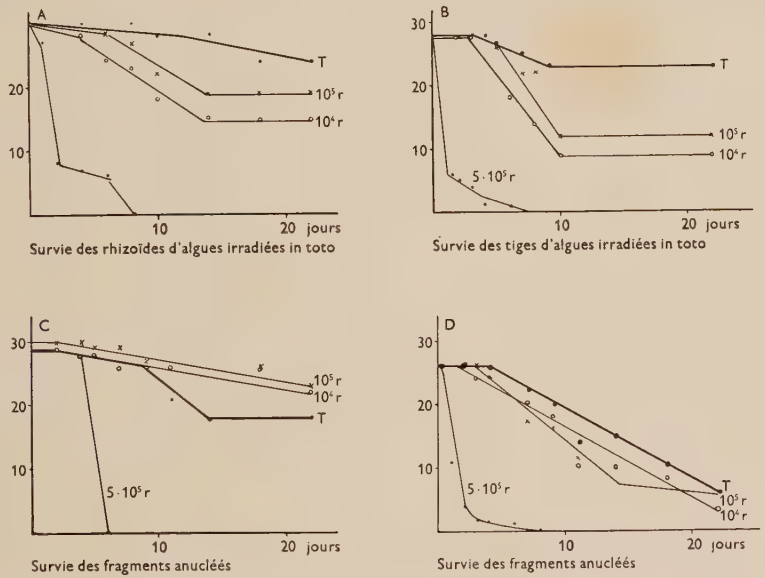

Fig. 1. Effets des rayons X sur la survie d'*Acetabularia*. Abscisses : nombre d'algues.

est épaisse et incrustée de calcaire : la partie qui régénère apparaît plus verte que le restant.

Algues entières : Nous avons suivi deux séries d'algues d'âges différents. La première (fig. 2, *A* à *D*) (celles dont la mortalité a déjà été observée fig. 1) concerne des algues ne formant pas de chapeaux, la seconde (*E*, *F*) se rapporte à des algues qui sont au contraire sur le point d'en former.

Dans la première expérience, il n'y a pas de différences après 50 jours d'observation entre la croissance des témoins et celle des algues entières irradiées *in toto* sauf pour la dose de $5 \cdot 10^5$ r (fig. 2, *A* et *B*). Or pour ces mêmes algues, la survie après irradiation est moins bonne que celle des témoins, on peut donc en conclure que les algues qui survivent à l'irradiation sont celles qui sont dans de bonnes conditions de croissance. Notons encore que, dans les jours qui suivent l'irradiation, la croissance des algues ayant subi 10^5 r semble meilleure que celle des algues n'ayant reçu que

10^4 r. Il pourrait s'agir du même effet paradoxal déjà constaté. Les algues sur le point d'effectuer leur morphogénèse survivent toutes et se développent normalement même après 10^5 r.

Fragments : Si l'on passe maintenant aux *fragments* nucléés et anucléés, on constate (fig. 2 *C* à *F*) que, dans les deux séries, on obtient après irradiation une *amélioration* de la régénération des fragments nucléés, pas très importante mais cependant reproductible. La régénération des fragments nu-

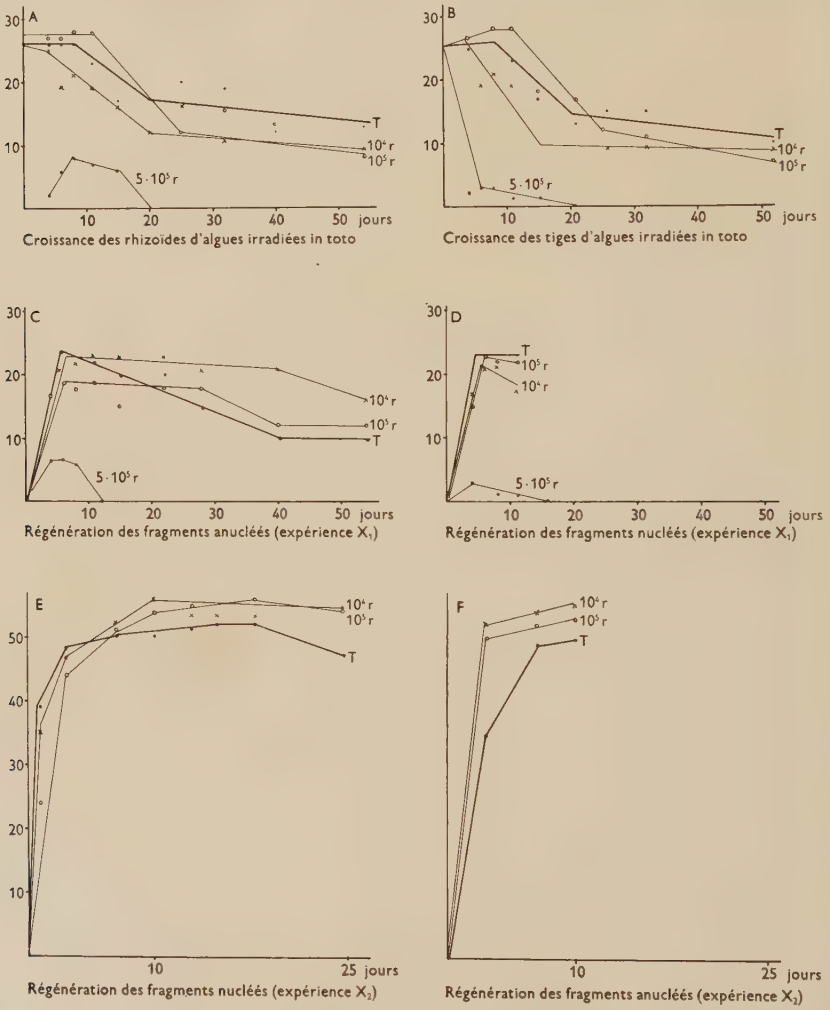

Fig. 2. Effets de l'irradiation X sur la croissance et la régénération d'*Acetabularia*. Abscisses : nombre d'algues.

cléés irradiés est d'abord plus lente que celle des témoins non irradiés, mais finalement le nombre des fragments nucléés qui régénère est plus grand que dans le lot témoin (fig. 2, *C* et *E*.) La régénération des fragments anucléés est accélérée dans le cas des algues plus âgées (2, *F*); elle est à peine ralentie chez les jeunes algues (2, *D*).

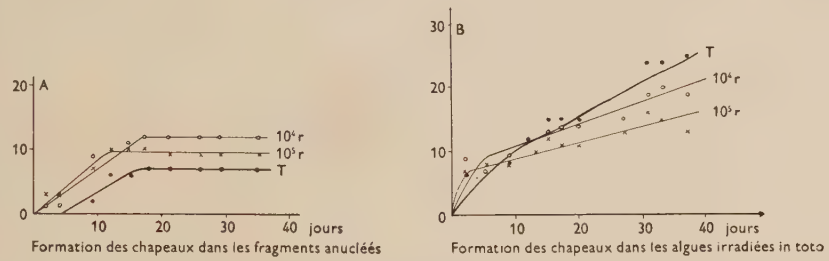

Fig. 3. Effets de l'irradiation X sur la morphogénèse d'*Acetabularia*. Abscisses : nombre d'algues.

Morphogénèse.—La formation de chapeaux a été observée très régulièrement dans des lots d'algues irradiées jusqu'à 240.000 r; ceux-ci ont également formé des cystes, mais généralement avec un retard considérable sur les témoins (1 mois). Pour rendre l'observation quantitative, nous avons noté pour les fragments d'algues du lot déjà décrit fig. 2, *B–F*, et pour des algues entières de la même culture irradiées *in toto*, l'apparition des chapeaux au cours du temps.

Dans le cas des *algues entières* (fig. 3, *A*), des doses n'affectant pas la *survie* inhibent cependant la formation des chapeaux chez un nombre d'individus d'autant plus important que la dose a été plus forte. L'inhibition n'apparaît que tardivement : pendant les 15 premiers jours, le nombre des chapeaux formés est sensiblement le même pour les témoins et pour les algues irradiées; ce n'est que par la suite que la morphogénèse se ralentit chez les algues irradiées. Tout se passe comme si les chapeaux prêts à se former au moment de l'irradiation avaient pu se différencier, tandis que les individus qui ne possédaient pas encore les « substances morphogénétiques » [6] nécessaires à la formation des chapeaux seraient incapables de les former après l'irradiation.

Dans le cas des *fragments* irradiés, seuls les fragments anucléés ont formé des chapeaux au cours de l'expérience. On assiste chez ceux-ci à une morphogénèse rapide et plus importante que normalement : ce phénomène rappelle ce qui a été observé pour la régénération (fig. 2, *F*).

On n'a pas suivi la morphogénèse des fragments nuclées irradiés.

DISCUSSION

L'un des phénomènes les plus frappants qui ressort de l'étude de la survie des algues est que le *cytoplasme*, qu'il fasse partie d'une algue entière ou qu'il soit séparé de son noyau, est moins résistant aux rayons X que le rhizoïde. Un phénomène analogue a été observé sur le même matériel après irradiation U.V. par Hämmerling [7] et nous-mêmes [15]; et sur les amibes par Mazia et Hirshfield [8] et par Skreb [13].

Cependant, dans le cas d'*Acetabularia*, il est difficile de conclure que le cytoplasme est réellement plus sensible que le noyau pour les raisons énumérées dans l'introduction (différences entre le rhizoïde et la tige en ce qui concerne l'hydratation et l'épaisseur des membranes).

Il ne fait aucun doute que le cytoplasme subit, indépendamment du noyau, des altérations importantes; de plus, des altérations tardives du cytoplasme peuvent résulter de l'irradiation de la partie nucléée seule.

Des altérations par les rayons X du cytoplasme irradié ont aussi été observées par Duryee [4] dans le cas des oocytes de grenouilles, et par Danielli [9] dans le cas des amibes, puisque ces deux auteurs ont provoqué des altérations de noyaux sains en les implantant dans un cytoplasme irradié.

Nous avons de plus, noté un phénomène apparamment paradoxal : la survie d'algues entières ou de tiges isolées est souvent *meilleure* après 10^5 r qu'après des doses inférieures à 40^4 r. Un tel phénomène pourrait résulter de l'inhibition d'un mécanisme biochimique qui mettrait ainsi à la disposition du phénomène observé des sources d'énergie et de métabolites ou des enzymes rendus disponibles.

Si on examine maintenant la croissance des algues et la régénération des fragments, on observe que les algues qui survivent à l'irradiation continuent à croître ou sont capables de régénérer. Dans certains cas, on observe même (*E*, *F*) que les fragments irradiés régénèrent *mieux*, plus vite (fig. 2, *F*) ou plus longtemps (fig. 2, *C* et *E*) que les algues témoins. Ici également il se pourrait que l'inhibition d'un mécanisme particulier ait pour effet de favoriser la croissance de la cellule irradiée.

En ce qui concerne la morphogénèse, on observe que celle-ci est encore possible jusqu'à des doses de 240.000 r. C'est d'ailleurs aux mêmes conclusions qu'arrive Hämmerling pour des doses allant jusqu'à 300.000 r. Nous avons cependant observé que pour les algues entières, celle-ci est d'autant moins bonne que la dose est plus forte; le phénomène se passe comme si des « substances morphogénétiques » présentes au moment de l'irradiation restaient biologiquement actives; l'arrêt tardif s'expliquerait par une *inhibi-*

on de la *formation* de ces substances, probablement d'origine nucléaire [6]. a fig. 3, *A*, confirme cette manière de voir : des fragments dépourvus de oyau ne peuvent continuer à former des chapeaux que pendant une uinzaine de jours après la section. Pendant cette période il semble qu'il y t également une *stimulation* des algues qu'elles contiennent un noyau ou on (3, *A* et *B*) : l'irradiation X semble encore accroître le phénomène que on observe généralement après l'énucléation.

Dans un travail qu'il vient de publier, Six [12] constate que la morphogé-èse des fragments anucléés est complètement bloquée après 40.000 r et ue ce phénomène est plus sensible que la croissance et que la survie. La iscordance entre ces résultats et les nôtres pourraient résulter du fait que ix n'utilise que la partie distale de l'algue (1 cm) tandis que nos fragments nucléés comptent les $\frac{2}{3}$ de l'algue (env. 2.5 cm). Quand il irradie la partie édiane de la tige les doses d'inhibition de la morphogénèse deviennent mparables aux nôtres.

Hämmerling [7] a observé que jusqu'à 18.000 r les noyaux et les cystes forment normalement. Même pour des doses de plusieurs centaines de nous avons encore constaté l'apparition des cystes, mais il y aurait alors énéralement une production moins abondante de gamètes.

RÉSUMÉ

L'irradiation affecte davantage la survie des fragments anucléés que celle es fragments nucléés d'*Acetabularia mediterranea*. L'irradiation de l'algue ntière produit aussi davantage de lésions irréversibles dans la partie distale, ytoplasmique de l'algue que dans la partie basale, nucléée.

Toutefois, la mortalité n'est pas proportionnelle à la dose administrée : ne dose $3 \cdot 10^3$ r entraîne plus rapidement la mort des algues que des doses lus élevées (10^4 r et 10^5 r).

La croissance et la morphogénèse des algues ou des fragments d'algues qui urvivent à l'irradiation est aussi bonne ou meilleure que celle des témoins. ette stimulation de la croissance est indépendante de la présence du noyau. ans le cas de la morphogénèse, cependant, une inhibition tardive de celle-ci e produit dans les algues entières, irradiées.

SUMMARY

The survival of anucleate fragments of *Acetabularia mediterranea* is less han the nucleate fragments, following X-irradiation. Upon X-irradiation of

the whole cell, the cytoplasm of the cell furthest from the nucleus dies quicker and in a higher percentage of cases than the region surrounding the nucleus.

However, the mortality rate of the cell and fragments is not proportional to the administered dose: dosages of $3 \cdot 10^3$ r result in a more rapid death than dosages of 10^4 and 10^5 r.

The growth and morphogenesis of the surviving irradiated algae at all dosages are identical to or better than the controls. This stimulation of growth is not dependent upon the presence of the nucleus.

The rate of cap formation (in total irradiated cells), which is stimulated in the beginning, is retarded from that of the controls after 15 days.

BIBLIOGRAPHIE

1. Astaurof, B. L., *Chem. Abstr.* **42**, 8233 (1948).
2. Bacq, Z. M., Damblon, J., et Herve, A., *Compt. Rend. Soc. Biol.* **149**, 1512 (1955).
3. Brachet, J., Chantrenne, H., et Vanderhaeghe, F., *Biochim. et biophys. Acta* **18**, 544 (1956).
4. Duryee, W. R., *J. Natl. Cancer Inst.* **10**, 735 (1949).
5. Errera, M., *Protoplasmatologia* (sous presse) (1956).
6. Hämmerling, J., *Internatl. Rev. Cytology* **2**, 475 (1952).
7. —— *Z. Naturforsch.* **II b**, 217 (1956).
8. Mazia, D. et Hirschfield, H., *Exptl. Cell Research*, **2**, 58 (1951).
9. Ord, M. J. et Danielli, J. F., *Quart. J. Microscop. Sci.* **97**, 29 (1956).
10. Petrova, S., *Botan. Centr. Beih. A* **61**, 399 (1942).
11. Schleip, W., *Arch. Zellforsch.* **17**, 289 (1923).
12. Six, E., *Z. Naturforsch.* **11 b**, 598 (1956).
13. Skreb, Y., communication personnelle.
14. Ulrich, H., *Naturwissenschaften* **42**, 468 (1955).
15. Vanderhaeghe, F. et Errera, M. (sous presse) (1956).
16. Whiting, A. R., *Proc. Natl. Acad. Sci.* **36**, 368 (1950).

ACTION DES RAYONS U.V. SUR DES FRAGMENTS NUCLÉÉS ET ANUCLÉÉS D'AMIBES

Y. SKREB[1] et M. ERRERA

Institut de Biologie de la Faculté de Médecine de Zagreb, Yougoslavie, et Laboratoire de Morphologie animale, Université libre de Bruxelles, Belgique

Reçu le 8 décembre 1956

Comme il a souvent été démontré par de nombreux auteurs, en particulier Brachet [2, 4] et Mazia [8], les amibes (*Amoeba proteus*) constituent un matériel de choix pour étudier les interactions entre le noyau et le cytoplasme.

Ceci résulte de la possibilité de les couper en deux fragments, nucléé et anucléé, dont on peut suivre indépendamment le comportement.

Il nous a paru intéressant d'entreprendre, comme l'ont déjà fait Mazia et Hirshfield [8] l'étude des effets des rayons U.V. sur les deux types de fragments, dans le but de comprendre les rôles respectifs du noyau et du cytoplasme dans la production et dans l'évolution des lésions dues à l'irradiation. Des travaux récents de Ord et Danielli [9], au cours desquels étaient effectués des transferts de noyaux sains dans du cytoplasme irradié aux rayons X ont permis d'établir un certain nombre de ces interactions.

Dans le présent travail, nous avons voulu étudier : (1) la sensibilité respective du noyau et du cytoplasme, (2) l'effet de la durée de l'énucléation sur la sensibilité à l'irradiation, (3) le rôle éventuel du noyau dans les phénomènes de photorestauration et (4) à l'aide de techniques cytochimiques, nous avons observé le métabolisme de l'acide ribonucléique (ARN) et du glycogène dans les fragments irradiés.

MATÉRIEL ET MÉTHODES

Ce travail, commencé dans le laboratoire du Professeur J. Brachet à Bruxelles, a été continué à Zagreb. Les amibes utilisées proviennent des cultures de Mr Brachet; nous le remercions vivement; elles ont été cultivées dans des conditions identiques aux siennes. Les techniques de section en fragments nucléés et anucléés, de même que les manipulations cytologiques, sont également identiques [4].

Irradiation : un arc au mercure à basse pression, soit Mineralight, soit Philips[2] donnant une forte intensité à 2537 Å a été utilisée; l'intensité est exprimée en ergs/mm² et est contrôlée à l'aide du dosimètre U.V. de Latarjet [7].

[1] Collaboratrice scientifique à l'Académie des Sciences Yougoslaves.

[2] Nous remercions vivement la firme Philips de Zagreb pour le prêt de cette lampe.

L'irradiation a porté sur des lots de 15 ou 20 moitiés d'amibes maintenues l'obscurité après l'irradiation ou illuminées immédiatement après l'irradiation.

Des amibes entières ont toujours été utilisées dans des expériences parallèles pou contrôler l'état de la culture. Au cours de l'irradiation, les amibes sont disposé dans des « salières » où elles sont cultivées et elles baignent dans le milieu de Chalkle Ce milieu, ne comportant que quelques sels minéraux, n'absorbe pas l'U.V. à l longueur d'onde utilisée.

L'illumination est obtenue à l'aide d'une lampe Philips Philora HP 125 à trave 5 mm de verre et 5 mm d'eau. L'intensité utilisée n'a pas été mesurée.

En plus de la durée de l'irradiation, nous avons étudié les facteurs suivants : dur du jeûne précédant la section et intervalle de temps entre la section et l'irradiatio

RÉSULTATS EXPÉRIMENTAUX

Survie en fonction de la dose d'U.V.

La fig. 1 représente l'évolution journalière d'une culture de fragment nucléés et anucléés, coupés après deux jours de jeûne et irradiés quelque heures après la section. On constate, surtout pour les doses faibles, que l survie des amibes anucléées est moins bonne que celle des amibes nucléées Ceci s'observe surtout dans les premiers jours qui suivent l'irradiation. E effet, pour les fortes doses (plus de 1000 ergs/mm²), les fragments anucléé commencent à se cytolyser dès le lendemain de l'irradiation alors que le fragments nucléés ne commencent à se cytolyser qu'à partir du 3e jour. Pa la suite, les différences sont souvent moins nettes du fait que les témoins no irradiés peuvent commencer à se cytolyser eux-mêmes.

Comme dans les jours qui suivent la section des amibes, les fragment anucléés s'appauvrissent en ribonucléoprotéines plus rapidement que le

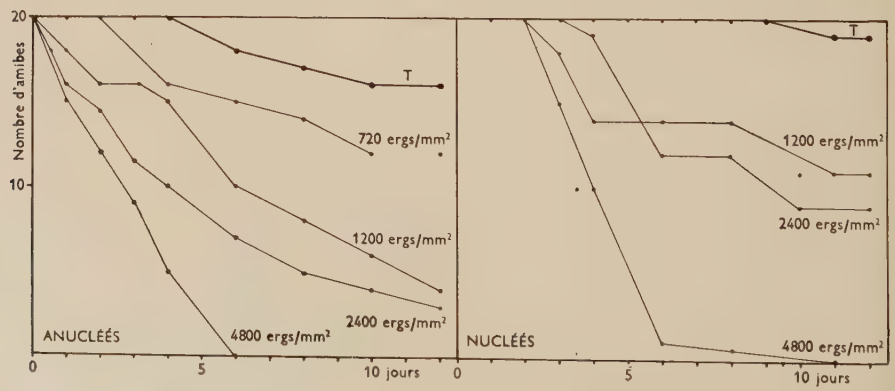

Fig. 1. Survie des fragments d'amibes. Ordonnées : nombre de fragments survivants.

fragments nucléés [4], nous avons pensé qu'il serait intéressant de rechercher l'effet de ce jeûne sur la survie des fragments irradiés. A cet effet, deux jours après la mise à jeûn, les amibes sont coupées et séparées en plusieurs lots qui sont irradiés (1200 ergs/mm2), 3 et 10 jours après la section. On constate

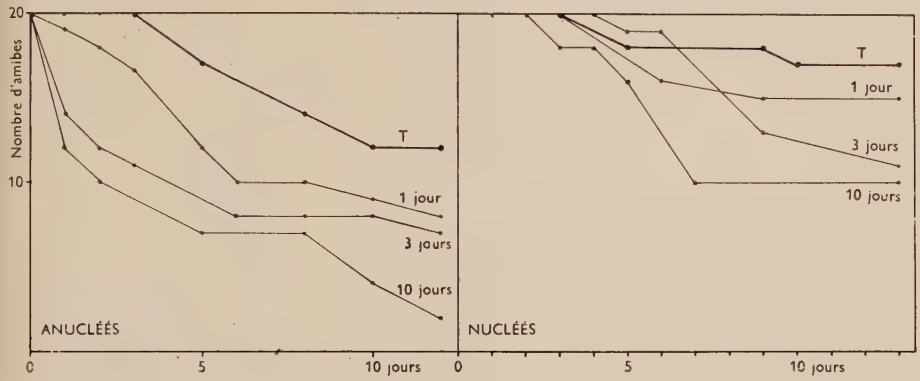

Fig. 2. Survie des fragments d'amibes irradiés aux U.V. (1200 ergs/mm²) après un jeûne de 1, 3 et 10 jours après la section. Ordonnées : nombre de fragments survivants.

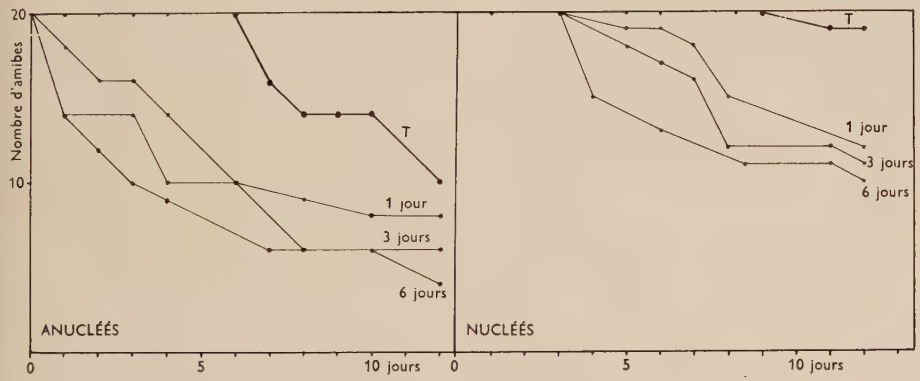

Fig. 3. Survie des fragments d'amibes irradiés (1200 ergs/mm²) quelques heures après la section et celle-ci ayant eu lieu après un jeûne de 1, 3 et 6 jours.

(fig. 2), surtout au cours des premiers jours (avant que les témoins ne commencent à péricliter) un net accroissement de la sensibilité des fragments anucléés. Cette différence peut dans certains cas devenir très considérable comme c'est le cas pour les amibes de la fig. 4. Une diminution des nucléoprotéines cytoplasmiques semble donc augmenter la sensibilité des amibes aux U.V.

Dans le but de nous rendre compte du rôle que le noyau pourrait jouer au

cours de ce jeûne, nous avons mis des amibes entières à jeûn pendant des temps croissants, elles ont été coupées après 1, 3 et 6 jours de jeûne et ensuite irradiées quelques heures après. Les résultats fig. 3 ne sont pas fort différents de ceux de l'expérience précédente. Comme la perte des ribonucléoprotéines

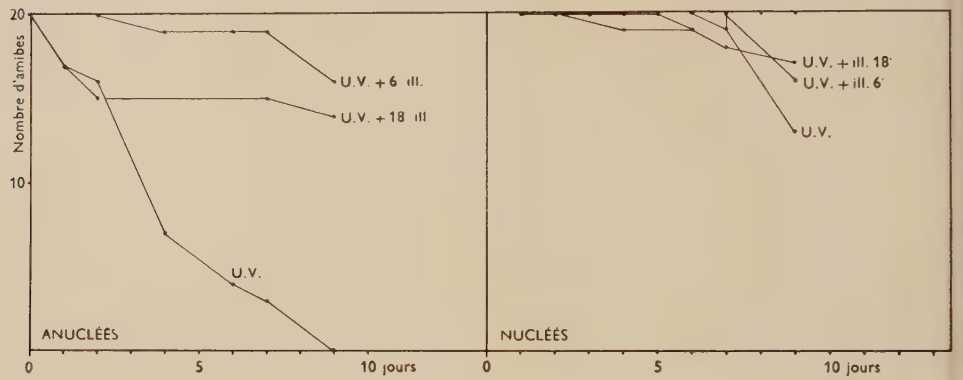

Fig. 4. Photo-restauration de fragments d'amibes coupées après 6 jours de jeûne et irradiés 3 jours après la section (2000 ergs/mm²). Ordonnées : nombre de fragments survivants.

dans les amibes entières à jeûn est moins rapide que dans les fragments anucléés, on ne peut conclure avec certitude que l'augmentation de la sensibilité résulte d'un appauvrissement en nucléoprotéines.

Dans le but de savoir si la *photorestauration* est un phénomène nécessitant à la fois le cytoplasme et le noyau comme on pouvait le supposer à la suite des expériences de Blum [1], nous avons soumis à diverses durées d'illumination des fragments nucléés et anucléés immédiatement après les avoir irradiés à l'aide de 2000 ergs/mm². Comme l'indique la fig. 4, la lumière visible a un effet restaurateur important sur les fragments anucléés irradiés. Dans le cas des fragments nucléés, la restauration existe également, mais les conditions expérimentales de cette expérience (où la survie après U.V. est bonne) ne sont pas favorables à la démonstration de restaurations spectaculaires.

Notons encore que trop de lumière visible semble être défavorable : la photorestauration est moins bonne après une forte illumination.

Cette expérience a été réalisée sur des amibes ayant été maintenues à jeun pendant 6 jours avant d'être coupées et n'ayant été irradiées que 3 jours après cette opération : cette longue période de jeûne semble ne pas avoir entamé les éléments cellulaires responsables de la photo-restauration.

Cependant, une étude critique de ce point mériterait d'être entreprise.

Etude cytochimique des amibes après l'irradiation

Des amibes sont coupées après deux jours de jeûne, puis irradiées le lendemain de la section (1200 ergs/mm²). Elles sont ensuite fixées au mélange de Serra, enrobées successivement dans de la gélose et de la paraffine et coupées. Les coupes (10 μ) des fragments nucléés et non nucléés d'un même lot (irradiés et irradiés + illuminés) sont disposées sur la même lame porte-objet de manière à subir un traitement tout à fait identique.

Acide ribonucléique.—Les lames ont été colorées par la méthode de Unna-Brachet [2] et la localisation de l'ARN a été plusieurs fois contrôlée après action de la ribonucléase. Les résultats peuvent se schématiser de la manière suivante :

Les *fragments anucléés* paraissent dès les premières heures après l'irradiation plus pâles que les fragments témoins qui ne commencent à pâlir que le deuxième jour. La perte de l'ARN qui détermine selon toute vraisemblance la diminution de l'affinité cytoplasmique pour la pyronine continue à être plus marquée dans les fragments irradiés. L'illumination après irradiation semble atténuer la perte de la basophilie cytoplasmique — mais la méthode cytochimique est certainement trop peu quantitative pour que l'on puisse rien conclure de définitif à cet égard.

Les *fragments nucléés* irradiés commencent à perdre leur basophilie vers le deuxième jour alors que les témoins ne commencent à le perdre que vers le sixième jour. Cette diminution n'est d'ailleurs pas identique dans tous les fragments nucléés irradiés et certains individus conservent leur basophilie beaucoup plus longtemps que d'autres. Les nucléoles perdent leur basophilie en même temps que le cytoplasme. Dans le cas des fragments nucléés, on peut nettement observer que la perte de la basophilie est *moins* rapide quand l'irradiation est suivie d'une illumination.

Si on prolonge le jeûne à trois et six jours avant d'irradier les fragments, on constate que la perte de la basophilie consécutive à l'irradiation se fait de manière encore plus précoce.

En conclusion, il semble que l'irradiation des fragments *anucléés* aggrave encore les effets de l'énucléation et détermine une perte plus rapide de l'ARN. Les fragments nucléés également subissent un appauvrissement plus précoce en ARN, tant nucléolaire que cytoplasmique; aux doses utilisées, les fragments nucléés irradiés perdent leur ARN cytoplasmique presqu'aussi rapidement que les fragments anucléés non irradiés : l'irradiation semble avoir entraîné des effets dans une certaine mesure comparables à l'énucléation.

Métabolisme du glycogène.—Les coupes de fragments d'amibes fixées au mélange de serra sont ensuite traîtées par la méthode de MacManus qui colore le glycogène en violet vif. La localisation de ce dernier a été contrôlée à l'aide d'une digestion préalable par l'amylase salivaire.

Brachet [4] avait observé que l'énucléation produit une forte diminution de la consommation du glycogène. Nous avons observé en effet que les fragments *anucléés* conservent leur glycogène pendant les douze jours que durent les observations. L'irradiation ne modifie en rien ce comportement.

Les *fragments nucléés* non irradiés ont visiblement commencé à utiliser leur glycogène dès le second jour, tandis que le lot *irradié* ne semble en avoir utilisé une quantité décelable que le quatrième jour : l'irradiation a donc pour effet de *retarder* la glycogénolyse; celle-ci s'effectue néanmoins car douze jours après l'irradiation, il n'y a pratiquement plus de différence entre témoins et irradiés. L'illumination des fragments nucléés irradiés *restaure* la faculté qu'ont ces amibes d'utiliser le glycogène : elles se comportent de manière tout à fait identique aux fragments nucléés non irradiés.

DISCUSSION

Survie des fragments.—La sensibilité plus grande des fragments observée par Mazia et Hirschfield se retrouve ici, mais peut-être d'une manière moins spectaculaire. La différence de sensibilité entre fragments nucléés et anucléés est moins grande que celle constatée par ces auteurs. Elle concerne principalement les premiers jours consécutifs à l'irradiation : on observe que certains fragments anucléés se cytolysent dès le premier jour alors que les fragments nucléés survivent tous au moins deux jours.

Les effets de la durée de la période de jeûne entre la section et l'irradiation ont été étudiés. Comme on le voit, la sensibilité des fragments anucléés augmente considérablement : et le nombre de fragments cytolysés le lendemain de l'irradiation est d'autant plus grand que le jeûne est prolongé. Dans les fragments nucléés, la cytolyse s'effectue surtout après le deuxième jour — et ici encore le jeûne augmente certainement la sensibilité de ce type de fragments. Que la période de jeûne précède ou suive la section en deux fragments importe peu. Il est difficile d'interpréter ces résultats du point de vue cytochimique. On sait que le jeûne entraîne une perte d'ARN beaucoup plus rapide dans les fragments anucléés que dans les fragments nucléés ou dans les amibes entières [4]. Il ne semble donc pas à première vue que la survie des fragments dépend de leur teneur en nucléoprotéines. Mais ceci

pourrait résulter de différences des quantités d'énergie U.V absorbées, que l'on peut difficilement calculer, mais qui sont vraisemblablement *beaucoup moins grandes* après quelques jours de jeûne dans le cas des fragments anucléés, du fait de la perte de constituants absorbant l'U.V. L'accroissement de la sensibilité aux U.V. en fonction du jeûne mériterait d'autres recherches pour en établir l'origine.

Photorestauration.—On sait que la photorestauration des phénomènes biologiques concernant *l'ADN* (spermatozoïdes (Blum) [1], bactériophages [5]) ne peut exister qu'en présence de cytoplasme; il est donc intéressant de constater que des dégâts *purement cytoplasmiques* peuvent être restaurés par la lumière visible en l'absence du noyau cellulaire; il est possible que des lésions *nucléaires* produites après irradiation du *cytoplasme* seul ne soient pas empêchées par l'illumination du cytoplasme; ceci pourrait expliquer le résultat de Von Borstel et Wolff [10] qui n'observent pas plus d'éclosions de larves d'Habrobracon dont seul le cytoplasme a été irradié, que celui-ci ait été illuminé ou non. Il est possible qu'une altération nucléaire sous l'effet de l'irradiation cytoplasmique se produise très rapidement dans le cas des amibes, comme Errera et Vanderhaeghe [6] l'ont observé dans le cas d'*Acetabularia mediterranea.*

Résultats cytochimiques.—Ceux-ci indiquent que, *grosso modo,* l'effet de l'irradiation se superpose à l'effet de l'énucléation : la basophilie cytoplasmique diminue plus rapidement dans les fragments d'amibes; dans les fragments anucléés, l'irradiation accentue les effets de l'énucléation, tandis que dans les fragments nucléés, l'irradiation entraîne des lésions voisines de celles de l'énucléation. Notons encore que les fragments anucléés commencent à se cytolyser dès le lendemain de l'irradiation, au moment où leur basophilie diminue; dans les fragments nucléés, celle-ci ne diminue que deux jours après l'irradiation et c'est également à ce moment que ce type de fragments commence à se cytolyser. Il semble donc exister une relation entre la survie des fragments et leur teneur en ARN. Nous avons constate que l'irradiation ralentit fortement la consommation du glycogène. Ce dernier résultat pourrait servir de base pour expliquer les nombreux cas d'accumulation de glycogène dans le foie d'animaux irradiés (références dans Errera 1952). Dans nos expériences il est fort difficile de savoir s'il faut attribuer ces effets de l'irradiation à une superposition d'effets cytoplasmiques et nucléaires; il faudrait avoir recours à des expériences de transfert de noyaux comme l'ont fait Ord et Danielli pour éclaircir cet aspect du problème.

RÉSUMÉ

L'irradiation U.V. affecte davantage la survie des fragments anucléés que celle des fragments nucléés d'amibes.

La mise à jeûn des fragments d'amibes avant l'irradiation augmente leur sensibilité à celle-ci.

La photorestauration des effets de l'irradiation U.V. se produit aussi bien dans les fragments anucléés que dans les moitiés nucléées.

Des observations cytochimiques montrent que l'irradiation provoque une chute de la basophilie du noyau et du cytoplasme dans les fragments nucléés et de la basophilie du cytoplasme dans les fragments anucléés. La consommation de l'amidon semble ralentie dans les fragments nucléés et anucléés après l'irradiation.

SUMMARY

Nucleate *Amoeba* fragments are less injured by U.V. irradiation than anucleate ones.

Both nucleate and anucleate *Amoeba* fragments starved for ten days exhibit a greater U.V. sensitivity than amoebae starved only for one or three days.

Photoreversal of the U.V. injury has been demonstrated in anucleate as well as in nucleate fragments.

As demonstrated cytochemically, U.V. irradiation results in a decrease of nuclear and cytoplasmic basophilia in nucleate amoebae and of cytoplasmic basophilia in anucleate ones; the rate of glycogen utilization by nucleate and anucleate amoebae was decreased by U.V. irradiation.

BIBLIOGRAPHIE

1. Blum, H. F., Robinson, J. C., et Loos, G. M., *Proc. Natl. Acad. Sci.* **36**, 623 (1950).
2. Brachet, J., Le rôle des acides nucléiques dans la vie de la cellule et de l'embryon. Desoer. Liège, 1952.
3. —— *Quart. J. Microscop. Sci.* **94**, 1 (1953).
4. —— *Biochim. et biophys. Acta* **18**, 247 (1955).
5. Dulbecco, R., *J. Bacteriol.* **58**, 329 (1950).
6. Errera, M. et Vanderhaeghe, F., *Exptl. Cell Research* (sous presse).
7. Latarjet, R., Morenne, M., et Berger, R., *Ann. Inst. Pasteur* **85**, 174 (1953).
8. Mazia, D. et Hirschfield, H., *Exptl. Cell Research* **2**, 58 (1951).
9. Ord, M. J. et Danielli, D. F., *Quart. J. Microscop. Sci.* **97**, 29 (1956).
10. Van Borstel, R. C. et Wolff, Sh., *Proc. Natl. Acad. Sci.* **41**, 1004 (1955).

BRIEF NOTES

A NOTE ON THE RELATIONSHIP BETWEEN THE GRAM REACTION AND PLASMOLYTIC EFFECTS IN BACTERIA

C. M. F. HALE

Department of Bacteriology, University of Birmingham, England

Received February 17, 1957

The effects of plasmolysis upon bacteria have been very variously described, especially in respect of whether a clear distinction exists between the reactions of Gram-positive and Gram-negative bacteria. The problem is well summarised by Knaysi [4]. A technique employed by Hale and Bisset [3] for the demonstration of bacterial cell walls provides evidence which helps to account for some of these divergences of opinion.

The method consists of immersing air dried smears for 20 min. in a saturated solution of $Ca(OH)_2$ at 90–100°, and staining for a few seconds in 0.1 per cent crystal violet. The results are seen in Figs. 1–6. A comparison was made of three strains of *Bacillus cereus*, and one each of *B. subtilis*, *Escherichia coli*, *Aerobacter aerogenes*, *Proteus vulgaris* and *Pseudomonas fluorescens*. With these were also compared three strains of *Azotobacter chroococcum* and one of *Rhizobium* sp. from lupin; organisms which normally stain Gram-negatively but which have been claimed to have Gram-positive affiliations [1, 2, 5]. All strains were isolated in this laboratory.

The reactions shown by *Bacillus cereus* (Figs. 1, 2) are typical of the Gram-positive, and by *Escherichia coli* (Figs. 3, 4) of the Gram-negative genera except *Azotobacter* and *Rhizobium*, which reacted in the same manner as the Gram-positive genera (Figs. 5, 6).

In smears of the *Bacillus*, *Azotobacter* and *Rhizobium* species when treated in this way, the cells appeared either to resist plasmolysis almost completely except at the poles or else to collapse internally, so that the cell wall alone remained, clearly stained with crystal-violet, more or less intact (Figs. 1, 2, 5, 6). All the Gram-negative bacteria appeared greatly shrunken, with a small, darkly-stained protoplast surrounded by an indefinite, polar area, representing the remnants of the cell envelopes (Figs. 3, 4). Probably this indicates general plasmolysis, whereas the Gram-positive genera and the nitrogen-fixers do not truly plasmolyse but collapse when the cell contents are destroyed. Thus the reactions of the two types of bacteria have been variously reported accordingly to the criteria of plasmolysis adopted by different workers in the past. At the same time, these experiments tend to support the view that *Azotobacter* and *Rhizobium*, although normally staining Gram-negatively, have certain of the characters of the Gram-positive bacteria.

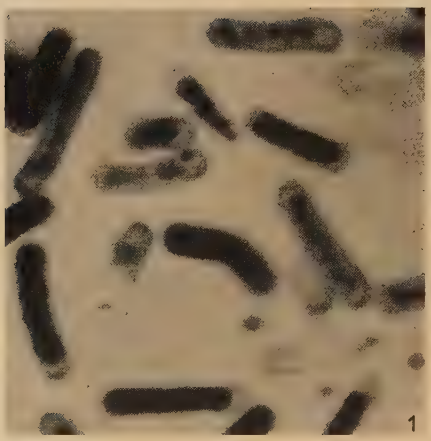

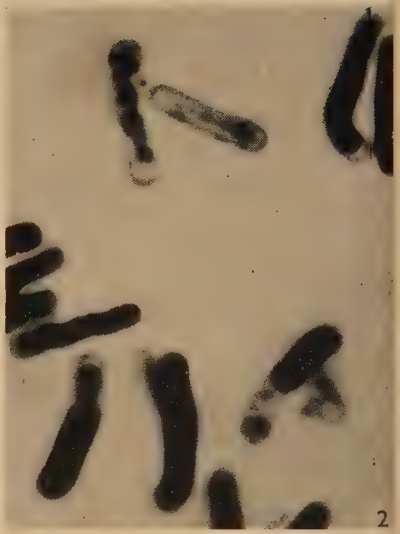

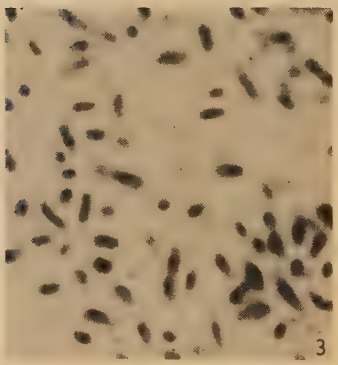

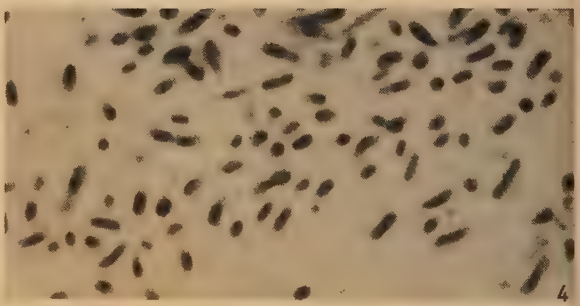

Illustrations (Photomicrographs, ×3000).

Figs. 1, 2.—*Bacillus cereus.*
Figs. 3, 4.—*Escherichia coli.*
Fig. 5.—*Rhizobium* sp.
Fig. 6.—*Azotobacter chroococcum.* (Explanations in text.)

REFERENCES

1. Bisset, K. A., *J. gen. Microbiol.* **7**, 233 (1952).
2. —— *ibid.* **13**, 442 (1955).
3. Hale, C. M. F. and Bisset, K. A., *ibid.* **15**, 423 (1956).
4. Knaysi, G., Elements of bacterial cytology, pp. 159 162. 2nd Ed., Comstock Pub. Co., Ithaca, New York, 1951.
5. Löhnis, F. and Smith, N. R., *J. agr. Research* **23**, 401 (1923).

TURNOVER OF THE SULPHATE GROUPS IN MAST CELLS OF YOUNG AND ADULT RATS

QUANTITATIVE AUTORADIOGRAPHIC STUDY

G. GUIDOTTI

Istituto di Patologia Generale, University of Milan, Italy

Received February 20, 1957

According to previous investigations radioactive sulphate is easily incorporated *in vivo* and *in vitro* in the sulphate groups of chondroitinsulphuric acid [3, 5] and of some other sulphomucopolysaccharides like heparin and precursors [7].

The injected radiosulphate was autoradiographically recovered in the mast cells of the rats' skin by Boström *et al.* [4] and in the mast cells of some experimental skin tumours by Asboe-Hansen [1, 2]. Furthermore the uptake of ^{35}S-labelled sodium sulphate by the cutaneous mast cells of young rats was studied by means of stripping film autoradiography [7].

This paper is concerned with the uptake of radioactive sulphate by the mast cells of the rats' skin; experimental animals of different ages were chosen in order to determine both the intensity of incorporation and the rate of exchange of the SO_4 groups according to the body senescence. This investigation was carried out quantitatively by means of a modified autoradiographic technique.

Twenty-seven rats, weighing about 70 g and 18 adult rats weighing about 220 g were given a single subcutaneous injection of ^{35}S-labelled sodium sulphate (0.75 μC/g body Wt.).

Three animals of the first group were killed at times after 15′, 45′, 90′, 3, 6, 12, 24, 48, 144 hours following the injection and three animals at the time of the second group were killed after 3, 6, 12, 24, 48, 144 hours following the injection.

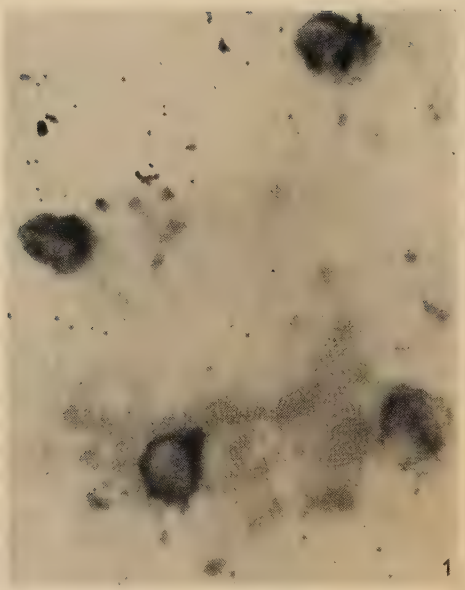

Fig. 1.—Skin of young rat. Electron-track autoradiography. Emulsion Ilford G5, thickness 50μ. Alcian 8 GN staining. 800 ×, immersion. Animal killed 15′ after the injection of the radiosulphate. No electron track is emerging from the mast cells.
Fig. 2.—Skin of young rat. Same details as for Fig. 1. Animal killed 6 hrs after the injection of the radiosulphate. Several electron tracks, emerging from the mast cells, are here clearly identifiable.

The abdominal region was shaved; a skin specimen was removed, fixed in Carnoy's fluid and embedded in paraffin. Sections 5μ thick were mounted on gelatin subbed glass slides, deparaffinized, hydrated and stained for 15′ with a 0.5 per cent solution of alcian 8 GN in Walpole buffer, pH 2.5. The dried sections were coated with Ilford G5 photographic emulsion (gel form) to a thickness of 50μ. The plates were desiccated for 2 hrs at 20°C in a slow current of dry air. The exposure at 0°C lasted 40 hrs.

Our routine processing was previously described [6].

Four sections for each animal including a total of 150 mast cells with related electron tracks were counted on the screen of a photographic microscope. All results were corrected according to the isotope decay and referred to the time of injection of the labelled sulphate.

Autoradiographic pictures obtained by our technique are shown in Figs. 1 and 2.

The results of the count of the tracks emerging from the cutaneous mast cells of the young and adult rats are reported in Figs. 3 and 4. In both of them the number of counted tracks for 100 mast cells, together with its standard error, has been indicated on the ordinate; the logarithm of the time intervals elapsed between the injection and the killing of the single groups of rats has been indicated on the abscissa. Our results show that the maximum of radioactivity is practically the same in the mast cells of either young or adult rats; however the incorporation rate of

the tracer appears to depend upon the age of the animals: as shown in Figs. 3 and 4 the maximum of radioactivity in the mast cells of young and adult rats was reached in about 6 and 24 hrs respectively.

According to these observations the radiosulphate is easily incorporated *in vivo* into the heparin or into the heparin-like compounds present in the mast cells of the rats.

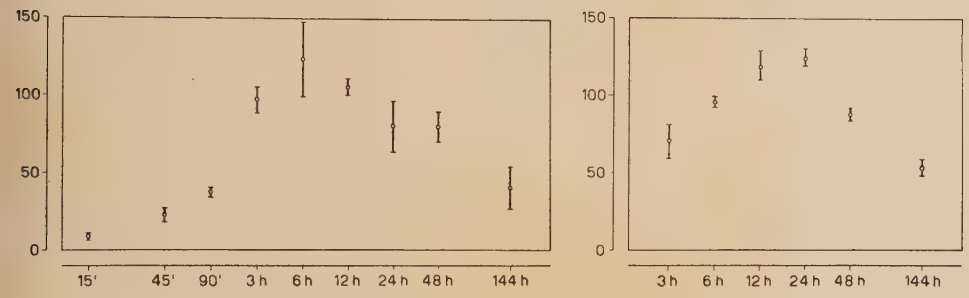

Fig. 3 (left).—Young rats. The number of the tracks counted for 100 mast cells with its standard error is reported on the ordinate; the logarithm of the time intervals between the injection of the radiosulphate and the killing of the single groups of rats has been indicated on the abscissa.
Fig. 4 (right).—Adult rats. Same details as for Fig. 3.

In the limits of our experience and, as far as the age of the experimental animals is concerned, these mast cells do not show significantly different exchange intensities. This lack of variability of the single cells to take up the sulphate groups could mean that no metabolic alterations bound to the ageing of the enzymatic systems of the protoplasm is brought about the senescence.

However, since the exchange rate is higher in the younger animals, the slowing of the ^{35}S uptake of the adult rats could be explained with the interference of some other causes like the state of vascularization of the skin, the membrane permeability or some undefined conditions bound to the whole animal body.

Experiments are in progress in order to clarify this point.

REFERENCES

1. Asboe-Hansen, G., *Cancer Research* **13**, 587 (1953).
2. —— *ibid.* **14**, 94 (1954).
3. Boström, H., *J. Biol. Chem.* **196**, 477 (1952).
4. Boström, H., Odeblad, E. and Friberg, U., *Acta Pathol. Microbiol. Scand.* **32**, 516 (1953).
5. Dziewiatkowski, D. D., *J. Biol. Chem.* **189**, 187 (1951).
6. Guidotti, G. and Levi-Setti, R., *Stain Technol.* **31**, 57 (1956).
7. Jorpes, E., Odeblad, E. and Boström, H., *Acta Haematol.* **9**, 273 (1953).

THE ULTRASTRUCTURE OF NORMAL AND DENERVATED NEUROMUSCULAR SYNAPSES IN MOUSE GASTROCNEMIUS MUSCLE[1]

J. F. REGER

Department of Anatomy, University of Colorado Medical Center, Denver, Colorado, U.S.A.

Received March 4, 1956

Studies on the ultrastructure of the normal neuromuscular synapse [1, 5, 7, 8, 9, 10] furnish a basis for experimental investigations using the electron microscope. Further investigation is needed in an attempt to learn more about the synaptic vesicles and membranes and their possible role in neuromuscular transmission. The following is a preliminary report of a study on the normal and denervated neuromuscular ultrastructure.

Material and methods. Gastrocnemius muscles of mice were denervated by sciatic section. Normal and denervated muscle were prepared identically. Tissue was fixed in buffered osmium tetroxide (pH 7.6) and subsequently dehydrated, embedded and sectioned for electron microscopy. Several hundred micrographs from 25 normal and 25 experimental preparations were made, of which the 2 included are representatives.

Observations.—Normal neuromuscular junction. In the normal motor end-plate from gastrocnemius muscle of mice the synapse consists of closely apposed axolemma and sarcolemma (Fig. 1). The resulting synaptolemma is 500–600 Å in thickness and composed of five differentially osmicated layers, best seen at arrows in Fig. 1. From the presynaptic axoplasmic to the postsynaptic sarcoplasmic side there are (1) densely osmicated axolemma, 100 Å in thickness, (2) an area of light osmification, 150 Å in thickness, (3) a middle densely osmicated region, which appears beaded in certain regions (best seen at arrows, Fig. 1), 100 Å in thickness, (4) another light zone, 150 Å in thickness, and (5) the dense inner layer of sarcolemma, 100 Å in thickness. The postsynaptic membrane (sarcolemma) is deeply infolded at the synapse forming a series of lamellae. The middle dense layer of the synaptolemma may be seen to assume the same infolding as that of the postsynaptic membrane. The axoplasm contains mitochondria, synaptic vesicles and endoplasmic reticulum (Fig. 1). Synaptic vesicles are 300–500 Å in size; they are found in the postsynaptic sarcoplasm as well, though fewer in number. The sarcoplasm of the end-plate also contains granules approximately 100 Å in size.

Denervated neuromuscular junction. After 48 hours denervation the axolemmal portion of the synaptolemma has almost completely retracted from the sarcolemma and lysis of the axolemma has begun (Fig. 2). A postsynaptic membrane free of axolemma remains, except in one area where a definitive axolemma may be seen

[1] Supported by grants from the Muscular Dystrophy Associations of America, Incorporated and U.S. Public Health Grant No. B-605.

The axon appears to have undergone considerable lysis and no recognizable mitochondria, synaptic vesicles, or endoplasmic reticulum are evident.

Discussion.—The normal ultrastructure of the synaptolemma described here is similar to that reported by Robertson [10]. The middle dense layer of the synaptolemma is probably sarcolemmal because of its continuation into the junctional folds of the postsynaptic membrane. Further support to this interpretation is given by the fact that after 48 hours denervation this layer is still observed intact as part of the postsynaptic membrane. The intervening dense layer of the synaptolemma may then be interpreted as an outer dense layer of postsynaptic membrane complex. The significance of its vesicular or beaded appearance is not known.

The infolding of the sarcolemma might be thought of as increasing the available postsynaptic surface area. Such an infolding of postsynaptic membranes has not been observed in most other types of synapses studied with the electron microscope [3, 5, 6], although Luft [4] reported similar infoldings of the electroplaque membranes of eel electric organs. Couteaux [2] first described the laminated structure of the neuromuscular postsynaptic membrane and by cytochemical methods identified the presence of acetylcholinesterase. In view of the complex nature of neuromuscular transmission, further studies of this membrane by electron microscopy and cytochemistry are warranted.

Synaptic vesicles of the type observed in the junctional axo- and sarcoplasm in this study have been reported for other synapses [3, 4, 5, 6]. Their function at the synapse remains a subject of speculation, although suggestions have been made that they may contain small quantities of chemical transmitter substance [3, 6, 10]. Confirmation of this will have to await investigation of the biochemical properties of synaptic vesicles. The close association of synaptic vesicles and endoplasmic reticulum in the axoplasm may be significant. De Robertis and Bennett [3] have suggested that synaptic vesicles may be formed by the endoplasmic reticulum.

Summary.—Normal and 48 hour denervated neuromuscular synapses of mouse gastrocnemius were studied. Axolemmal retraction from sarcolemma was observed after 48 hours denervation. The postsynaptic sarcolemma is described as a three layered membrane complex. This membrane is deeply infolded resulting in an increase in surface area. The normal axon contains mitochondria, endoplasmic reticulum and synaptic vesicles 300–500 Å in size. After 48 hours denervation the axon and its contents display considerable lysis. The normal sarcoplasm contains synaptic vesicles and granules approximately 100 Å in size.

REFERENCES

1. Beams, H. W. and Evans, T. C., *Proc. Soc. Exptl. Biol. Med.* **82**, 344 (1953).
2. Couteaux, R., *Rev. Can. Biol.* **6**, 563 (1947).
3. De Robertis, E. D. P. and Bennett, H. S., *J. Biophys. Biochem. Cytol.* **1**, 47 (1955).
4. Luft, J. H., *J. Biophys. Biochem. Cytol.* **2** (Supplement), 229 (1956).
5. Palade, G. E., *Anat. Rec.* **118**, 335 (1954). Abstract.
6. Palay, S. L., *J. Biophys. Biochem. Cytol.* **2** (Supplement), 193 (1956).
7. Reger, J. F., *Anat. Rec.* **118**, 344 (1954). Abstract.
8. —— *ibid.* **122**, 1 (1955).
9. Robertson, J. D., *Anat. Rec.* **118**, 346 (1954). Abstract.
10. —— *J. Biophys. Biochem. Cytol.* **2**, 381 (1956).

Fig. 1.—Normal neuromuscular synapse. Axon (*Ao*) in upper fourth of figure contains a mitochondrion (*M*), synaptic vesicles (*SV*) and endoplasmic reticulum (*ER*). Axolemma (*Al*) is closely apposed to sarcolemma (*Sl*). Arrows delimit synaptolemma. The sarcoplasm (*So*) contains granules and synaptic vesicles (*SV*). A portion of a myofibril (*Mf*) appears in the lower right.

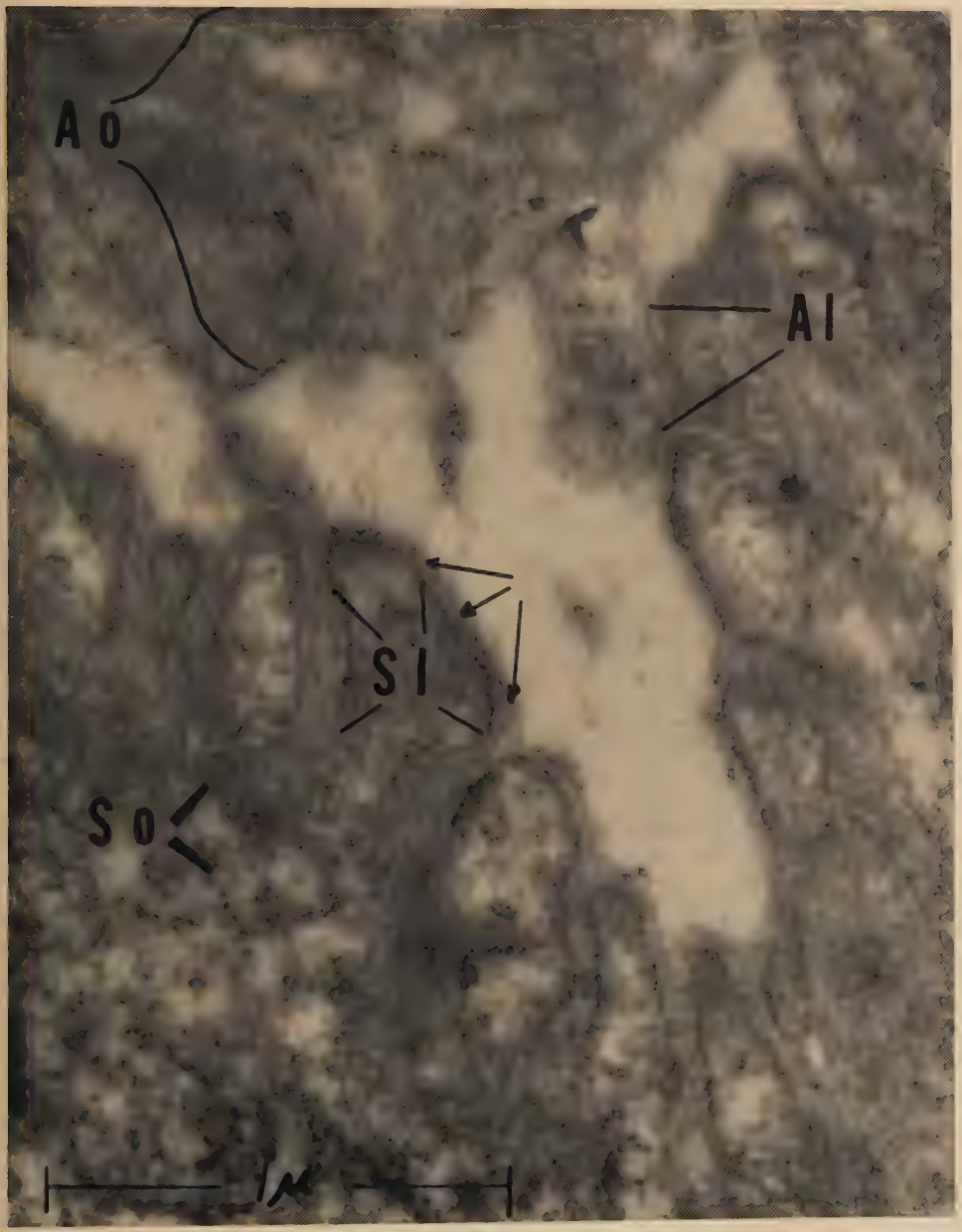

Fig. 2.—Neuromuscular synapse after 18 hours' denervation. The axon (*Ao*) undergoing lysis is seen retracted from sarcolemma (*Si*). Small portions of axolemma (*Ai*) may be seen. Arrows indicate middle dense layer of synaptolemma. Postsynaptic sarcoplasm (*So*) is in the lower left.

A MECHANICAL MICRO-SCANNER

S. LARSSON

Department of Histology, University of Göteborg, Sweden

Received March 15, 1957

With the present trends and scope in cell research there is a demand of scanning devices which are able continuously to scan a small or large part of a microscopic object. Recently some constructions of this type have been described in the literature, but none has the advantage of being directly applicable to an ordinary type of a microscope.

Scanning of a microscopic object can be arranged in one of the following three ways, or by a combination of these methods.

(1) Scanning in the plane of the image with a disc or a thin steel belt perforated with holes which are small in comparison with the structures in the image. The best-known examples are furnished by the scanning device described by Nipkow. Other systems are described by Deeley [2], and Bourghardt, Hydén and Nyqvist [1].

(2) The scanning is performed by moving the object against a stationary field stop.

(3) Scanning by flying-spot, i.e. the radiating spot of the cathode tube, is projected by means of a lens system in the plane of the object.

A combination of two of these methods is described by Tolles [4]. According to this method the object is moved in one direction and a scanning of the image is performed in the other direction.

When the object is scanned according to the well-known Nipkow principle and the aim is to perform an intensity measurement with high resolution of a certain area, then an error may be introduced. This is due to a gradient in the peripheral part of the area scanned, which in turn is due to light reflection and scattering in the spherical lens surfaces in the microscopic optical system. If the object is moved and only the rays in the optic axis are used at the scanning, this gradient can be excluded. The present paper describes a mechanical micro-scanner constructed according to the latter principle. The apparatus is now used as a scanning system in the cell analyser previously described [1, 3].

It may be noted that the micro-scanner here described can be fixed on any microscope table, and is thus ready for use in any part of the electromagnetic spectrum. The axial ray through the microscope system emerging from the object is projected on a field-stop which is shaped as a quadrangle, the side of which is 3 μ in relation to the microscopic sample. The radiation leaving the field-stop is thrown on a photomultiplier which is connected to a registering part via an amplifier.

The micro-scanner consists of three plates (Fig. 1, *1*, *2* and *3*) which are movable against each other in pairs. The preparation holder is fitted to the top-plate, but on the same level as it is ordinarily placed when no scanner is used. The bottom-plate

(Fig. 1, *1*) is attached to the microscope table and hence it is still possible to move the preparation in two dimensions. In this plate three V-formed grooves are ground. In each of these there is a steel ball. These balls support the middle plate (Fig. 2, *2*) in which two corresponding V-formed grooves are ground. The position of the third steel-ball is ground as a flat face. In this way a stable three-point suspension is obtained which is movable in the longitudinal direction of the grooves. The top-

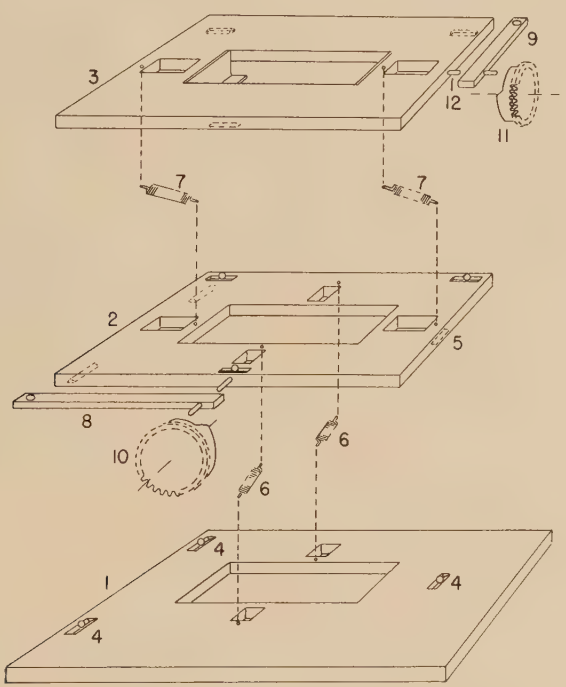

Fig. 1.—Principle drawing of the micro-scanner.

plate is connected with a middle-plate in a corresponding way. The direction of the V-formed grooves is, however, perpendicular to that of the bottom-plate. In this way a two-dimensional movement is obtained.

In order to obtain a good contact surface of the plates against the balls, two pairs of springs are arranged as is seen from Fig. 1, *6* and *7*. Furthermore, by the action of the springs, the top-plate and the middle-plate will be pressed against the levers at *8* and *9* in Fig. 1. The levers can be turned in the horizontal plane and will each press against its own cam profile (Fig. 1, *10* and *11*). The contact surface consists of small rounded-off and hardened steel-pins which are fixed in the plates and the levers respectively. In order to avoid a distorting *momentum*, steel-pins of the plates and the springs are arranged linearly. The cam profile at *11*, Fig. 1, consists of a steel cog wheel rotating on an axis which is parallel with the direction of movement of the top-plate. The plane face of the cog wheel facing the plate has been given the shape of one single thread, the lead of which is 320 μ. As the support of the cog wheel is

fixed in relation to the bottom plate, and through this in relation to the microscopic optics, the following cycle will be carried through when the cam-profile (=the cog wheel) rotates one turn: the top-plate is moved in one direction with an even velocity and returns to the initial position when the turning of the thread has been completed. The cam profile of the top-plate is driven by a synchronous motor with a gear ratio of 60/64. The number of revolutions of the motor is 30 rpm. The velocity is adjusted

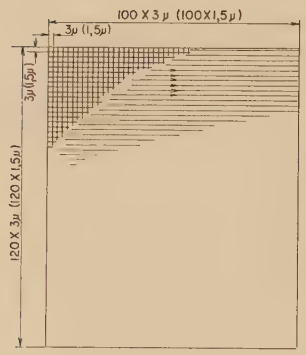

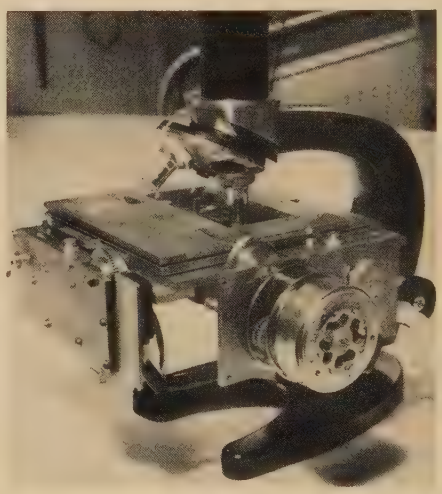

Fig. 2 (*left*).—The scanned area.
Fig. 3 (*right*).—The micro-scanner applied to the microscope.

to the measuring frequency of the cell analyser, which is 50 measuring points per second. In two seconds the cam wheel turns $\frac{60}{64}$ of a whole revolution and thus the top-plate, on which the object is attached, is moved 300 μ. During this movement the transmission value of 100 measuring points is registered. During the remaining $\frac{4}{60}$ seconds, the cam wheel completes the remaining $\frac{4}{64}$ of the revolution. Concomitantly with the returning to the original position an impulse from a micro-switch is emitted. The micro-switch is actuated by a cam, projecting from the periphery of the cam profile. The impulse goes to a relay which actuates a ratchet-wheel with 90 teeth. Through a gear this wheel drives the second cam profile which in its turn actuates the middle plate. This last cam profile has a lead of 380 μ. Through this mechanism the middle-plate is moved 3 μ in one direction by each impulse. The movement is transferred via the top-plate to the object. In that way the subject will undergo a continuous movement in the horizontal direction in relation to the optic axis of the microscope. At this process 100 measuring points, 3×3 μ each, are registered. When one line is scanned, the preparation is moved 3 μ along the Y-axis and 100 new measuring points are calculated, and so on, until 120 lines are scanned. At this moment the calculation by the cell analyzer is automatically stopped and a surface of 300×360 μ has thus been scanned, calculated and registered (Fig. 2).

The movement along X and Y can be diminished by changing the attachment for the levers *8* and *9* in Fig. 1 and the cam-profiles in relation to the lower plate. 150 × 180 μ seems to be a suitable range for a smaller area. Using the same stop-field in front of the photo-multiplier and doubling the lateral magnification, a scanning with higher resolution can be attained.

It is important to obtain a linear ratio between the movement of the object and time. Therefore, the grinding of the cam profile has to be performed with precision. A test showed that the maximum deviation at a movement of 300 μ of an object is less than *1* μ, i.e. measuring points situated in the middle of one line are "delayed" by less than 1 μ. The bearing surface of the cam profiles has been made rather large and produced in the same chucking as the grinding of the profiles. The bearing surface of the axial shaft has been made so large that a counter-force for the spring pressure of the plates is obtained.

Usually the details of a construction can be carried out in many ways. One point may be commented upon. The pressure of the top plate against its own cam profile will result in a lateral pressure in the bearing between the bottom plate and the middle part. This, however, has not proved to be a weak point, the bottom pair of springs (*6* in Fig. 1) having been constructed more rigid than the top pair (*7* in Fig. 1). Furthermore, the steel pin of the top plate (*12* in Fig. 1) will not adhere at the same point of the lever when the top plate follows the movement of the middle plate. When the area scanned is 300 × 360 μ, the length of the lever is 50 mm. Then the 60th-line scanning will be 300 μ whereas the first and the 120th will be:

$$\text{The first scanning line:} \quad \frac{300(50 + 0.360/2)}{50} = 301.08\ \mu.$$

$$\text{The 120th scanning line:} \quad \frac{300(50 - 0.360/2)}{50} = 298.92\ \mu.$$

The main point is that the surface of the measuring points is determined by the size of the field stop. These points are all of similar size, although their geometrical localization differs from the correct position, except in the 60th line. The deviations are, however, so small, that it was considered preferable to accept this error instead of the inconvenience of having the cam profile and motor movable in relation to the microscope.

REFERENCES

1. Bourghardt, S., Hydén, H. and Nyqvist, B., *J. Sci. Instr.* **32**, 186 (1955).
2. Deeley, E. M., *J. Sci. Instr.* **32**, 263 (1955).
3. Hydén, H. and Larsson, S., *J. Neurochem.* **1**, 134 (1956).
4. Tolles, W. E., *Trans. New York Acad. Sci. Ser. II* **17**, 250 (1955).

THE FINE STRUCTURE OF THE MESONEPHROS OF THE 17-DAY RABBIT EMBRYO

T. S. LEESON

University College of South Wales & Monmouthshire, Cardiff, U.K.

Received March 15, 1957

This is a preliminary report of a more extensive investigation into the embryonic and foetal kidneys of the rabbit. It has been shown by Gersh [1] and by Leeson and Baxter [3] that by 17 days the rabbit mesonephros is a large organ, fully formed and fully differentiated. The most rostral one or two nephrons, i.e., the oldest, may be degenerate.

Since 1950, many studies have been made of the ultrastructure of the adult metanephros in many vertebrates but the embryonic kidney has been singularly neglected.

Material and Methods.—The embryos were obtained from does 17 days after observed matings and varied in size from 17.8 to 19.2 mm C.R. before fixation. The mesonephroi, which measured about 2.5 × 0.5 mm were dissected gently from the embryos with glass needles and either fixed whole or cut into cubes of side 0.5 mm. Fixation and preparation were routine, the sections being cut on a Sims–Leeson heat-advance ultramicrotome [5] and examined in a Metropolitan-Vickers E.M.3 electron microscope.

Results.—The similarity between the fully-developed mesonephric glomerulus and that of the adult metanephros is most striking, although at low magnifications the arrangement of the capillary loops seemed more 'open' than in the metanephros. The 'basement membrane' of light microscopy is seen by electron microscopy to

---

All figures are of the 17-day rabbit embryo mesonephros.

Fig. 1. This is a visceral epithelial cell of Bowman's capsule or podocyte with its nucleus (*N*), mitochondria (*M*) and elements of the endoplasmic reticulum (*E. R.*). Processes of this cell, pedicels (*P*) extend to be attached to the lamina densa (*B*) of the glomerular capillary lined by a thin endothelial sheet (*E*). These pedicels may branch (arrows). × 10,000.

Fig. 2.—A higher power of the "basement membrane" to show pedicels (*P*), some of which branch (arrow), attached to lamina densa (*B*) with endothelial cytoplasm (*E*). × 16,000.

Fig. 3.—This shows the complexity of the mesonephric glomerulus. The lamina densa (*B*) is cut tangentially and attached to it are numerous interlacing pedicels (*P*). × 16,000.

Fig. 4. –A cell of the proximal segment of the tubule showing nucleus (*N*), lumen (*L*), microvilli (*A*), mitochondria (*M*) and numerous large vesicles (*V*). × 4,500.

Fig. 5.—A higher power of the brush border of the proximal segment showing microvilli and the numerous small vesicles. Lumen (*L*) and plasma membrane (*C*) between two cells are shown. × 16,000.

Fig. 6.—Cells of distal segment with basement membrane (*B*), lumen (*L*), nuclei (*N*), mitochondria (*M*) and infoldings of the basal layer of the plasma membrane at arrow. × 4,500.

Fig. 7.—Two adjacent collecting ducts with sparse microvilli (*A*). × 3,000.

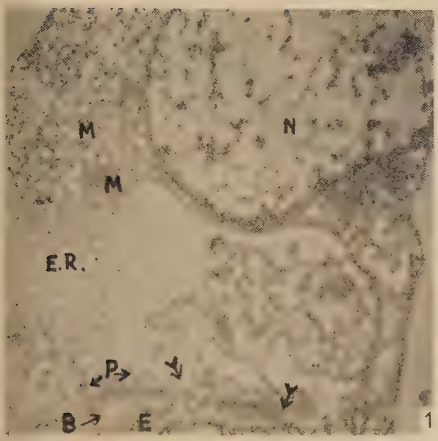

1

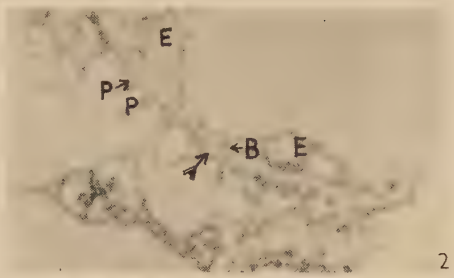

2

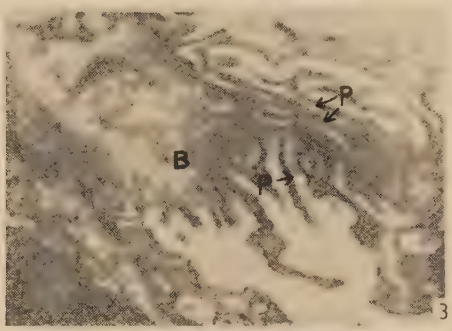

3

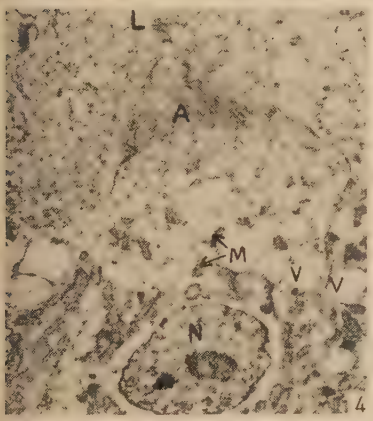

4

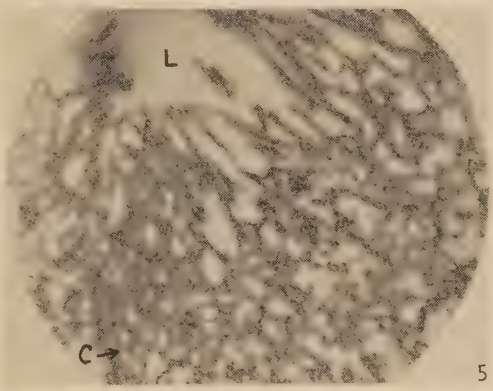

5

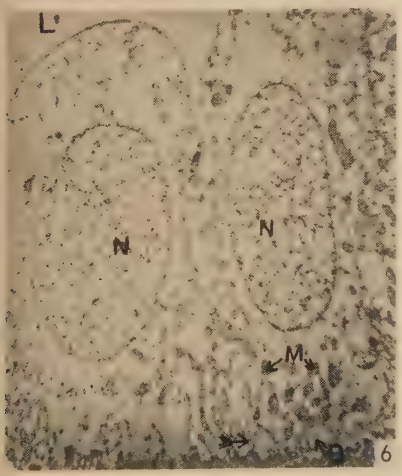

6

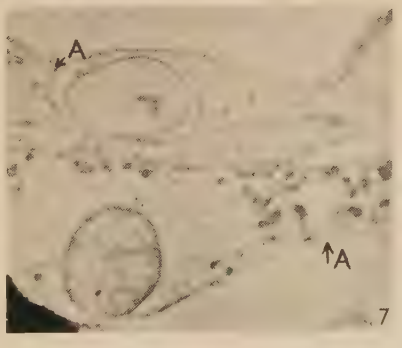

7

consist of three layers, as has been described by many authors in the adult metanephros, for example Hall [2]. Lining the glomerular capillary is a thin attenuated sheet of endothelial cytoplasm which in suitable tangential sections is seen to be perforate. External to this is a dense, homogenous definitive basement membrane to which are attached on its outer surface numerous small foot processes or pedicels of the visceral epithelial cells or podocytes. These pedicels are of a uniform cross-section and some appear to bifurcate to form a Y-shape at their attachment to the basement membrane. Between them are filtration slits of the urinary or capsular space. Excluding blood cells, only endothelial and epithelial or podocyte cells have been seen and no intercapillary elements, or mesangium, have been noted.

In the adult mouse, Rhodin [4] described the lumen of the proximal tubular segment as collapsed but in the mesonephros a lumen has always been observed. There is a well marked basement membrane around the tubule and in both proximal and distal segments the basal layer of the plasma membrane is infolded to form pockets in the cytoplasm. These infoldings are more complex in the metanephric distal segment. In the pockets so formed are long filamentous mitochondria. In the apical region of the proximal segment cell are situated numerous large vesicles which may be identical with the fluorescent granules described in 1945 by Sjöstrand [6] and later identified in an electron-microscope study by Sjöstrand and Rhodin [7]. The plasma membrane in the apical region of the proximal segment cell is evaginated to form numerous microvilli which form the brush-border and are associated with very many small vesicles. In the distal segment, the apical plasma membrane is either smooth with marked clefts between adjacent cells or may show a few sparse, short microvilli scattered indiscriminately. These may also be seen in the collecting ducts.

Conclusion. At this preliminary stage, to draw any conclusions would be unwise but it is fair to comment on the extreme degree of similarity in structure between the 17-day mesonephros and adult metanephros of the rabbit, and to suggest that this complexity of structure in the mesonephros, and particularly in the mesonephric glomerulus, is probably associated with a urinary function.

REFERENCES

1. Gersh, I., *Contr. Embryol.* No. 153 (1937).
2. Hall, V., Proceedings of the 6th Annual Nephrotic Conference, p. 1, 1954.
3. Leeson, T. S. and Baxter (In preparation).
4. Rhodin, J., Correlation of Ultrastructural Organization and Function in Normal and Experimentally Changed Proximal Convoluted Tubule Cells of the Mouse Kidney. Stockholm, 1954.
5. Sims, A. L. and Leeson, T. S., *J. Sci. Instr.* (1957). In press.
6. Sjöstrand, F., *Acta Anat. Suppl.* **1**. (1945).
7. Sjöstrand, F. and Rhodin, J., *Exptl. Cell Research* **4**, 426 (1953).

A DEVICE FOR SEPARATING FRACTIONS AFTER GRADIENT DENSITY CENTRIFUGING

J. W. P. PHELPSTEAD and D. B. ROODYN

Medical Research Council Radiobiological Research Unit, A.E.R.E., Harwell, Berks., England

Received March 17, 1957

Since the report by Brakke in 1951 [2] of the use of a medium of graded specific gravity for the fractionation of virus particles, many workers have used continuously or discontinuously graded media for the fractionation of cell homogenates (for example see [4, 5, 1, 7]). One of the difficulties in such a technique is in cleanly removing the various layers at the end of the centrifuging without causing mixing. A Lucite sampling device has been described by Hogeboom and Kuff [3] in which the fractions are passed through a perforated plate before removal. The authors mention difficulties in effecting complete removal of fluid from the sampling device and present evidence for the possible spreading of the sedimentation boundary of protein solutions because of the sampling technique. Kuff and Schneider [5] mention the use of a special knife described by Randolph and Ryan [6], that cuts the centrifuge tube but refer to problems of leakage around the blade. A perspex apparatus that avoids the use of metal parts has been described by Anderson [1]. The following apparatus is based on similar principles except that an enclosed perspex shutter is used, resulting in greater ease of operation and negligible leakage of fluid.

The apparatus (Fig. 1) consists essentially of two blocks of perspex *U* and *L* separated by a thin perspex sheet *C*. A channel in the sheet *C* allows a disc-shaped shutter to slide on the upper surface of the block *L*. A hole passes through *U*, *C* and *L*. The plastic centrifuge tube is pushed into position over a collar *K* projecting from the lower surface of the block *L*. Heavy fluid is flowed from a hypodermic syringe into the bottom of the centrifuge tube via a thin glass tube *T* which tightly fits into a hole under the shutter and the entire contents of the tube is pushed up into the central hole. When a suitable quantity of liquid has passed the shutter, it is closed and the fraction is sucked off.

The apparatus is constructed as follows: The blocks *U* and *L* and the sheet *C* are screwed together and a hole 1″ diameter drilled and bored through them. In the bottom of the lower block *L*, the hole is enlarged with a boring tool for a depth of $\frac{1}{4}$″ to a diameter of $1\frac{1}{2}$″. The collar *K* is then made as follows: perspex rod of $1\frac{1}{2}$″ diameter is drilled out with a $\frac{1}{2}$″ drill and a length of $\frac{1}{2}$″ from the end turned down to an outside diameter of $1-\frac{1}{16}$″ so that the plastic centrifuge tubes used (4″ long and $1-\frac{1}{16}$″ internal diameter) fit firmly over the collar. The wide part of the rod is then trimmed to a length of $\frac{1}{4}$″ and firmly cemented with chloroform into the $1\frac{1}{2}$″ diameter hole in the bottom of the lower block *L*. The $\frac{1}{2}$″ hole in the centre of the rod is then enlarged to 1″ so as to be continuous with the central hole through *U*, *C* and *L*. As a result the collar projects $\frac{1}{2}$″ from the bottom of the apparatus and has a final wall thickness of $^1/_{32}$″.

The shutter mechanism is made as follows: a slot is cut through the $\frac{1}{16}$″ thick

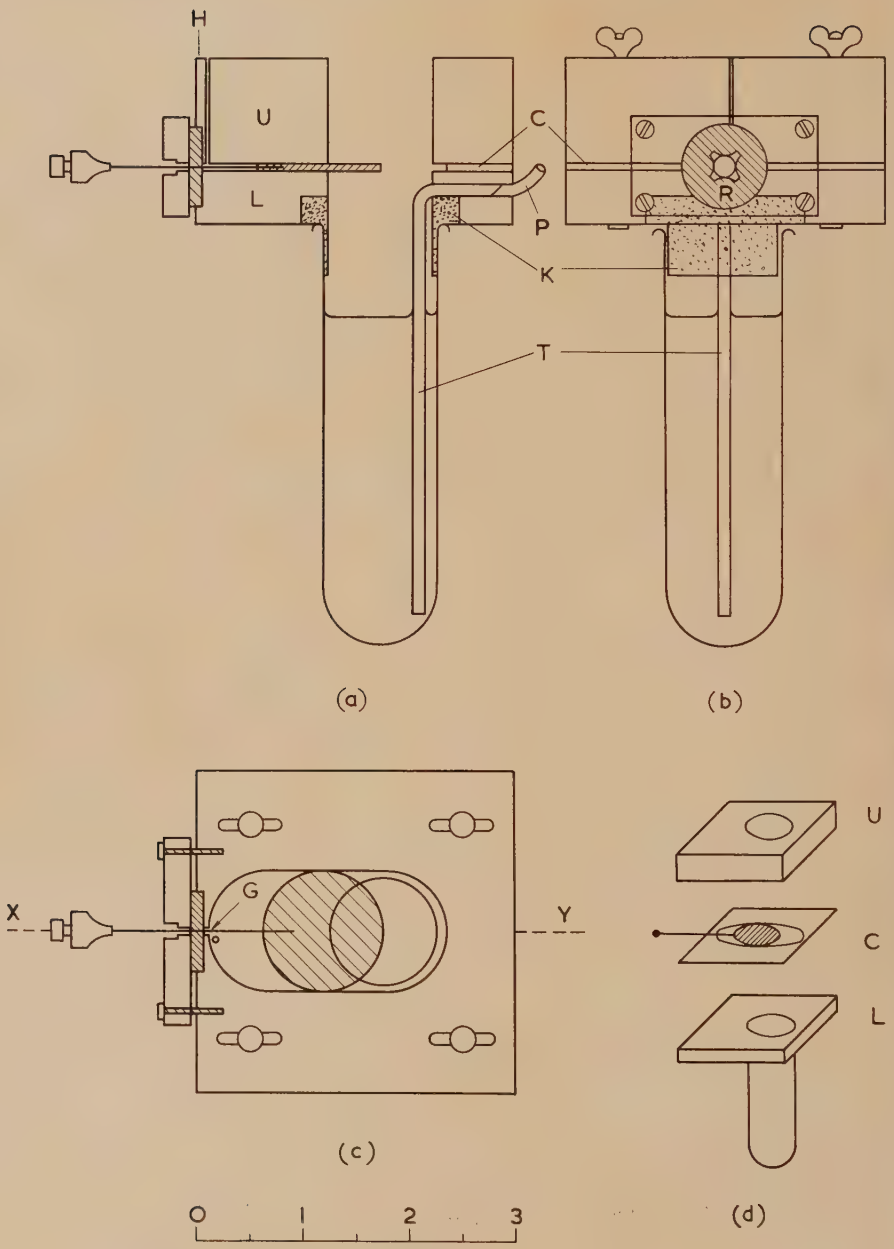

Fig. 1 (*b*).—Side view (*c*) Plan (*a*) Section through XY.
Fig. 1 (*d*). —Simplified diagram of shutter mechanism. Scale in inches. *P* is polythene tubing connecting to a hypodermic syringe. Other symbols explained in text.

perspex sheet *C* with a $1\frac{1}{8}''$ end mill and a disc slightly wider than the channel is turned from similar sheet. Opposite edges of the disc are then filed until the disc can just slide freely in the channel without rotating or sticking. The shutter is moved by a size *O* hypodermic syringe needle cemented into a hole drilled in it. Leakage from the shutter space through the gap *G* is prevented by a $\frac{1}{8}''$ rubber washer *R* sunk into the side of the apparatus. Sheet *C* is cemented onto block *L* but the upper block is only held in position by screws and wing nuts so that the apparatus can be dismantled and cleaned. A small hole *H* diameter 0.03″ is drilled from the upper surface of the block *U* into the edge of the space enclosing the shutter to allow air to enter and leave as the shutter is moved. The apparatus is polished so that the fractions can be observed during cutting.

The efficiency of the apparatus was tested as follows: 10 ml of 50 per cent v/v glycerol containing some methyl violet was put in the bottom of the centrifuge tube and 30 ml of 40 per cent v/v glycerol was layered over it. 70 per cent v/v glycerol was introduced into the bottom of the tube until the dyed layer had been removed. 97 per cent of the dye was removed in two consecutive 5.0 ml fractions and the total recovery of dye in all fractions was 99.5 per cent showing that losses through leakage are negligible and that disturbances of the layer during fraction cutting only resulted in a loss to other fractions of 3 per cent of the material present.

The authors would like to thank Mr. J. St. L. Philpot and Mr. D. Stock for kind help and advice.

REFERENCES

1. Anderson, N. G., *Exptl Cell. Research* **9**, 446 (1955).
2. Brakke, M. K., *J. Am. Chem. Soc.* **73**, 1847 (1951).
3. Hogeboom, G. H. and Kuff, E. L., *J. Biol. Chem.* **210**, 733 (1954).
4. Holter, H., Ottesen, M. and Weber, R., *Experientia* **IX**, 346 (1953).
5. Kuff, E. L. and Schneider, W. C., *J. Biol. Chem.* **206**, 677 (1954).
6. Randolph, M. L. and Ryan, R. R., *Science* **112**, 528 (1950).
7. Roodyn, D. B. *Biochem. J.* **64**, 361 (1956).

THE EFFECTS OF RIBONUCLEASE AND OTHER BASIC PROTEINS ON THE INCORPORATION OF C^{14}-L-LEUCINE INTO LIVER PROTEINS *IN VITRO*

T. HULTIN, ALEXANDRA VON DER DECKEN and GUNILLA BESKOW

The Wenner-Gren Institute for Experimental Biology, University of Stockholm, Sweden

Received March 28, 1957

A considerable number of experiments, both on living cells and on cell-free cytoplasmic systems, suggest a functional connection between protein metabolism and structural ribonucleoproteins [cf. 7, 3, 10, 19, 11, 15, 12]. In support of this concept

it has been demonstrated that ribonuclease inhibits the incorporation of labeled amino acids into proteins in cellular as well as in non-cellular systems [1, 14, 8, 19, 4, 5]. Recent experiments by Brachet [5, 6] have shown that in the cells of living root tips basic proteins (histone, protamine, cytochrome *c*) exert a similar inhibitory effect, presumably by forming a complex with the nucleic acids. It was observed that in the same cells the inhibition of amino acid incorporation by ribonuclease

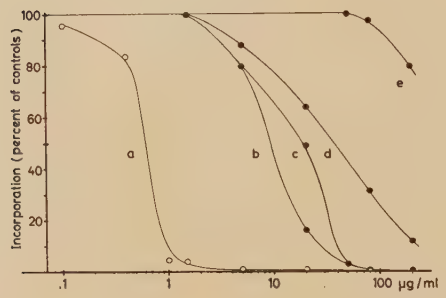

Fig. 1.—The incorporation of C^{14}-L-leucine into the proteins of a cell-free rat liver system containing microsomes and cell fluid. The effects on the incorporation of different concentrations (μg per ml) of (*a*) ribonuclease, (*b*) clupein, (*c*) echinoderm sperm protein, (*d*) lysozyme and (*e*) cytochrome *c*. The specific activities of the control samples were approximately 600 c.p.m. per cm^2 (indefinite sample thickness).

took place more rapidly than the disappearance of the cytoplasmic basophily. For these and other reasons it was propounded as a possibility that also ribonuclease in the inhibition of amino acid incorporation may primarily act as a basic protein, not as a specific enzyme.

In order to examine this possibility under more easily controled conditions the inhibitory effect of ribonuclease on the incorporation of C^{14}-L-leucine into proteins was compared with the effects of other basic proteins in a cell-free liver system.

Experimental.—Male albino rats (150–200 g) were used in the experiments. The incubation medium contained KCl (0.025 *M*), $MgCl_2$ (0.01 *M*), potassium phosphate (0.02 *M*, pH 7.8), tris (hydroxymethyl)aminomethane (0.03 *M*, pH 7.8), and sucrose (0.25 *M*). The livers were minced and washed in this medium, and then homogenized in 2.5 volumes of the same solution by means of a glass homogenizer. The homogenates were centrifuged for 5 minutes at 12000 × g (mean gravitation) in order to remove tissue fragments, nuclei and mitochondria. Of the supernates 0.7 ml were added to test tubes containing, in a volume of 0.2 ml, 0.08 μM-L-leucine (1.5 mc per m*M*), 10 μM phosphoenolpyruvate, and varied amounts of ribonuclease or other basic proteins. Immediately after the addition of the homogenate 1 μM of ATP (0.1 ml) was added to the samples. (ATP was added as the last constituent in order not to form precipitates with the basic sperm proteins in the higher concentrations.) The preparation of the incubation samples was carried out at nearly 0°C.

The samples were incubated at 35°C for 15 minutes. Immediately after the incubations L-leucine in large excess was added to the samples for the purpose of isotope dilution, followed by trichloroacetic acid to a final concentration of 10 per cent. The precipitated proteins were purified by a slightly modified Schneider procedure [17]. The activity of the protein samples, determined by a thin mica window counter, was recalculated for indefinite sample thickness (1 cm^2 plate area) on the basis of an empirical activity saturation curve.

Effects of ribonuclease and other basic proteins on the incorporation.—As is shown by the figure the incorporation of C^{14}-L-leucine was strongly inhibited by ribonuclease (Sigma, "5 × crystallized"). The inhibition was almost complete already at a ribonuclease concentration of 1 μg per ml. Since no preincubation was carried out, the inhibition must have been nearly instantaneous. Ribonuclease is a weakly basic protein (isoelectric point 9.45 [2]). If the rapid inhibition of the incorporation were primarily due to non-specific ionic interaction between the ribonuclease molecules and vital centra in the ribonucleoprotein structure, inhibitory effects of at least similar strength should be expected in the case of proteins of more pronounced basic character. The following basic proteins were tested in the incorporation system: cytochrome *c* (I.E.P. 10.65 [18], a Sigma preparation), lysozyme (I.E.P. 11.0 [2], Nutritional Biochemicals Co.) clupein (I.E.P. about 12 [16], British Drug House), and a basic sperm protein from the echinoderm *Brissopsis lyrifera* (Forb.), containing approximately 23 per cent lysine, 14 per cent arginine and 1 per cent histidine [9, 13]. It was observed that even the extremely basic sperm proteins had to be added in about 20 times larger amounts than ribonuclease in order to inhibit the incorporation process to the same extent. Lysozyme, and particularly cytochrome *c* were considerably weaker inhibitors.

The experiments show that ribonuclease inhibits the incorporation process in a distinctly specific way. The rapid onset of the inhibition may be taken as an indication that the effect is primarily due to a formation of specific complexes between the enzyme and the ribonucleoprotein structures, conceivably of the enzyme-substrate type. It would be difficult, however, under such conditions, to exclude the possibility of a simultaneous, rapid disconnection of a critical number of nucleotide groups of vital significance for the incorporation reaction.

REFERENCES

1. Allfrey, V., Daly, M. M. and Mirsky, A. E., *J. Gen. Physiol.* **37**, 157 (1953).
2. Anderson, E. A. and Alberty, R. A., *J. Phys. Colloid. Chem.* **52**, 1345 (1948).
3. Brachet, J., *Arch. Biol., Liège* **53**, 207 (1941).
4. —— *Nature* **174**, 876 (1954).
5. —— *Biochim. et Biophys. Acta* **16**, 611 (1955).
6. —— *ibid.* **19**, 583 (1956).
7. Caspersson, T., *Naturwissenschaften* **29**, 33 (1941).
8. Gale, E. F. and Folkes, J. P., *Nature* **173**, 1223 (1954).
9. Hultin, T., *Pubbl. Staz. Zool. Napoli* **21**, 153 (1947).
10. —— *Exptl. Cell Research* **1**, 376 (1950).
11. —— *ibid. Suppl.* **3**, 210 (1955).
12. Hultin, T. and von der Decken, A., *Exptl. Cell Research* (in press).
13. Hultin, T. and Herne, R., *Arkiv Kemi, Mineral. Geol.* **26** *A*, No. 20 (1948).
14. Lester, R. L., *J. Am. Chem. Soc.* **75**, 5448 (1953).
15. Littlefield, J. W., Keller, E. B., Gross, J. and Zamecnik, P. C., *J. Biol. Chem.* **217**, 111 (1955).
16. Mujake, S., *Hoppe-Seyl. Z.* **172**, 225 (1927).
17. Schneider, W. C., *J. Biol. Chem.* **161**, 293 (1945).
18. Theorell, H., *J. Am. Chem. Soc.* **63**, 1820 (1941).
19. Zamecnik, P. C. and Keller, E. B., *J. Biol. Chem.* **209**, 337 (1954).

LIGHT SCATTERING STUDIES ON SINGLE ASCITES CARCINOMA CELLS[1]

J. R. MEYER-ARENDT and A. P. HORAVA

Department of Pathology, Ohio State University, Columbus, Ohio, U.S.A.

Received April 1, 1957

Light scattering usually represents one of the potential pitfalls in microspectrophotometry [3, 5, 7]. On the other hand, light scattering studies are widely used to gain information on molecular weights and shapes [1, 6]. Light scattering, or, better, turbidimetric measurements on blood serum have also been proposed [2, 4] as a means for distinguishing cancer patients from healthy individuals.

To perform similar studies at a strictly cellular level, an optical arrangement has been designed that permits scattered light measurements on single tissue cells of cell nuclei or other cellular components *in situ*. The principle of the optical set-up is shown in Fig. 1. Two pinholes, each measuring 40 μ in diameter, are provided for projecting, by means of an objective of 50 mm focal length, f:9, a narrow light

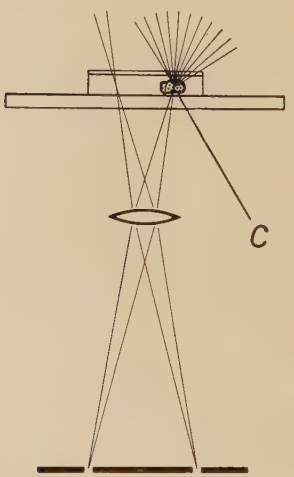

Fig. 1.—Ray diagram showing the optical arrangement used for microscopic light scattering studies. C = cell object.

[1] This investigation was supported by a research grant (C-2834 BBC) from the National Cancer Institute, Public Health Service, Department of Health, Education, and Welfare; and by an Institutional Grant of the American Cancer Society to the Ohio State University College of Medicine.

Fig. 2.—Above, ascites carcinoma cells, Papanicolaou stain, normal photomicrograph. Center: light scattering pattern arising from a single ascites carcinoma cells nucleus (right). At left: control beam; below: densitometer readings derived from the scattering pattern above. The scattering pattern printed here shows, of course, less details than the densitometer reading taken from the original negative.

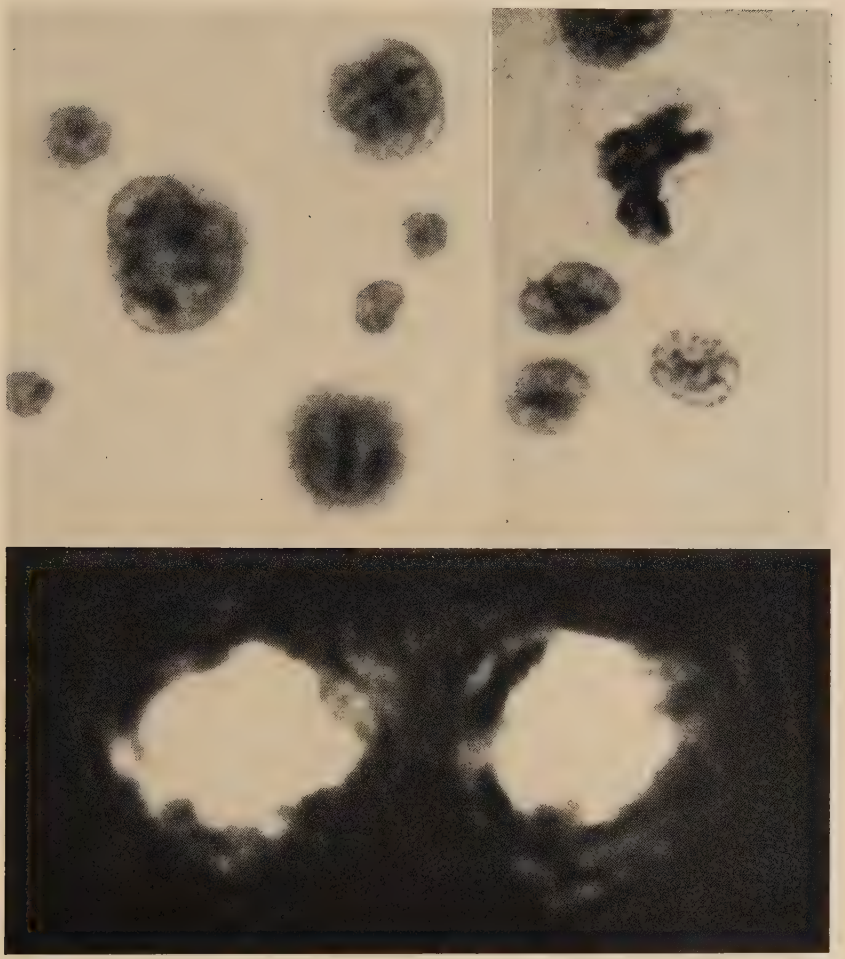

beam of not more than 4 μ in diameter when entering the specimen. Monochromatic light of 546.1 mμ wavelength is obtained from a mercury vapor lamp. One of the light beams is directed onto the structure detail under investigation (designated "C" in Fig. 1); the other beam serves as a reference. Using a reference beam is necessary, since in many cases some diffraction and scattering effects do occur also within empty areas of the specimen, due to impurities and inhomogeneities in the mounting medium, glass slides, etc. The polarization of the incident beams has been neglected. As the microscope objective, a high-power oil immersion planachromatic Zeiss objective has been used. If the objective is slightly out of focus by a given degree, the distribution of the scattered light around the detail of the microscopic structure will be imaged as shown in Fig. 2, center.

We carried out measurements on the nuclei of single tumor cells from a transplantable mouse Ehrlich's ascites carcinoma with modal tetraploid chromosome number.[1] The tumor is composed of a fluid which is exudative in nature and a cell population containing 90 to 95 per cent of tumor cells and 5 to 10 per cent inflammatory cells. The tumor cells show a scant faintly basophilic vacuolated cytoplasma and a rather prominent vesicular nucleus. The nuclear membrane is clearly visible in non-stained smears by phase-contrast microscopy, and also in stained smears. There are usually one or two prominent nucleoli. The distribution of the chromatin assumes a pattern of irregularly scattered large but smoothly delineated clumps. The average tumor cell diameter is 15.4 μ (fresh, non-fixed preparation); the nuclear diameter (long axis) is 12.1 μ; and the average tumor-cell and tumor-nucleus-volume were calculated: cell-volume 2070 cu. μ, nucleus 1450 cu. μ.

Fig. 2 shows, on top, a normal photomicrograph of mouse ascites tumor cells and, center, the distribution of the scattered light arising from the nucleus of one of such a carcinoma cell.[2] The cell suspension was spread onto a microscopic slide, air-dried, and simply covered with a coverslip, thus mounted only in air as used occasionally for microscopic interferometer measurements [2]. No special fixing, embedding, or staining procedures have be to employed. The light beam passing through the carcinoma cell nucleus, at the right in Fig. 2, center, is considerably scattered by the fine structure of the chromatin; usually, also the reference beam, on the left, is partially broadened by scattering and refraction effects due to irregularities on the surface of the air-mounted specimen. Quantitative evaluation is possible by scanning across the diffraction photomicrographs by means of a microdensitometer (Fig. 2, below). Curves obtained in this manner, indicating the light distribution behind the structure detail and behind the reference, enclose areas that are related in a ratio of 73 (reference) to 68 (cancer cell nucleus), i.e. they were approximately equal in size as they should. However, the light beam passing through the cancer cell nucleus shows a markedly broader splitting and scattering compared with the reference beam, only a part of which seems to be due, as suggested by some well defined peaks in the densitometer readings, to Fresnel diffraction on somewhat larger, visible structures within the cancer cell nucleus. At an out-of-focus distance of 106 μ, the 100 $\times$ objective used in this study still collects light from the object within an angle of 49° from the optical axis. Thus, the most peripheral light effects seen in the

[1] Made available to us by the courtesy of Dr. T. S. Hauschka.
[2] The photographs were taken by Mr. Gilford R. Millard.

scattering pattern represent stray light emitted from the specimen under this angle. Other angles can be derived by extrapolation, permitting the computing of optical data as in ordinary light scattering work. Purely empirical findings like those reported here are theoretically not yet fully explained. However, they seem to depend, in part, upon molecular characteristics (turbidity) of the substrate itself and, in part, upon the roughness of its surface when drying. Such surface characteristics themselves seem likewise to be related to the physicochemical composition of the matter under investigation. Together, the evaluation of such characteristics seems to represent a new addition to already known optical investigation methods such as ultraviolet absorptiometry, and interference and phase-contrast microscopy.

Summary.—Light scattering usually limits the validity of optical microscopic measurements. To overcome this limit, an optical arrangement has been designed that utilizes just such light scattering phenomena as a means for obtaining information on biological material. Measurements on ascites carcinoma cells indicate that this method permits the study of light scattering arising from minute cell components such as cell nuclei *in situ*.

REFERENCES

1. Edsall, J. T., *in* The Proteins, Chemistry, Biological Activity and Methods. H. Neurath and K. Bailey, eds., Vol. *I*, part *B*, pp. 602–616, Academic Press, New York, 1953.
2. Mellors, R. C., Kupfer, A. and Hollænder, A., *Cancer* **6**, 372 (1953).
3. Ornstein, L., *Lab. Invest.* **1**, 250 (1952).
4. Quinn, J. A., Katz, St. A. and Rappoport, A. E., *Am. J. Clin. Pathol.* **25**, 1128 (1955).
5. Scott, J. F., *Lab. Invest.* **1**, 73 (1952).
6. Stacey, K. A., Light-Scattering in Physical Chemistry. Academic Press, New York, 1956.
7. Svensson, G., *Exptl. Cell Research* **6**, 529 (1954).

ELECTRON MICROSCOPE STUDIES ON THE FINE STRUCTURE OF THE OVARY

I. STUDIES ON THE ORIGIN OF YOLK

G. YASUZUMI and H. TANAKA

Electron Microscope Research Laboratory, Department of Anatomy, Nara Medical College, Kashihara, Nara Pref., Japan

Received April 4, 1957

Although the process of formation of yolk has been studied by classical cytological methods [2, 3, 5–7, 10], many details of the complex cytological differentiation involved have remained obscure because of the limited resolving power of the light microscope. The present electron microscope study on the formation of yolk in the pond-snail provides detailed and accurate information regarding the relationship between the chromidal substance and Golgi complex suggested by light microscopy.

The tissue of the ovary of *Cipangopaludina malleata* was fixed in 1 per cent osmium tetroxide solution (pH 7.3) [9, 11], and embedded in a mixture of butyl methacrylate and methyl methacrylate, containing by weight 0.2 per cent benzol peroxide 8. After being polymerized the tissue was sectioned with a Shimadzu-ultramicrotome and examined in low power in an Akashi electron microscope model TRS–50.

The juxtanuclear region of an undifferentiated germinal cell is seen to be composed of a set of parallel rods which appear as a set of loops strung in a line. The rods are the double-walled lamellae in which their outside surface is covered by small, dense granules (Figs. 1 and 2). In the advanced stage of maturation of the oocyte, many circular or ovoid bodies 0.4–0.8 μ in the diameter appear in the juxtanuclear region. They are surrounded by a clearly defined limiting membrane, and some (G_1) of them contain a light substance and a few masses of dense substance, and others (G_2) a considerable number of fine granules of intermediate density (Fig. 3). The prominent cytoplasmic organelle in the juxtanuclear region of the oocyte has been called by Hertwig (1899) "Chromidien" in German [4]. Numerous authors since the time of Hertwig have thought that the chromidal substance is chemically similar to the nucleolar substance and even supported the idea of its nuclear region. With the help of absorption microspectrophotometry, it has been found that the chromidal substance contains nucleoproteins of the ribonucleic acid type [1].

The chromidal bodies migrate to come into close contact with the Golgi complex, and thus a number of chromidal bodies are found scattered in the matrix of the ground substance between the Golgi complex (Fig. 4). In this stage the bodies are filled up with dense osmiophilic substances. As the differentiation of the oocyte proceeds, the chromidal bodies are subsequently surrounded by the Golgi complex (Figs. 5 and 6). In a little more advanced oocyte, the dense, granular character of the chromidal substance is gradually lost and is replaced by a pattern of the less opaque, homogeneous substance (Fig. 7). The chromidal substance is perfectly enveloped by the Golgi complex, and at the same time the spaces of parallel double membranes have become progressively wider. Thus the yolk granule is completed, showing a feature resemble that of the Vater-Pacini corpuscle in an elliptical form measuring about 2.0 2.5 × 2.5 3.0 μ. There is little or no electron-scattering material between the lamellar structure of the yolk granule and in its center. The lamellae are probably separated from one another by a clear fluid or semi-fluid substance in life (Fig. 8). Concurrently with the formation of yolk the lipid granule (L) appears in the cytoplasm, suggesting to be orginated from the chromidal substance as a result of separation of its chemical composition (Fig 9).

Fig. 1.—Low power electron micrograph showing the fine structure of endoplasmic reticulum of an undifferentiated germinal cell. The endoplasmic reticulum shown by this micrograph appears to be roughly parallel to the nuclear membrane. × 16,720.

Fig. 2.—Low power electron micrograph of the endoplasmic reticulum of an undifferentiated germinal cell, showing particles adhering to the membrane of the endoplasmic reticulum. × 25,500.

Fig. 3.—Low power electron micrograph of the advanced stage of the oocyte, showing part of the nucleus (N) and the cytoplasm including the chromidal bodies (G_1 and G_2). × 25,200.

Fig. 4.—A section through a little more advanced oocyte including the chromidal bodies between the Golgi complex. The chromidal bodies comprise dense osmiophilic granules. × 21,300.

1

2

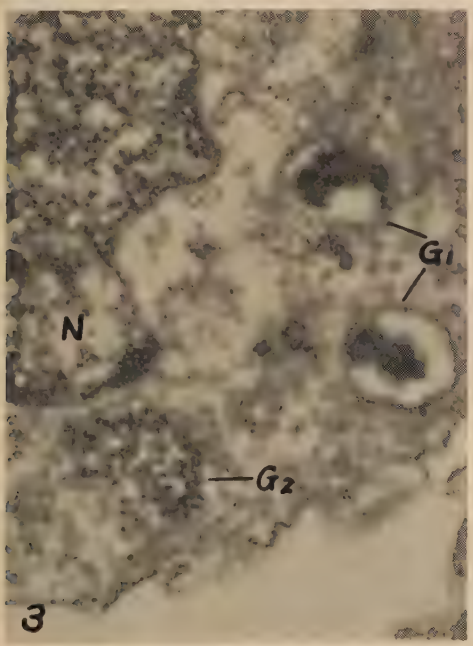
N
G1
G2
3

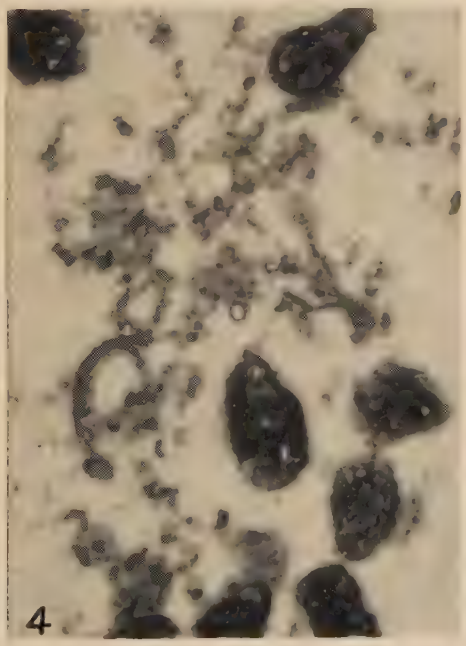
4

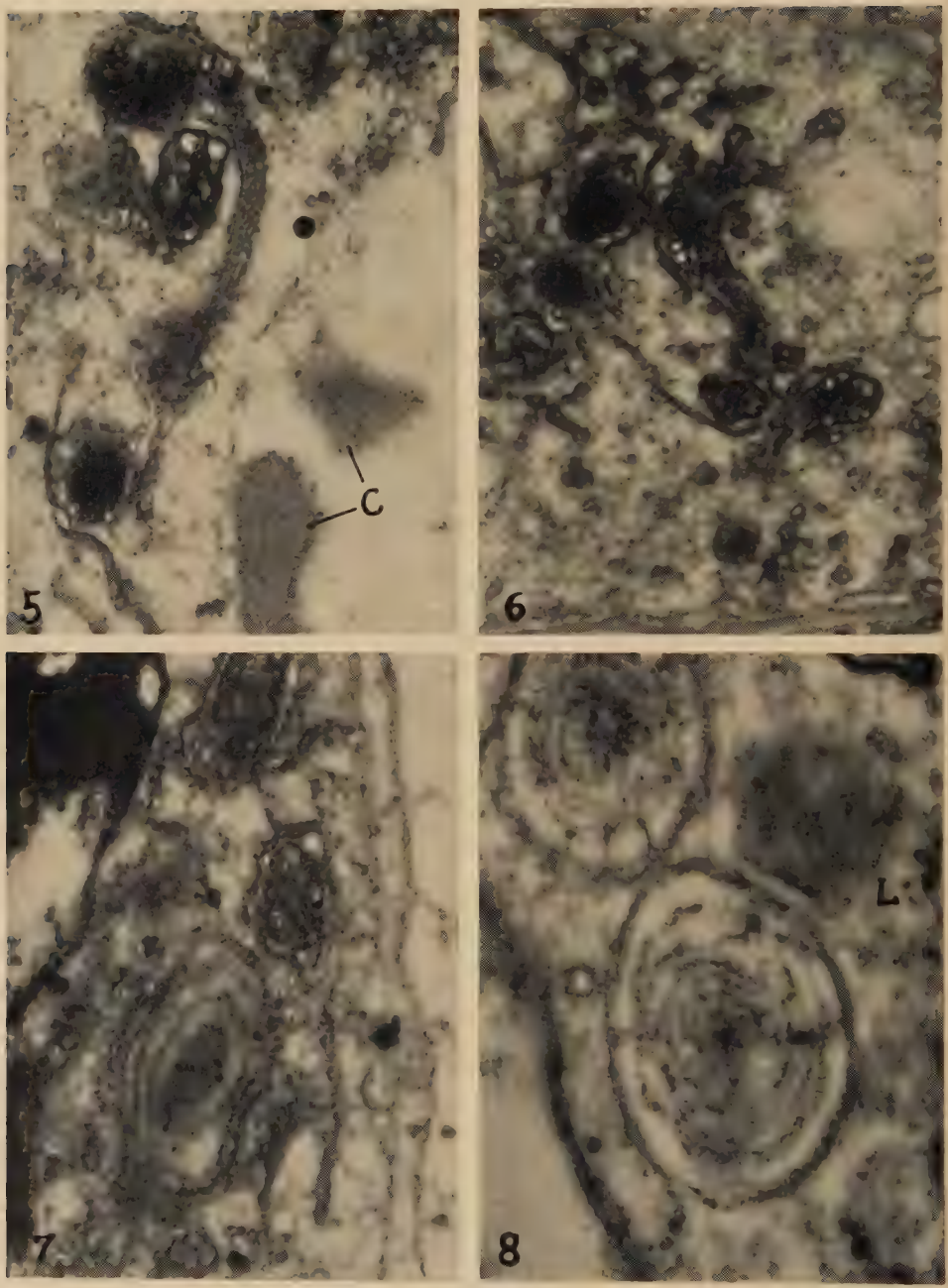
C
5
6
7
L
8

Nucleolar extrusions preceding the appearance of yolk [2, 3, 6, 7, 10], development of yolk out of the Golgi complex [6, 7] and simultaneous appearance of lipid granules [10] have been described by a number of skilled observers. The relationship between these three substances has been elucidated by means of an electron microscope study on thin sections of the ovary of *Cipangopaludina malleata.*

REFERENCES

1. Caspersson, T., Cell Growth and Cell function. New York, W. W. Norton & Co. 1950.
2. Gatenby, J. B., *Quart. J. Microscop. Sci.* **63**, 445 (1919).
3. —— *ibid.* **66**, 1 (1922).
4. Meves, F. (1899). Cited by Popoff [10].
5. —— *Arch. mikroskop. Anat. Entwicklungsgeschichte* **61**, 1 (1901).
6. Nath, V., *Quart. J. Microscop. Sci.* **72**, 403 (1929).
7. Nath, V. and Mehta, D. R., *Quart. J. Microscop. Sci.* **73**, 7 (1930).
8. Newman, S. B., Borysko, E. and Swerdlow, M., *J. Research Natl. Bureau Standards* **43**, 183 (1949).
9. Palade, G. E., *Anat. Rec.* **114**, 427 (1952).
10. Popoff, M., *Arch. mikroskop. Anat. Entwicklungsgeschichte* **70**, 43 (1907).
11. Yasuzumi, G., *J. Biophys. and Biochem. Cytology* **3** (1957) (in press).

Fig. 5.—The Golgi complex comes into contact with the limiting membrane of the chromidal bodies. A portion of the nucleus shows chromosomes (*C*) believed to be in very early prophase. × 36,000.
Fig. 6.—A section through an advanced oocyte showing the chromidal bodies surrounded by the Golgi complex. × 25,200.
Fig. 7.—Low power electron micrograph of three developing yolk granules. One of them has a core with intermediate density, which is surrounded by three layers. × 33,000.
Fig. 8.—Low power electron micrograph of two completed yolk granules and a lipid granule (*L*). × 24,000.

HISTOCHEMICAL STUDIES OF SULFO-MUCOPOLYSACCHARIDES IN THE ORGANIC MATRICES OF MINERALIZED TISSUES[1]

R. C. GREULICH[2] and U. FRIBERG

Department of Medical Physics and Department of Histology, Karolinska Institutet, Stockholm, Sweden

Received April 6, 1957

Radiosulfate ion is known to be incorporated into the sulfo–mucopolysaccharides (SMP) of mesenchymal tissues, both *in vivo* and *in vitro* [3]. In the present investiga-

[1] Supported in part by research grant D–177 from the National Institute of Dental Research, United States Public Health Service (RCG), and by a grant from "Konung Gustaf V:s 80-årsfond", Stockholm (UF). The technical assistance of Mrs. Monica Björkman and Miss Gun Ekbladh is gratefully acknowledged.

[2] Bank of America—Giannini Foundation Fellow, on leave from Department of Anatomy University of California Medical Center, Los Angeles, U.S.A.

tion, observations have been made which suggest a relationship between SMP and ribonucleic acid (RNA) in the organic matrices of all mineralized tissues.

Experimental.—Histochemical and autoradiographic observations have been made on decalcified bones and teeth taken from normally growing guinea pigs. These animals were sacrificed at various intervals following a single intra-peritoneal injection of sodium S^{35}-sulfate in a dose of 2.4 μC/g. Specimens were fixed a 3:1 (v/v) mixture of 96 per cent ethanol and 40 per cent neutral formalin. Decalcification was carried out in daily changes of a 34 per cent aqueous solution of disodium–dihydrogen ethylene diamine tetra-acetate (Na_2H_2–EDTA), pH 7.3, for 7 to 8 days at 37°C, and was controlled by radiography. The decalcified tissues were embedded in paraffin. Semi serial 8 μ sections were affixed to glass slides, were deparaffinized, and the slides were then divided into four similar groups. One group was immersed in a 0.05 per cent aqueous unbuffered solution of crystalline ribonuclease[1] (RNA-se) for 4 hours at 37°C, followed by 12 hours in a 0.06 per cent aqueous solution of the same enzyme at room temperature (Group I). Group II was placed in a 0.1 per cent aqueous unbuffered solution of testicular hyaluronidase (H-dase, 100–200 TRU/mg) for 4 hours at 37°C. Group III was placed for 2 hours in a 0.5 per cent solution of β-amylase at 37°C. Group IV was immersed in distilled water at room temperature for 4 hours at 37°C, and then in a second change of distilled water at room temperature for 12 hours. Additional samples from each group were removed at intervals during incubation in order to follow the progress of the hydrolyses histologically. After incubation, the four group of slides were autoradiographed by the "coated" method of Belanger and Leblond [2, 8], using NTB-3 liquid experimental emulsion.[2] All samples exposed for three weeks at 4°C, and were then developed and fixed simultaneously. Autoradiographic processing and all subsequent treatments of the four groups were comparable.

Results.—The success of the enzyme incubations was established by comparing stained sections from the control Group (IV) with those of the treated groups (I–III). Cytoplasmic basophilia of the tissues in group I was progressively lost during treatment with RNA-se (Figs. 1, 2). Metachromatic staining with toluidine blue of Group II (H-dase), demonstrated a progressive loss of metachromasia from cartilage and dentin matrix during the hydrolysis, this loss being complete at the end of 4 hours (Figs. 3, 4). Glycogen deposits in liver, muscle, cartilage, etc., were lost during treatment with β-amylase (Group III), as determined by staining with Best's carmine hematoxylin, and the PAS technique. Incubation in water (Group IV) had no apparent effect upon these various staining characteristics, as compared to normal histological preparations.

Fig. 5 summarizes the effect of the control and the various enzyme incubations on the S^{35}, which could be demonstrated autoradiographically, at 24 hours after the isotope injection. Neither β-amylase nor control incubation altered the normal distribution or intensity of the autoradiographic reactions known to occur in untreated control autoradiograms at this time. Testicular hyaluronidase, however, removed nearly all of the S^{35} label from epiphyseal cartilage (Figs. 6, 7). It did *not*

[1] All enzyme preparations obtained from Nutritional Biochemicals Corp., Cleveland, Ohio, U.S.A.

[2] Kindly supplied by Eastman Kodak Co., Rochester, New York, U.S.A.

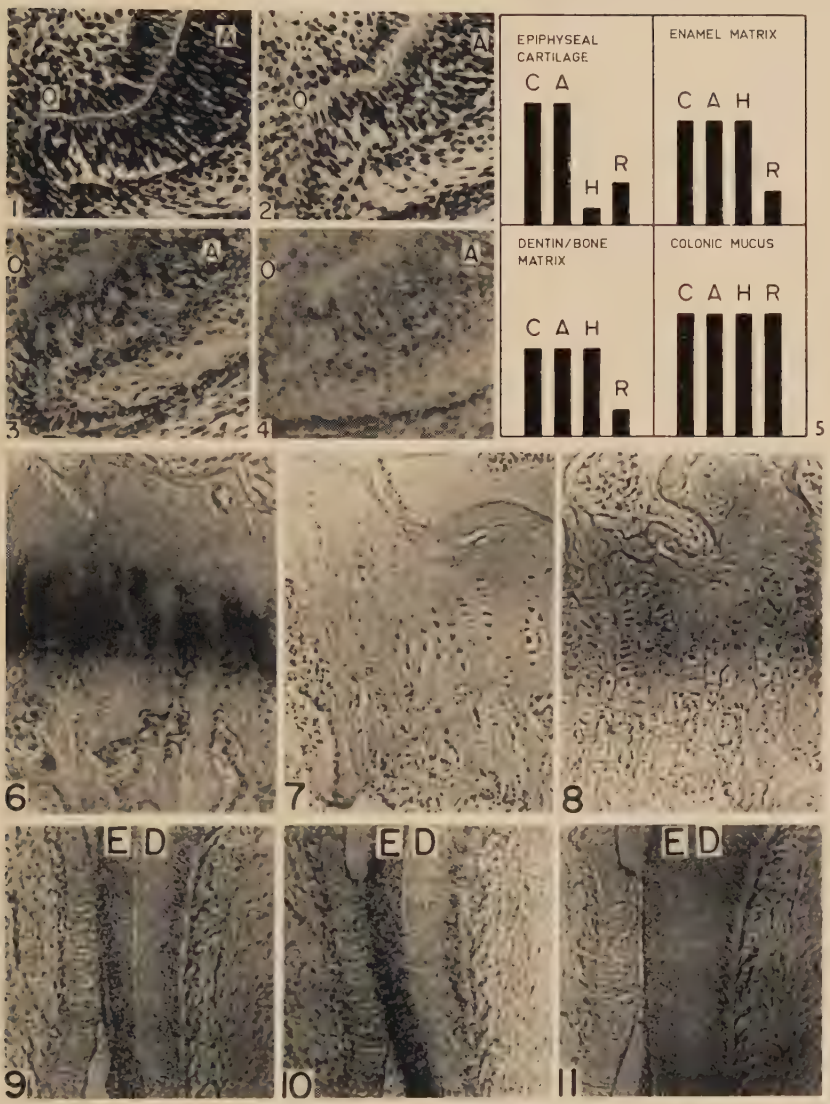

Figs. 1–4.—Semi-serial sections taken at the base of a decalcified molar tooth. Stained with hematoxylin–eosin (Figs. 1, 2), and with toluidine blue (Figs. 3, 4). The sections in Figs. 2 and 4 have been incubated with RNA-se and H-dase, respectively, while those in Figs. 1 and 3 have been incubated with water. The loss of cytoplasmic basophilia and metachromasia indicated successful removal of RNA and CSA, respectively. *A* ameloblasts; *O* odontoblasts.

Fig. 5. Relative effect of various enzyme treatments on the residual content of S^{35} in several tissues visualized autoradiographically. Note the more pronounced action of ribonuclease. *C* control; *A* β-amylase; *H* hyaluronidase; *R* ribonuclease.

Fig. 6–11.—Alteration of S^{35} autoradiograms (as seen in phase contrast) of semi serial sections of decalcified epiphyseal cartilage (Figs. 6–8) and teeth (Figs. 9–11), following incubation with water (Figs. 6, 9), hyaluronidase (Figs. 7, 10), and ribonuclease (Figs. 8, 11). Note that hyaluronidase causes a loss of S^{35} in cartilage only, while ribonuclease removes most reactivity from cartilage, enamel matrix, and dentin matrix. *E* enamel matrix; *D* dentin matrix.

alter the intensity of the reactions seen in the organic matrices of enamel and dentin (Figs. 9, 10), or of bone, nor did it affect any of the mucus-containing tissues which ordinarily exhibit strong autoradiographic reactions after S^{35}-sulfate administration (Fig. 5). RNA-se was also effective in removing S^{35}-label from epiphyseal cartilage, although not to the same extent as was H-dase (Figs. 6, 7, 8, cf. Fig. 5). Moreover, unlike the H-dase, *the RNA-se also removed the greatest share of bound sulfur from the matrices of enamel and dentin* (Figs. 9, 11), *and from bone matrix*. It did not, however, affect the intensity of the autoradiographic reactions of mucus-containing tissues.

Discussion.—Experimental attention has recently turned toward the possible role in the mineralization process of mucoprotein and mucopolysaccharides of the matrix ground substance. Chief among the recognized and well-characterized components of the ground substance is chondroitin sulfuric acid (CSA), which has been isolated in significant amounts from cartilage, bone matrix, and dentin matrix [6, 5, 9]. Its occurrence in enamel is less certain [14]. It seems likely that this substance occurs in conjunction with a protein moiety other than collagen in cartilage, bone and dentin, although the nature of this structural association is unknown [11, 13].

Previous investigations using combined autoradiographic and histochemical methods have provided contradictory data regarding the incorporation of S^{35}-sulfate into SMP. Bélanger [1] stated that H-dase treatment of acid-demineralized bones and teeth removed metachromasia and S^{35}-label from almost all cartilage, from bone matrix, and from dentin matrix. More recently [7], it has been shown that, after EDTA-demineralization, H-dase will remove the S^{35}-label from cartilage only, and does not affect the label in the matrices of bone, dentin and enamel.

Another SMP, keratosulfate, has been isolated chemically from bone matrix, and additional ones are thought to occur in the matrix ground substance [12]. The functional significance of these compounds is not known. A recent isotopic and chemical study of bone matrix has suggested that almost all of the uptake of S^{35}-sulfate occurred in the formation of labeled CSA [10], and thus this substance is believed to be responsible for the autoradiographic images in the present study. Our observations suggest the existence of a close relationship between CSA and RNA in the organic matrices of calcified tissues as well as in cartilage. This relationship is apparently such as to hinder the action of H-dase upon the labeled CSA moiety in the matrices of bones and teeth. RNA-se, however, a truly specific enzyme [4], removes the S^{35}-label from the matrices, presumably by freeing CSA (or its label) from its association with RNA. This effect of enzyme incubation is common to *all* mineralized tissue matrices. As far as we are aware, this is the only chemical-functional feature, other than the presence of mineral salts, which has been shown to be common to enamel matrix and to the matrices of the other mineralized tissues. It is tempting to suggest that this association of SMP (CSA?) and RNA (and protein?) may be of fundamental importance to the process of mineralization.

REFERENCES

1. Bélanger, L., *Can. J. Biochem. Physiol.* **32**, 161 (1954).
2. Bélanger, L. and Leblond, C., *Endocrinology* **39**, 8 (1946).
3. Boström, H. and Jorpes, E., *Experientia* **10**, 392 (1954).
4. Brown, D. and Todd, A., *in* The Nucleic Acids, p. 409. Academic Press, New York, 1955.

5. Eastoe, J. and Eastoe, B., *Biochem. J.* **57**, 453 (1954).
6. Einbinder, J. and Schubert, M., *J. Biol. Chem.* **185**, 725 (1950).
7. Greulich, R., *Anat. Rec.* **124**, 404 (1956).
8. Gross, J., Bogoroch, R., Nadler, N. and Leblond, C., *Am. J. Roentgenol.* **65**, 420 (1951).
9. Hess, W. and Lee, C., *J. Dent. Research* **31**, 793 (1952).
10. Kent, P., Jowsey, J., Steddon, L., Oliver, R. and Vaughan, J., *Biochem. J.* **62**, 470 (1956).
11. Meyer, K., *Ann. N.Y. Acad. Sci.* **60**, 803 (1955).
12. —— *in* Bone Structure and Metabolism, p. 65. J. & A. Churchill, London, 1956.
13. Shatton, J. and Schubert, M., *J. Biol. Chem.* **211**, 565 (1954).
14. Stack, M., *J. Am. Dent. Assoc.* **48**, 297 (1954).

THE INTRACELLULAR DISTRIBUTION OF AMINO ACID INCORPORATION BY SLICES OF LIVER AND LIVER TUMOURS AND BY ASCITES CELLS

P. N. CAMPBELL, OLGA GREENGARD and H. E. H. JONES

Courtauld Institute of Biochemistry, Middlesex Hospital, London, England

Received April 7, 1957

Since growth is undoubtedly closely associated with protein synthesis it might be expected that tumour tissue would have an increased ability to synthesise protein. A comparison of liver and liver tumour slices [10] or whole homogenates [9] incubated with C^{14}-alanine showed, in fact, a greater incorporation of radioactivity into the tumour than into the liver protein. Similar results have since been obtained with C^{14}-glycine under conditions in which a net synthesis of serum albumin both by liver and tumour slices could be demonstrated [1, 2].

In order to gain some understanding of the nature of these differences in the two types of tissue, subcellular fractions of whole preparations were studied from the point of view of their relative capacities to incorporate amino acids under *in vitro* conditions. For this purpose normal liver, regenerating liver and liver tumour slices and Krebs II mouse ascites tumour cells were used.

Experimental. —Liver tumours were induced in rats by feeding them on a diet containing 0.06 per cent *4*-dimethylaminoazobenzene. Regenerating liver was obtained from rats which had been partially hepatectomised by the method of Higgins and Anderson [3]. They were used 48 hours after the operation at which time the mitotic rate was found to be high. The ascites tumour cells were obtained from mice 7–9 days after inoculation. The tissues were incubated in Krebs–Ringer-bicarbonate-glucose-saline aerobically (O_2 + 5 per cent CO_2) at 37° in the presence of approximately 1 μ C of uniformly labelled C^{14}-glycine. The quantities used were 800 mg of slices in 4 ml of medium, or 1 ml of washed, packed cells, suspended in 3 ml of medium. After incubation the slices were homogenised in a Potter-type glass homogeniser and the ascites cells were disrupted in an ultra-sonic disintegrator. For liver the subcellular fractionation in sucrose solution was carried out as described by Palade [5]. The ascites cells were fractioned either by the latter method with an

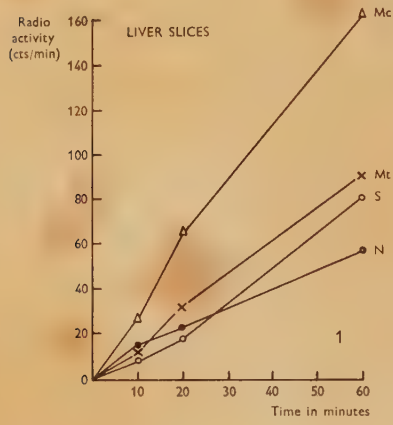

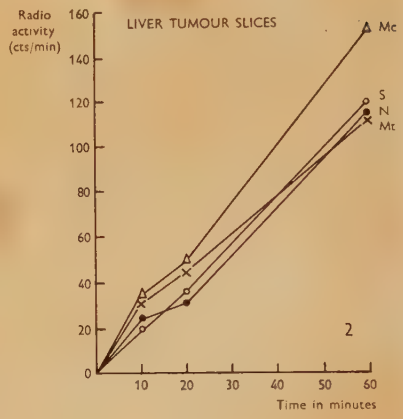

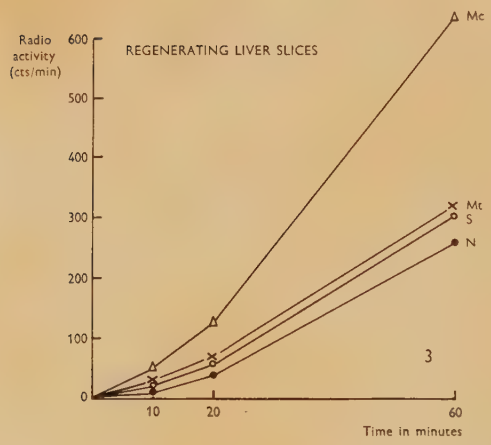

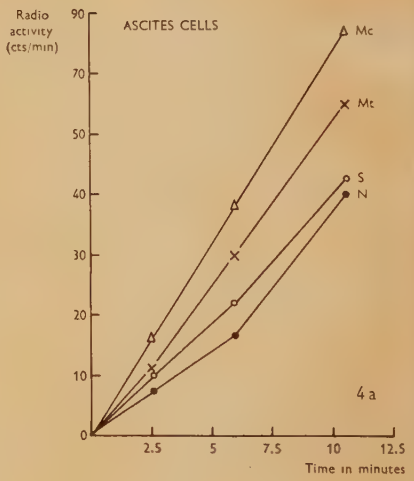

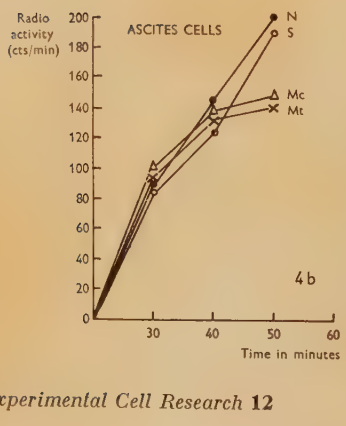

Fig. 1.—The incorporation of C^{14}-glycine into liver slices.
Fig. 2.—The incorporation of C^{14}-glycine into liver tumour slices.
Fig. 3.—The incorporation of C^{14}-glycine into slices from regenerating liver.
Fig. 4.—The incorporation of C^{14}-glycine into suspended ascites cells. Fractionated in Krebs-Ringer saline. (*a*) Short term incubation. (*b*) Long term incubation.

initial sucrose concentration of 0.88 *M*, or in the incubating medium. The four fractions obtained were as follows: (1) Nuclear (N), (2) large granules containing most of the mitochondria (Mt), (3) small granules containing most of the microsomes (Mc) and (4) supernatant (S).

The proteins were precipitated by the addition of an equal volume of 10 per cent trichloroacetic acid and the precipitates heated and washed to remove non-protein material as described by Zamecnik *et al.* [10]. The radioactivity was measured at "infinite thickness" on 0.28 cm^2. Perspex disks.

Results and discussion.—Fig. 1 shows the increase with time of the radioactivity of the proteins of the four fractions derived from liver slices. Fig. 2 represents the corresponding curves obtained in simultaneous experiments with slices of liver tumour. A comparison of the two figures shows that the most striking difference occurs in the nuclear fractions; that from liver tumour slices having a specific activity more than twice as high as that derived from liver slices after one hour of incubation. Since the protein content of the nuclear fraction represents a considerable proportion of the total protein in the slices, it is evident that the difference in this fraction makes an important contribution to the difference previously observed between unfractionated slices of liver and liver tumour. It was therefore of interest to see whether this greater ability of the nuclear proteins to incorporate amino acids is shown by regenerating liver and by other tumour cells.

Fig. 3 represents the findings with regenerating liver slices. On comparing these curves with those of Fig. 1, it can be seen that after one hour incubation the proteins of all fractions of the regenerating liver slices incorporated about 4 times as much radioactivity as the corresponding fractions from normal liver. Similarly, when using alanine as the labelled amino acid, all protein fractions of regenerating liver attained higher specific activities than those of the normal liver. The incorporation into both tissues, however, was much lower with alanine than with glycine, as expected on the basis of other *in vitro* liver studies [9]. Therefore unlike liver tumour there is no preferential incorporation of amino acids into the nuclear fraction of regenerating liver slices.

The results obtained with ascites cells are shown in Fig. 4 a and 4 b in which the fractionation was carried out in the saline medium. In the first few minutes the incorporation into the microsomal fraction is highest. Thus these results with ascites are not inconsistent with the hypothesis that the microsomal ribonucleoprotein is the initial site of incorporation of amino acids (e.g. [4]). It is of considerable interest that the nuclear fraction, after a lag period, reaches values even higher than the other particulate fractions. Identical results were obtained when applying sucrose fractionation, except that the mitochondrial fractions tended to show lower rates of incorporation.

Preliminary results indicate that the difference in the pattern of amino acid incorporation between hamster kidney and transplanted, stilboestrol-induced, renal tumour slices is very similar to that found between liver and liver tumour. Thus the enhanced incorporation of amino acids into the nuclear proteins appears to be a characteristic of the tumours studied.

The present studies on regenerating liver slices, showing an enhanced incorporation of amino acids into all fractions may be associated with the finding [6] that in this tissue the relative amount of protein both in the nuclei and in the cytoplasmic

granules is greater than in normal liver. Furthermore, our results with tumour tissue may be a reflection of the observation [7, 8] that in this tissue an increase occurs in the ratio of nuclear to cytoplasmic protein.

We are grateful to Dr. J. G. Bennette for supplying the ascites cells.

REFERENCES

1. Campbell, P. N. and Stone, N. E., *Biochem. J.* **61**, XX (1955).
2. —— *ibid.* **66** 19 (1957).
3. Higgins, G. M. and Anderson, R. M., *Arch. Pathol. (Lab. Med.).* **12**, 186 (1931).
4. Hultin, T., *Exptl. Cell Research Suppl.* **3**, 210 (1955).
5. Palade, G. E., *Arch. Biochem.* **30**, 144 (1951).
6. Price, J. M. and Laird, A. K., *Cancer Research* **10**, 650 (1950).
7. Price, J. M., Miller, J. A. and Miller, E. C., *Cancer Research* **2**, 96 (1949).
8. Rutman, R. J., Cantarow, A. and Paschkis, K. E., *Cancer Research* **14**, 115 (1954).
9. Winnick, T., *Arch. Biochem.* **27**, 65 (1950).
10. Zamecnik, P. C., Loftfield, R. B., Stephenson, M. L. and Steele, J. B., *Cancer Research* **11**, 592 (1951).

THE MODIFYING EFFECT OF CULTURE AGE ON HEAT SENSITIVITY OF YEAST[1]

A. M. ROSENBERG and T. H. WOOD

Department of Physics, University of Pennsylvania, Philadelphia, Penna., U.S.A.

Received April 12, 1957

On the basis of the shape of thermal survival curves Rahn [2] and Wood [6] have suggested that thermal inactivation of microorganisms is due to damage of the reproductive apparatus. Additivity studies of X-ray and thermal damage in yeast further suggest that these two injurious agents act on the same biological site [5]. The variation of X-ray sensitivity with various culture conditions has been studied in yeast [4]; thus it is desirable to obtain information on thermal sensitivity as a function of different culture conditions, primarily culture age.

The yeast used was a haploid strain originally designated by Zirkle and Tobias as SC-7 [7]. Cells from a stock culture were streaked on potato dextrose agar (Difco) slants and grown at 25°C for different lengths of time (1-day to 48-days). Yeast cells were harvested from these slants, washed by repeated centrifugation, and suspended in $M/15$ KH_2PO_4 at a concentration of 10^6 cells/ml. These suspensions were agitated on a rotary shaker for several hours before using. Aliquots of 0.1 ml of yeast sus-

[1] This investigation was supported by a research grant (C-2390) from the National Cancer Institute, U.S. Public Health Service.

pension were added to 9.9 ml of $M/15$ KH_2PO_4 held within a temperature bath at 56.2°C. Samples were removed at various time intervals, properly diluted, and plated on potato dextrose agar plates. Visible colonies were counted after incubation for 3 days at 30°C. Surviving fractions were computed from suitable controls; complete survival curves were plotted as the logarithm of the fraction of the original population surviving various time exposures at 56.2°C for culture ages from 1- to 48-days.

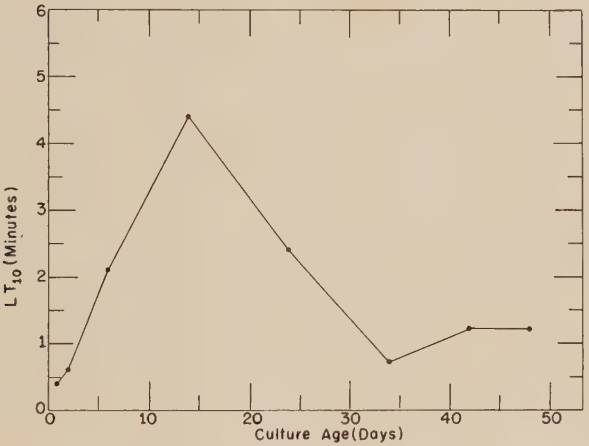

Fig. 1.—The time in minutes required to inactivate a haploid yeast population to the 10 per cent survival level (LT_{10}) as a function of culture age.

These survival curves are sigmoid in shape and display "tails" (an upward concavity) at low survival levels (below 1 per cent) [6]; for such curves a convenient and meaningful index of thermal resistance is the time required to inactivate the population to the 10 per cent survival level (LT_{10}). A plot of the LT_{10} as a function of the age of culture is shown in Fig. 1.

It can be seen from this figure that the yeast from 1- and 2-day-old cultures are approximately 10 times as sensitive to thermal inactivation as those from 14-day-old cultures. However, as the culture age is varied from 14- to 48-days, thermal resistance decreases by a factor of 3.

The increased thermal sensitivity in the very young cultures (1- and 2-day) could be related to either a higher rate of metabolism or increased frequency of budding. Beam *et al.* [1] have shown that in "tail" formation in X-ray survival curves of yeast the survival level at which the "tails" occur is directly correlated with the fraction of budding cells and that the X-ray resistance of this budding fraction is greater than that of the remaining population. However, in these studies on thermal inactivation, the "tail" position is always below the 1 per cent survival level (i.e., no more than 1 per cent of the original population has an unusually high thermal resistance) even though $^1/_3$ of the population may be budding. Hence there is not this correlation between "tail" position of thermal inactivation curves and the fraction of the population undergoing budding.

It would be expected that the addition of glucose to 14-day-old cultures (normally considered to be "resting") would increase their metabolic activity. Although glucose addition does not change appreciably the level of the "tail", the thermal

resistance as measured by the LT_{10} can be reduced by such addition of glucose to a value typical of much younger cells. Thus the progressive decrease in thermal sensitivity displayed in the 2- to 14-day old region is probably due to decreased metabolic activity. The increased thermal sensitivity of cultures over a month old is unexplained. Changes in the water content of the cell with aging may be responsible, and investigation of this possibility with partially desiccated yeast cells is planned.

In preliminary experiments we have found 14-day old diploid yeast to be more thermally resistant than 2-day-old diploids, in confirmation of Sherman's work [3].

REFERENCES

1. Beam, C. A., Mortimer, R. K., Wolfe, R. G. and Tobias, C. A., *Arch. Biochem. and Biophys.* **49**, 110 (1954).
2. Rahn, O., *Bacteriol. Revs.* **9**, 1 (1945).
3. Sherman, R., *Exptl. Cell Research* **11**, 659 (1956).
4. Wood, T. H., *Proc. Soc. Exptl. Biol. Med.* **84**, 446 (1953)
5. —— *Arch. Biochem. and Biophys.* **52**, 157 (1954).
6. —— *in* Advances in Biological and Medical Physics, Chapt. 4, Vol. IV. J. H. Lawrence and C. A. Tobias, Eds., Academic Press, New York, 1956.
7. Zirkle, R. E. and Tobias, C. A., *Arch. Biochem. and Biophys.* **47**, 282 (1953).

Errata.—In the Brief Note by E. Scarano and R. Maggio, "An exchange between ^{32}P-labeled pyrophosphate and ATP catalyzed by amino acids in unfertilized sea urchin eggs", This Journal, **12**, 403 ff. the following corrections should be made:

Under the authors' names, insert: Centro di Studi per la Biologia del Consiglio Nazionale delle Ricerche, Stazione Zoologica, Napoli.

Table I, column 1, last line: For $E - {}^{32}PP$ *read* $E + {}^{32}PP$.

Table I, column 2, line 9: to be deleted.

P. 404, reference in penultimate line of first paragraph: for [12] *read* [2].

P. 405, second line of first paragraph: For there is a formation of hydroxamine acids *read* there is no formation of hydroxamic acids.

AUTHOR INDEX

A

Afzelius, B. A. and Murray, A., 325

B

Bacq, Z. M. *et al.*, 639
Bahr, G. F. *et al.*, 342
Bahr, G. F. and Zeitler, E., 44
Bell, L. G. E. See McLeish 120
Beskow, G. See Hultin, 675
Bloom, G. See Bahr, 342
Bomstein, R. A. and Steberl, E. A., 254
Bos, C. J. See Emmelot, 191

C

Campbell, P. N. *et al.*, 689
Chapman-Andresen, C., 397
Chayen, J. See Deeley, 582; McLeish, 120
Collet, A. See Policard, 400

D

Damblon, J. See Bacq, 639
Danes, S. B., 169
Daoust, R., 203
Davies, H. G. See Deeley, 582
Davis, M. and Smith, C. L., 15
De, D. N., 181
Decken, A., von. See Hultin, 675
Deeley, E. M. *et al.*, 582
De Robertis, E. and Franco Raffo, H., 66
De Robertis, E. and Vaz Ferreira, A., 568, 575

E

Emmelot, P. See Bos, 191
England, M. C. and Mayer, D. T., 249
Engström, A. *et al.*, 592
Engström, A. and Lundberg, B., 198
Errera, M. See Bacq, 639; Skreb, 649

F

Fajer, A. See Junqueira, 338
Fauré-Fremiet, E. *et al.*, 135
Finamore, F. J., 356
Fjelde, A., 35
Forro, F., 363
Franco Raffo, H. See De Robertis, 66
Friberg, U. See Bahr, 342; Greulich, 685

G

Gauchery, M. See Fauré-Fremiet, 135
Gezelius, K. and Rånby, B. G., 265
Goldman, D. E. and Lepeschkin, W. W., 507
Graham, A. F. See Siminovitch, 299
Greengard, O. See Campbell, 689
Greulich, R. C. and Friberg, U., 685
Guidotti, G., 659

H

Hagström, B. E. See Perlmann, 418
Hale, C. M. F., 657
Harvey, A. N. See Sacks, 537
Hellström, K. E. and Nilsson, O., 180
Henry, B. S. See O'Hern, 115
Herve, A. See Bacq, 639
Hino, S. See Lindegren, 163
Hlinka, J. See Mellors, 560
Holmstrand, K. See Wallgren, 188
Horava, A. P. See Meyer-Arendt, 678
Hultin, T., 290, 413, 518, 675

I

Immers, J., 145

J

Johnston, P. M. See Sacks, 537
Jones, H. E. H. See Campbell, 689
Junqueira, L. C. U. *et al.*, 338

K

Kaltenbach, J. C. See Perlmann, 185
Kaplan, W. D. See Ohno, 395
Kaufmann, B. P. See McDonald, 415
Kinosita, R. See Ohno, 395
Kriszat, G. See Runnström, 526
Kruszynski, J., 108

L

La Cour, L. F. See McLeish, 120
Lagergren, C. See Engström, 592
Larsson, S., 666
Lawrence, J. C. and Ricketts, C. R., 633
Leeson, T. S., 670
Lepeschkin, W. W. See Goldman, 507
Lesley, S. M. See Siminovitch, 299
Lindegren, C. C. and Hino, S., 163
Lundberg, B. See Engström, 198, 592

M

Maggio, R. See Scarano, 403
Makinodan, T. See Ruth, 309
Markman, B., 424
Marshak, A., 599
Mayer, D. T. See England, 249
McDonald, M. R. and Kaufmann, B. P., 415
McLeish, J. *et al.*, 120
Mellors, R. C. *et al.*, 560
Meyer-Arendt, J. R. and Horava, A. P., 678
Morton, J. H. See Sacks, 537
Murray, A. See Afzelius, 325

N

Nakamura, M., 200
Naora, H., 1
Nilsson, O. See Hellström, 180
Nevill, A. See Siminovitch, 299

O

O'Hern, E. M. and Henry, B. S., 115
Ohno, S. *et al.*, 395
Ortega, L. G. See Mellors, 560

P

Paul, J. and Pearson, E. S., 212, 223
Pearson, E. S. See Paul, 212, 223
Pelc, S. R., 320
Perlmann, P. and Hagström, B. E., 418
Perlmann, P. and Kaltenbach, J. C., 185
Perry, R. P., 546
Phelpstead, J. W. P. and Roodyn, D. B., 673
Policard, A. *et al.*, 400
Pregermain, S. See Policard, 400
Prescott, D. M., 126, 196

R

Reger, J. F., 662
Ricketts, C. R. See Lawrence, 633
Roodyn, D. B. See Phelpstead, 673
Rosenberg, A. M. and Wood, T. H., 692
Rothschild, H. A. See Junqueira, 338
Rouiller, Ch. See Fauré-Fremiet, 135
Runnström, J., 374
Runnström, J. and Kriszat, G., 526
Ruth, R. F. *et al.* 309
Rånby, B. G. See Gezelius, 265

S

Sacks, J. *et al.*, 537
Salzen, E. A., 615
Scarano, E. and Maggio, R., 403
Scherr, G. H., 92
Sevastikoglou, J., 80
Siminovitch, L. *et al.*, 299
Skreb, Y. and Errera, M., 649
Smith, C. L. See Davis, 15
Steberl, E. A. See Bomstein, 254
Stenram, U., 626
Stoholski, A. See Mellors, 560
Svensson, G., 406

T

Tanaka, H. See Yasuzumi, 681

V

Vanderhaeghe, F. See Bacq, 639
Vaz Ferreira, A. See de Robertis, 568, 575
de Villafranca, G. W., 410
Vincent, J., 422
Vorbrodt, A., 154

W

Wallgren, G. and Holmstrand, K., 188
Wettstein, D., 427
Wolfe, H. R. See Ruth, 309
Wolman, M., 231, 241
Wood, T. H. See Rosenberg, 692

Y

Yasuzumi, G. and Tanaka, H., 681

Z

Zeitler, E. and Bahr, G. F., 44

SUBJECT INDEX

A

Acetabularia mediterranea, effect of X-ray on, BACQ *et al.*, 639
Acrosomal reaction of spermatozoa during fertilization, AFZELIUS and MURRAY, 325
Adrenal medulla—electron microscopy of excretion of cathecol-containing droplets in, DE ROBERTIS and VAZ FERREIRA, 568; multivesicular cathecol-containing body of, DE ROBERTIS and VAZ FERREIRA, 575
Amino acid incorporation, intracellular distribution of, CAMPBELL *et al.*, 689
Amoebae—nucleated and enucleated fragments of, effect of U.V. on, SKREB and ERRERA, 649; nucleus and ribonucleic acid synthesis in, PRESCOTT, 196
Anaerobiosis, effect of, on origin of respiratory-deficient yeast, LINDEGREN and HINO, 163
Antibody, cytochemical morphology of production of, RUTH *et al.*, 309
Antigens, quantitative changes in, during early development of sea urchin, PERLMANN and KALTENBACH, 185
Antiserum, cortical inhibitions and polyspermy caused by, in sea urchin eggs, PERLMANN and HAGSTRÖM, 418
Arginine, quantitative cytochemical estimation of, MCLEISH *et al.*, 120
Ascites—carcinoma cells, light scattering studies on, MEYER-ARENDT and HORAVA, 678; cells, intracellular distribution of amino acid incorporation, CAMPBELL *et al.*, 689
Asterias eggs, nuclear swelling in, in relation to passage of materials into and out of nuclei, MARSHAK, 599
Autoradiography, turnover of in mast cells, studied by, GUIDOTTI, 659

B

Brush borders of kidney and intestine, species differences in, KRUSZYNSKI, 108

C

Cancer cells—chromosomes of, MELLORS *et al.*, 560; human, growth in tissue culture, FJELDE, 35
Cell membranes, a method for staining of, WOLMAN, 241
Chick embryo—metabolism of heart explants during transition from *in vivo* to *in vitro* conditions, PAUL and PEARSON, 212; metabolism of liver explants during transition from *in vivo* to *in vitro* conditions, PAUL and PEARSON, 223
Chromosomes—mass of, in germinal and cancer cells of mouse, MELLORS *et al.*, 560; X and Y, conjugation of in rat spermatocyte, 395
Coccidioides immitis, effect of ribonuclease on, O'HERN and HENRY, 115
Cross-striated muscle, anisotropic band of, VILLAFRANCA, 410

D

Deoxyribonucleic acid—connection between synthesis of, in testis of mouse, PELC, 320; content of cells in the root of *Vicia faba*, DEELEY *et al.*, 582; egg extracts interfering with diphenylamine reaction for, FINAMORE, 356; localization of, in tissue sections, 203; of individual nuclei, NAORA, 1
Dictyostelium discoideum, morphology and fine structure of, GEZELIUS and RÅNBY, 265

E

Electron microscopy—of cathecol-containing droplets in adrenal medulla, DE ROBERTIS and VAZ FERREIRA, 568; of cytoplasmic modifications on contact with silica particles, POLICARD *et al.*, 400; of fine structure of ovary, YASUZUMI and TANAKA, 681; of macronuclear reorganisation in euplotes, FAURÉ-FREMIET, 135; quantitative interpretation of, ZEITLER and BAHR, 44
Embryos, density of, SALZEN 615
Endamoeba histolytica, methylthioadenosine as a growth factor for, NAKAMURA, 200
Ethylene-diaminetetraacetic acid, production of mitotic abnormalities by, MCDONALD and KAUFMANN, 415
Euplotes, macronuclear reorganization in, FAURÉ-FREMIET *et al.*, 135

F

Fallopian tube, ciliated and secretory cells in, HELLSTRÖM and NILSSON, 180
Fertilization, cytochemical studies of, in sea urchin egg, IMMERS, 145
Feulgen reaction, nuclei stained with, NAORA, 1
Formaldehyde, volume changes during fixation in, BAHR *et al.*, 342

G

Glycogen, liver, intracellular distribution of, SACKS *et al.*, 537
Gradient density centrifuging, a device for separating fractions, PHELPSTEAD and ROODYN, 673
Gram reaction, relationship with plasmolytic effects in bacteria, HALE, 657
Growth—change in the physiological state of a cell population in, as a function of, PRESCOTT, 126; of human cancer cells, FJELDE, 35; postnatal, DNA content of individual nuclei in, NAORA, 1

H

Heat sensitivity, modifying effect of culture age on, in yeast, ROSENBERG and WOOD, 692
Histoplasma capsulatum, dimorphism of, SCHERR, 92

I

Irradiation effect of, on ultraviolet absorption spectrum of parts of living cells, PERRY, 546

L

Larvae, density of, SALZEN, 615
L strain mouse—propagation of cells in suspension, SIMINOVITCH *et al.*, 299; suspension cultures of fibroblasts of, DANES, 169

M

Mast cells, sulphate, turnover in, GUIDOTTI, 659
Mesonephros, fine structure of, LEESON, 670
Methylthioadenosine as a growth factor for *Endamoeba histolytica*, NAKAMURA, 200
Microphotometer, scanning interference, SVENSSON, 406
Microradiography—correlation to polarised light-picture of secondary bone, VINCENT, 422; high resolution, midget X-ray tube for, ENGSTRÖM and LUNDBERG, 198; technical considerations on, WALLGREN and HOLMSTRAND, 188
Micro-scanner, mechanical, LARSSON, 666
Microsomes, liver, characteristics of extracts from, HULTIN, 290
Mitochondria—submicroscopic organization of, in insect testis, DE ROBERTIS and FRANCO RAFFO, 66; thyroxine and swelling of EMMELOT and BOS, 191
Mycobacterium tuberculosis, growth pattern of human cancer cells in, FJELDE, 35

N

Neuromuscular synapses, ultrastructure of, in mouse gastrocnemius muscle, REGER, 662
Nuclear membrane, ultrastructure of, of plant cells, DE, 181
Nuclei—comparative nucleic acid content of, in frog, ENGLAND and MAYER, 29; microspectrophotometry of, with Feulgen reaction, NAORA, 1; passage of materials, in nuclear swelling in *Asterias*, MARSHAK, 599
Nucleic acid, comparative, content of liver nuclei, ova nuclei and spermatozoa, ENGLAND and MAYER, 249
Nucleoli, interferometric dry matter determinations of, STENRAM, 626
Nucleotides, acid-soluble, in development of *P. miliaris*, HULTIN, 413

O

Osmium tetroxide—reaction of, with tissue components, WOLMAN, 231; volume changes during fixation in, BAHR *et al.*, 342
Osteogenesis, endochondral, in tissue culture, SEVASTIKOGLOU, 80
Oxidation-reduction indicators, solidifying effect of, on surface of unfertilized sea urchin egg, RUNNSTRÖM and KRISZAT, 526
Oxidative phosphorylation, effect of some inhibitors of, on phosphatases, VORBRODT, 154

P

Pancreas, protein production by, JUNQUEIRA *et al.*, 338
α-Particles, irradiation of single cells with, DAVIS and SMITH, 15
Phase contrast microscopy, species differences in brush borders of kidney and intestine, KRUSZYNSKI, 108
Phosphatases, histochemical demonstration of effect of inhibitors on, VORBRODT, 154
Phospholipides, utilization of, by bovine spermatozoa, BOMSTEIN and STEBERL, 254
Phosphorus, distribution of, among progeny of a single labeled bacterium, FORRO, 363
Pinocytosis in leucocytes, CHAPMAN-ANDRESEN, 397
Plastides, chlorophyll lethals and submicroscopic alterations of, VON WETTSTEIN, 427
Porphyrexid, effect on, on fertilization of sea urchin egg, RUNNSTRÖM, 374
Porphyrindin, effect on, on fertilization of sea urchin egg, RUNNSTRÖM, 374
Psammechinus miliaris, acid-soluble nucleotides in development of, HULTIN, 413
Pyrophosphate—ATP-exchange, catalyzed by amino acids in unfertilized sea urchin eggs, SCARANO and MAGGIO, 403

R

Refractometry, species differences in brush borders of kidney and intestine as revealed by, KRUSZYNSKI, 108
Ribonuclease—effect of, on *Coccidioides immitis*, O'HERN and HENRY, 115; effects of, on incorporation of C^{14}-L-leucine into liver proteins, HULTIN *et al.*, 675
Ribonucleic acid—synthesis of, and nucleus in *Amoeba*, PRESCOTT, 196; synthesis of, in mouse testis, PELC, 320

S

Sea urchin, soluble protein antigens during early development of, PERLMANN and KALTENBACH, 185
Sea urchin eggs—cortical inhibitions and polyspermy caused by, in, PERLMANN and HAGSTRÖM, 418; cytochemical studies of fertilization and first mitosis of, IMMERS, 145; effect of porphyrexid and porphyrindin on fertilization of, RUNNSTRÖM, 374; unfertilized—amino acids in, catalyzed by, pyrophosphate—ATP exchange in, SCARANO and MAGGIO, 403; solidifying effect of oxidation-reduction indicators on surface of, RUNNSTRÖM and KRISZAT, 526
Sea urchin embryos—metabolic utilization of C^{14}-formate in, HULTIN, 518; nuclear activity in differentiation of, MARKMAN, 424
SH-groups, roles of in dimorphism of *Histoplasma capsulatum*, SCHERR, 92
Spirogyra, injury and recovery of, after exposure to ultrasound, GOLDMAN and LEPESCHKIN, 507
Sulfo-mucopolysaccharides, histochemical studies of, in organic matrices of mineralized tissues, GREULICH and FRIBERG, 685
Sulphate—turnover in rat mast cells, studied by autoradiography, GUIDOTTI, 659; uptake of by skin, LAWRENCE and RICKETTS, 633

T

Testis—connection between RNA and DNA in, PELC, 320; insect, mitochondria and other cytoplasmic structures of, DE ROBERTIS and FRANCO RAFFO, 66
Tetrahymena geleii, change in physiological state of a cell population as a function of growth and age, PRESCOTT, 126
Tissue culture—change in physiological state of a cell population in, as a function of growth, PRESCOTT, 126; endochondral osteogenesis in, SEVASTIKOGLOU, 80; growth pattern of human cancer cells in, FJELDE, 35; irradiation of, with α-particles, DAVIS and SMITH, 15

U

Ultraviolet rays, effect of, on fragments of amoebae, SKREB and ERRERA, 649

V

Vicia faba, DNA content of cells in root of, DEELEY *et al.*, 582

X

X-ray—absorptiometry, determination of strontium and calcium in bone by, ENGSTRÖM *et al.*, 592; effect on *Acetabularia mediterranea*, BACQ *et al.*, 639

NOTICE TO AUTHORS

Experimental Cell Research publishes papers dealing with the experimental analysis of the activity and of the biochemical and biophysical organization of the cell and its subunits. Technical or theoretical papers aiming at the further development of methods in the field of experimental and ultrastructural cytology will also be acceptable.

Address: The author's complete address should be placed on each manuscript.

Manuscript: Authors residing in the Western hemisphere should send their manuscripts in duplicate to the U.S. editors; others to the European editors or to the Editorial Office, Norrtullsgatan 16, Stockholm Va, Sweden. Manuscripts in English, French, or German are accepted. The grammar and style of the manuscripts should be carefully checked before they are handed over to the Editors. The manuscripts should be typed double spaced on one side of the paper only and should not exceed *fifteen printed* pages, including figures and tables. Footnotes should be avoided, but if used they must be numbered consecutively and placed on a separate sheet at the end of the manuscript. Authors are requested to conclude their manuscripts with a brief summary and to indicate an *abbreviated running title* on the title page. Descriptions of technique and sections of minor importance will be printed in small type.

Brief Notes not longer than *three printed* pages will be published in the next forthcoming issue, if possible. Only those papers will be accepted as *Brief Notes*, which are to be considered as preliminary communications or which contain viewpoints that may essentially contribute to the discussion of current problems or technical advances.

N.B.—No proof will be sent to authors of *Brief Notes*. Therefore, typescripts prepared for this section are in every detail equivalent to proofs approved by the author.

Manuscripts should be submitted in complete and final form for publication. Approved manuscripts that are not in proper form will be returned for revision. Galley proofs will be sent to the authors who are requested to return them together with proofs of the figures immediately by airmail to the Editorial Office. The point of insertion of each figure should be indicated.

Tables and Figures: The dimensions of the printed page, 125 × 175 mm, should be kept in mind in preparing figures and tables for publication. Each table should be typewritten on a separate sheet and all figures and tables should be marked with the author's name. Figure legends should be typed in sequence on a separate sheet. Graphs and diagrams should be carefully drawn in black ink on white paper or blue coordinate paper, and all drawings should be so prepared and lettered that they can stand a reduction of 50 per cent. The amount of illustration material must not exceed a total of four pages, unless funds are raised by the author to defray the extra cost. No illustrations in color will be accepted unless the author is prepared to cover the cost of reproduction.

Literature cited: Papers referred to in the manuscript should be listed on a separate page and headed "References." The journal, volume, page number and year of publication should be mentioned. The system of abbreviation given in "List of Periodicals" in *Chemical Abstracts*, **45**, No. 24, Part II (1951), should be followed. The references should be arranged in alphabetical order according to the (first) author's surname. They should also be numbered so that each may be referred to in the text by number only. Please follow carefully the following style for punctuation and order of listing:

1. Bahr, G. F., *Exptl. Cell Research* **1**, 603 (1950).
2. Kidder, G. W. and Dewey, V. C., Biochemistry and Physiology of Protozoa. Vol. I, p. 392. Academic Press Inc., New York, 1951.
3. Oppenheimer, B. S., Oppenheimer, E. T., Stout, A. P. and Danishefsky, I., *Science* **118**, 305 (1953).

Reprints: Authors will be furnished, free of charge, with fifty reprints without covers. Additional reprints may be obtained at cost. Order forms will be submitted with the galley proofs. These should be filled in, indicating shipping and billing instructions, and returned with the proofs.

Abstracts: Authors are requested to provide an abstract for *Biological Abstracts* on a special form which is submitted with the galley proofs.